THÈSE

Pour l'obtention du grade de
DOCTEUR DE L'UNIVERSITÉ DE POITIERS
UFR des sciences fondamentales et appliquées
Écologie et biologie des interactions - EBI (Poitiers)
(Diplôme National - Arrêté du 25 mai 2016)

École doctorale : Chimie, Écologie, Géosciences et AgroSciences Théodore Monod (Poitiers)
Secteur de recherche : Physiologie végétale

Présentée par :
Abir Israel

Functional diversity of AtESL sugar transporters in development and response of Arabidopsis thaliana to abiotic constraints

Directeur(s) de Thèse :
Maryse Laloi, Fabienne Dédaldéchamp, Rossitza Atanassova

Soutenue le 01 avril 2021 devant le jury

Jury :

Président	**Éric Gomes**	Professeur, ISVV, Université de Bordeaux
Rapporteur	**Marie-Pascale Prud'homme**	Professeur, INRAE, Université de Caen
Rapporteur	**Soulaïman Sakr**	Professeur, IRHS, Agrocampus Ouest, Université d'Angers
Membre	**Maryse Laloi**	Maître de conférences , EBI, Université de Poitiers
Membre	**Fabienne Dédaldéchamp**	Maître de conférences, EBI, Université de Poitiers
Membre	**Rossitza Atanassova**	Professeur, EBI, Université de Poitiers
Membre	**Vincent Courdavault**	Maître de conférences, Université de Tours

Pour citer cette thèse :
Abir Israel. *Functional diversity of AtESL sugar transporters in development and response of Arabidopsis thaliana to abiotic constraints* [En ligne]. Thèse Physiologie végétale. Poitiers : Université de Poitiers, 2021. Disponible sur Internet <http://theses.univ-poitiers.fr>

THESE

Pour l'obtention du Grade de

DOCTEUR DE L'UNIVERSITE DE POITIERS

(Faculté des Sciences Fondamentales et Appliquées)
(Diplôme National - Arrêté du 25 mai 2016)

Ecole Doctorale : Chimie Ecologie Géosciences Agrosciences « *Théodore Monod* »

Secteur de Recherche : Physiologie végétale

Présentée par :

Abir ISRAEL

****

Diversité fonctionnelle des transporteurs de sucres AtESL dans le développement et la réponse d'*Arabidopsis thaliana* aux contraintes abiotiques

****

Directrices de Thèse :
Maryse LALOI
Fabienne DEDALDECHAMP
Rossitza ATANASSOVA

****

Soutenue le 01 Avril 2021 devant la Commission d'Examen

****

JURY

Marie-Pascale PRUD'HOMME	Professeur, Université de Caen	Rapporteur
Soulaiman SAKR	Professeur, IRHS Agrocampus-Ouest, Angers	Rapporteur
Vincent COURDAVAULT	Maître de conférences, Université de Tours	Examinateur
Éric GOMES	Professeur, ISVV, Université de Bordeaux	Examinateur
Maryse LALOI	Maître de conférences, Université de Poitiers	Examinateur
Fabienne DEDALDECHAMP	Maître de conférences, Université de Poitiers	Examinateur
Rossitza ATANASSOVA	Professeur, Université de Poitiers	Examinateur

ACKNOWLEDGMENTS

My thesis would never have been possible without the support and guidance of many people, to whom I express my gratitude.

Foremost, I would like to thank the members of my thesis Jury. First of all, my thesis reporters ***Prof. Marie-Pascale PRUD'HOMME*** *and* ***Prof. Soulaiman SAKR*** *for their valuable time to read and evaluate my dissertation. I would like to thank* ***Dr. Vincent COURDAVAULT*** *and* ***Prof. Eric GOMES*** *for having agreed to participate in my thesis Jury as examiners.*

I would like to express my sincere thanks to ***Prof. Jean-Marc BERJEAUD*** *and* ***Prof. Pierre COUTOS-THEVENOT****, for having accepted me in the EBI laboratory and SEVE team.*

I would like to express my special gratitude to my scientific supervisors, ***Dr. Maryse LALOI****,* ***Dr. Fabienne DEDALDECHAMP*** *and* ***Prof. Rossitza ATANASSOVA*** *for their valuable scientific help, support and useful criticism throughout my thesis. I highly appreciated their ideas and suggestions to make my experience productive and enthusiastic. Their guidance helped and motivated me enormously, and I have learned so much during the countless hours spent together at the laboratory bench. In particular, I will never forget our morning scratching of hundreds of leaves for the vacuoles' experiments. Thanks to all three of them for having written the articles and for their precious corrections of the whole manuscript. Finally, I am particularly grateful to my supervisors for having given me the opportunity to teach, and for their generous help in my first steps as university lecturer.*

NO WORDS can sum up the gratitude that I owe to ***Rossitza****. I deeply appreciate how you have been continuously encouraging and guiding me throughout my thesis, and for having always been by my side, when I needed help. I would also like to thank you for your scientific advice, assistance and criticism. Thank you again for the peach jam I really liked it :-). I am heartily thankful to you,* ***Rossi****, for all you have done for me.*

Fabienne*, thank you for your empathy, great sense of humor, motivation, and encouragement that came at the right moment when desperation set in. Thanks, Fabienne, for spending much time with me grinding hundreds of plants to find our "princess". I am so thankful for what you did for me… Thank you for your support during the lockdown, bringing me water packs, Leclerc drive…*

Maryse*, thank you for your indispensable critiques during this thesis and for helping me so much in the teaching. I will keep a good memory of our pleasant and enriching trip to Glasgow. I cannot express my gratitude for your continuous support during the lockdown.*

I gratefully thank ***Dr. Hristo ATANASSOV*** *for his kindness, the magic formula (which helped me a lot), and especially, for the corrections of my manuscript.*

*I would like to thank **Prof. Enrico MARTINOIA** for the fruitful scientific discussions on vacuoles' isolation, and **Dr. Vincent COURDAVAULT** for kindly providing us the protocol for tobacco protoplasts' isolation.*

*Many, many thanks to **Mrs. Caroline PAILLOT** for her technical help, especially during the days when I worked alone. Caro, thank you for your help as well as your reliable and accurate work. I really appreciate the time I spent working with you.*

*Thanks to **Mr. Vincent LEBEURRE** for helping me in the preparation of my plant cultures. Vincent, thank you for the attentive eye that you were able to keep on my plants.*

*I would like to thank **Mr. Benoît PORCHERON** for his technical help and advices I received from him in the yeast experiment.*

*I want to thank also **Mrs. Cécile GAILLARD** for our scientific discussions. Thank you for your thinking of me, and for other many things.*

*I would like to thank all the members of the laboratory, **Mrs. Geneviève HARIKA, Mrs. Sylvie CLERCY-MOREL, Dr. Joan DOIDY, Mr. William BEUZEBOC, Dr. Sylvain LA CAMERA, Dr. Laurence MAUROUSSET, Dr. Nathalie POURTAU, Dr. Cécile VRIET, Dr. Rémi LEMOINE, Mrs. Florence THIBAULT, Mr. Mickeal DURAND, and Mrs. Magali LALLEMAND** for their kindness.*

*I would like to thank the former Ph.D. student and actual **Dr. Antoine DESRUT**. Thank you for your kindness. I wish you all the best and every success in your life.*

*To my colleague in office, **Mrs. Amélie MORIN**, thank you for your help in statistical analysis, and I wish you all the best for finalizing your thesis and in the future. I would like to thank **Mrs. Marie BOURGEAIS**; I wish you all the best.*

*I am indeed grateful to my great family in Poitiers, and particularly to **Rana AWAD**, **Sarah MANTASH**, **Zeinab MCHEIK**, who are special and dear to me. Thank you all for the unfailing support, which I will never forget. To **Maha CHIEB**: thank you for having always been present, whenever I needed a friend.*

*I am indebted and indeed grateful to my family without whom nothing would have been possible. To my **parents**, thank you for your continuous support throughout these years. You have always been there for me, even if you were so far away. I LOVE you all very much. To my **Mom** and **Dad**: I wish to thank you, over and over again, for having always felt your tender presence by my side. You indefinitely believed, supported and pushed me forward, to give the best of myself. I LOVE you so much.*

LIST OF ABBREVIATIONS

ABA	ABscisic Acid
ABRE	ABA Responsive Element
ADH	Alcohol-DeHydrogenase
ATP	Adenosine triphosphate
ATPase	ATP-synthase
BAP	6-benzylaminopurine
bp	Base Pair
BSA	Bovin serum albumin
b-ZIP	basic leucine Zipper Protein
$CaCl_2$	Calcium Chloride
CC-SE	Companion Cell - Sieve Element complex
cDNA	Complementary DNA
CDS	Coding DNA Sequence
CO2	Dioxyde de carbone
Col-0	Colombia
CS	Casparian Strip
dNTP	Nucleoside TriPhosphate
DPS	Day Post Sowing
DPS	Day Post Sowing
DRE	Drought Responsive Element
DREB	Drought Responsive Element Binding protein
DST	Disaccharide transporter
DTT	Dithiothreitol
DW	Dry Weight
EDTA	Ethylenediaminetetraacetic acid
ERF	Ethylene Response Factor
ESL	Early-responsive to dehydration Six-Like
EtOH	Ethanol
FW	Fresh Weight
GA	Gibberelline
GFP	Green Fluorescent Protein
Glc	Glucose
GMO	Genetically Modified Organism

GUS	Beta-glucuronidase
h	Hour
H^+	Proton
HEPES	(4-(2-HydroxyEthyl)-1-PiperazinEethaneSulfonic acid
HXK	Hexokinase
INT	INositol Transporter
K^+	potassium ion
Kb	kilo base pair
KCl	Potassium Chloride
KOH	Potassium Hydroxide
LB	Luria Broth
LEA	Late Embryogenesis Aboundant
MFS	Major Facilitator Superfamily
$MgCl_2$	Magnesium Chloride
MS	Murashige and Skoog
MST	Monosaccharide transporter
MYB	Myeloblastosis virus
MYC	Muelocytomatsosis virus
NaCl	Sodium chloride
NEB	New England Bio labs
OD	Optical Density
OD	Optical Density
PCR	Polymerase Chain Reaction
PEG	PolyEthylene Glycol
pGlcT	plastidic Glucose Transporter
pH	Potential of Hydrogen
PMA	Plasma Membrane ATPase 1
PMT	Polyol/Monosaccharide Transporter
PRA	Project Rosette Area
qPCR	Quantitative PCR
RFO	Raffinose Family Oligosaccharide
Rgt	Restors Glucose Transport
ROS	Reactive oxygen species
RWC	Relative Water Content
SBG1	Supressor of G protein beta1
SC	Stomatal Conductance
SDS	Sodium Dodecyl Sulfate
SE	Sieve Element
Snf	Sucrose Non Fermenting

SnRK	Sucrose Related Kinase
STP	Sugar transporter protein
SUC or SUT	SUcrose Transporter
SWEET	Sugar Will Eventually be Exported Transporter
TAE	Tris-Acetate-EDTA
TF	Transcription factor
TIP	Tonoplast Intrinsic Protein
TMT	Tonoplast Membrane Transporter
Tris-HCL	Tris hydrochloride
TSS	Transcription Start Site
TW	Turgid Weight
ura	Uracil
UV	Ultra-Violet
v/v	Volume/Volume
v/v/v	Volume/Volume/ Volume
VGT	Vacuolar Glucose Transporter
w/v	Weight/Volume
WC	Water Content
YEB	Yeast Extract Beef
YNB	Yeast Nitrogen base (without amino acids)
YPM	Yeast extract-Peptone-Maltose

TABLE OF CONTENT

CHAPTER I 1
INTRODUCTION & LITERATURE REVIEW 1
Introduction 2
Literature Review 3
1. Biosynthesis and translocation of sugars in plants 3
1.1. Sugars biosynthesis 3
1.2. Source organs and sink organs 3
1.3. Translocation of sugars: Sources to Sinks 3
1.3.1. Phloem loading 3
1.3.2. Long-distance transport 5
1.3.3. Phloem unloading 5
2. State of the art of Sugar Transporters 5
2.1. The Major Facilitator Superfamily 6
2.1.1. Overview 6
2.1.2. Sucrose Transporters: SUC 6
2.1.3. Monosaccharide transporters : MST 15
2.2. SWEET family 15
2.3. The implication of tonoplast transporters in the intracellular transport 16
3. Water deficit 17
3.1. Plant/water relations: Water potential 17
3.2. Water path in the soil-plant-atmosphere system 18
3.2.1. Soil water is absorbed by the roots 18
3.2.2. Ascension of water through the plant vascular system: Xylem 19
3.3. Plants survival strategies to cope with water deficit 20
3.4. How plants respond to water deficit 21
3.4.1. At whole-plant level 21
3.4.2. Metabolic and cellular level 24
3.4.2.1. Osmotic adjustment 24
3.4.2.2. Photosynthesis level 24
3.4.3. Gene level 25
3.4.3.1. Stress responsive genes 25
3.4.3.2. Transcriptional regulation of gene expression 26
4. Sugar signaling in plants 32
4.1. Glucose signaling pathways 32
4.1.1. Hexokinase-dependent glucose-signaling pathway 32
4.1.1. Hexokinase-independent glucose-signaling pathway 33
4.1.2. Glucose-dependent pathway of glucose signaling 33
4.2. Sugar and Hormone Crosstalk 34
4.3. Disaccharide signaling pathway 36
4.4. Signal transduction 36
5. Evolutionary history of the monosaccharide transporters (MST) family of land plants 37
CHAPTER II 41
MATERIALS & METHODS 41
Materials and methods 42
1. Biological material 42
1.1. Plant material 42
1.2. Bacterial strains 42

1.3. Yeast strains 42
2. Growth conditions 42
2.1. *Arabidopsis* cultivation under normal conditions 42
2.2. Cultivation under water deficit condition 43
2.3. Tobacco cultivation 43
2.4. Arabidopsis in vitro cultivation 43
2.4.1. Seed surface sterilization 43
2.4.2. Seed germination experiments 44
3. Growth and Physiological parameters of Col 0 and *atesl3.05* mutant leaves 44
3.1. Rosette sampling 44
3.2. Physiological phenotyping of plants 45
3.2.1. Leaf water status: relative water content (RWC) and water content (WC) .. 45
3.2.2. Follow-up of rosette development: Measurement of project rosette area (PRA) 45
3.2.3. Measurements of stomatal conductance (SC) 46
3.2.4. Estimation of osmotic pressure in the cells of leaves 46
3.2.5. Analysis of leaf cell anatomy by light microscopy 46
3.2.6. Soluble sugars extraction and content measurement 47
4. Basic methods in Molecular biology 48
4.1. RNA extraction 48
4.2. Yesat RNA extraction 48
4.3. cDNA synthesis 49
4.4. qPCR 49
4.5. Heat shock transformation of *E. coli* competent cell 49
4.6. *A. tumefaciens* transformation 50
4.6.1. Production of electrocompetent *A. tumefaciens* cells strain EHA105 50
4.6.2. Transformation of *A. tumefaciens,* strain EHA105, competent cells by electroporation 50
4.6.3. Heat shock of *A. tumefaciens* strain GV3101 competent cells 51
4.7. Yeast transformation 51
4.8. Bacterial and yeast colony PCR 51
4.9. Plasmid extraction from bacteria 52
4.10. DNA electrophoresis on agarose gel 52
4.11. Digestion of plasmid DNA 52
5. Mutant characterization 52
5.1. Rapid extraction of genomic DNA 52
5.2. DNA extraction by NucleoSpin® Plant II kit (Macherey-Nage) 53
5.3. Plant genotyping using PCR 53
5.4. DNA amplification by PCR 53
5.5. Generation of double, triple and quadruple mutants 53
5.5.1. Crossing 53
5.5.2. Generation of multiple double mutants atesl 54
5.5.3. Generation of multiple triple mutants *atesl* 54
5.5.4. Generation of the *esl1.02esl3.03esl3.05esl3.07* quadruple mutant 54
6. Cloning of *AtESL1.02*, *AtESL3.03*, *AtESL3.05* and *AtESL3.07* by Gateway® technology for heterologous expression in yeast 54
6.1. Amplification of *AtESL* gene via PCR 54
6.2. Cloning AtESLs PCR products via the TOPO cloning reaction 55
6.3. LR reaction 55
7. Cloning of the AtESL3.05 and AtESL3.03 using restriction enzymes for heterologous expression in yeast 56

7.1. PCR amplification 56
7.2. Cloning of AtESLs coding region into pGemT-easy vector 56
7.3. Digestion and cloning of AtESLs coding region into PDR195 vector 57
8. Functional analysis of AtESLs in yeast: Drop test yeast complementation assay 57
9. Subcellular localization of *AtESL3.05* 58
9.1. Plasmid construction using Gateway® technology 58
9.2. Transient expression in *Nicotiana benthamiana* leaves by agroinfiltration 59
9.3. Isolation of protoplasts from agroinfiltrated tobacco leaves 59
9.4. Confocal microscopy 60
10. Stable transformation in *A. thaliana*: transgenic plants overexpressing *AtESL3.05* gene 60
11. Isolation of vacuoles 61
11.1. Plant material and growth conditions 61
11.2. Vacuoles' isolation - methods 62
12. In *silico* analysis 63
CHAPTER III 64
Early-response-to-dehydration Six-Like (ESL) transporter family: emergence in Charophytes and evolution in the land plants 64
1. Introduction 65
2. Article 1 66
CHAPTER IV 96
Responsiveness of ESL (Early-response-to-dehydration Six-Like) transporter genes to water deficit in *Arabidopsis thaliana* plants 96
1. Introduction 97
2. Article 2 98
CHAPTER V 124
Arabidopsis ESL1.02, ESL3.03, ESL3.05 and ESL3.07 sugars transporters in seed germination and early seedling development in response to endogenous and exogenous cues 124
1. Introduction 125
2. Experimental results 127
3. Results 128
4. Discussion 139
CHAPTER VI 146
Towards the deciphering of transport activity and subcellular localization of AtESL monosaccharide transporters 146
1. Introduction 147
2. Experimental results 149
3. Results 150
4. Discussion 156
CHAPTER VII 160
Conclusion & Perspectives 161
REFERENCES 167
ANNEXES 195

CHAPTER I

INTRODUCTION & LITERATURE REVIEW

Introduction

Life on earth depends on photosynthesis. Photosynthesis is the only biological process that converts the light energy from the sun into chemical compounds, mainly sugars, and oxygen, which is necessary for respiration. Indeed, plants are photosynthetic organisms producing sugars (glucose, fructose, maltose, sucrose), that are essential to primary metabolism and serve as a source of energy, of carbon skeletons for the biosynthesis of other metabolites, but they can also act as signal molecules involved in metabolic signaling and its crosstalk with hormonal pathways. The soluble sugars produced are transiently stored in the form of starch within the chloroplast or imported to the vacuoles for transient or long-term storage. In animals, glucose is the main form of transported sugars and the key source of energy, while, in plants, sucrose is the most commonly transported form and is translocated from source organs to sink organs. This allocation is mediated by phloem sieve tubes, in which long-distance transport takes place. Glucose and fructose are mostly distributed from cell to cell and between organelles at a subcellular level. The process of sugars partitioning requires the activity of sugar transporters, specialized transmembrane proteins, involved in the directed distribution of these solutes at the subcellular and whole-plant levels. Plants, owing to their immobility, have evolved many mechanisms to respond and acclimate to their close environment, for their survival. Physiological, biochemical, and molecular modifications play a crucial role in the adaptation of plants to unfavorable environments, in terms of biotic and abiotic stresses. To improve crop tolerance, it is important to understand how plants respond to environmental cues.

Literature Review

1. Biosynthesis and translocation of sugars in plants

1.1.Sugars biosynthesis

Photosynthesis is the only process that uses light energy to produce sugar and takes place in the chloroplast of leaf mesophyll cells. Photosynthesis happens in two stages. The first stage is the light-dependent reaction where the light is used to produce chemical energy compounds including ATP and NADPH. These two products are then used in the light-independent reaction through the Calvin cycle to generate triose-phosphates (Taiz and Zeiger 1998). The end products of photosynthesis are either used in the chloroplast for starch synthesis or exported to the cytosol for sucrose synthesis (Frommer and Sonnewald, 1995). In higher plants, sucrose is the sugar most commonly found in the phloem (Lemoine, 2000). This is due to its non-reducing nature, which is being unaffected by metabolism (only two types of enzymes can cleave sucrose: sucrose synthase and invertases). Sucrose is therefore very stable, which contributes to its long-distance transport and vacuolar storage (Lemoine, 2000).

1.2.Source organs and sink organs

In higher plants, not all cells can perform photosynthesis (Truernit, 2001). Therefore, plant organs can be divided into two types: source and sink organs (Turgeon, 1989). Source organs such as mature leaves are photosynthetic sites and they produce an excess of carbohydrates, which is exported to other organs of the plants. On the other hand, sink organs such as roots, tubers, and fruits, are non-photosynthetically active and they must import carbohydrates from source organs to support their growth (Turgeon, 1989; Truernit, 2001). Consequently, source organs are defined as net exporters of carbohydrates and sink organs as net importers of carbohydrates (Truernit, 2001). In plants, the patterns translocation of sucrose is from source organs to sink organs via the phloem. Such long-distance transport requires the loading of sucrose in the phloem at the level of source organs and its discharge from the phloem at the level of sink organs.

1.3.Translocation of sugars: Sources to Sinks

1.3.1. Phloem loading

Sucrose synthesized in the mesophyll cells is transported to sink organs via the phloem. Before reaching the phloem, sucrose must first move from mesophyll cells to the parenchyma cells via the symplastic pathway. This movement occurs from cell to cell through

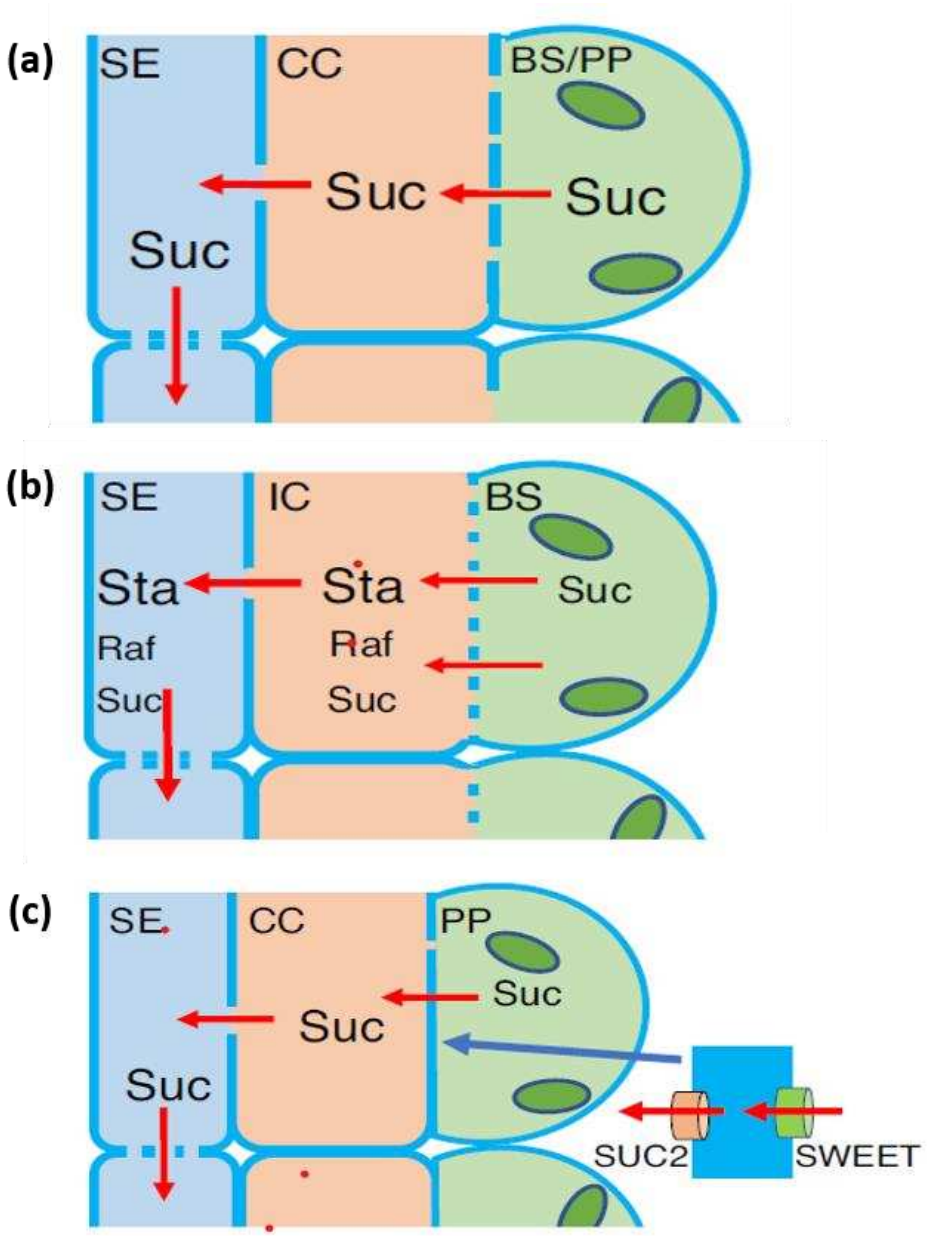

Ch.I-Fig. 1 : The three strategies for sucrose loading into the phloem.
(a) Symplastic sucrose loading. (b) Polymer trapping. (c) Apoplastic sucrose loading. (Suc), (PP), (BS) (CC), (IC), (SE), (Raf) and (Sta) represents the sucrose, the parenchyma cells, the bundle sheath cells, the companion cells, the sieve element, the intermediary cells, the raffinose, and the stachyose, respectively. Adapted from Zhang and Turgeon (2018).

plasmodesmata according to the concentration gradient (Lalonde et al., 2003). The sucrose is then loaded into the sieve elements and companion cells, which represent a functional unit, called a sieve element-companion cell complex (CC-SE) (Taiz and Zeiger 1998). Two transport pathways are involved in sucrose loading: the symplastic pathway and the apoplastic pathway (Kühn et al., 1999; Truernit, 2001).

In the symplastic pathway, sucrose is passively moved from parenchyma to the companion cells via plasmodesmata. Such transport requires a high number of plasmodesmata between the parenchyma cells and the CC-SE and a high concentration of sucrose in the mesophyll cells (Ch.I-Fig. 1a). Plants of the *Cucurbitaceae*, *Onagraceae*, and *Oleaceae* families, the process of polymer trapping is prevalent. In this process, sucrose loaded into parenchymal cells is passed to specific companion cells, known as intermediary cells, via plasmodesmata, and then sucrose is converted into raffinose and stachyose (RFOs: raffinose family oligosaccharides (RFOs) (Ch.I-Fig. 1b). These molecules are larger than sucrose and cannot return to the mesophyll cells via plasmodesmata (Rennie and Turgeon, 2009; Zhang and Turgeon, 2018).

On the other hand, in the case of the apoplastic pathway, sucrose is transferred from the parenchyma cells to the apoplast, defined as the extracellular cell wall space (Gottwald et al., 2000). In *Arabidopsis*, this efflux involved the presence of two facilitators: *AtSWEET11* and *AtSWEET12* (discovered by Chen et al., 2012). Consequently, the two transporters do not require energy to function. Once, in the apoplast, the sucrose is then loaded into the companion cells of the phloem. Since the concentration of sucrose in the phloem is higher than in the apoplast, active transport is required. This active transport is mediated by sugar transporters located in the plasma membranes of the companion cells (Gottwald et al., 2000; Sauer, 2007). These transporters are known as sucrose/proton symporters (Gottwald et al., 2000) called SUC or SUT proteins for Sucrose Transporters (Sauer, 2007). SUC have to load the sucrose against its concentration gradient using a proton motive force generated by proton pumps (H^+-ATPases) (Ch.I-Fig. 1c) (Gottwald et al., 2000; Sauer, 2007). In *Arabidopsis thaliana*, the active transport is mediated by a sucrose-H^+- symporters called SUC 2 (Truernit and Sauer, 1995; Gottwald et al., 2000), located in the plasma membrane of the companion (Stadler and Sauer, 1996). However, in *Solanaceous* species such as tobacco, potato, and tomato, the sucrose transporter SUT1 is located in the plasma membrane of the sieve elements (Kuhn, 1997). The loaded sucrose reaches the sieve tubes *via* many plasmodesmata, which connect the companion cells to the sieve tubes.

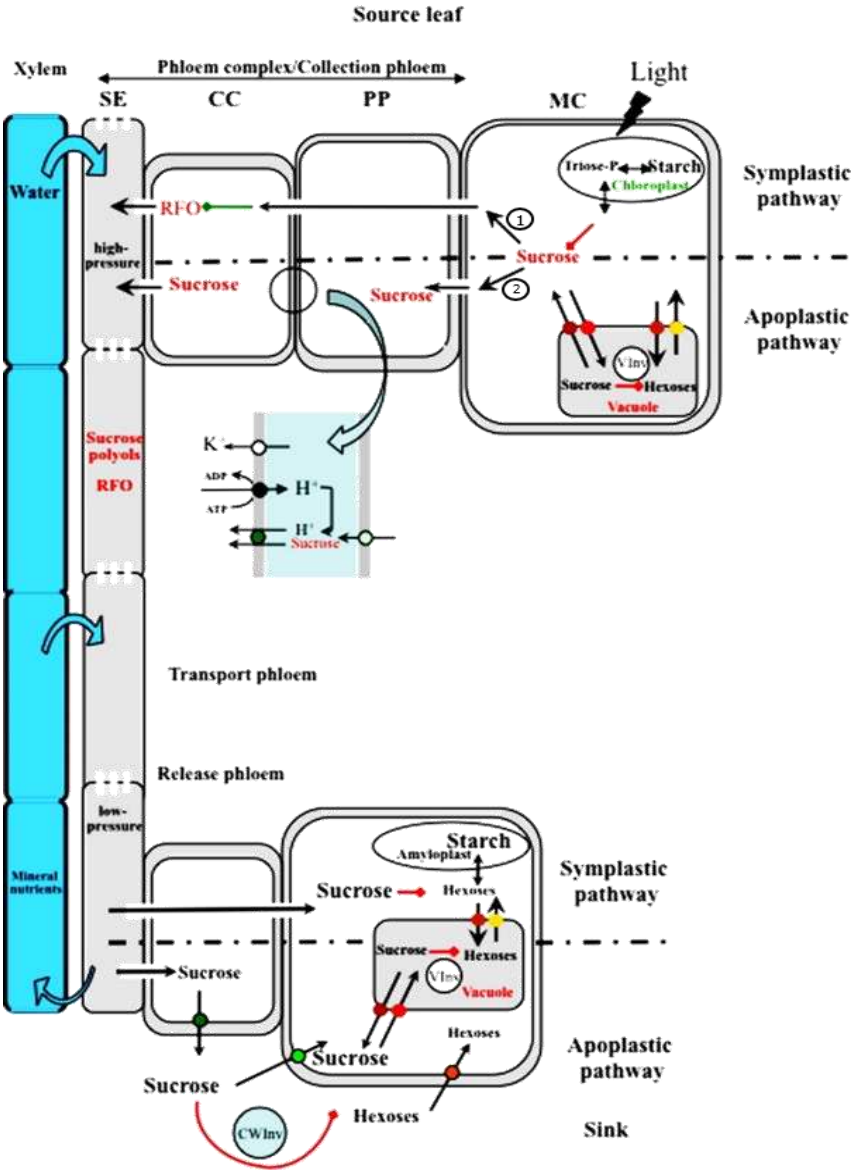

Ch.I-Fig. 2 : Schematic diagram showing the long-distance transport of sucrose from source to sink organs. In plants, sucrose is produced in the mesophyll cells and is considered as the main form of sugar transported in the phloem. Several transport steps are implicated in the long-distance transport. In step one, sucrose moves from mesophyll cells (MC) to parenchyma cells (PP) in the plasmodesmata. In step two, sucrose is loaded from PP into the sieve element-companion cell complex (SE/ CC) *via* two possible pathways. In the symplastic pathway, sucrose is transported from PP to SE/CC via plasmodesmata. In some species, sucrose is converted to large molecules (RFOs: Raffinose Family oligosaccharides) in the CC cells. These larger molecules are transferred and accumulated in sieve tubes (SE). In the apoplastic pathway, sucrose enters the apoplast between the PP and the CC *via* facilitators that belong to the SWEET family (pale green circle) and is then exported to the CC by SUT/SUC (green circle) by active sucrose/proton symporters. The proton pump (H+-ATPases) (black circle) produces proton motive force as source energy. Finally, sucrose reaches the sieve tubes through many plasmodesmata, which connect the CC to the sieve elements. In both loading paths, once sucrose is loaded in the sieve tubes hydrostatic pressure is generated, which attracts water from the xylem. This enables the translocation of sucrose from source organs to sink organs by mass flow. Upon its release from the phloem, sucrose is either unloaded in the sink organs *via* the symplastic pathway or *via* the apoplastic pathway. In the latter case, sucrose is unloaded into the apoplast by a sucrose transporter, SUT1/SUC2 type (green circle). Sucrose released in the apoplast is imported by a sink sucrose transporter of the same SUT1/SUC2 (light green circle) or can be hydrolyzed by a cell-wall invertase (CWInv) to produce glucose and fructose. Hexoses are taken up by specific hexose transporters localized at the plasma membrane (orange circle) or on the tonoplast (yellow and brown circles). Sucrose in sink organs can be metabolized to support growth and development, stored as starch in amyloplasts, or stored into the vacuoles (red circles), where it can be hydrolyzed by vacuolar invertases (VInv) (Lemoine et al., 2013).

1.3.2. Long-distance transport

Once sucrose is loaded into the phloem sap, it is translocated by mass flow from source organs to sink organs following the pressure-flow model proposed by Münch 1930. This model states that the translocation of the photosynthates in the sieve elements is driven by a pressure (or turgor) gradient between the sources and sinks organs (De Schepper et al., 2013). The pressure gradient is generated by the high turgor pressure in the sieve elements of the source organ, due to the massive accumulation of photosynthates (loading) and by the low turgor pressure in the sieve elements of the sink organ due to the release of photosynthates (unloading) (De Schepper et al., 2013, Taiz and Zeiger 1998). Moreover, the sieve tubes are channels that are not tightly closed, so sucrose can be unloaded or retrieved along the translocation pathway to supply the surrounding tissues (axial sink) (Bel, 2003).

1.3.3. Phloem unloading

In sinks, the imported sucrose moves out from the sieve elements to supply the surrounding tissues. The phloem unloading occurs via symplastic and/or apoplastic pathways depending on the sink types (Patrick, 1997). Furthermore, phloem unloading relies also on the stage of development of the sink organs. Indeed, in 1995 Ruan and Patrick, showed that during the development of the tomato fruit, the phloem unloading switches from the symplasmic pathway at early stages to the apoplastic pathway during the late stage of fruit development (Ruan and Patrick, 1995). Moreover, in the apoplastic unloading pathway, sucrose released into the apoplast can either directly enter the receiver cells by sucrose transporters (SUC), or it can be cleaved into glucose and fructose by cell wall-bound invertases. Hexoses are then entered the sink cells *via* hexose transporters (Büttner and Sauer, 2000; Sauer, 2007). After that, sucrose or hexoses are either metabolized to supply energy and carbon skeletons for growth and development of the sink organs, or they are stored as sucrose in sugar beet (*Beta vulgaris*) and grapevine (*Vitis vinifera*), or as starch in potato (*Solanum tuberosum*) tubers (Lemoine, 2000; Ludewig and Flügge, 2013). Ch.I-Fig. 2 resumes the long-distance transport of sucrose from the source- to the sink organs.

2. State of the art of Sugar Transporters

Complete sequencing of the genome of *Arabidopsis thaliana* has showed the presence of several sugar transporter genes. Two different families of sugar transporters have been identified: the disaccharide transporters (Williams et al., 2000) and the monosaccharide transporters (Büttner, 2007). These two families belong to the Major Facilitator Superfamily –

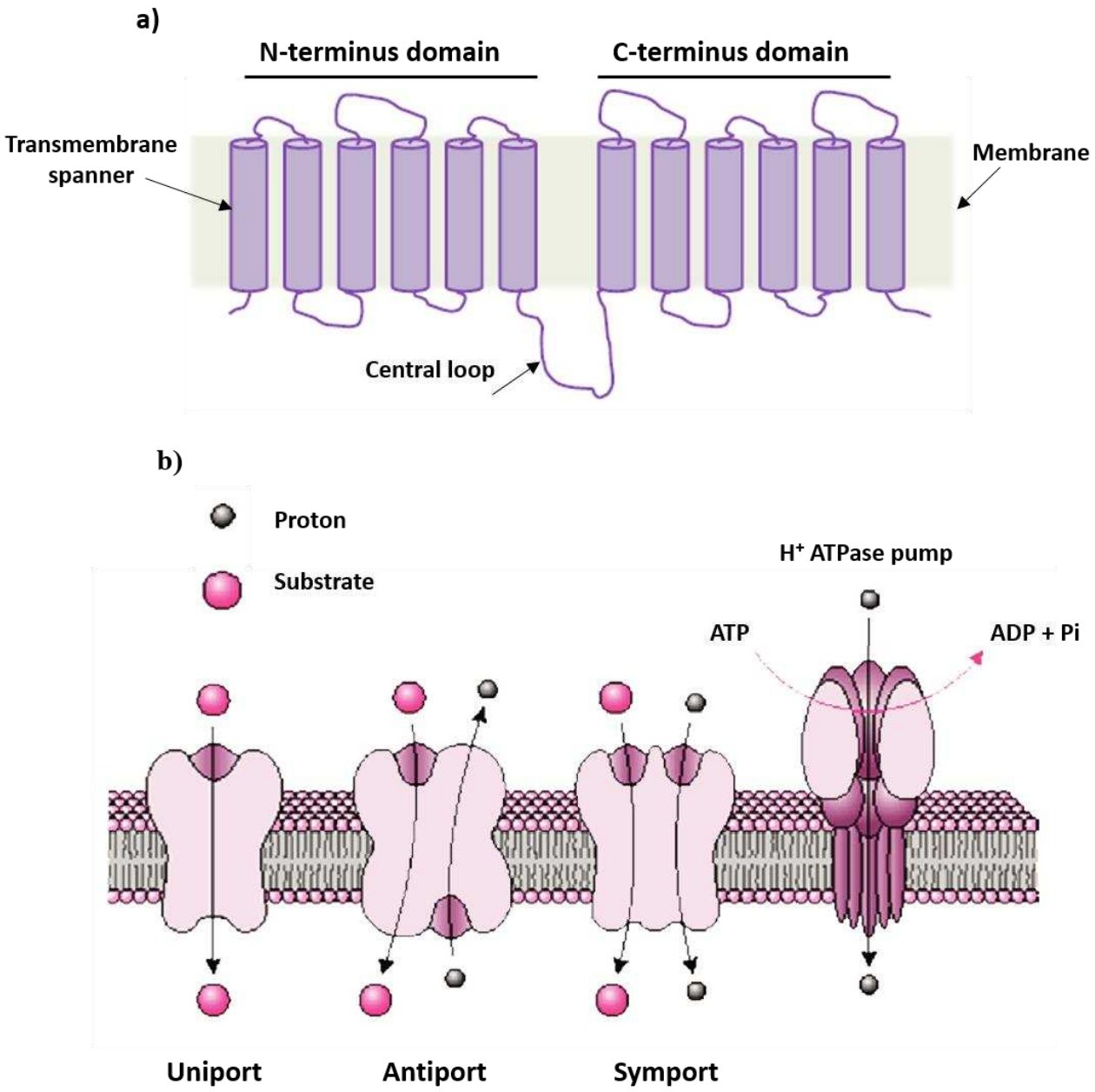

Ch.I-Fig. 3 : Structure and mode of action of transporters belonging to the Major Facilitator Superfamily.

(a) General representation of the structure of a Major Facilitator Superfamily Transporter.

(b) Uniporters translocate substrate according to their gradient. Symporters transport substrates into the same direction, while antiporters transport substrates in the opposite direction. Symporters and antiporters both use electrochemical gradient (proton-dring force created by H^+ ATPase pumps) to move substrates (adapted from Afoufa-Bastien, 2010).

MFS, (Marger and Saier, 1993; Reddy et al., 2012). Later, a new family of sugar transporters, named SWEETs, has been discovered (Chen et al., 2010a). Sugar transporters play an essential role in the carbohydrate allocation, which is a process of sugar transport and redistribution from photosynthetic source-organs to nonphotosynthetic sink-organs (Bush, 1999; Julius et al., 2017).

2.1.The Major Facilitator Superfamily

2.1.1. Overview

The major facilitator superfamily (MFS) is the largest recognized superfamily of secondary transporters in the life kingdom (Pao et al., 1998; Reddy et al., 2012; Yan, 2013). The MFS comprises 76 families that transport various types of substrates (e.g., carbohydrates, lipids, amino acids, peptides, vitamins, drugs, ions, and other molecules). The majority of MFS members possess a twelve transmembrane α-helices arranged into two groups of six transmembrane segments linked by a central loop (Ch.I-Fig. 3a) (Pao et al., 1998; Lemoine, 2000; Reddy et al., 2012; Yan, 2013). Mechanistically, MFS transporters transport their substrates across the membrane by three different kinetic mechanisms: uniporters, symporters, and antiporters. Uniporters translocate one type of substrate depending on the substrate gradient. Symporters transport two or more substrates in the same direction. Antiporters translocate two or more substrates in the opposite direction. Both symporters and antiporters use the electrochemical gradient of one substrate as a driving force (Ch.I-Fig. 3b) (Pao et al., 1998; Law et al., 2008). The MFS transporters that transport sugars belong to the subfamily known as Sugar Porter (SP) (Yan, 2013), which is classified into the disaccharide transporters (DST) family and the monosaccharide transporters (MST) family. In *Arabidopsis*, the DSTs are represented by the sucrose transporters (SUC), for whom nine genes have been identified, named from *AtSUC1* to *AtSUC9* (Sauer, 2007). Contrary to DST, in *Arabidopsis* the MST family displays 53 genes, divided into seven subfamilies (Büttner, 2007).

2.1.2. Sucrose Transporters: SUC

Sucrose is known as a very stable molecule which contributes to its long-distance transport from source organs to sink organs. Sucrose transporters play an essential role in phloem loading and unloading where they act as sucrose/proton symporters in plants and may have two nomenclatures according to the literature; SUT (Sucrose Transporters)

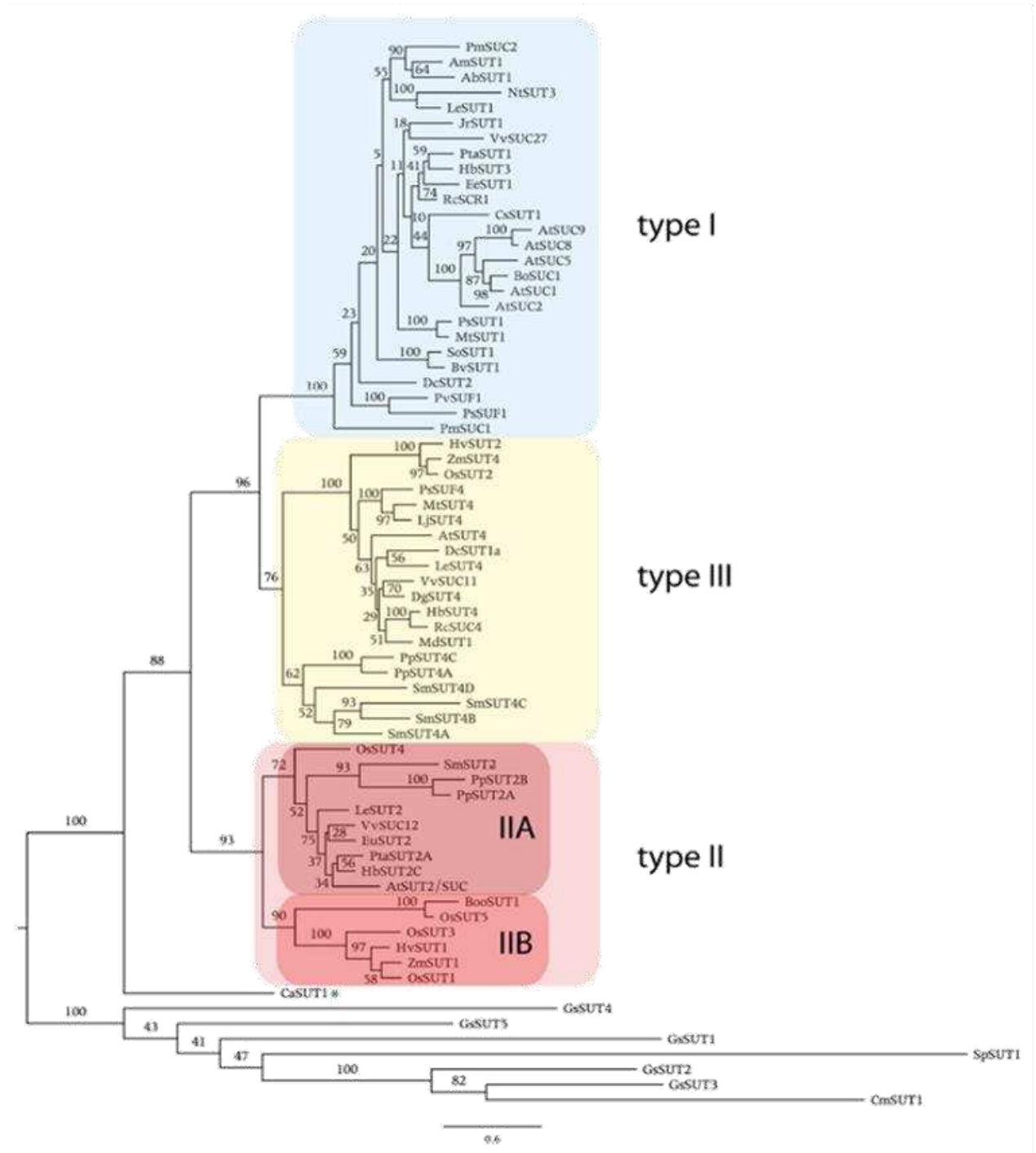

Ch.I-Fig. 4 : Phylogenetic tree defining the distribution of plant sucrose transporters and homologs (Reinders et al, 2012)

or SUC (Sucrose carriers) (Sauer, 2007; Ayre, 2011). Several phylogenetic analyses have been conducted to classify the sucrose transporters. The first phylogenetic analysis classified SUTs into three types or clades (Aoki et al., 2003; Lalonde et al., 2004), and soon after they were divided into four groups according to Sauer (2007). Lately, with the increasing number of new SUTs sequences, group one, which is unique to monocotyledonous species, was divided to five different groups (Braun and Slewinski, 2009; Kühn and Grof, 2010). In this manuscript, the phylogenetic analysis performed by Reinders et al. (2012), is described. According to their analysis, SUTs are classified into three phylogenetic groups: type I, type II, and type III (Ch.I-Fig. 4).

- **Type I SUTs**

Type I contains only sequences from dicot species, including five SUC transporters of *Arabidopsis*, AtSUC 1, 2, 5, 8 and 9 and two additional, AtSUC6 and AtSUC7, which are not included in their study since their encoding genes are considered as pseudogenes (Sauer et al., 2004). *AtSUC* 1 is expressed in the flower organs such as pollen, where the encoded protein is involved in the pollen germination (Stadler et al., 1999; Sivitz et al., 2008), but also in trichomes and roots (Sivitz et al., 2007). Another member of the type I, *AtSUC2,* is expressed in the companion cells of the leaves and this transporter is implicated in the phloem loading. Remarkably, a study conducted by Gottwald et al. (2000), reported that *atsuc2* homozygous mutant shows an extremely stunted growth. *AtSUC5* is highly expressed in seeds specifically in the endosperm and *atsuc5* mutant showed an alteration of fatty acid concentration during early seed development and retardation in embryo development (Baud et al., 2005). Moreover, *AtSUC6* is expressed in the reproductive tissues (Rottmann et al., 2018b). Since AtSUC6 and AtSUC7 are considered as aberrant proteins, a recent study confirms that *AtSUC7* is a non-functional pseudogene and revealed that AtSUC6 can transport sucrose and maltose across the plasma membrane (Rottmann et al., 2018b). Lastly, there are A*tSUC8* and *AtSUC9* which are expressed in floral tissues (Sauer et al., 2004) and *atsuc9* mutant has been reported to exhibit earlier flowering under short-day conditions (Sivitz et al., 2007).

- **Type II SUTs**

Type II includes sequences of dicot and monocot species. This group can be split into two sub-groups IIA and IIB. Type IIA proteins are larger (587 amino acids) than type IIB proteins (523 amino acids), owing to the presence of a longer central cytoplasmic loop (Reinders et al., 2012).

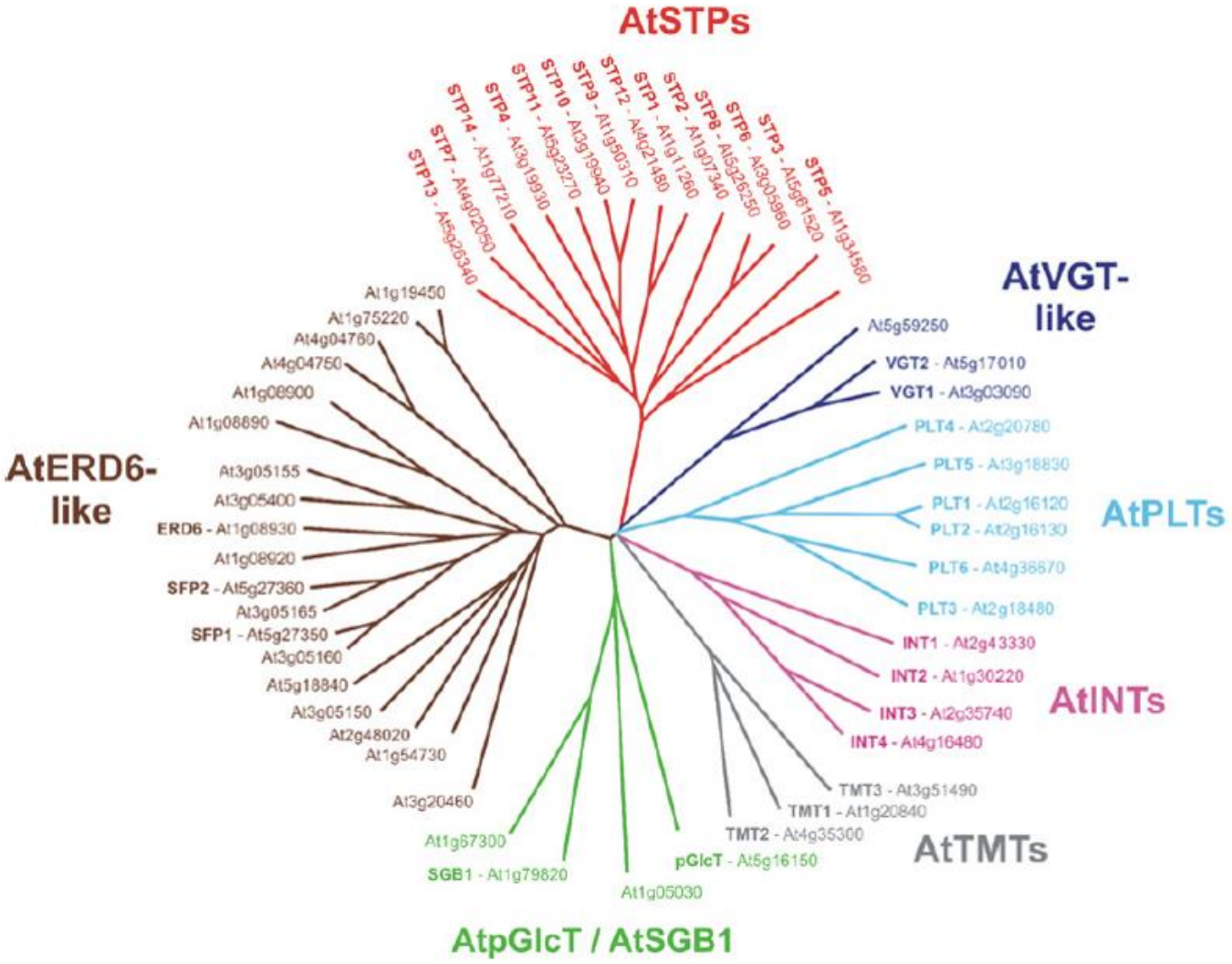

Ch.I-Fig. 5 : Phylogenetic tree of the monosaccharide transporter family (MSTs) from *A. thaliana*.
The genome of *A. thaliana* has 53 MSTs genes divided in seven subfamilies (Büttner, 2007)

AtSUT2/AtSUC3 transporter belongs to the sub-group IIA and is mainly expressed into sinks such as guard cells, pollen, root tips, and others. AtSUT2/AtSUC3 is localized in the sieve elements of the phloem and might most likely be responsible for the retrieval of sucrose in long-distance transport as suggested by Meyer et al. (2004).

- **Type III SUTs**

Type III also contains sequences from dicot and monocot species, including AtSUC4 from *Arabidopsis*. The expression of *AtSUC4* is limited to the stele of the root, developing anthers and meristems of the aerial parts (Schneider et al., 2012). Furthermore, using the GFP as reporter gene, AtSU4-GFP was exclusively localized in the tonoplast (Endler et al., 2006; Schneider et al., 2012). AtSUC4 has also been shown to participate in the release of sucrose from the vacuole to the cytosol (Schulz et al., 2011; Schneider et al., 2012).

2.1.3. Monosaccharide transporters : MST

When sucrose is released into the apoplastic space of the sink organs, it can be transported by SUTs, or cleaved by cell wall invertases to produce hexoses (glucose and fructose), which are then carried by monosaccharide transporters. These transporters play a role at the sub-cellular level by controlling the distribution of glucose and fructose among cell compartments. Although monosaccharide transporters do not participate directly in the long-distance transport, their indirectly role affect the carbon allocation and sugar flux at the whole plant level (Büttner, 2007; Slewinski, 2011). In *Arabidopsis*, the MST family encompasses 53 genes clustered into 7 subfamilies: two large and five small subfamilies (Ch.I-Fig. 5). The two large subfamilies are STP (sugar transport proteins) and ESL (Early Response to Dehydration Six-Like). The five small subfamilies are pGlucT/SBG1 (plastidic glucose transporter/Supressor of G protein beta1), INT (inositol or cyclic polyol transporters), PMT (linear polyol transporters, formerly PLT), TMT (tonoplastic monosaccharide transporters), and VGT (vacuolar glucose transporters) (Slewinski, 2011).

- **The STP subfamily**

In *Arabidopsis*, the STP subfamily composed of fourteen members (AtSTP1-14) is the best characterized one. All studied AtSTPs have been localized to the plasma membrane and act as hexoses /H^+ symporters (Büttner, 2007). In higher plants, the first identified hexose transporter was AtSTP1 (Sauer et al., 1990), which is expressed in germinating seeds and roots of seedlings (Sherson et al., 2000). In 2003 Stadler et al. showed that *AtSTP1* is detected in several organs, such as guard cells of cotyledons, rosette leaves, sepals, ovaries, and stems

(Stadler et al., 2003). Interestingly, four *AtSTPs* (2, 6, 9, and 11) are expressed mainly in pollen at different stages of development (Büttner, 2007; Büttner, 2010). *AtSTP4*, *AtSTP10*, and *AtSTP7* which are all expressed in pollen and root tissues (Truernit et al., 1996; Rottmann et al., 2016; Rottmann et al., 2018a). *AtSTP12* and *AtSTP8* are expressed in reproductive organs such as ovules, *AtSTP12* is also detected in root tissues (Rottmann et al., 2018a). *AtSTP* expression has been found for *AtSTP5* in the seed coat (Büttner, 2010), for *AtSTP14* and *AtSTP3* in source leaves, and for *AtSTP14* in the seed endosperm (Büttner, 2007; Poschet et al., 2010). The expression of *AtSTP13* is detected in the vascular tissue of emerging petals (Norholm et al., 2006).

- **The ESL subfamily**

In a previous thesis work realized by Lucie Slawinski (2017), an evolutionary genomics approach was performed to study the evolution of ESL (Early Response to Dehydration Six-Like) transporters in the genome of 60 species representative of the plant kingdom (from algae to Angiosperms). Phylogenetic analysis of the 520 identified protein sequences showed that the ESL transporters fell into three major groups of ESL (ESL1, ESL2, and ESL3). Based on their phylogenetic position, a new nomenclature was suggested to name these transporters. The nomenclature proposed by Lucie is as follows: for example, the name ESL1 meaning that this transporter, belonging to group ESL1, then an additional number was added when several members were present within the same group (e.g. ESL1.01, ESL1.02).

In *Arabidopsis*, the nineteen ESL transporters constitute the largest subfamily in the MSTs family. To date, only six AtESL members have been characterized. The first evidence for the existence of this subfamily was derived from experiments performed under dehydration conditions. In 1994 Kiyosue et al. using the differential hybridization technique demonstrated the presence of twenty-six clones that strongly hybridize with cDNA prepared from 4-weeks old plants subjected to dehydration for one hour (Kiyosue et al., 1994). The twenty-six cDNA clones were divided into sixteen groups, from ERD1 to ERD16 by Southern blot hybridization (Kiyosue et al., 1994).

Four years later, one of these ERD clones, ESL3.08 (also called ERD6), which belongs to group ESL3c, was characterized by Kiyouse et al.,1998. The cDNA of *AtESL3.08* consists of 1741bp in length and encodes a protein of 496 amino acids with a predicted molecular mass of 54 kDa (Kiyosue et al., 1998). Sequence analysis of ESL3.8 showed that it encodes a sugar transporter according to several features, such as the presence of 12 transmembrane domains and a central hydrophilic region. In addition, the presence of PESPRXL and PETKGXXXE motifs at the end of the 6th and 12th transmembrane domains, respectively

(Kiyosue et al., 1998). These features are common for sugar transporters belonging to the MFS superfamily. Northern blot analysis showed that the *AtESL3.08* mRNA accumulates strongly after one and two hours of dehydration or drought stress, as well as under cold (4°C) or high salinity (250 mM NaCl) treatment, whereas the *AtESL3.08* mRNA was decreased after five hours of ABA treatment (100 µM) (Kiyosue et al., 1998; Yamada et al., 2010). The qRT-PCR analysis revealed that the expression level of *AtESL3.08* was the same in leaves and roots, however, under high salinity (125 mM NaCl) or ABA (100 µM) conditions, its expression decreased in leaves, whereas, it remained unchanged in roots (Yamada et al., 2010). Transgenic lines expressing *GUS* or *TM-GFP* (GFP located in the membrane and fused with the N-terminal part of *AtSTP9*) under the control of the *AtESL3.08* promoter, revealed the activity of the promoter in sepals and in roots, especially in the cortex cells of the latter (Yamada et al., 2010). Although the function of the AtESL3.08/AtERD6 is not yet elucidated, it could be involved in the redistribution of sugars to protect plant cells from the detrimental effects of dehydration (Kiyosue et al., 1998).

Thereafter, in 2001 Quirino et al. identified two genes duplicated in tandem on chromosome 5, *AtESL3.13* (also named *AtSFP1)* and *AtESL3.14* (also named *AtSFP2)* (Sugar-porter Family Protein), which belong to group ESL3c. These two genes displayed different expression patterns during leaf development. Northern blot analysis showed that the expression of *AtESL3.13* was detected in seedlings nine days after germination, but not in mature plant organs (leaves, flowers, flower buds, stem, and roots), while *AtESL3.14* was expressed in all tested plants organs, and in seedlings. Further analysis showed that only *AtESL3.13* is induced during leaf senescence but the expression of *AtESL3.14* remains stable during this process. In addition, promoter analysis of *AtESL3.13* and *AtESL3.14* was realized using the reporter gene, GUS, and the results obtained concur well with RNA gel blots results. Therefore, *AtESL3.13* and *AtESL3.14* appeared to be differently expressed, spatially and temporally (Quirino et al., 2001). It should be noted that nothing is still known about the transport activity of these two sugar carriers.

The first member characterized within the ESL subfamily is ESL3.07, which is also called ESL1 in some publications (Yamada et al., 2010) and belonged to group ESL3c. AtESL3.07 and its homology AtESL3.08/ERD6, are duplicated in tandem and localized on chromosome 1. These genes respond differently to various abiotic stresses. Northern blot analysis showed that the expression of *AtESL3.07* was induced after one hour by drought, high salinity (250 mM NaCl), and ABA (100 µM) treatment and showed a high induction after 5

hours under these stresses. In addition, the qRT-PCR analysis revealed that the expression of *AtESL3.07* was higher in the roots than in the leaves under normal conditions, while the expression of *AtESL3.07* was strongly induced in the roots than in the leaves under high salinity and ABA treatment (Yamada et al., 2010). The *AtESL3.07* promoter was fused to GUS or TM-GFP reporter genes to identify its promoter activity. The analysis revealed that the promoter activity of *AtESL3.07* was detected in aerial parts and roots as *AtESL3.08* promoter activity. Furthermore, the promoter activity of *AtESL1* was detected in pericycle and xylem parenchyma cells of roots and within the root endodermis (Yamada et al., 2010). Taken together, these results indicate that the physiological functions of AtERD6 and AtESL1 may be different, as suggested by Yamada et al., 2010. Using the GFP reporter gene in protoplasts as well as in transgenic *Arabidopsis* plants, it has been shown that the AtESL3.07 protein is primarily localized at the tonoplast *via* an N-terminal LXXXLL motif, which is present in most of the transporters within the ESL subfamily (Yamada et al., 2010). The characterization of the transport activity of AtESL3.07 was carried out using the transgenic tobacco BY-2 cells expressing a modified AtESL3.07 protein in which the tri-leucine was mutated into a tri-alanine in a way to shift its localization from the tonoplast to the plasma membrane. This analysis revealed that AtESL3.07/ESL1 is a low-affinity glucose transporter with a high Km value (102.2 mM). In the stated study, the authors concluded that AtESL3.07/ESL1 acts as a facilitator because the addition of protonophore (CCCP) does not affect its uptake activity (Yamada et al., 2010).

One year later, another member of the ESL subfamily, the AtESL1.02 (also known as AtERDL6), which belongs to group ESL1, was characterized by (Poschet et al., 2011). During plant development, *AtESL1.02* was characterized by a wide expression pattern in photosynthetic tissues as well as non-photosynthetic tissues as sink organs, particularly, its expression was marked in organs and developmental phases with high metabolic turnover, like seed germination, abscission, wound responses, and others (Poschet et al., 2011). The localization of AtESL1.2-GFP constructs was tested by transient expression in *Arabidopsis* and tobacco (*Nicotiana benthamiana*). The results showed that AtESL1.02 was localized at the tonoplast in the protoplasts of *Arabidopsis* and tobacco. Poschet and coworkers demonstrated that the *AtESL1.02* expression is regulated in conditions that trigger the mobilization of vacuolar carbohydrate storage. Indeed, the expression of *AtESL1.02* was induced in conditions that need the release of glucose from the vacuole, such as darkness, heat stress, and wounding leaves. On the other hand, the *AtESL1.02* expression was dropped under cold stress and external glucose supply during which glucose accumulates in the vacuole. However, the

atesl1.02 mutant showed a raised vacuolar glucose content (more than 90 %) compared to the wild type (86%). Furthermore, in the *atesl1.02* mutant, the glucose content was slowly released as compared to the wild type during a rewarming phase after cold treatment (passage from 4°C to 22°C) and the seed weight increased by 10% (Poschet et al., 2011). Conversely, *Arabidopsis* lines overexpressing *AtESL1.02* had lower glucose levels than wild-type plants (Poschet et al., 2011). Taken together, these data indicate that AtESL1.02 functions as a vacuolar glucose exporter, as assumed by Poschet et al., 2011. The transport activity of AtESL1.02 has been studied using the patch-clamp technique on isolated vacuoles prepared from the double mutant *attmt1/attmt2* and the triple mutant *attmt1/attmt2/aterdl6* (Klemens et al., 2014). It has been suggested that AtESL1.02/AtERDL6 may acts as a H^+/glucose symporter by exporting glucose from the vacuole to the cytosol (Klemens et al., 2014).

The apple MdERDL6-1, an orthologue of ERDL6 in *Arabidopsis*, was recently identified by (Zhu et al., 2021). The authors showed that the expression level of *MdERDL6-1* was high in fruits and that its encoded protein seems to be localized at the tonoplast by transient assays in *Arabidopsis* and apple calli protoplasts. Using yeast as a heterologous expression, the authors succeed to decipher the transport activity of MdERDL6-1. They showed that MdERDL6-1 acts as an H^+/glucose symporter with a low affinity for glucose (Km=21.7 mM). This suggested that MdERDL6-1 function similarly as the ERDL6 in *Arabidopsis*, to export glucose from the vacuoles to the cytosol. Interestingly, in their study, the authors showed that the overexpression of MdERDL6-1 leads to an increase rather than a decrease in the sugar levels in apple and tomato leaves and fruits. Also, the overexpression of *MdERDL6-1* induces the expressions of *MdTST1/2* and *SlTST1/2*. TSTs are well-known to import sugars into the vacuole, and thus the high concentration of sugars in the overexpression lines is due to the induction of *TSTs*. This suggested that the MdERDL6-1, TST1, and TST2 work coordinately to maintain vacuolar sugar hemostasis (Zhu et al., 2021).

The last characterized member of the ESL subfamily is AtESL2.01 (also called AtZIF2), which belongs to group ESL2a. The promoter region from *AtESL2.01* was cloned and fused to the reporter gene (GUS) and the promoter activity of *AtESL2.01* was detected to remain active in some plant organs, such as in leaf mesophyll cells, flower organs, and was especially strong in root tissues, such as the primary and lateral roots and at the root tip (Remy et al., 2014). Furthermore, the promoter activity of *AtESL2.01* was analyzed using the GFP reporter gene, and this revealed that *pAtESL2.01* confers gene expression in the endodermis and the cortex of the primary root tip (Remy et al., 2014). Moreover, the subcellular

Ch.I-Table 1 : Different features of the six *AtESL* genes.

(Adapted from: Kiyosue et al., 1994 ; Yamada et al., 2010 ; Quirino et al., 2001 ; Poschet et al., 2011 ; Klemens et al., 2014 ; Remy et al., 2014 ; Slawinski, 2017)

Designation	Accession number	Phylogentic group	Sub-cellullar localisation	Tissue localization	Transport activity	Environmental factors
ESL3.08/ERD6	At1g08930	ESL3c	n.d.	Shoots, sepals of flowers, epidermis and cortex cells of roots	n.d.	+ Dehydration, cold, salt stress − ABA
ESL3.13/SFP1	At5g27350	ESL3c	n.d.	Young seedlings (stomates, at the end of the cotyleond)	n.d.	+ Leaf senescence
ESL3.14/SFP2	At5g27360	ESL3c	n.d.	Youn seddlings (vascular of cotyledons), mature plants (stems, flowers)	n.d.	− Leaf senescence
ESL3.07/ESL1	At1g08920	ESL3c	Tonoplast	Shoots, sepals of flowers, pericycle and xylem parenchyma cells of roots , root endodermis	Hexose transport (glucose, fructose, galactose…): Facilitator	+ Dehydration, ABA, Salt stress
ESL1.02/ERDL6	At1g75220	ESL1	Tonoplast	Leaves, flowers, roots	Vacuolar glucose exporters: symport H+/glucose	+ Darkness, heat stress, wounding − Cold stress, external glucose supply
ESL2.01/ZIF2	At2g48020	ESL2a	Tonoplast	Leaf mesophyll cell, flowers, roots	n.d.	+ Zinc

Abbreviations: AGI, *Arabidopsis* Genome Initiative; n.d.: not defined; (+): induction of gene expression; (−): repression of gene expression.

localization of AtZIF2 -YFP or GFP was determined by transient and stable assays in *Arabidopsis* protoplasts or root tips. This analysis revealed that the transporter AtESL2.01 was mainly localized at the tonoplast. In response to a high concentration of zinc (Zn), the expression of two splicin variants of *AtESL2.01* was induced in *Arabidopsis* roots, while the loss of function of *AtESL2.01* causes plant hypersensitivity to Zn, whereas its overexpression enhances plant tolerance to Zn (Remy et al., 2014). Taken together, AtESL2.01/AtZIF2 mediates the root vacuolar sequestration of zinc to avoid its translocation to the shoot and thereby enhances plant tolerance to heavy metals (Remy et al., 2014).

More recently, Breia et al., 2020 showed that the grapevine *VvERD6l13* was induced in the grape berries upon infection by a necrotrophic or biotrophic pathogen such as *botrytis cinerea* and *Erysiphe necator*, respectively. So far, the characterized ESL sugar transporters are localized at the tonoplast, unexpectedly the VvERD6l13 was localized at the plasma membrane in the tobacco epidermal cells. Using yeast as a heterologous system, the VvERD6l13 functions as an H+/sucrose symporter with low affinity (Breia et al., 2020). Moreover, Desrut et al., 2020 showed that six *ESL* genes were differentially regulated in the presence of PGPR (plant growth promoting rhizobacteria). Indeed, three *ESL* genes, *ERD6-like7/ESL2.01*, *ERD6-like12/ESL3.10*, and *ERD6-like16/ESL2.03*, as well as *ERD6-like18/ESL3.14*, were down-regulated in the shoots and roots, respectively. And, it was shown that only *ERD6-like13/ESL3.04* and *ERD6-like15/ESL3.03* were up-regulated in the roots in the response of PGPR (Desrut et al., 2020).

The characterization of the six AtESL is summarized in the Ch.I-Table 1.

- **The pGlucT/SBG1 subfamily**

In *Arabidopsis*, four genes code for the transporters of the pluck/SBG1 subfamily. One of these genes, AtpGlucT acts as a translocator of glucose from the chloroplasts (Weber et al., 2000). Cho et al. (2011) demonstrated that in *Arabidopsis* leaves, AtpGlucT interacts with the maltose transporter (MEX1) to export products of starch degradation from the chloroplast to the cytosol, thereby regulating plant growth and development. Another member of this subfamily, AtSGB1, has been characterized as a hexose transporter, which is localized in the Golgi membrane (Wang et al., 2006).

- **The INT subfamily**

The INT subfamily comprises four members in *Arabidopsis*, but only three of them encode functional proteins, while the fourth member, *AtINT3*, is considered as a pseudogene. AtINT2 and AtINT4 are targeted to the plasma membrane and function as H^+/myoinositol symporters (Schneider et al., 2006; Schneider et al., 2007).

AtINT4 is expressed in the pollen and phloem companion cells of source leaves (Schneider et al., 2006) while the *AtINT2* promoter/reporter gene is weakly expressed the anther tapetum and leaf vasculature (Schneider et al., 2007). Unlike the two aforementioned, AtINT1 is localized to the tonoplast,and Schneider et al., 2008 suggested that AtINT1 is implicated in the export of myoinositol produced from the degradation of inositol compounds contained in the vacuolar lumen (Schneider et al., 2008).

- **The PMT subfamily**

Polyols (also called sugar alcohols) are reduced forms of aldoses and ketoses, which act as osmotic active solutes in plant cells, where they accumulate under abiotic stresses such as drought, salt stress, or cold (Noiraud et al., 2001a). In celery, AgMaT1 was identified as the first mannitol transporter by a heterologous system (Noiraud et al., 2001b). *A. thaliana* has 6 PMT members sharing homology with the polyol transporters (Büttner, 2007). The physiological function is difficult to attribute to this group in *Arabidopsis*, which translocate sucrose in its phloem but not polyols (Klepek et al., 2005). Of these six genes, only three genes have been characterized: *AtPMT1*, *AtPMT2*, and *AtPMT5*. AtPMT5 was characterized as a low-affinity H^+/symporter and it transports a wide variety of sugars including cyclic and linear polyols (sorbitol, xylitol) as well as monosaccharides (hexoses, and pentoses) (Klepek et al., 2005; Reinders et al., 2005; Klepek et al., 2010). *AtPMT5* is expressed in roots, in the vascular tissue of leaves and in floral organs (Klepek et al., 2005). AtPMT1 and AtPMT2 were recently characterized as fructose and xylitol / H^+ symporters and are found in pollen plants, pollen tubes, and young xylem cells (Klepek et al., 2010).

- **The TMT subfamily**

The TMT subfamily consists of three members in *Arabidopsis*, TMT1-3, encoding proteins targeted to the vacuolar membrane (Wormit et al., 2006). Wormit and coworkers carried out a GUS assay to analyze the promoter activity of the three TMTs. Their analysis revealed that *AtTMT1* and *AtTMT2* had a tissue- and cell type-specific expression pattern, unlike *AtTMT3* which displayed a weak expressed (Wormit et al., 2006). Moreover, AtTMT1 and AtTMT2 have been suggested to function as H^+/glucose antiporters (Wormit et al., 2006) and have been later on characterized as H^+/sucrose antiporters (Schulz et al., 2011). AtTMT1 and AtTMT2 can import glucose and sucrose into the vacuole. The expression of *AtTMT1* and *AtTMT2* has also been induced in abiotic stresses like drought, salt, and cold, as well as by sugars (Wormit et al., 2006).

- **The VGT subfamily**

In *Arabidopsis*, the VGT subfamily consists of three members. Only two members, AtVGT1 and AtVGT2 have been detected in the tonoplast, whilst the third member (product of the gene At5g59250) seems to be localized on the chloroplast membrane (Aluri and Büttner, 2007; Büttner, 2007). AtVGT1 has been shown to act as a glucose/H^+ antiporter to import hexoses into the vacuole during sugar compartmentation, and it is expressed in pollen, in leaves and stems, but not in roots (Aluri and Büttner, 2007).

2.2. SWEET family

Unlike SUTs and MSTs, the SWEET family does not belong to MFS superfamily owing to its distinct structure. SWEETs are small proteins that are predicted to have seven transmembrane segments (TMs) arising from an ancient duplication of a 3-transmembrane-helix-domain polypeptide fused to the central TM helix (TM4). The N and C termini have been located in the extracellular and the cytoplasmic side, respectively (Chen et al., 2010a). The SWEETs family splits into 4 subclades and includes 17, 16, and 21 members in *Arabidopsi*s, grapevine, and rice, respectively (Chen et al., 2010a; Lecourieux et al., 2014). AtSWEET1 has been the first member characterized as a low-affinity uniporter with a Km value of 9 mM and acts as a facilitator to mediate both efflux and uptake of glucose at the plasma membrane (Chen et al., 2010a). Five AtSWEETs members (AtSWEET4, 5, 7, 8, and 13) have been detected to transport glucose (Chen et al., 2010a). AtSWEET16 and AtSWEET17 have been localized at the tonoplast and shown to transport fructose (Chardon et al., 2013; Klemens et al., 2013). AtSWEET16 has been also demonstrated to transport glucose and sucrose (Klemens et al., 2013). SWEETs belonging to the clades III have a preference to transport sucrose rather than glucose. This clade encompasses AtSWEET10-15, OsSWEET1, and OsSWEET14 (Chen et al., 2012). The latter authors focused on *AtSWEET11* and *AtSWEET12*, which are strongly expressed in the leaves of *Arabidopsis*. AtSWEET12 acts as a low-affinity sucrose uniporter (Km = 70 mM for influx and Km >10 mM for efflux). The double mutant *atsweet11/12* showed higher accumulation of sugars (sucrose, hexoses, and starch) in leaves, where photosynthetic capacity and leaf size are affected, while the root length is reduced. AtSWEET11 and AtSWEET12-GFP fusions are targeted to the plasma membrane, both of which are localized phloem parenchyma cells in *Arabidopsis.* Taken

together, these results have shown that both AtSWEET11 and AtSWEET12 are involved in a two-step mechanism of SWEET-mediated export from parenchyma cells feeding H^+-coupled import into the SE-CC complex as suggested by Chen et al. (2012). *AtSWEET8*, also known as AtRPG1 (*Ruptured Pollen Grain1*) is expressed in the tapetum and its mutation leads to male sterility, due to involvement in glucose efflux that is essential for pollen nutrition (Guan et al., 2008). *AtSWEET5*, also known as AtVEX1 (*Vegetative Cell Expressed1*), is found in the vegetative cell of the pollen grains and plays a role in supplying the generative cells with sugars (Engel et al., 2005). *AtSWEET15*, also known as SAG29 (*Senescence-Associated Gene29*), is highly expressed in leaves during senescence (Chen et al., 2015). The expression of some *AtSWEETs* is modified during a challenge by a pathogen invasion. *AtSWEET4*, *5*, *7*, *8*, *10*, *12*, and *15* are highly induced in leaves of *Arabidopsis* infected with the bacteria *Pseudomonas syringae*. More precisely, *AtSWEET12* is induced by the fungus *Golovinomyces cichoracearum*, and *AtSWEET4*, *15*, and *17* are induced by the fungus *Botrytis cinerea* (Chen et al., 2010a). Certain *AtSWEETs* may be involved in response to abiotic stresses, such as *AtSWEET16,* which is repressed under cold, osmotic stress, or low nitrogen (Klemens et al., 2013).

2.3. The implication of tonoplast transporters in the intracellular transport

The vacuole is considered to be the largest organelle, as it may occupy more than 80% of the total cell volume (Martinoia et al., 2000; Martinoia et al., 2012). The tonoplast is a membrane surrounded the vacuole and separates it from the surrounding organelles (Hedrich et al., 2015). The vacuole serves as an intermediate storage compartment for a variety of compounds such as sugars, poly-alcohols, organic, and amino acids (Hedrich et al., 2015), but it also takes part in stress tolerance, where some of the stored compounds, like sugars, act as compatible osmolytes. In the source leaves, more specifically in the mesophyll cells, synthesized sugars can be temporarily stored in the vacuole when the export of sucrose to the phloem is limited (Martinoia et al., 2000). Hence, it is no wonder that such temporary storage requires the existence of many types of influx and efflux sugar transporters at the tonoplast membrane (Martinoia et al., 2000; Hedrich et al., 2015). The carriers TMT and VGT are responsible for the influx of sugars into the vacuole (glucose for VGT; glucose and sucrose for TMT) (Wormit et al., 2006; Aluri and Büttner, 2007). The import of sugars against their concentration gradient requires energy supplied by two types of vacuolar pumps: the V-pyrophosphatase (V-PPase) and the V-ATPase (Hedrich et al., 2015). In addition to the two

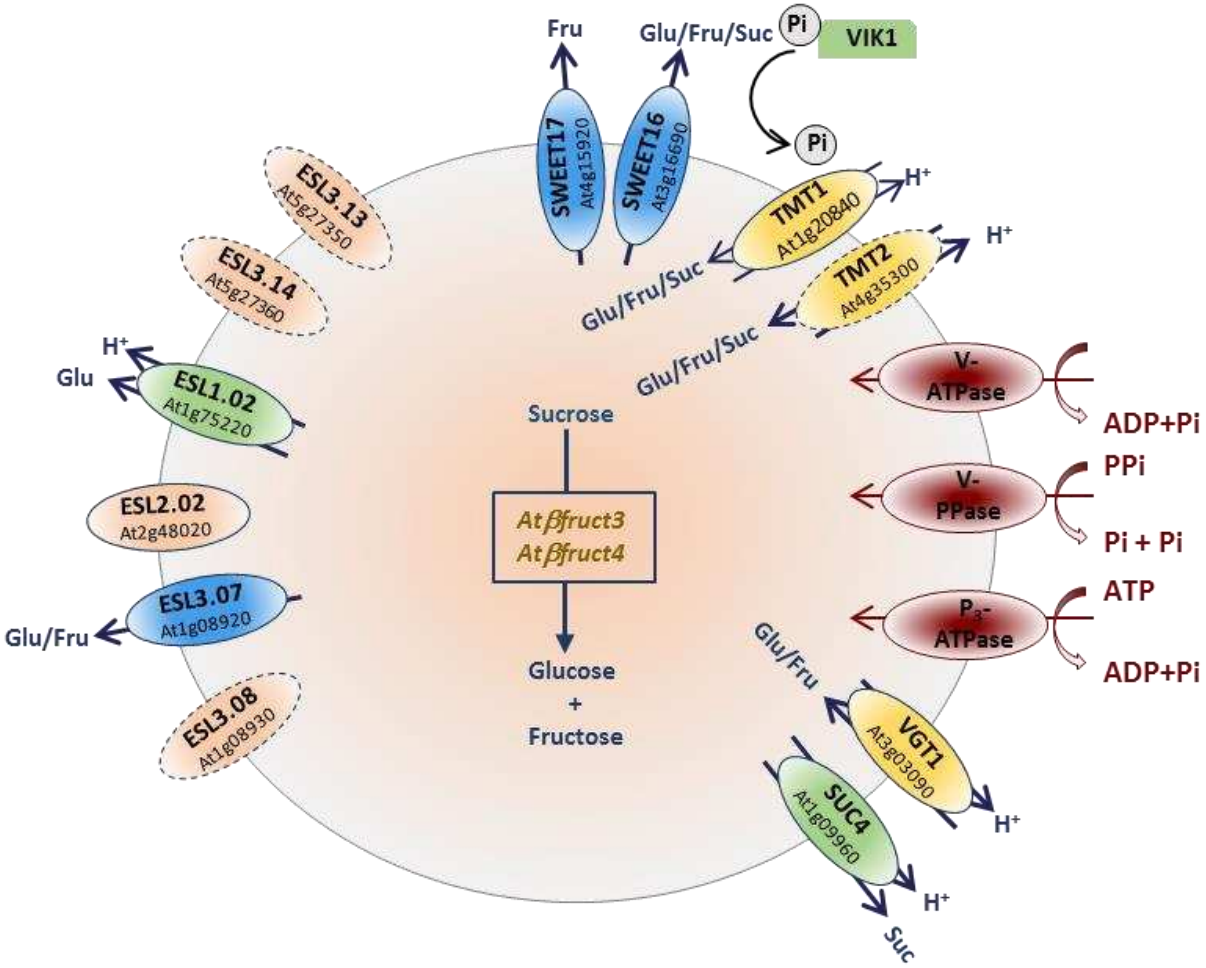

Ch.I-Fig. 6 : Simplified scheme summarizing current data on sugar transporters located on tonoplast.
Fru: fructose, Glu: glucose, Suc: sucrose. Circles in solid lines: sugar transporters located on the tonoplast; circles in dashed lines: sugar transporters putatively located on the tonoplast (adapted from Slawinski, 2017).

proton/sugar antiporters, two types of proton-driven sugar symporters are identified at the tonoplast, SUC4 (Schneider et al., 2012), and ESL1.02/ERDL6 (Klemens et al., 2014). Three facilitators ESL3.07/ESL1 (Yamada et al., 2010), SWEET16 (Klemens et al., 2013), and SWEET17 (Chardon et al., 2013), have been identified as responsible for the export of hexoses to the cytosol. Ch.I-Fig. 6 shows the above-mentioned vacuolar sugar transporters.

3. Water deficit

With climate change, crops are more vulnerable to drought and other stresses such as salinity and high temperature, and these restrictions may affect food security around the world. Indeed, agriculture and climate changes are tightly connected, as climate change is the main cause of environmental stresses adversely impacting the agriculture of a region (Raza et al., 2019). Nowadays, the agriculture sector is the main consumer of water, where approximately 70% of the water available is used in this sector (Somerville and Briscoe, 2001), and 40% of the world food is generated in irrigated soils (Chaves and Oliveira, 2004). Depending on the cultivated species, the quantity of water required for their development is variable. For example, the production of 1 kg of cotton necessitates 5263 L, whereas 1 kg of wheat and potatoes require 590 L (CNRS – Dossier scientifique: l'eau).

Drought is considered as one of the main abiotic stresses, which severely affects plant growth, development, and crop yield (Boyer, 1982). Since plants cannot move, they have evolved numerous programs to cope with the adverse effects of water deficit by making changes at physiological, metabolic, and molecular levels. In this context, improving crop tolerance to drought requires a deep knowledge of physiological mechanisms and genetic control of the contributing traits at different plant developmental stages (Farooq et al., 2009).

3.1.Plant/water relations: Water potential

Water is essential for the growth and development of the plant. It is involved in several metabolic and physiological processes. It is important to understand the relations between plant and water and the effects of insufficient water supply (Chavarria and dos Santos, 2012). Plants require a significant volume of water to meet their metabolic needs. Water is absorbed from the soil by the roots (97%), and the majority of absorbed water is lost by the transpiration process. Only a small part of the absorbed water remains for plant growth (2%) or is used in biochemical reactions such as photosynthesis and other metabolic processes (1%) (Taiz et al., 2014).

Water potential (Ψ_w) is commonly defined as the water content in the soil, plants, and atmosphere (Chavarria and dos Santos, 2012). In general, water potential may be influenced by concentration, pressure, and gravity (Taiz et al., 2014). Thus, the water potential is the result of four components and can be written using the following equation: $\Psi_w = \Psi_s + \Psi_p + \Psi_g + \Psi_m$. Where, these terms represent osmotic potential, hydrostatic potential, gravitational potential, and matrix potential, respectively. However, in the case for herbaceous plants, this equation can be reduced to $\Psi_w = \Psi_s + \Psi_p$ because Ψ_g is negligible in most cases when the height of the plant is less than 5 m and can be considered in studies of tree species (height more than 10 m) (Chavarria and dos Santos, 2012) - Ψ_m is also ignored except for severe dehydration conditions (Taiz et al., 2014).

In most cases, the water potential is negative except for pure water its Ψ_W is equal to 0 MPa at 20℃ (Taiz et al., 2014). Water always moves from a compartment with higher water potential (less negative) to a compartment with lower water potential (more negative). The osmotic potential is the effect of dissolved substances (solutes) on water potential (Chavarria and dos Santos, 2012; Taiz et al., 2014). It is negative since the water moves from a region of lower concentration to a region of higher concentration (Chavarria and dos Santos, 2012). Therefore, the presence of more solutes in water, reduces the osmotic potential, and decreases the water potential (Chavarria and dos Santos, 2012; Taiz et al., 2014). The hydrostatic potential is directly related to the turgor pressure. A positive Ψ_p increases the water potential, whereas a negative Ψp decreases the water potential (Taiz et al., 2014).

3.2. Water path in the soil-plant-atmosphere system

3.2.1. Soil water is absorbed by the roots

In the majority of plants, the surface area for water uptake is represented by the close contact between the surface of the root, especially the root hairs, and the soil particles (Taiz and Zeiger, 1998). The absorption of water by the roots causes a reduction in the water potential of the soil that is near the roots (rhizosphere) (Chavarria and dos Santos, 2012). This process creates a water potential gradient between the rhizosphere and the near region of soil that has a higher water potential. Then, this gradient attracts water from the soil towards the roots of the plant. In this way the water moves to the roots through the mass flow, since the water-filled pore spaces in the soil are interconnected (Taiz and Zeiger, 1998; Chavarria and dos Santos, 2012).

3.2.2. Ascension of water through the plant vascular system: Xylem

In the soil, water moves to the roots of the plant by mass flow. The water enters into contact with the roots, it takes the direction from the epidermis to the endodermis of the roots, and in this direction, water may travel *via* three pathways: the apoplastic, the symplastic, and the transmembrane pathway (Chavarria and dos Santos, 2012; Taiz et al., 2014).

In the apoplastic pathway, water moves from soil to xylem through the apoplast which is a continuous network of cell walls and intercellular air spaces in plant tissues. In the symplastic pathway, water passes from one cell to a neighbor cell via plasmodesmata connections. In the transmembrane pathway, the water enters a cell on one side, leaves the cell on the other side, then enters the next one in the chain, and so on.

Also, an important detail concerning these three different paths is that the movement of water through the apoplast pathway may be blocked by the Casparian strip at the endodermis level (Chavarria and dos Santos, 2012; Barberon and Geldner, 2014; Taiz et al., 2014). The Casparian strip (CS) is a hydrophobic barrier deposited as a band in the radial and transverse sections of endodermal cells and is impregnated with wax, lignin, and suberin. It should be noted, that not always the CS form a barrier to block the movement of water and solutes. For example, in the young part of the root, the water moves from the soil to enter the endodermis before the differentiation of the CS or at sites that can break the CS like the sites of the emergence of the lateral roots (Barberon and Geldner, 2014). Once the CS is differentiated, water may be transported into the endodermis via transporters localized at the endodermal plasma membrane (Barberon and Geldner, 2014). Aquaporins or called water channel proteins belong to the family of membrane channel proteins that facilitate the transport of water and can be implicated in this transport (Maurel et al., 2008; Maurel et al., 2015).

The roots absorb water and ions from the soil and transport them via the xylem to the aerial parts of the plant. But how are the water and solutes pushed up to the shoot when there is no pump to do this transport? Once these solutes have accumulated in the xylem, this contributes to a decrease in the osmotic potential of the xylem, which in turn will decrease the water potential of the xylem. This decrease would cause the absorption of water, which in turn contributes to positive hydrostatic pressure in the xylem, this phenomenon called root pressure. Therefore, root pressure combines with the transpiration for driving up water via the xylem to the shoots. However, the role of root pressure is less predominant in conditions where the transpiration rate is high. Instead, the water is pushed up to the shoot of the plants by the evaporative demand. Indeed, the water at the top of the plant negative hydrostatic

pressure, also called tension, this tension created by transpiration pulls the water in the xylem to the aerial parts of the plant. This mechanism is called the cohesion-tension theory (Taiz and Zeiger, 1998). Once the water in the xylem vessels is transported to the aerial parts of the plant a small part of it is used for metabolism, while the majority is evaporated through leaf stomata.

3.3.Plants survival strategies to cope with water deficit

Stress is usually defined as an external factor that negatively affects the plant. In the field, plants are subjected to several unfavorable environments that may induce stress. Water deficit, heat stress, salinity, and others are major abiotic stress factors that adversely affect plant growth, productivity, and reproductive capacity (Rhodes and Nadolska-Orczyk, 2001; Taiz and Zeiger 1998). In plants, water deficit occurs when the evaporative demand inside leaves is greater than the availability of water in the soil (Bray, 1997).

As sessile organisms, plants have established several mechanisms at the morphological, physiological, biochemical, cellular, and molecular levels to cope with the detrimental effects of water deficit or drought (Fang and Xiong, 2015). Drought resistance mechanisms are divided into 4 types: drought escape, drought avoidance, drought tolerance, and drought survival (Lawlor, 2013).

- **Drought escape**

This type comprises plants that complete their life cycle under well-hydrated conditions, before the onset of drought (Taiz and Zeiger, 1998; Chaves et al., 2003; Lawlor, 2013). Such plants are characterized by a strong degree of developmental plasticity (Chaves et al., 2003). Plants are therefore not affected by drought which may happen in their environment at another time; for that, the term escape is used (Lawlor, 2013).This strategy is important from an agronomic point of view. In the annual plants such as cereals, the development cycle generally coincides with climatic conditions: the vegetative growth is associated with the rainy season and the grain maturation occurs in the dry season (Lawlor, 2013).

- **Drought avoidance**

Avoidance is the ability of plants to grow during periods of drought, while maintaining their water status by adapting the following methods: **i)** By limiting water loss and conserving soil water. This requires a decrease in transpiration by reducing the surface area and stomatal conductance. Reduced leaf area may occur in the early stage of drought by the production of smaller leaves, and later, with more extreme drought by senescence of older leaves (Lawlor, 2013). In addition to these, plants tend to reduce the absorption of light by rolling the leaves

and to increase the reflection by a high density of trichomes (Chaves et al., 2003). In general, these modifications lead to a decrease in assimilation and photosynthesis and thus to loss of productivity (Lawlor, 2013). **ii)** By optimizing the water supply with deeper roots to exploit the maximum water from the soil (Lawlor, 2013). Indeed, the water uptake is maximized by adjusting the allocation of assimilates to the roots where their growth is promoted, thus increasing the water absorption capacity of the roots (Jackson et al., 2000; Chaves et al., 2003). **iii)** Finally, the storage of water in organs (trunk, stem) is also possible, as in the case of annual plants cultivated in agriculture (Lawlor, 2013).

- **Drought tolerance**

The term tolerance is often used to describe a metabolic mechanism for drought resistance (Lawlor, 2013). The mechanisms that are known to confer drought tolerance in preserving the water content and the turgor pressure of the tissues, even when the water supply is limited, include decreased osmotic potential via accumulation of proline (Morgan, 1984; Hare et al., 1998) or increasing the water flow in the cells via the additional presence of aquaporins (Maurel et al., 2008).

- **Drought survival**

Survival is a type of drought resistance, where cells, tissues, and organs that have stopped to grow during drought period are able to sustain cellular function and recover quickly after drought their previous vital functions, such as photosynthesis (Lawlor, 2013). For example, resurrection plants such as *Craterostigma plantagineum* belong to the *Scrophulariaceae* family, which is capable of reviving after a period of drought during which it becomes entirely dry and may stay alive for many years in this state. Upon watering, this plant recovers completely within 48 hours. The re-mobilization of sugars and the presence of LEA (Late Embryogenesis Abundant) proteins are responsible for this spectacular recovery capacity of growth (Scott, 2000).

3.4. How plants respond to water deficit

3.4.1. At whole-plant level

Some of the earliest responses to water deficit at the leaf level are a reduction in leaf growth and the closure of stomata (Chaves, 1991; Damour et al., 2010), both of which entail limiting water loss. Inhibition of cell expansion results in a reduction of leaf area during water deficit (Taiz and Zeiger, 1998). This is attributed to many factors: (1) the reduction in turgor pressure, (2) the decreases in the rate of cell division (Tardieu, 2013) and (3) the reduction in

cell wall plasticity, and its hardening (Chazen and Neumann, 1994). Water deficit can also contribute to a decrease in the number of leaves, at the example of the *Arabidopsis* Col-0 ecotype (Aguirrezabal et al., 2006; Hummel et al., 2010). It should be noted that the reduction in the leaf area and the stomatal conductance will affect the plant capacity to intercept the light and CO_2 capture and, consequently, its ability to produce biomass (Tardieu et al., 2011). It is noteworthy that the leaf expansion rate is decreased early before the onset of the reduced photosynthesis (Tardieu et al., 1999; Hummel et al., 2010).

Stomatal closure in response to water deficit presents the advantage to reduce water losses, despite the limitation of the CO_2 entrance, which results in a delayed decrease of the photosynthesis rate (Scharwies and Dinneny, 2019). Absorption and loss of water in guard cells affect their turgor and thereby modulate opening and closing of the stomata. Metabolic energy and changes in membrane permeability are both involved as well (Chaves et al., 2003). Abscisic acid (ABA) has been described as one of the key chemical signals involved in the control of stomatal behavior (Davies and Zhang, 1991). In dry soil, the closure of stomata was observed by split-roots experiments, in which part of the roots became dehydrated while the water status in the shoots stay unchanged (Neales et al., 1989; Khalil and Grace, 1993). This indicating that ABA produced by dehydrating roots and is subsequently transported to the aerial parts of the plant, was primarily involved in the control of stomatal closure. The regulation of stomata by ABA relies not only on the long-distance signaling mechanism but also on the modulation of the concentration of this hormone at the level of the guard cells themselves (Wilkinson and Davies, 2002). ABA concentration in the guard cells can originate not only from roots, but mainly from ABA synthesized in leaves and the guard cells themselves (Cornish and Zeevaart, 1986). When the leaves and roots of Arabidopsis are divided and imposed on water stress, ABA concentrations increase in the leaves but not in the roots (Ikegami et al., 2009). In *Arabidopsis* plants, immunohistochemical localization has been conducted using specific antibodies to ABA biosynthesis enzymes: AtNCED3, AtABA2, AtAAO3) (Endo et al., 2008). This study revealed that such enzymes are localized in the vascular parenchyma cells of leaves (Endo et al., 2008). The stomatal regulation depends also on the pH of xylem sap and leaf tissue which may increase in response to severe water deficit, high light intensity, and high leaf temperature (Wilkinson and Davies, 2002). Changes in the pH of xylem sap may act as a chemical signal from root to leaves in response to water deficit. When plants are under drought conditions, the pH of xylem sap becomes more alkaline, where the pH of xylem sap increases from 6.3 to about 7.2 (Wilkinson, 1999). The alkalinization of the apoplast adjacent to the stomatal guard cells in the leaf epidermis favors the accumulation

of the dissociated form of ABA (ABA^-), which can reach the guard cells instead of being sequestered by the leaf symplastic reservoir (the mesophyll cells) (Wilkinson, 1999; Wilkinson and Davies, 2002). As a consequence ABA binds to guard cell ABA receptors found on the outer surface of the guard cells, which leads directly to the closure of the stomata (Wilkinson, 1999).

ABA is distinguished by its weak acidic properties, which is present in an undissociated form (ABAH) in the presence of the slightly acidic medium, whereas in an alkaline medium, ABAH is dissociated into ABA^- and H^+. Like other acids, the protonated form will cross the lipid bilayer of the plasma membrane in which the ABAH is taken by the mesophyll cells under normal conditions, and that a low concentration of ABAH will reach the guard cells. However, during water deficit, the pH of xylem sap becomes slightly alkaline, favoring the deprotonated form (ABA^-), which cannot pass through the plasma membrane and stays trapped inside the cells. As a result, less ABA is taken by the mesophyll cells and a high concentration of ABA accumulates in the apoplast near the stomatal guard cells to induce their closure (Wilkinson, 1999). When the ABA reaches the plasma membrane of guard cells, it binds to the ABA receptors of the guard cells and triggers a signaling cascade leading to the closing of the stomata. PYR/PYL/RCAR proteins have been identified as ABA receptors (Ma et al., 2009; Park et al., 2009). Once bound, ABA triggers the production of ROS (reactive oxygen species), a phenomenon called oxidative burst, which results in the release of Ca^{2+} from the intracellular store and the influx of calcium across the plasma membrane (Cho et al., 2009). Calcium signaling triggers the release of Cl^- anions into the apoplast, which leads to the depolarization of the plasma membrane. This depolarization activates the massive efflux of K^+ by the opening of K^+ efflux channels, which induces a decrease in the turgor pressure of the guard cells leading to stomatal closure (Blatt, 2000; Sirichandra et al., 2009; Kim et al., 2010).

Roots are the first organs in contact with the water deficit, and they are able to sense a decrease in the water potential of the soil. Plants have to make changes at the root level to overcome the water deficit. They maintain the growth of root in density and depth, in which roots can uptake the maximum of water from the soil even at low soil water potential (Chaves et al., 2002; Sharp et al., 2004). The decrease in shoot growth during water stress is not generally associated with a reduced growth of the root system contributing to an augmentation in the root/shoot ratio (Chaves et al., 2002; Sharp et al., 2004; Verslues et al., 2006). Furthermore, it has been shown that the leaf expansion and leaf area are reduced during water deficit as well as the stomatal conductance. However, photosynthesis is maintained and

becomes inhibited over a long period of severe water deficit and hence, photosynthetic assimilates (sugars) from source organs are largely redistributed to sink organs, such as roots, to promote their growth (Hummel et al., 2010; Muller et al., 2011; Durand et al., 2016). In parallel, ABA produced by roots may also act as a signal to modify the root architecture (e.g. suppression of lateral root development) in response to water deficit, thereby facilitating water absorption from the sol improve their chances of obtaining water from the soil (Xiong et al., 2006; Roycewicz and Malamy, 2012).

3.4.2. Metabolic and cellular level

3.4.2.1. Osmotic adjustment

Osmotic adjustment is a biochemical mechanism used by plants to cope with water deficit. Under this constraint, plants accumulate many molecules known as osmolytes, osmoticum, or compatible solutes. Such osmolytes are not harmful to cells even at higher concentrations. Accumulated osmolytes in plants reduce the water potential of cells thereby preventing the efflux of water or enable water to move into cells, to maintain turgor pressure and sustain their growth (Hare and Cress, 1997; Hare et al., 1998). Osmolytes involved in osmotic adjustment during water deficit are variable, amino acids (e.g. proline), sugars (e.g. sucrose, hexoses, polyols), and quaternary ammonium compounds (e.g. glycine-betaine) (Munns, 2002; Moore et al., 2008; Hummel et al., 2010). Accumulation of soluble sugars in *A. thaliana* leaves is a process generally observed during water deficit (Taji et al., 2002; Hummel et al., 2010; Mewis et al., 2012; Sperdouli and Moustakas, 2012). In *Craterostigma plantagineum* sucrose is accumulated in significant amounts during drought, which may stabilize enzymes and cellular structures in water deprivation (Scott, 2000). It has been assumed that the accumulation of soluble sugars in poplar, grown in *vitro,* enhances osmotic and salt tolerance (Watanabe et al., 2000). Under salt stress, much more soluble sugars accumulate in salt-tolerant rice varieties than in salt-sensitive ones (Cha-um et al., 2009).

3.4.2.2. Photosynthesis level

In the early stages of water deficit, the stomatal conductance decreases because stomatal closure causes a reduction in the CO_2 availability. As stress becomes more severe, usually the efficiency of photosynthesis decreases (Lawlor and Cornic, 2002). Experiments, in which different levels of drought have been imposed on various species of almond trees, have shown that at an early stage of stress, a slight decrease in stomatal conductance has a less pronounced effect on the net CO_2 assimilation (Rouhi et al., 2007). In other terms, a slight

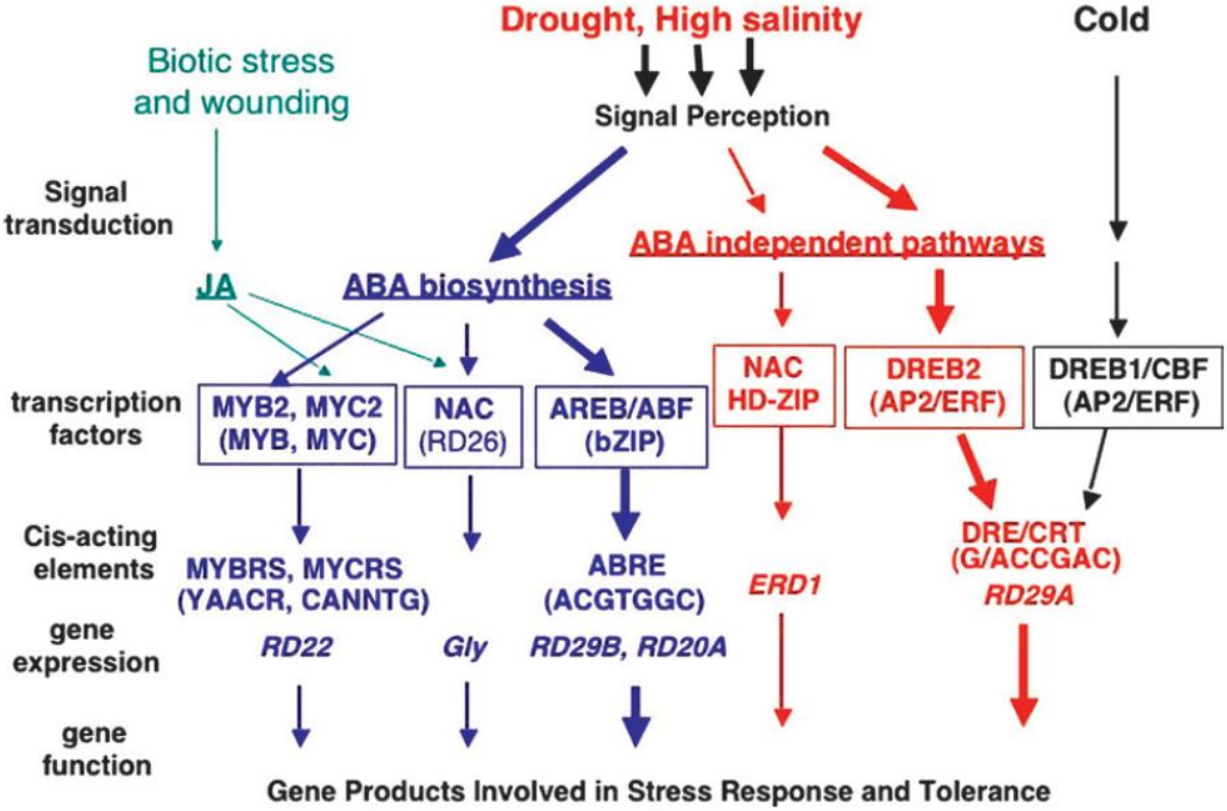

Ch.I-Fig. 7 : *Cis*-elements and transcription factors involved in the regulation of gene expression in response to abiotic stresses. Two pathways are involved in the gene regulation in response to water deficit, ABA-dependent pathway (blue) and ABA-independent pathway (red), with their respective transcription factors and promoter *cis*-acting elements (Shinozaki and Yamaguchi- Shinozaki, 2007).

closure of the stomata does not prevent photosynthesis to take place in which the synthesized sugars are stored in the vacuole as soluble sugars or in chloroplasts in the form of starch, or exported to sink organs such as roots, to increase their growth (Muller et al., 2011).

The reduction of photosynthesis may result directly from the restriction of CO_2 diffusion through stomata (known as stomatal limitation), the decrease of mesophyll conductance, and the modification of photosynthetic metabolism (known as non-stomatal limitation) or indirectly, such as oxidative stress caused by the accumulation of ROS (Chaves et al., 2009). Plant mechanisms to protect the photosynthetic apparatus from oxidative stress imply two categories of detoxification systems: enzymatic and non-enzymatic (Apel and Hirt, 2004). The enzymatic antioxidant systems include superoxide dismutase (SOD), peroxidase (POD), catalase (CAT) and glutathione reductase (GR). The non-enzymatic antioxidants include ascorbic acid (Conklin, 2001), glutathione and pigments, such as carotenoids, flavonoids (Jung, 2004) and anthocyanins (Chalker and Scott, 1999), acting as scavengers of ROS.

3.4.3. Gene level

3.4.3.1. Stress responsive genes

The molecular response to stress involves activation of large sets of genes, which enable plants to withstand environmental constraints (Shinozaki and Yamaguchi-Shinozaki, 2000). Many of the stress-inducible genes have been detected by microarray technology (Shinozaki et al., 2003). The proteins encoded by these genes are divided in two categories. The first category includes proteins that are directly involved in plant protection against abiotic, e.g. LEA (Late Embryogenesis Abundant) proteins, enzymes for the synthesis of osmolytes, aquaporins, sugar and proline transporters, as well as enzymes involved in ROS detoxification. The second category encompasses regulatory proteins that are involved in signal transduction and regulation of gene expressions, such as transcription factors, protein kinases, protein phosphatases, and calmodulin-binding proteins (Shinozaki and Yamaguchi-Shinozaki, 2000; Shinozaki et al., 2003; Ni et al., 2009; Lata and Prasad, 2011). Many of the drought-inducible genes are ABA regulated, while others are not. This indicates the existence of two regulatory systems, ABA-dependent and ABA-independent Ch.I-Fig. 7, that are involved in the regulation of gene expression in response to abiotic stresses (Yamaguchi-Shinozaki and Shinozaki, 2005, 2006; Yoshida et al., 2014; Liu et al., 2018).

3.4.3.2. Transcriptional regulation of gene expression

In eukaryotes, the gene expression is regulated at epigenetic, transcriptional and post-transcriptional levels (Hernandez-Garcia and Finer, 2014). At the level of transcription, the modulation of gene activation and repression results from interactions between *cis*-acting elements, short DNA intersect regulatory sequences, and *trans*-acting factors, transcription factors or DNA-binding regulatory proteins (Zou et al., 2011; Hernandez-Garcia and Finer, 2014). *Cis*-acting elements are defined as non-coding DNA sequences encompassing 4 to 12 bases, found in non-transcribed gene promoter regions, up-stream of the gene transcription start site (TSS), which provide the binding motifs for specific trans-acting regulatory proteins involved in the initiation and the regulation of transcription (Venter and Botha, 2010; Hernandez-Garcia and Finer, 2014; Biłas et al., 2016). The promoters may be defined as core promoters (regions situated ca. 100 bp up-stream and down-stream of the transcription starting site – TSS), proximal promoters (ca. 500 pb up-stream of TSS) and distal promoters (ca. 1kb, 2 kb, 3 kb upstream of TSS). The core promoter carrying canonical (TATA box) or non-canonical (GC box) conserved sequences allows the assembly of RNA polymerase II and general transcription factors involved in the complex triggering of the initiation of transcription. The activation of the full promoter depends on the relative position of the core promoter and combinatorial interaction of *cis*-regulatory elements found in both the proximal and distal regions (Hernandez-Garcia and Finer, 2014). The efficiency of gene expression is based on proteins/DNA interaction, where this complex can turn on or turn off transcription. Therefore, the transcriptional regulation depends on the presence or absence of the transcription factors and on the type, number, and location of *cis*-regulatory elements in the promoter (Hernandez-Garcia and Finer, 2014). In addition, enhancers and silencers are short DNA sequences that serve as binding sites for specific transcription factors, but are typically located up-stream or down-stream, too far away from the TSS (ca. 10 kb), and within introns (Lee and Young, 2000; Riethoven, 2010; Tora and Timmers, 2010; Hernandez-Garcia and Finer, 2014; Biłas et al., 2016).

In addition to the regulatory elements found in the promoter regions, 5'UTR, 3'UTR, and introns have been shown to regulate gene expression (Hernandez-Garcia and Finer, 2014; Gallegos and Rose, 2019). The positive impact of introns on gene expression was referred to as an intron-mediated enhancement (IME), that remains largely unknown (Laxa, 2016). Through functional analysis with the *GUS* reporter gene, Weise et al. (2008) showed that the promoter activity of the tomato *LeSUT1* sucrose transporter gene was very low and restricted in the phloem. Inversely, the whole gene sequence encompassing the promoter, the exons, the

introns and the 3'UTR fused to the reporter gene resulted in a high GUS activity. Analyzing the role of each intron, the authors determined that the three introns were responsible for regulating the *LeSUT1* expression. The introns 2 and 3 were responsible for expression in the companion cells, guard cells and trichomes, respectively. This shows that these two introns can act as transcriptional enhancers. As the construct containing the intron 1 did not show GUS activity, it has been considered functioning as a repressor. It has been concluded, that the promoter region alone did not contain all the information required for the *LeSUT1* transcriptional activity, and that the presence of *cis*-regulatory elements in all three introns was required for the regulation of its proper expression (Weise et al., 2008). In addition to the aforementioned, gene expression is regulated not only by DNA sequences but also by epigenetic events, including DNA methylation, histone post-translational modifications through methylation, acetylation, ubiquitinylation, and phosphorylation (Chen and Tian, 2007; Chen et al., 2010b). The histone modifications can activate or repress gene expression in response to abiotic stress. In this regard, Zhao et al. (2014) have reported that the high levels of histones H3K9 and H4K5 acetylatilatio, in the promoter region of the gene encoding the transcription factor ZmDREB2A (*Zea mays* dehydration-responsive element-binding protein 2A) were essential for the induction of *ZmDREB2A* under osmotic stress (Zhao et al., 2014). In *Arabidopsis*, the expression level of *ABI2*, *DREB2A*, *RD29A*, and *RD29B* has been found induced under ABA or NaCl treatment. Using chromatin immunoprecipitation (ChIP) assays, this induction was associated with an increase in the level of the gene activation histone marks, H3K9K14ac (acetylation) and H3K4me3 (trimethylation) (Chen et al., 2010b). Under drought stress, the level of the gene activation marks, H3K9ac and H3K4me3, gradually increased on the coding regions of drought-inducible genes (*RD29A*, *RD29B*, *RD20*, and *RAP2.4*), and such enrichment of histone marks related to the active chromatin state was correlated with the up-regulation of these stress-responsive genes (Kim et al., 2008). The above-cited studies suggest a link between the different changes of histone modifications and the induction of abiotic stress-responsive genes.

Overall, the transcription factors are DNA-binding proteins that function as activators or repressors of the transcription and are the master regulators in controlling numerous biological processes such as growth, development, and responses to various abiotic and biotic stresses. So far, fifty-eight families of transcription factors (TF) have been identified in plants, covering large number TF families common for eukaryotes and a non-neglected number of plant specific TF families. Among them, at least six TF families are involved in plant response to abiotic and biotic stresses, and may function in both ABA-dependent and ABA-independent

signaling pathways. These families are bZIP, MYB, MYC, AP2/ERF, NAC, and WRKY (Agarwal et al., 2006; Ng et al., 2018; Baillo et al., 2019).

- **bZIP family**

The transcription factors belonging to the bZIP (basic region leucine zipper) family are involved in the control various biological processes such as morphogenesis, seed formation, and response to various stresses (Jakoby et al., 2002). These transcription factors are characterized by a bZIP domain composed of two motifs: a basic region for DNA binding and a leucine zipper domain for the dimerization of the transcription factor (Jakoby et al., 2002; Corrêa et al., 2008). Several bZIP TFs referred to as AREB (ABRE-Binding protein) and ABF (ABRE Binding Factors) are involved in the ABA-dependent pathway. The promoter regions of most ABA-inducible genes contain a conserved *cis*-element named ABA-Responsive Element (ABRE; PyACGTGG/TC), with ACGT core sequence (Uno et al., 2000; Zhang et al., 2005; Gómez-Porras et al., 2007; Roychoudhury et al., 2013). A single copy of ABRE is insufficient to activate the expression of ABA-responsive genes. The latter requires additional copies of ABRE or ABRE combined with coupling element (CE) such as two CEs (CE1 and CE3), *motifII*, and DRE/CRT (Narusaka et al., 2003; Zhang et al., 2005; Gómez-Porras et al., 2007). The promoter region of the drought-responsive gene *RD29B* contains two AREB *cis*-elements necessary for its expression in response to ABA (Uno et al., 2000). Until now, nine members of AREB/ABFs have been identified in *Arabidopsis* (Liu et al., 2019). Among them, three AREB/ABFs (AREB1/ABF2, AREB2/ABF4, and ABF3) are strongly induced by abiotic stresses such as dehydration and high salinity, whilst ABF1 is also up-regulated under the same stresses but at a lower level than that of AREB1/ABF2, AREB2/ABF4, and ABF3 (Fujita et al., 2005; Yoshida et al., 2015). Analysis of the overexpression of AREB1/ABF2, AREB2/ABF4 and ABF3 in transgenic *Arabidopsis* plants has shown to improve the tolerance to water stress (Kang et al., 2002; Kim et al., 2004; Fujita et al., 2005). It has been reported that AREB1/ABF2 is also implicated in glucose signaling (Kim et al., 2004). The genome-wide transcriptome analysis performed by Yoshida et al. (2010) demonstrated that the expression of several downstream stress-responsive genes was significantly disrupted in the *areb1 areb2 abf3* triple mutant, and novel AREB/ABF target genes, such as LEA and group-A PP2C genes and transcription factors have also been identified (Yoshida et al., 2010). Under stress conditions, the *areb1 areb2 abf3* triple mutant exhibits improved insensitivity to ABA and reduced tolerance to drought, when compared with the single and double mutants. These data allow to conclude that AREB1/ABF2, AREB2/ABF4, and ABF3 act as transcriptional

activators cooperatively regulating ABRE-dependent gene expression through ABA signaling during osmotic stress (Yoshida et al., 2010).

- **MYB and MYC families**

The proteins of the MYB and MYC families are present in both plants and animals and are involved in numerous plant processes including metabolism, differentiation, cell shape, hormones response, and response to biotic and abiotic stress (Ambawat et al., 2013). As a common feature, MYB proteins contain three conserved MYB repeats (R1R2R3), which are involved in DNA-binding and protein-protein interactions (Feller et al., 2011). In plants, most MYB factors belong to the R2R3-MYBs group displaying only two repeats (Feller et al., 2011). It has been shown that the transcriptional activity of certain MYB proteins is based on the interaction with MYC2-type basic Helix-Loop-Helix (bHLH) transcription factor (Feller et al. 2011). AtMYB2 and AtMYC2 TFs bind to MYBRS and MYCRS *cis*-elements, respectively, and cooperatively activates the expression of the *RD22* gene induced by ABA and drought stress (Abe et al., 1997; Abe et al., 2003; Yamaguchi-Shinozaki and Shinozaki, 2005; Yamaguchi-Shinozaki and Shinozaki, 2006). The MYB and MYC transcription factors bind to (C/T) NGTT(G/A) and CANNTG (E-box) *cis*-elements, respectively (Fujita et al., 2011; Prouse and Campbell, 2012). MYB and MYC transcription factors are involved in the regulation of gene expression under abiotic stress in ABA-dependent manner (Fujita et al., 2011; Roychoudhury et al., 2013). *AtMYB96* and *AtMYB102* are strongly induced in response to ABA and drought stress. It has also been shown that *AtMYB102* is induced under salinity stress and that its complete up-regulation requires a combination of osmotic and wounding stresses. *In silico* analysis revealed that the transcription activity of *AtMYB102* depends on the presence of two conserved regulatory elements, such as ABRE- coupling elements (CE1) and W-box, and their interacting factors in the promoter (Denekamp and Smeekens, 2003). *AtMYB44* is activated by ABA and various abiotic stresses such as dehydration, salinity, and cold. The transcription factor AtMYB44 is also involved in the ABA-dependent signaling pathway that confers tolerance to abiotic stresses by triggering stomatal closure (Jung et al., 2008). *AtMYB70*, *AtMYB73*, and *AtMYB77* are up-regulated by wounding, white light, salinity and cold stresses (Jung et al., 2008; Lata and Prasad, 2011). The transcription factor AtMYB41 also plays important role in response to abiotic stresses, and its expression level is extremely up-regulated by drought, ABA and salt stress (Cominelli et al., 2008).

- **AP2/ERF family**

AP2/ERF (APETALA2/Ethylene Response Factor) is a transcription factor family that is predominantly found in plants (Kim et al., 2006). This family has a DNA-binding domain, called AP2/ERF, which consists of approximately 60-70 amino acids (Nakano et al., 2006). In plants, the AP2/ERF family encompasses four subfamilies: AP2, ERF, RAV, and DREB (Nakano et al., 2006; Sakuma et al., 2006). DREB proteins can bind to the DRE *cis*-element (A/GCCGAC), a motif found in the promoter of many genes induced by drought and cold stress. As ABRE, the presence of one copy of the DRE *cis*-element is sufficient for gene expression, which has to be present in multiple copies for ABA-responsive gene expression. Some proteins of this subfamily have been found to recognize the C-repeat (CRT) and the Low-Temperature-Responsive Element (LTRE) *cis*-elements, which are similar to the DRE sequence. Transcription factors that can bind to the CRT *cis*-elements are DREB/CBF (DRE-binding proteins/CRT-binding factors) (Yamaguchi-Shinozaki and Shinozaki, 2005, 2006; Fujita et al., 2011; Mizoi et al., 2012). The promoter of the drought-cold inducible gene, *RD29A*, contains ABRE, as well as DR/CRT DREB *cis*-elements, each of which, is involved in the ABA-dependent and ABA-independent signaling pathway, respectively (Yamaguchi-Shinozaki and Shinozaki, 2005). The DREB proteins are important transcription factors that are involved in abiotic stress signaling (Fujita et al., 2011). DREB proteins contain two subclasses: DREB1/CBF and DREB2. DREB1/CBFs are involved in the cold signaling pathway, while DREB2s are implicated in the dehydration signaling pathway (Agarwal et al., 2006; Roychoudhury et al., 2013). In *Arabidopsis*, the DREB1 subclass contains six members. Only three of them are up-regulated by cold stress (*DREB1A/CBF3*, *DREB1B/CBF1*, and *DREB1C/CBF2*), while the three others are responding to different abiotic stresses. *DREB1D/CBF4* is induced by dehydration and ABA, whilst *DREB1E/DDF2* and *DREB1F/DDF1* are responsive to salinity stress (Liu et al., 1998; Haake et al., 2002; Magome et al., 2008; Fujita et al., 2011). The DREB2 subclass consists of eight members in *Arabidopsis* that are not induced by cold stress. Among them, *DREB2A* and *DREB2B* are responsive to dehydration, salinity, and heat stress, whereas *DREB2C* is up-regulated under heat stress. Besides, *DREB2A*, *DREB2D*, and *DREB2F* are highly inducible by salinity stress, and *DREB2E* - by ABA (Liu et al., 1998; Sakuma et al., 2006; Fujita et al., 2011) .

- **NAC family**

The NAC is a plant-specific transcription factor family with 117 and 151 members in *Arabidopsis* and rice, receptively (Shao et al., 2015). The name NAC is derived from the names of three distinct genes, whose encoded proteins contain a particular NAC domain, i.e.

NAM (No Apical Meristem), ATAF1-2, and CUC2 (Cup-Shaped Cotyledons) (Souer et al., 1996; Aida et al., 1997). The NAC TFs are involved in numerous developmental processes such as seed development, embryo development, leaf senescence, cell division, and responses to abiotic and biotic stresses (Shao et al., 2015). The NAC proteins are characterized by the presence of a conserved NAC domain in the N-terminus that targets specific DNA sequence (Ooka et al., 2003; Olsen et al., 2005). NAC transcription factors can bind to the NAC recognition motif (NACRS) containing the CACG core sequence. This *cis*-acting element is found in the promoter region of *ERD1* (Early Responsive to Dehydration stress 1) gene (Tran et al., 2004; Tran et al., 2007). *ANAC019*, *ANAC055*, and *ANAC072* are up-regulated by ABA and various abiotic stresses such as drought and salinity. Their proteins ANAC019, ANAC055, and ANAC072 recognize CATGTG *cis*-elements (Tran et al., 2004). *Arabidopsis* transgenic plants overexpressing either *ANAC019*, *ANAC055*, or *ANAC072/RD26* exhibit elevated tolerance to drought stress (Tran et al., 2004). Some NAC TFs have been reported to regulate the expression of stress-responsive genes in cooperation with other transcription factors, such as those belonging to the ZF-HD (zinc finger homeodomain) TF family. The transcription factors ANAC019, ANAC055, and ANAC072 have been shown to interact with the ZF-HD1 to regulate the expression of *ERD1* (Tran et al., 2007).

- **WRKY family**

The WRKY family of 74 plant-specific transcription factors (*Arabidopsis*) is involved in various plant biological processes such as leaf senescence, seed development, seed dormancy and germination, and in response to biotic and abiotic stresses (Eulgem et al., 2000; Rushton et al., 2010). The common feature of WRKY TFs is a DNA-binding domain consisting of a conserved amino acid sequence WRKYGQK and a zinc-finger-like motif. This feature allows the WRKY TF to repress or activate transcription by binding to the *cis*-element named W-box (C/T) TGAC(C/T) with TGAC core located in the promoter of target genes (Eulgem et al., 2000; Rushton et al., 2010). Certain WRKY TFs can also bind to non-W box elements such as SUSIBA2/HvWRKY46 (sugar signaling in barley), which can recognize both the W-box and the SURE (sugar-responsive) elements (TAAAGATTACTAATAGGAA), whereas NtWRKY12 transcription factor can only target the SURE-like element, but not the W-box (Sun et al., 2003). It has been reported that the ABO3/WRKY63 transcription factor is involved in response to ABA and drought stress (Ren et al., 2010).

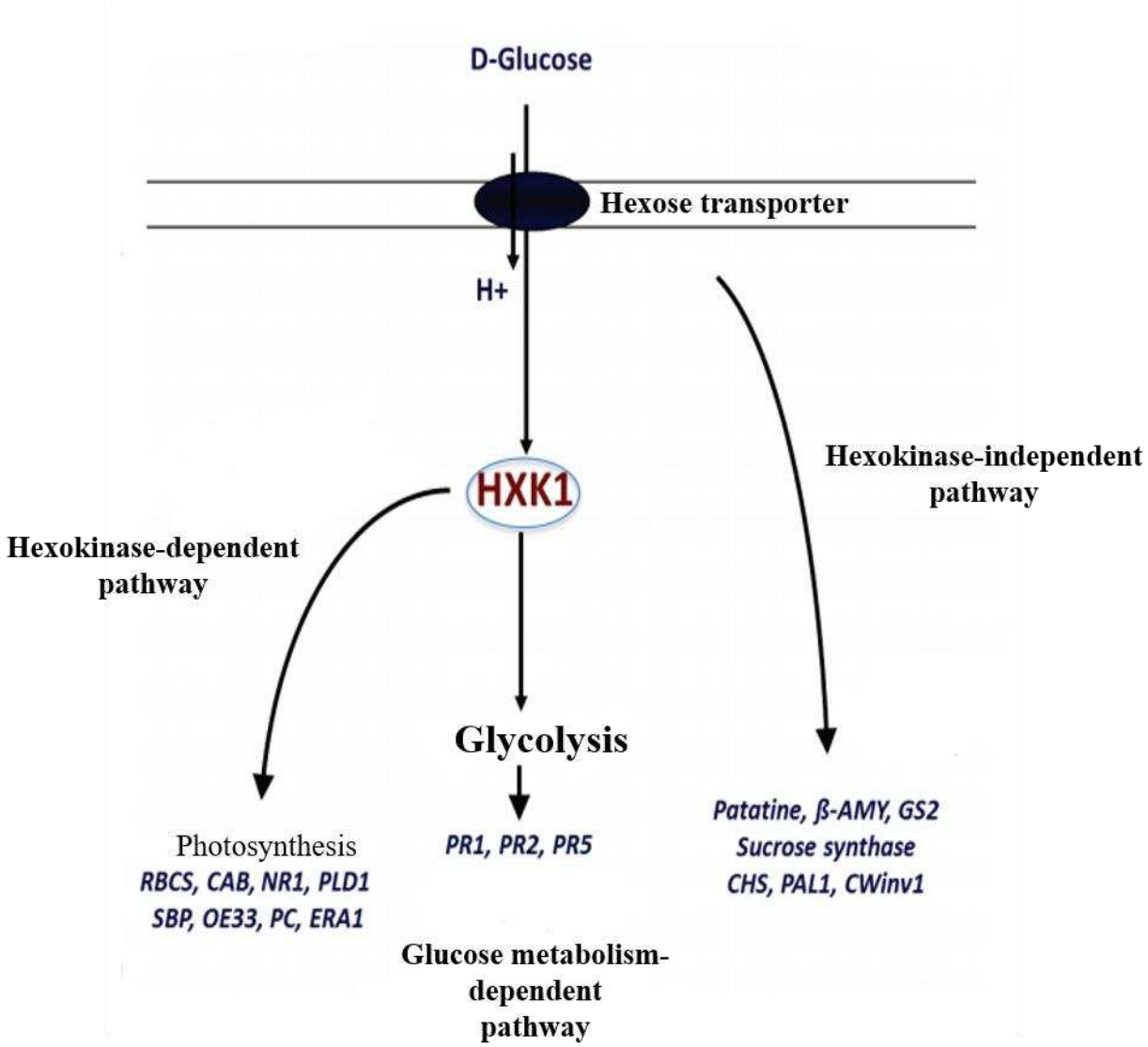

Ch.I-Fig. 8 : Diagram showing the three pathways of glucose signaling, defined with respect to the cytoplasmic glucose sensor HXK1, as well as a list of genes regulated by the different pathways. The hexokinase-dependent pathway regulates the expression of RBCS (Rubisco Small Subunit), CAB (Chlorophyll A/B Binding protein), NR1 (Nitrate Reductase 1), PLD1 (Phospholipase D 1), SBP (Sedoheptulose-1,7-bisphosphatase), OE33(Oxygen-Evolving Enhancer 33), PC (Plastocyanin), ERA1 (Enhanced Response to ABA). The glycolysis pathway, which relies only on the catalytic activity of hexokinase, induces the expression of PR1, 2, 5 (Pathogenesis-Related Proteins 1, 2, 5). The HXK1 independent pathway is involved in the regulation of patatin, sucrose synthase, β-AMY (β amylase), GS2 (Glutamine Synthase 2), CHS (Chalcone Synthase), PAL1 (Phenylalanine Ammonia Lyase 1), CWinv1 (Cell Wall invertase 1). (Adapted from Parrilla, 2015)

4. Sugar signaling in plants

Sugar sensing and signaling pathways are well known in unicellular organisms such as yeast (*Saccharomyces cerevisiae*), which represents the most well studied eukaryotic model. However, sugar sensing and signaling are much more complex in plants (Rolland et al., 2006). Plants as multicellular organisms need long-distance and cell-specific signaling pathways during growth, development and in response to environmental cues (Rolland et al., 2006). As autotrophic organisms plants use their proper photoassimilates, namely sugars, to build carbon skeletons, to fuel growth and development, and also as metabolic signaling molecules (Rolland et al., 2006; Ramon et al., 2008). Sugars play a pivotal role in the regulation of genes in plants and other organisms. Glucose is the most studied carbohydrate signal in plants. The plant first senses glucose through sensor proteins and then this interaction triggers a signal transduction pathway (Smeekens, 2000; Rolland et al., 2002). The first glucose sensor recognized in plants is the Hexokinase 1, which is a core component of glucose sensing and signaling in the cytoplasm (Jang et al., 1997; Moore et al., 2003; Rolland et al., 2006). In plants, three different pathways of glucose signaling have been suggested: (i) a HXK1-dependent pathway, (ii) a HXK1-independent pathway, and (iii) a glycolysis-dependent pathway that depends on the enzymatic activity of HXK1 (Xiao et al., 2000) (Ch.I-Fig. 8). Moreover, sugar signaling mechanisms are strongly connected to plant hormones such as abscisic acid, ethylene, auxin, and cytokinin (León and Sheen, 2003; Ramon et al., 2008).

4.1. Glucose signaling pathways

4.1.1. Hexokinase-dependent glucose-signaling pathway

The first evidence of the role of hexokinase as an intracellular glucose sensor has been provided by (Jang and Sheen, 1994) through studying the glucose mediated repression of some photosynthesis genes in isolated protoplasts of maize (*Zea mays*). This hypothesis has experimentally been corroborated in transgenic *Arabidopsis* lines under- or over-expressing *AtHXK1* (Jang et al., 1997). The latter study revealed that plants expressing the *AtHXK1* antisense gene become hyposensitive to glucose, whereas plants overexpressing the *AtHXK1* gene turn out hypersensitive to glucose (Jang et al., 1997). Some physiological functions of HXK1 have been unraveled by the identification and characterization of the *Arabidopsis* glucose insensitive mutants (*gin2*), affected in the enzymatic activity of hexokinase1, but still preserving its sensor function (Moore et al., 2003). Using this mutant, it has been demonstrated that the glucose sensing function of AtHXK1 is independent of its metabolic

activity (Moore et al., 2003). In the nucleus, AtHXK1 interacts with two unconventional partners to form a multimeric protein complex: the vacuolar H^+-ATPase B1 (VHA-B1) and the 19S regulatory particle of proteasome subunit (RPT5B) (Cho et al., 2006). The *vha-B1* and *rpt5b* mutants displayed insensitivity to glucose similar to that found for *gin2* mutants, including a defect in glucose repression of the CAB2 gene (Cho et al., 2006). The latter study implies that the HXK1 nuclear complex is crucial for glucose mediated gene repression.

4.1.1. Hexokinase-independent glucose-signaling pathway

Evidence for a hexokinase-independent pathway has been provided by using non-phosphorylable glucose analogs, which can mimic glucose-dependent regulation of gene expression. Indeed, 6-deoxyglucose (6-DG) is a glucose analog transported across the plasma membrane into the cytosol, and even though it cannot be phosphorylated by HXK1, it activates the expression of genes encoding cell-wall invertase (*CwINV1*), sucrose synthase (SuSy), and phenylalanine ammonia-lyase1 (P*AL1*) (Godt et al., 1995; Roitsch et al., 1995; Ehness et al., 1997). Further evidence for the existence of the hexokinase-independent pathway has been provided by experiments using 3-O-methyl glucose (3-O-MG), another transportable but non-phosphorylable glucose analog, displaying the ability to activate a patatin class I promoter in transgenic *Arabidopsis* (Martin et al., 1997). The expression of the genes encoding AGPase (ADP-glucose pyrophosphorylase), CHS (chalcone synthase), PAL1 (phenylalanine ammonia-lyase), and AS1(asparagine synthetase) is regulated through the HXK1-independent pathway of glucose signaling (Xiao et al., 2000).

4.1.2. Glucose-dependent pathway of glucose signaling

Evidence of the third glucose signaling pathway, referred to as glycolysis-dependent, has been provided in *Arabidopsis thaliana* (Xiao et al., 2000). This pathway is independent on HXK1 sensor function and depends only on the catalytic activity of hexokinase. The expression of the pathogenesis-related genes *PR1* and *PR5* is induced in plants overexpressing *AtHXK1*. Inversely, their expression is lost in plants under-expressing *AtHXK1*. In parallel, the *PR1* and *PR5* are also induced in plants overexpressing the yeast *HXK2*. These data showed that *PR5* and *PR1* gene expression is regulated by glucose signaling dependent only on HXK1 catalytic activity, without implication of its sensor function. The induction of the pathogenesis-related genes *PR1* and *PR5* genes by glucose may be indirect and, therefore, mediated downstream of HXK1 by the perception of an intermediate or final product of the glycolytic pathway (Xiao et al., 2000).

4.2.Sugar and Hormone Crosstalk

The deciphering the sugar signaling pathways relies on the elucidation of the crosstalk between metabolic and hormonal signals. The interaction between sugar and hormone signaling pathways has been highlighted by analyzing early seedling development in the presence of high sugar concentrations (e.g. sucrose, glucose). Under such conditions, the seedlings with altered growth also displayed inhibition of hypocotyl elongation, cotyledon greening and expansion (Smeekens, 2000; Rolland et al., 2006). Genetic screening for developmental arrest phenotype has allowed isolation of many glucose-insensitive and glucose-hypersensitive mutants in *Arabidopsis*. It appears that these mutants are allelic to genes affected in hormone biosynthesis and hormone signaling pathways (Rolland et al., 2006). There is now evidence for the intimate connection between sugar and hormone signal transduction pathways (e.g. abscisic acid, ethylene) (Arenas-Huertero et al., 2000; Cheng et al., 2002; Arroyo et al., 2003; León and Sheen, 2003; Price et al., 2003; Rook and Bevan, 2003; Lin et al., 2007). Remarkably, several of the sugar mutants are allelic to *Arabidopsis* mutants affected in ABA biosynthesis (*aba*) or ABA signaling (*abi*). For example, the two glucose insensitive mutants *gin6* and *gin5* are allelic to *abi4* and *aba3* mutants, respectively. *ABI4* gene encodes an AP2-type transcription factor involved in the signaling of ABA in seeds (Finkelstein et al., 1998). The fact that the *abi4* mutant is insensitive to glucose implies fine-tuning interplay between ABA and glucose signaling pathways. Not all *abi* mutants are insensitive to glucose. While *abi4* and *abi5* are glucose insensitive, *abi1-1*, *abi2-1*, and *abi3-1* display a glucose-sensitive phenotype. The fact that all *abi* mutants are not glucose-insensitive suggests the existence of two signaling pathways, one ABA-specific and another one ABA/glucose-dependent (Arenas-Huertero et al., 2000; León and Sheen, 2003).

The *ABA3* gene is required for the biosynthesis of ABA. It has been shown that accumulation of ABA is essential for the establishment of a response related to the perception of a glucose signal. Consistent with this finding, a number of ABA-deficient mutants (*aba1-1*, *aba2-1*, and *aba3-2*) are also insensitive to glucose, suggesting that ABA may decrease their glucose sensitivity. In addition, the glucose-insensitive phenotype of the *gin5/aba3* mutants can be reverted by the addition of exogenous ABA at 100 nM physiological concentration (Arenas-Huertero et al., 2000). Thus, *GIN5* plays an essential role in the regulation of ABA levels in response to glucose signaling (Arenas-Huertero et al., 2000).

The identification and the characterization of the *gin1* mutant revealed an interaction between glucose and ethylene signaling pathways (Zhou et al., 1998). This conclusion is supported by experiments where the ethylene overproduction (*eto1)* and the constitutive ethylene triple response (*ctr1)* mutants display insensitivity to glucose. Consistent with this, the ethylene-insensitive mutants (*etr1, ein2,* and *ein3*) display hypersensitivity to glucose (Zhou et al., 1998; Cheng et al., 2002). Further evidence has been provided by functional experiments where two mutants *gin4* and *sis1* (sugar insensitive) turn out to be mutant alleles of *CTR1*, which acts as a negative regulator of ethylene signaling (Kieber et al., 1993; Gibson et al., 2001; León and Sheen, 2003; Rolland et al., 2006). It has been shown that *gin1* is allelic to *aba2*, and *ABA2/GIN1* encodes the SDR1 protein (short-chain dehydrogenase/reductase) involved in the ABA biosynthesis (Cheng et al., 2002). The *gin1* mutant displays a phenotype similar to that of the ethylene hypertensive mutant (*ctr1*), which is presumably due to a defect in the biosynthesis of ABA. It appears plausible that the antagonistic effect of ethylene on glucose signaling may be a consequence of the ethylene inhibitory effect exerted on ABA biosynthesis and signaling (Cheng et al., 2002). The interaction between ABA and ethylene signaling pathways has been further corroborated by the isolation of alleles of *ctr1* and ethylene-insensitive *(ein2*), as enhancer and suppressor allelic mutations of the *abi1* mutant respectively (Beaudoin et al., 2000). Along the same line, the *era3* mutant (enhanced response to ABA) is allelic to *ein2* (Ghassemian et al., 2000). These results illustrate an antagonistic relationship between ABA and ethylene signaling during germination and seedling development.

Interestingly, glucose has been shown to regulate the expression of ABA biosynthesis genes *ABA1*, *ABA2*, *ABA3*, and *AA03* (Cheng et al., 2002). Furthermore, glucose triggers the degradation of the regulatory element EIN3 (ETHYLENE INSENSITIVE 3) in the ethylene signaling pathway, through the hexokinase-dependent pathway, while the ethylene favors its stability. *Arabidopsis* transgenic lines underexpressing or overexpressing *EIN3* display, respectively, hypersensitivity or insensitivity to glucose (Yanagisawa et al., 2003). Glucose seems to inhibit the development of young seedlings by stimulating the synthesis of ABA, and probably, by inhibiting ethylene-dependent signaling, which itself acts antagonistically to the ABA signaling. Glucose not only inhibits the early seedling development but also delays the germination of *Arabidopsis* seeds (Price et al., 2003; Dekkers et al., 2004). Glucose and endogenous plant hormones play a crucial role in the regulation of the germination process. The main hormonal crosstalk orchestrating the transition from seed dormancy to seed germination concerns the balance between ABA and gibberellins (GAs). ABA inhibits

germination, while gibberellins (GAs), brassinosteroids (BRs), and ethylene promote germination (Dekkers et al., 2004). High glucose concentrations inhibit seed germination by increasing endogenous ABA (Price et al., 2003). This indicates the involvement of glucose in the control of ABA level during the early stages of plant development (Price et al., 2003). The mechanism of perception and transduction of the glucose signal during germination seems to be different from that found during early seedling development. Indeed, during germination, the mutants *abi2*, *abi4*, and *abi5* act in a similar way to that of the wild-type in response to glucose treatment. Therefore, it seems plausible that HXK1 is probably not involved in the perception of the glucose signal during germination (Price et al., 2003)

4.3.Disaccharide signaling pathway

For several genes, their expression is regulated by sucrose, but not by its derivative hexoses (glucose and fructose). Sucrose-specific signaling is involved in the regulation of the patatin gene in potatoes (Jefferson et al., 1990), and the AtATB2 bZIP transcription factor in *Arabidopsis thaliana* (Rook et al., 1998). Several non-metabolizable sucrose analogs, such as palatinose and turanose, have revealed the existence of a specific disaccharide signal, independent of metabolism. These molecules were found to regulate the activity of alpha-amylase in barley embryos (Loreti et al., 2000). Trehalose is metabolized by plants and was found to increase the expression of APL3 gene in *Arabidopsis*, which encodes an ADP-glucose pyrophosphorylase subunit (Wingler et al., 2000). Trehalose is hydrolyzed by trehalase to glucose and the inhibition of this enzyme leads to a reduction of starch and sucrose accumulation. Therefore, trehalose might be involved in the regulation of carbohydrate metabolism in plants (Müller et al., 2001). Some authors suggest that certain SUT2 group disaccharides' transporters, at the example of AtSUT2/SUC3, might function as sucrose sensors in plants. This is supported by the fact that the structure of these transporters display structural homology with that of the Snf3 and Rgt2 glucose sensors in yeast (Barker et al., 2000).

4.4.Signal transduction

Although sugar-signaling mechanisms in yeasts and mammals are well elucidated, little is known about the transduction pathways of sugar signals in plants. The involvement of protein kinases, protein phosphatases, and other secondary messengers such as calcium or calmodulin have been suggested (Smeekens, 2000). SnRK1 (Snf1 Related Kinase) is a plant protein kinase with a catalytic domain that shares high similarity with Snf1 (Sucrose Non-Fermentig 1) of yeast and AMPK of mammals (AMP-activated Protein Kinase)

(Halford et al., 2003; Rolland et al., 2006). The fact that proteins can rescue the *snf1*-mutant phenotype of yeast indicates that the function of these protein kinases is conserved during evolution. However, the SnRK1 family has increasingly diverged and expanded, as corroborated by the presence of specific regulatory subunits found in plants only (Halford et al., 2003; Polge and Thomas, 2007). In *Arabidopsis*, SnRK1/AtKIN10 may be involved in the regulation of the expression of more than 1000 genes encoding transcription factors and proteins involved in chromatin remodeling (Baena-González et al., 2007). These authors also showed a positive correlation between the expression profile of SNRK1/AtKIN10 regulated genes and that of genes regulated by sugar starvation (Baena-González et al., 2007).

5. Evolutionary history of the monosaccharide transporters (MST) family of land plants

Previous works have focused on the evolutionary history of the monosaccharide transporters (MST) in various species, such as in *Arabidopsis*, rice, *Medicago*, pea, and grapevine. *Arabidopsis thaliana* has 53 monosaccharide transporter (MST) genes which can be divided into seven subfamilies (Büttner, 2007). Of these STP (Sugar Transport Protein) and ESL (Early Response to Dehydration Six-Like) are considered as the two largest subfamilies (Johnson et al., 2006). By searching EST databases of various species representing all terrestrial plants, Johnson et al. (2006) detected only six subfamilies of monosaccharide transporters in the bryophyte *Physcomitrella patens*, the fern *Ceratopteris richardii* being the first lineage in which, PLT subfamily was identified (Johnson et al., 2006). They could detect one ESL in genomes of *Selaginella* and *P. patens*, 4 in *Pinus taeda* and *Zea Maize* and 5 in *Lycopersicum esculentum*. Few years after, identified 27 MST including only 1 ESL in the genome of *Selaginell*a and 8 MST with no ESL in *P. patens* genome. For the latter, this is not in accordance with Johnson et al, (2006). The comparison of the MST family in *Arabidopsis* and rice revealed that this family is larger in rice than in *Arabidopsis* with 65 and 53 MST genes, respectively (Johnson and Thomas, 2007). This difference is probably due to the number of tandem duplication events in their evolutionary histories. In rice, the STP and PLT subfamilies were greatly expanded, while the ESL subfamily was much larger in *Arabidopsis* (Johnson and Thomas, 2007). Johnson et al. (2006) proposed that the expansion of the ESL subfamily is due to three segmental duplications and six tandem duplications. In Fabaceae, the MST genes, are also split into seven clades. Pea (*Pisum sativum*) and Medicago (*Medicago truncatula*) possess 59 and 72 MST genes, respectively, indicating that the MST gene family is extremely large in Medicago (Doidy et al., 2019). It is noteworthy that STP, PLT, and INT

clades in Fabaceae are greatly expanded due to the presence of gene duplication events (Doidy et al., 2019). However, the ESL clade seems to be smaller than in other Eudicots species as Medicago and pea comprised 10 MtESL and 9 PsESL, respectively. The lineage *Brassica* present a very large MST family (175 MST genes were identified in *B. napus*, 87 in *B. oleracea* and 83 in *B. rapa)* divided also in seven sub-families. Gene redundancy occurred in the ESL sub-family as between 24 to 30 ESL copies are present in *B. rapa*, *B. oleracea* and *B. napus* (A and C sub-genomes) (Zhu et al., 2021). Grapevine (*Vitis vinifera*) comprises 59 MST genes divided into seven subfamilies. Twenty-two ORFs of putative VvESL transporters, with high similarity to the 19 AtESL proteins, have been identified (Afoufa-Bastien et al., 2010). Fourteen ORFs VvESL were found to be located in tandem on chromosome 14 (Afoufa-Bastien et al., 2010).

Altogether, these results put into question the biological necessity of so many duplicated *ESL* genes in some plant genomes. In this context, it is interesting to deepen our comprehension of the evolutionary history of the ESL (Early Response to Dehydration Six-Like) subfamily. To this end, Lucie Slawinski (2017) performed the first complete phylogenetic analysis of the ESL subfamily. Sixty-three representative species of the plant kingdom and algae were studied, including thirtheen algae, three bryophyte (moss), one lycophyte (spike moss), one gymnosperm, and fourty-eigth angiosperms. The investigation of the ESL sequences in nonvascular land plants and algae was important to understand the evolution of this family. She performed a BLASTp (Basic Local Alignment Search Tool) analysis, using as queries 18 ESL protein sequences identified in the grapevine proteome (Afoufa-Bastien et al., 2010), and identified 526 protein sequences in 50 Embryophyte proteomes. Furthermore, she could show the complete absence of ESL sequence in 12 algae proteomes (including rhodophytes, stramenopiles and chlorophytes) but succeeded to report a single ESL copie in the proteome of the Charophyte *Klebsormidium nitens.* Three and two ESL sequence proteins were also found in the non-vascular moss *Physcomitrella patens* and the vascular seedless spike moss *Selaginella moellendorffi*, respectively. Afterward, she performed a phylogenetic analysis with 519 putative ESL proteins to analyze the evolutionary history of the ESL family within the plant kingdom. This analysis revealed that these transporters could be divided into three major ESL groups named: ESL1, ESL2, and ESL3.

Group ESL1 comprised 133 ESL protein sequences derived from the 47 Embryophytes: Three and two ESL proteins sequences from the bryophyte *Physcomitrella patens* and the lycophyte *Selaginella moellendorffi,* respectively, five out of nine sequences from the gymnosperm *Pinus taeda* and 123 ESL protein sequences from angiosperms (44 species).

Each embryophyte genome proteome appears to have at least one ESL1 protein sequence, indicating that these sequences are conserved across the land plant evolution.

At the basis of Group ESL2 and Group ESL3 are located the 4 sequences of the Gymnosperm *P. taeda* and no sequences of moss and fern are present. This suggests a first duplication event in the common ancestor of seed plants (paleopolyploidy or ζ : 340Mya). Group ESL2 comprised 150 ESL protein sequences derived from the 44 angiosperms. Four out of five sequences from the basal angiosperm *Amborella trichopoda* were identified at the basis of the group ESL2 which is therefore specific to angiosperms.

In group ESL3, the complete absence of ESL protein sequences from bryophyte, lycophyte, gymnosperm and from *A. trichopoda* suggested a second whole-genome duplication event in the common ancestor of mesangiosperms (WGD ε: 170-235 MYa). ESL3 group is a mesangiosperms specific group and harbor 232 ESL protein sequences derived from 40 species. This group can be divided into 3 sub-groups. The fact that ESL3a contains sequences from basal eudicots (*A. coerulea and N. nucifera*) which are excluded from ESL3b and ESL3c suggest a third duplication event, probably the whole genome triplication event (WGT γ/1R: 117MYA). Furthermore, ESL3b and ESL3c are two groups specific for pentapetalae (rosids and asterids). Lucie identified a high number of tandem duplicated ESL (47%), demonstrating that monogenique duplications have also highly contributed to the evolution of ESL. The estimation of the synonymous and non-synonymous substitution dN/dS (also called Ka/Ks ratio) for the genus *Arabidospsis* showed that ESL genes are under purifying (negative) selection, which means a conservation of their function. However, the selection pressure for *ESL3* genes seems less stringent, which might lead to the emergence of new functions.

In summary, Lucie Slawinski highlighted the emergence of the ESL gene family with Streptophyta and stated that the expansion of this family coincided with the evolution of land plants according to whole genome duplication and specific tandem duplication. Her work will serve as a useful starting point to better understand the role of AtESL in sugar partitioning in plant cells.

Rationale

The main interests of our research team SEVE (Sucres Echanges Végétaux & Environnement) are focused on the biological roles of sugar transporters in plant development and responses to biotic and abiotic stresses through sugar allocation in the whole organism, as well as sugar partitioning between different compartments of the cell.

The main objective of my thesis work is to explore the functional diversity of monosaccharide transporters belonging to the ESL (Early Response to Dehydration Six-Like) subfamily in Arabidopsis.

At my arrival, Lucie Slawinski (PhD thesis, 2017) has analyzed the gene expression of 17 *AtESL* in response to water deficit in *Arabidopsis* leaves and has established the up-regulation of four *AtESL* genes: *ESL3.07*, *ESL1.02*, *ESL3.03*, and *ESL3.05*. To gain insight into the physiological function of three of them, *ESL3.07*, *ESL1.02*, *ESL3.03*, she has identified and characterized their single T-DNA insertional mutants under normal and water-deficit conditions.

In the continuity of this work and using reverse genetic approach, I had to identify the missing mutant for the fourth gene *AtESL3.05* (*atesl3.05*), perform its physiological phenotyping under normal and water-deficit conditions, and analyze gene expression of *ESLs* and other vacuolar sugar transporters in this mutant.

Since the *atesl* single mutants have not shown any specific phenotype under normal and water-deficit conditions, these sugar transporters might function redundantly. In the aim to overcome that plausible functional redundancy of ESL proteins, I had to generate double, triple and quadruple homozygous mutants.

In the line of the phylogenetic analysis and as a first step towards understanding the functional diversity of *ESLs*' genes, I had to perform *in silico* analysis of the 19 *AtESL* promoter sequences and identify their common and gene-specific *cis*-acting elements.

To better discriminate the mutant responsiveness to metabolic and hormonal signals, as well as to different abiotic stresses, I had to carry out seed germination assays on the generated single, double and triple *atesl* mutants.

The major challenge of my thesis work concerned the subcellular localization and the functional characterization of AtESL3.05 sugar transporter.

CHAPTER II

MATERIALS & METHODS

Materials and methods

1. Biological material

1.1. Plant material

The wild type *Arabidopsis thaliana*, ecotype Columbia 0 (Col 0) was used in all experiments. DNA insertional mutants *at1g75220* (SALK_106049) *atesl1.02*, *at4g04760* (SALK_132009)/ *atesl3.03, at1g08890* (SALK_047351)/ *atesl3.05* and *at1g08920* (SALK_025646)/ *atesl3.07* of the same genetic background were identified *via* SIGnAL site (SALK Institute Genomic Analysis Laboratory) and provided by NASC (the European Arabidopsis Stock Center). The presence of the T-DNA insert and the homozygosity of these mutant lines were confirmed by PCR analysis (Slawinski, 2017). *Nicotiana benthamiana* plants were leaf infiltrated with *Agrobacterium tumefaciens* cell suspensions.

1.2. Bacterial strains

- *Escherichia coli* strain One shot® Top10 (Invitrogen) was used for bacterial transformation and amplification of plasmids. Genotype: F- *mcr*A Δ(*mrr-hsd*RMS-*mcr*BC) φ80*lac*ZΔM15 Δ*lac*X74 *rec*A1 *ara*D139 Δ(*araleu*)7697 *gal*U *gal*K *rps*L (StrR) *end*A1 *nup*G.
- Transient expression experiments by agroinfiltration of *N. benthamiana* leaves were performed with *A. tumefaciens* strains GV3101 (pMp90) and EHA105. For the stable transformation of *A. thaliana* wild-type plants, the *A. tumefaciens* strain GV3101 (pMp90) was used.

1.3. Yeast strains

Saccharomyces cerevisiae EBY.VW4000 (Wieczorke et al., 1999) is a glucose deficient yeast due to lack of the twenty sugar transporter genes that could be necessary for hexose uptake and is thus mostly used for functional validation of monosaccharide transporters.

2. Growth conditions

2.1. *Arabidopsis* cultivation under normal conditions

Seeds of Col 0 and the SALK-mutants were sown in pots containing a sterile mixture of soil:vermiculite (3:1) and were then placed in darkness, at 4°C for two days. Such stratification synchronizes and improves the germination of seeds. Afterwards, sowing was

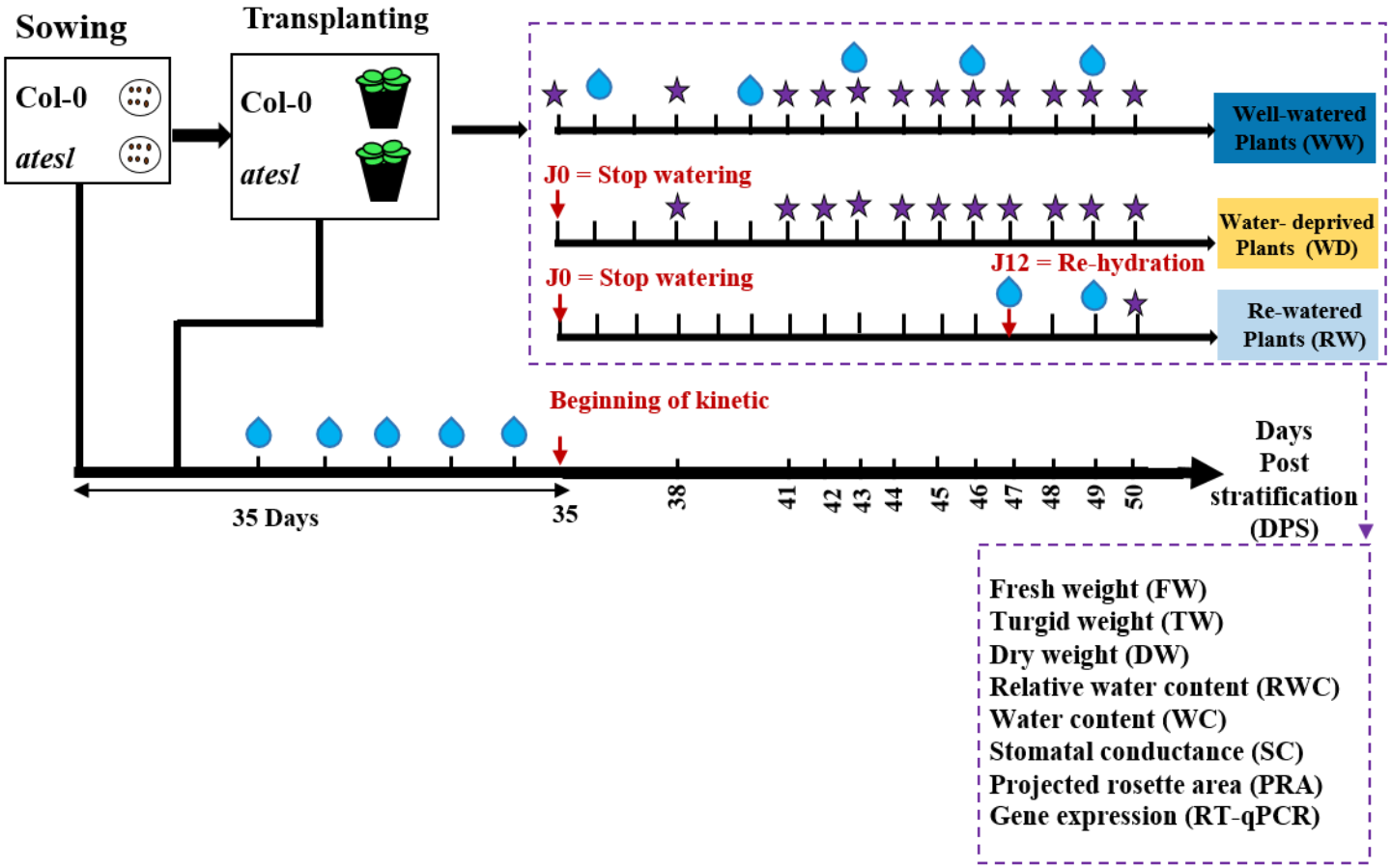

Ch.II-Fig. 1 : Protocol used for water deficit treatment and measurements. The days after the onset of watering are indicated at the bottom by the black arrow. Violet asterisks indicate time-point of sampling and blue droplet symbols - those of watering.

placed in a controlled phytotron under short photoperiod (10 h/14 h day/night), at 100 $\mu mol.m^{-2}.s^{-1}$ of light intensity, with 22/18°C (day/night) temperature and 50/90 % (day/night) relative humidity. After 13 days of growth, the young seedlings were individually transplanted into Arasystem™ (BETATECH bvba, Belgique), filled with 50 ± 2 g of soil:vermiculite (3:1) mixture. Until the 35th day of growth, the plants were watered once per week and for one hour, bottom-up by a water bath supplemented with fertilizer (PETERS (20/20/20; N/P/K).

In order to identify homozygous and heterozygous mutant lines through the presence of the T-DNA insertion, seeds of the heterozygous *esl3.05* mutant (Slawinski, 2017) and seeds derived from genetic crossings were grown under the same conditions as mentioned above, except that seeds were sown directly in the Arasystem™ (BETATECH bvba, Belgique).

In order to induce the flowering for seed production, all Arabidopsis plants cultivated in soil:vermiculite (3:1) mixture were transferred to a GMO certificated greenhouse compartment under long photoperiod (16 h light/ 8 h darkness). Individually harvested seeds were stored at room temperature until use.

2.2. Cultivation under water deficit condition

To characterize the effect of water deficit on the ecotype Col 0 and its *esl3.05* mutant, the seeds of each genotype were initially cultivated for 35 days as described above (see section 2.1). One group of plants was water-deprived for fifteen days, i.e. from the 35th to the 50th day post sowing (DPS). A second group of plants was water-deprived for twelve days, i.e. from the 35th to the 47th DPS, and further re-watered from the 48th to the 50th DPS. A third control group of plants was regularly watered every 3 days, without fertilizer, until the 50th DPS (Ch.II-Fig. 1). Throughout the following text these three groups are referred to as “water-deprived”, “re-watered” and “well-watered”.

2.3. Tobacco cultivation

Seeds of *N. benthamiana* were sown in pots containing a sterile soil:vermiculite (3:1) mixture. After 13 days, the seedlings were individually grown in pots (diameter) at 25°C in a phytotron under long-day conditions (16 h light/ 8 h darkness).

2.4. Arabidopsis in vitro cultivation

2.4.1. Seed surface sterilization

The seeds of different genotypes were surface-sterilized by soaking in 70% EtOH for 2 min, then in a sterilization solution (5% bleach, 60 µl of 20% Triton X-100, and sterile water

up to 60 ml) for 5 min, shaking every 60 s. The seeds were washed thoroughly by five washes with sterile distilled water and suspended in sterile water.

2.4.2. Seed germination experiments

Sterilized seeds were grown on Petri dishes containing minimal MS medium containing macro- and micro elements without sugar (annex I) or supplemented with: 7.2% glucose, or 7.2% mannitol, or 3 µM ABA, or 200 mM NaCl. Approximately 100 to 200 seeds per genotype were spread onto the plate divided on sectors in the aim to cultivate all studied genotypes on the same medium. Plated seeds were stratified in dark for 24 h at 4°C to remove residual dormancy, and after that transferred to a culture chamber under continuous light, at 22°C or 4°C (cold condition). Since the first day in light seeds were photographed daily for eight consecutive days using Nikon D5200 camera. Radicle protrusions from the seed coat were scored as germination events through using the cell counter plugin of the Fuji software, and respective germination percentage was calculated as well. All germination experiments were performed in at least three biological replicates.

3. Growth and Physiological parameters of Col 0 and *atesl3.05* mutant leaves

3.1.Rosette sampling

Arabidopsis rosettes were excised and immediately divided into two equal parts. The first half of the rosette was used to measure physiological parameters, while the second half was immediately frozen in liquid nitrogen for further RNA analyses and sugars extractions. Three independent biological experiments were carried out. Experiment with Col 0 and *atesl3.5* was performed on five plants for each of the three treatment conditions (well-watered, watered-deprived, and re-watered plants), twelve points of sampling (35th, 38th, 41th, 42th, 43th,44th, 45th, 46th, 47th, 48th, 49th, and 50th DPS) (Ch.II-Fig. 1). In addition, the rosettes of ten plants per condition (i.e. well-watered, water-deprived and re-watered plus Col 0 and *atesl3.05* mutant), were collected 12 times (i.e. on 35th, 38th, 41th DPS, and later on every next day until the 50th DPS) and photographed in order to calculate projected surface area (PRA). In parallel, other four groups of ten plants per group processed under the above-described conditions were used to determine stomatal conductance.

3.2.Physiological phenotyping of plants

3.2.1. Leaf water status: relative water content (RWC) and water content (WC)

The half-rosette was initially weighed to measure its fresh weight (FW). Afterwards it was let to float onto distilled water, at 4℃ for 24 h in darkness. After this 24-hour period the half-rosette was considered to reach constant weight, and a second measurement of its turgid weight (TW) was performed. The half-rosette was then dried at 80℃ for 24 h in order to measure its dry weight (DW). Based on these measurements, the relative water content and water content were calculated as follows:

$$RWC=\frac{(FW-DW)}{(TW-DW)}\times 100\%$$

$$WC=\frac{(FW-DW)}{(FW)}\times 100\%$$

3.2.2. Follow-up of rosette development: Measurement of project rosette area (PRA)

Projected rosette area (PRA) was determined through using the ImageJ software, version 1.53e (http://imagej.nih.gov/ij/). Rosettes of ten plants by condition were followed up during the 15 days of experimentation. For each photography, a scale calibration was initially set up. To that aim, the respective image was first selected through “File->Open”, and 1 cm-long straight line was drawn on a ruler photographed alongside the rosette. On the window which opened after “Analyze-> Set Scale”, the parameter “Known distance” was set to “1” (for 1 cm), and “cm” was selected as “Unit of length”. Scale calibration was completed and saved by “OK”. Next, the entire rosette form of the image was surrounded by approximate close circle or ellipse through “Image->Freehand”, and all residual area was deleted by subsequent “Edit->Clear outside”. The image was processed by “Image->Adjust->Color threshold”, manual cursor adjustment of the parameters “Hue”, “Saturation” and “Brightness”, and final saving by “Select”. The rosette area, in black on pastel blue background, appeared narrowly delimited by a yellow line, and was determined by “Analyze->Measure”. Measured values were visualized by “Window->Results”, selected and exported to an Excel file for further analysis.

Ch.II-Table 1 : The concentrations of sucrose solutions used to estimate the osmotic pressure of leaf cells and the osmotic pressure in Mpa corresponding to each sucrose solution

Concentration of sucrose (M)	Osmotic pressure of the solution (Mpa)
0	0
0,0625	0,2
0,125	0,3
0,188	0,5
0,25	0,6
0,3125	0,8
0,375	0,9
0,4375	1,1
0,5	1,2
0,5625	1,4
0,625	1,5
0,6875	1,7
0,75	1,8
0,8125	2
0,875	2,1
0,9375	2,3
1	2,4

Ch.II-Fig. 2 : Leaves' pieces after 24-hour incubation in sucrose solutions. From left to right: pieces of the leaf after soaking in sucrose solutions ranging from 0 to 1 M sucrose (see Ch.II-Table 2). The leaf pieces were obtained from three different plants of Col-0, at day 10, after the arrest of watering. Three biological and technical replicates were performed.

3.2.3. Measurements of stomatal conductance (SC)

Stomatal conductance (SC, mmol/m^2/s) was measured using a leaf porometer (Model SC-1, Decagon Devices Inc., USA). Measurements were taken daily after 5 h of illumination period, two measurements by plant (i.e. two leaves), and 10 plants for each of the conditions. As described in 3.1 the plants for SC measurements were tested in parallel with the plants used for sampling and photography.

3.2.4. Estimation of osmotic pressure in the cells of leaves

In order to estimate the osmotic equilibrium in cells, leaf fragments without the main vein were weighed immediately after excision (*T0 mass*) and placed into solutions with increasing sucrose concentration ranging from 0 M to 1 M (Ch.II-Fig. 2 and Ch.II-Table 1). After 24 h, at 4°C, the leaves' fragments were reweighed (*24h mass*) to calculate mass difference (*Δmass*):

$$\Delta mass = 24h\ mass - T0\ mass$$

This mass difference (vertical axis) was then plotted on a graph against the osmotic pressure of sucrose solutions (horizontal axis). The osmotic pressure (π) of the various sucrose solutions was calculated from the concentration of sucrose solutions by the following equation:

$$\pi = R \times T \times Cs$$

The unit of π in Pa when R is the ideal gas constant i.e. 8.32 J / mol / Kelvin; T is the temperature in Kelvin i.e. 239K and Cs is the concentration of the solution in mol/L. The osmotic pressure of the cells corresponds to the osmotic pressure of the solution, which does not cause a variation in mass. The osmotic pressure was determined for the Col-0 and the mutant *esl3.5* under well-watered and water-deprived conditions at 45th, 47th, and 49th DPS, days corresponding to the end of phase 2, phase 3, and phase 4, respectively (Slawinski, 2021). Three plants per genotype and condition were used for this analysis.

3.2.5. Analysis of leaf cell anatomy by light microscopy

The leaves of *A. thaliana* were sliced using a razor blade, perpendicularly to the central vein, and were fixed immediately with 0.5% glutaraldehyde and 2% paraformaldehyde in 0.05 M phosphate buffer, pH 7, 2, at 4°C for 1 h. After three washes, 20 min each, with 0.2 M phosphate buffer, pH 7.2 containing 7.5% sucrose, post-fixation was performed in 1% osmium tetroxide for 5 min followed by dehydration in ethanol at increasing concentrations of 20%, 50%, 70%, 95% and 100 %. The samples were then impregnated using successively two

Ch.II-Table 2 : Protocol for the enzymatic determination of soluble sugars.

	Sucrose reaction : Part (I)		Glucose/Fructose reaction: Part (II)	
	Blank	Sample	Blank	Sample
Sample (µl)	-	25	-	25
Water (µl)	25	-	75	50
β-fructosidase (µl)	50	50	-	-
Vortex , incubate for 5 min				
Water (µl)	475			
Buffer (µl)	25			
$NADP^+$/ATP (µl)	25			
Vortex, incubate for 5 min, read OD at 340 nm (read 1)				
Hexokinase/G6P-DH (µl)	5			
Vortex, incubate for 15 min, read OD at 340 nm (read 2)				
PGI (µl)	-		5	
Vortex, incubate for 15 min, read OD at 340 nm (read 3)				

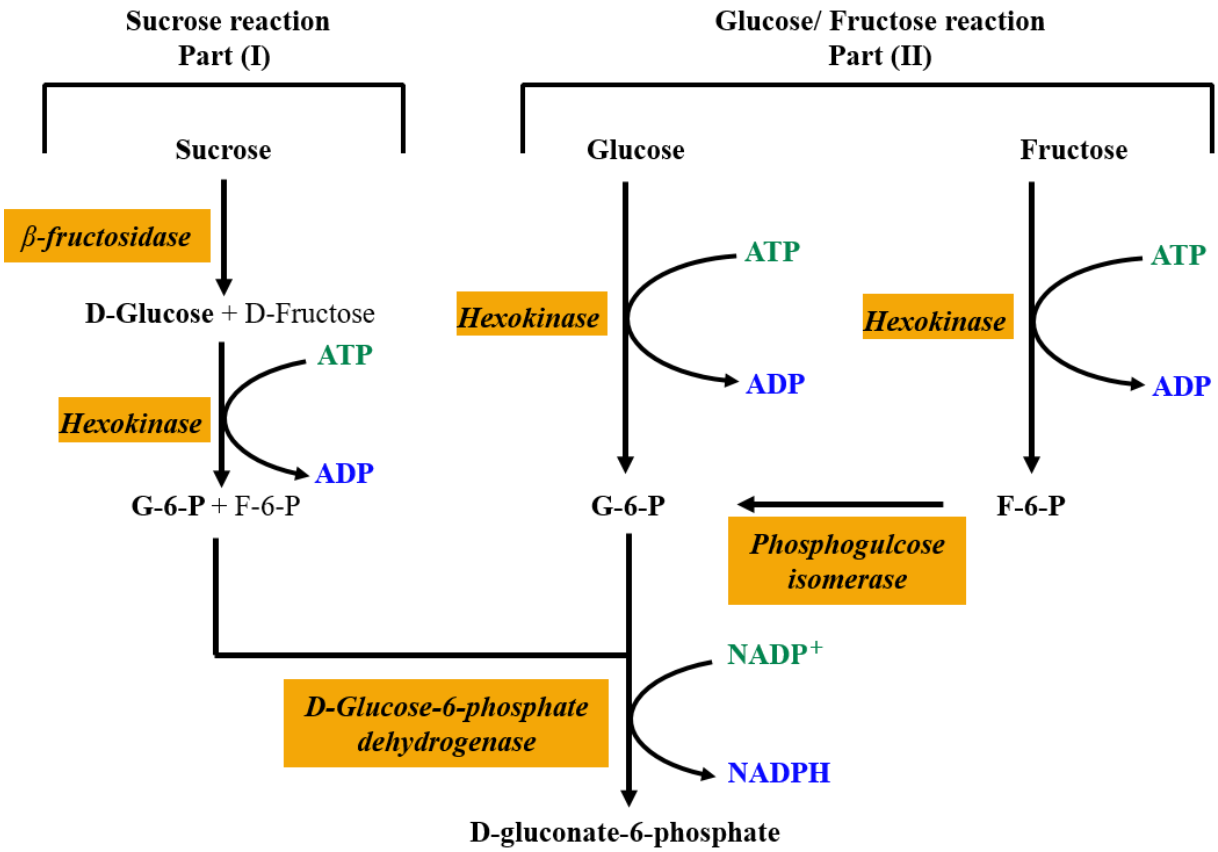

Ch.II-Fig. 3 : Enzymatic determination of soluble sugars (adapted from Megazyme)

incubations in a mixture of LRWhite resin and 100 % EtOH (1: 2, v/v) for 20 min, followed by two other prolonged incubations in the same mixture for 60 min, 60-minutes incubation in pure LRWhite resin, and final overnight incubation in pure LRWhite resin. All these steps were performed at 4°C. The polymerization of the resin was carried out at 60°C for 24 h. A 500-nm thick section obtained in a microtome (EMUC6, Leica) was stained with toluidine blue (prepared in Borax, pH 9) and observed on a light microscope (Zeiss Axioplan). The microscopic observations were conducted for the Col0 and the mutant *esl3.5* under well-watered and water-deprived conditions at 45th, 47th, and 49th DPS. Three independent biological replications were performed, only samples from the third repetition were used for analysis.

3.2.6. Soluble sugars extraction and content measurement

The contents of sucrose, glucose, and fructose were measured in the leaves of Col-0 and the mutant *esl3.5*. Extractions were conducted on material previously ground in liquid nitrogen (TissueLyser II, Qiagen) and lyophilized (5 days, -30°C; Freezone6, Labconco). Soluble sugars were extracted from 10 to 20 mg of powder by three washing with 1.5 ml of methanol:chloroform:water (12/5/3, v/v/v) and twice with 0.5 mL. After centrifugation at 12000 *g* for 10 min, the supernatants were collected, pooled and dried in a vacuum for 3 h at 50°C using MiVac Quattro; Genevac. The soluble sugars were dissolved in 0.3 or 0.5 ml of water depending on the amount of material used for the extraction and quantified using the Suc/Fru/D-Glc Assay Kit (Megazyme). The determination of soluble sugars was carried out by enzymatic determination using the kit "Sucrose/Fructose/D-Glucose Assay Kit" (Megazyme, USA) (Ch.II-Fig. 3 and Ch.II-Table 2).

In the first step, sucrose was hydrolyzed to glucose and fructose by β-fructosidase, and these sugars were phosphorylated by hexokinase (HK). Glucose-6-phosphate (G6P) was converted to gluconate-6-phosphate by glucose-6-phosphate dehydrogenase (G6PDH) in the presence of $NADP^+$. This reaction releases a NADPH molecule, which is stoichiometric with the amount of glucose molecule. The NADPH was measured with a spectrophotometer (λ = 340 nm). In this part, the endogenous glucose was determined in addition to glucose generated by sucrose degradation. In the second part, glucose and fructose were phosphorylated by hexokinase and the glucose-6-phosphate (G6P) product was converted to gluconate-6-phosphate by glucose-6- phosphate dehydrogenase (G6PDH) in the presence of $NADP^+$. This reaction releases a NADPH, which is stoichiometric with the amount of glucose. The NADPH was then measured with a spectrophotometer (λ = 340 nm). At this step, the endogenous

glucose was quantified. The fructose-6- phosphate (F6P) was converted to glucose-6-phosphate (G6P) by phosphoglucose isomerase (PGI) and converted to gluconate-6-phosphate by glucose-6-phosphate dehydrogenase in the presence of $NADP^+$. This reaction releases a molecule of NADPH for a molecule of glucose and therefore per fructose molecule. The NADPH was measured with a spectrophotometer (λ = 340 nm) to determine the amount of fructose. The amount of sucrose present in the sample was determined by the difference between total glucose measured after the breakdown of sucrose (part I sucrose dosage) and the amount of endogenous glucose (part II glucose dosage).

4. Basic methods in Molecular biology

4.1. RNA extraction

Frozen leaf samples were grounded using TissueLyser II QIAGEN and subsequently, total RNA was isolated from 100 mg of powder with RNA Extraction Buffer method (25 mM Tris HCl, pH 8; 25 mM EDTA; NaCl 75 mM; SDS 1% w/v; β-mercaptoethanol 7.8% v/v) adapted from (Kay et al., 1987). Quantity of RNA was measured using a spectrophotometer (Nanodrop 1000, Thermo Scientific) and RNA integrity was checked by 1.5 % (w/v) agarose gel electrophoresis.

4.2. Yesat RNA extraction

S. cerevisiae cells, EBYVW.4000 strain, were grown overnight in 10 ml of YNB medium at 28°C with shaking at 220 rpm to an OD_{600} of 0.8. The cells were harvested by centrifugation at 4000 *g* for 10 min, resuspended in 1ml of sterile water and then transferred into a 1.5 ml microcentrifuge tube. The washed cells were either frozen in liquid nitrogen before storage at -80°C or used directly for RNA extraction. Yeast cells were incubated with 400 µl of lysis buffer (50 mM Tris-HCl, pH 6.0; 10 mM EDTA; 5% SDS) at 65°C for 5 min, immediately placed on ice, then mixed by inversion with 200 µl of 0.3 M KCl, and centrifugated at 16 000 *g* for 10 min at 4°C to discard cellular debris. In order to isolate nucleic acids and eliminate proteins, the aqueous supernatant was supplemented with an equal volume of phenol/chloroform/isoamyl alcohol (25/24/1, v/v/v), mixed and centrifugated at 16 000 *g* for 10 min at 4°C. Then, the aqueous phase was mixed with one volume of chloroform and centrifugated again under the same conditions. Total nucleic acids were obtained after precipitation of the aqueous phase by adding 0.1 volume 3M sodium acetate and 0.6 volume isopropanol, and incubation for 30 min at -20°C. After centrifugation (16 000 *g*, 10 min, 4°C), the nucleic acid pellet was washed with 70% ethanol, air-dried and resuspended in 200 µl TE

buffer (10 mM Tris-HCl, pH 7.5; 1 mM EDTA pH 8.0). To allow differential precipitation of RNAs, 200 µl of 6M LiCl were added and the mixture was incubated for 30 min at -20°C. After centrifugation (16 000 *g*, 10 min, 4°C), the RNA pellet was washed with 70% ethanol, air-dried, resuspended in 50 µl of sterile water and stored at -80°C.

4.3. cDNA synthesis

Total RNA (1 µg) was treated with DNAse (SIGMA-ALDRICH) in a reaction volume of 10 µL consisted of 1 µg RNA,1 µl of 10X DNAse buffer, 1 µl of the DNase (1U), and water up to 8 µl. The mixture was incubated at 37°C for 30 min, then 1 µl of stop buffer was added before an incubation at 70°C for 10 min, followed by 2 min in ice. cDNA was synthesized by adding 14 µL of a reaction mixture to make a final volume of 25 µl. The reaction mixture consisted of 5 µl of 5X RT buffer (Promega), 1.25 µl of 10 mM dNTP, 2 µl of 10 µM oligo dT, 1 µl of MMLV reverse transcriptase (Promega), and 4.75 µl of H_2O. The mixture was incubated at 37°C for 90 min. The cDNA synthesized was diluted (1:10) with distilled water and stored at -20°C.

4.4. qPCR

The qPCR assays were performed in 96-well plate with the Master Cycler Realplex2 (Eppendorf), in 15 µl reaction mixture: 5 µl of diluted cDNA as template, 7.5 µl of 2 × SYBRGREEN® GoTaq qPCR Master Mix (Promega), 0.5 µl of each of the two gene-specific primers (10 mM) and 1.5 µl of water. The qPCR program was set at 95°C for 2 min, then 40 cycles of 15 s at 95°C, 1 min at 60°C. At the end of amplification, a melting curve was carried to check the specificity of the primers (95°C, 15 s; 60°C to 95°C, 20 min; 95°C, 15 s). The *AtPP2a* (At1g13320) (Czechowski et al., 2005) was used as a reference gene to normalize the expression of *AtESL* genes. The relative expression was determined according to the $2^{-\Delta Ct}$ method. Two or three technical replicates were performed per biological replicate. The sequences of primers used to amplify the cDNA samples are shown in annex V; Table 1.

4.5.Heat shock transformation of *E. coli* competent cell

Two µl of plasmid was added to a chemically competent One shot® Top10 (50 µl, Invitrogen) *E. coli* cells. The reaction was incubated on ice for 30 min and a heat shock was conducted at 42°C for 30 s and the competent cells were immediately returned to the ice for 2 min. 250 µl of SOC was added and the cells were grown at 37°C for 1 h and shaken horizontally (200 rpm). In a next step 100 µl of cells were spread onto LB (Annex II) plates

using the appropriate antibiotics for selection of resistance, and the plates were incubated overnight at 37°C. Colonies were picked for PCR analysis (see section 4.8) and positive clones were cultivated in 5 ml of LB media with antibiotics at 37°C overnight. Stocks in 50% glycerol were stored at -80°C.

4.6. *A. tumefaciens* transformation

Once plant expression constructs were generated they were transformed into *A. tumefaciens* for stable transformation of *A. thaliana* Col 0 or transient expression in *N. benthamiana* tobacco leaves.

4.6.1. Production of electrocompetent *A. tumefaciens* cells strain EHA105

A. tumefaciens competent cells were generated by inoculation of 400 ml YEB medium (Annex II) containing Rifampicin (100 µg/ml) with 4 ml of overnight bacterial culture. These were grown at 28°C, with shaking at 200 rpm, until reaching DO_{600} estimated concentration of 0.6-0.8 arbitrary units. Cells were centrifuged (2000 *g*, 15 min, 4°C) and the pellets were resuspended in 400 ml of ice-cold water and centrifuged again in the same conditions. The pellets were resuspended in 200 ml of ice-cold water and centrifuged again in the same conditions. After centrifugation, the pellets were resuspended with 100 ml of ice-cold water and centrifuged again. The cells were resuspended in 10 ml of ice-cold 10% glycerol and centrifuged (2000 *g*, 15 min, 4°C). Finally, the cells were resuspended in 1 ml of ice-cold 10% glycerol, and dispensed into 50-µl aliquots in sterile microfuge tubes, immediately frozen in liquid nitrogen and stored at -80°C.

4.6.2. Transformation of *A. tumefaciens,* strain EHA105, competent cells by electroporation

One µl to 2 µl of expression vector was added to 50 µl of electro-competent *A. tumefaciens* strain EHA105, mixed gently and left on ice 1 min and then transferred to an electroporation cuvette (Bio-Rad). A pulse was applied from the Bio-Rad Gene-Pulser on the electroporation cuvette. At room temperature, 1 ml of YEB medium was added and the transformed cells were incubated (1 h, 28°C with shaking at 225 rpm) and 100 µl of cells were plated on YEB plates containing rifampicin (25 µg/ml) and the appropriate antibiotics for selection of resistance. After 2 days at 28°C colonies were picked for a colony PCR analysis (see section 4.8), and positive clones were cultivated in 5 ml of YEB media with antibiotics at 28°C overnight and glycerol (20 %) stocks are stored at -80°C.

4.6.3. Heat shock of *A. tumefaciens* strain GV3101 competent cells

Plasmid DNA (2 µl) was mixed gently with 50 µl of competent *A. tumefaciens* strain GV3101 cells and left on ice for 30 min. Heat shock was performed in water bath at 42°C for 30 s and the competent cells were immediately returned to the ice for 2 min. LB medium (250 µl) was added and the cells were grown at 28°C for 1 h and shaken horizontally (200 rpm). After that 100 µl of cells were spread on LB plates using the appropriate antibiotics (Gentamycin, 25 µg/ml; Rifampicin, 100 µg/ml; Spectinomycin, 100 µg/ml) and the plates were incubated 2 days at 28°C. Colonies were screened by colony PCR (see section 4.8), and positive clones were cultivated in 5 ml of LB media with antibiotics at 28°C overnight and glycerol (20%) stocks are stored at -80°C.

4.7. Yeast transformation

S. cerevisiae (strain EBYVW.4000) cells were inoculated into fresh YPM (1% yeast extract,1% peptone, and 2% maltose) plate into 10 ml of YPM liquid medium (Annex III). The cells were incubated at 28°C overnight at 200 rpm. One ml of the yeast culture was centrifuged at 9860 *g* for 30 s and the cell pellet was resuspended in 100 µl of solution A (10 mM Tris-HCl, pH 7.5; 1.0 mM EDTA, pH 8; 0.1 M lithium acetate; 1 M sorbitol) and incubated for 1 h at 28°C. A second centrifugation was carried out for 30 s at 9860 *g*. Five 5 µl of plasmid DNA was added to the cell pellet and gently resuspended in 100 µl of solution B (10 mM Tris-HCl, pH 7.5; 1.0 mM EDTA, pH 8.0; 0.1 M lithium acetate; 40% PEG 4000). The transformation mix was incubated for 30 min at 28°C. A heat shock was then performed in a water bath for 5 min at 42°C. The yeasts were harvested for 30 s at 9860 *g* and resuspended in 100 µl of solution C (10 mM Tris-HCl, pH 7.5; 1.0 mM EDTA, pH 8.0; 0.6 M sorbitol). Eventually, 100 µl of the cell suspension was spread onto a selective medium (YNB) (Annex III) and incubated for 3-4 days at 28°C.

The screen for positive transformants by PCR analysis (see section 4.8) resulted in selection of clones that were cultivated overnight in 5 ml of appropriate auxotrophic YNB medium at 28°C. Stocks in 50% glycerol were stored at -80°C.

4.8. Bacterial and yeast colony PCR

A single colony was picked with a sterile pipette tip and directly dissolved in 50 µl of sterile water. Then, 5 µl of this mixture was used as the DNA template combined with 4 µl of 5X Green GoTaq® Flexi buffer (Promega), 1 µl of forward and reverse primers

(10 µM each primer), 0.4 µl of 10 mM of dNTP, 1.6 µl of 25 mM of $MgCl_2$, 0.5 µl Taq DNA polymerase (5 U/µl) and sterile water up to 20 µl.

The PCR program was 95°C initial denaturation for 2 or 7 min, followed by 35 cycles of 95°C denaturation for 30 s, primer annealing temperature (55 - 64°C) for 30 s, 72°C extension for 2 min and a final extension at 72°C for 5 min. The primer annealing to the template DNA was adapted to the melting temperatures (Tm) of the primer pair.

4.9. Plasmid extraction from bacteria

A 5 ml of LB medium with the appropriate antibiotics were inoculated with a single colony and incubated overnight at 37°C with shaking (200 rpm). After centrifugation (10 min, 4000 g) the DNA plasmids were extracted from the pellets using the QIAprep Miniprep Kit (Qiagen) according to the manufacturer's instructions.

4.10. DNA electrophoresis on agarose gel

5X Green GoTaq® Flexi buffer (Promega) was added to DNA samples, which were loaded on 1% agarose gel (1% agarose in 1X TAE buffer, 0.1 µg/µl Ethidium bromide) and separated at 100V in 0.5×TAE buffer for 20-30 min (depending on the concentration of agarose gel and DNA fragment size) and then the DNA was visualized using UV light.

4.11. Digestion of plasmid DNA

The vector and the insert were digested in a final volume of 20 µl with 2.5 µl of 10X of buffer restriction enzyme (Promega) and 1 U/µg of restriction enzyme and sterile water up to 20 µl. After 3 h of incubation at 37 ° C, the digestion products were loaded on an agarose gel (1 %).

5. Mutant characterization

5.1. Rapid extraction of genomic DNA

Plant DNA was isolated by a rapid DNA extraction method (Edwards et al., 1991). Rapid extraction of genomic DNA was done as follows: leaf tissue was ground with plastic cone shaped bluestick, four hundred µl of extraction buffer (200 mM Tris/HCl, pH 7.5; 250 mM NaCl; 25 mM EDTA, 0.5 % SDS) was added, followed by another grinding cycle under the same conditions as the first one. After centrifugation for 5 min at 16 000 g, 400 µl of supernatant was added to 400 µl of 100% isopropanol. After centrifugation for 10 min at 16 000 g the pellet was washed with 750 µl of 80 % ethanol before final centrifugation for 2 min

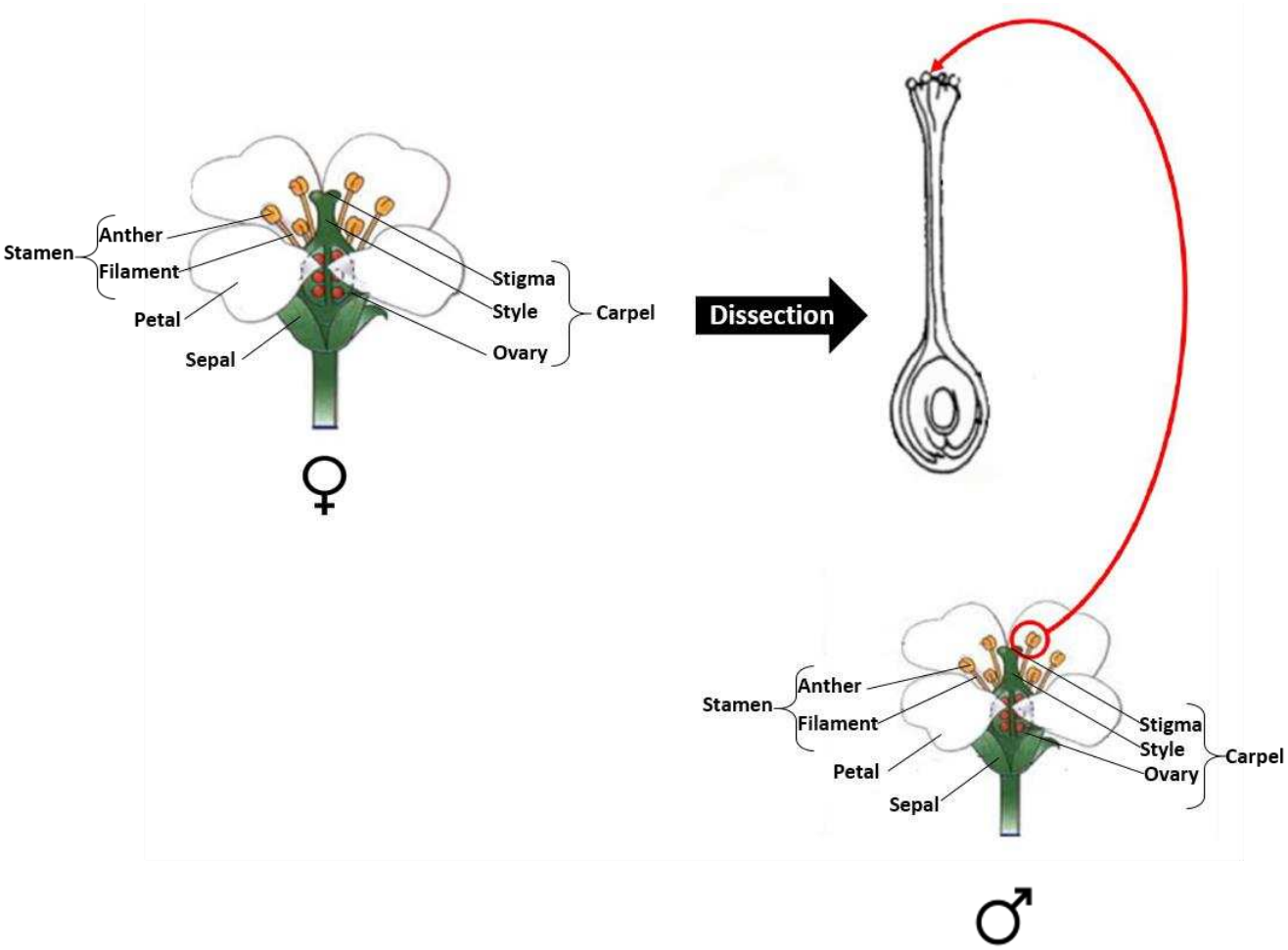

Ch.II-Fig. 4 : Principle of crossing between two individuals of *Arabidopsis thaliana.*
(Adapted from Monier, 2012).

at 16 000 g. The pellet containing DNA was air-dried and resuspended in 50 µl of MilliQ water.

5.2.DNA extraction by NucleoSpin® Plant II kit (Macherey-Nage)

The screening of the double, triple, and quadruple mutants generated by crossing the simple mutant plants, was carried out first by using the rapid DNA extraction method, and the DNA of the selected plants was extracted again using the NucleoSpin® Plant II kit (Macherey-Nagel) following the manufacturers' instructions.

5.3.Plant genotyping using PCR

In order to determine the presence of the T-DNA insertion in homozygous and heterozygous lines, a PCR-based genotyping was used. The genomic DNA was extracted using the rapid DNA extraction method described in section 5.1. Two PCR reactions were performed independently to detect wild-type and mutant alleles. The two primers LP and RP (gene-specific primers) were used to amplify the wild type allele. The primer pairs LP and LBb1.3 (T-DNA primer), as well as RP and LB (T-DNA primer), were used to amplify the mutant allele. The primers used for genotyping are listed in annex V; Table 2.

5.4.DNA amplification by PCR

Two µl of genomic DNA (1 µg) as a DNA template was mixed with 4 µl of 5X Green GoTaq® Flexi buffer (Promega), 1 µl of forward and reverse primers (10 µM each primer), 0.4 µl of 10 mM of dNTP, 1.6 µl of 25 mM of MgCl2, 0.3 µl Taq DNA polymerase (5 U/µl) and sterile water up to 20 µl. The PCR program was 95°C for 3 min, then 35 cycles of 95°C for 30 s, 52-60°C for 30 s, 72°C for 1 min 30 s and final extension 72°C for 2 min. The PCR products were loaded on 1% agarose gel.

5.5.Generation of double, triple and quadruple mutants

5.5.1. Crossing

The opened flowers were removed from the “mother plant” by scissors because all of these are self-fertilized and useless. The close flower buds were gently opened and the stamens were carefully dissected without damaging the stigmas (Ch.II-Fig. 1). Crossing was then carried out by rubbing the stamens of the desired genotype on the stigma. This operation was repeated several times. The buds pollinated in this way were marked by a thread, while the smaller surrounding buds were pinched to arrest their development.

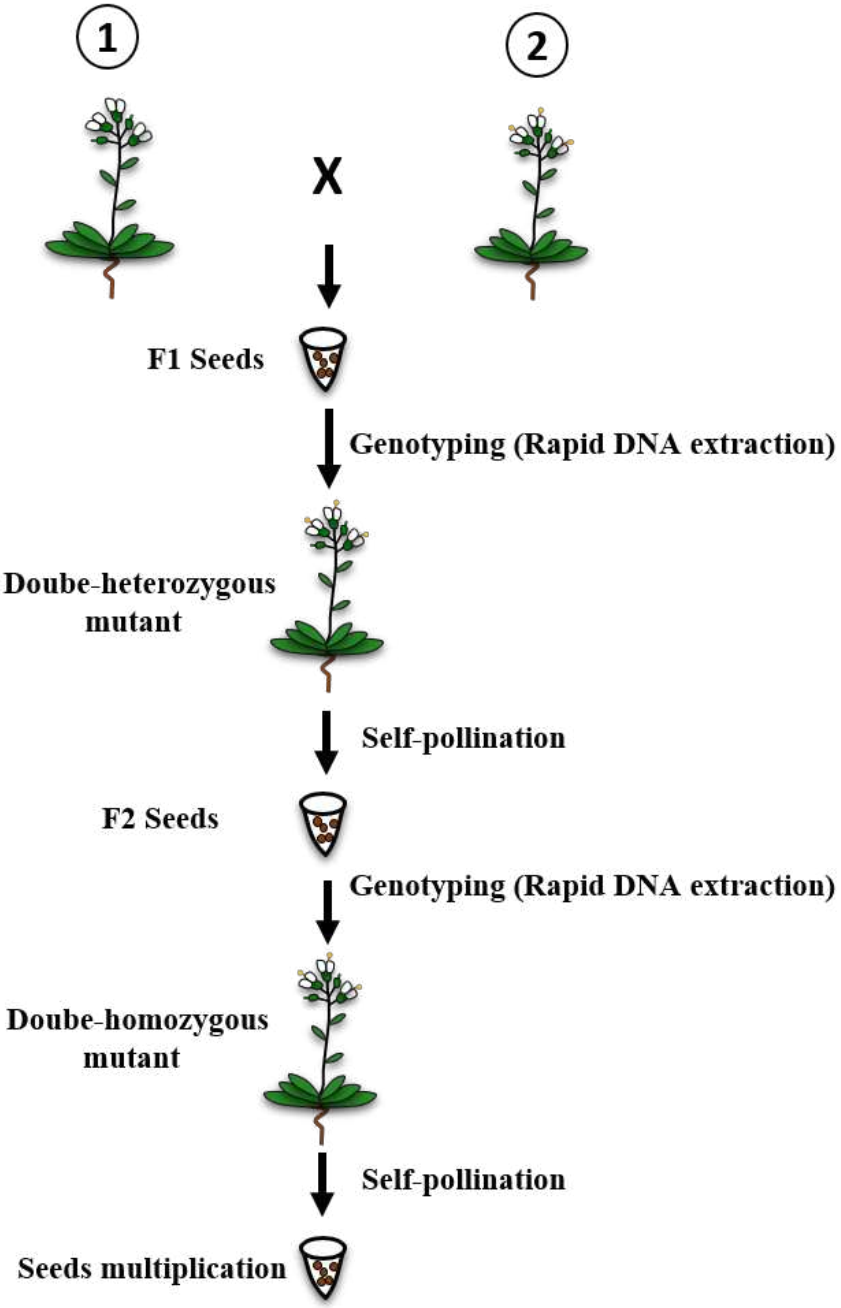

Ch.II-Fig. 5 : The producing and screening strategy used to generate multiple lines of double mutant *atesl*. Numbers 1 and 2 represents the four *atesl* homozygous mutants *esl3.07*, *esl1.02*, *esl3.03*, and *esl3.05* crossed to each other in all possible combinations.

5.5.2. Generation of multiple double mutants atesl

Double mutant lines, each lacking two AtESL transporters genes, were generated by crossing the four homozygous single mutants *esl3.07*, *esl1.02*, *esl3.03*, and *esl3.05* to each other in all possible combinations. The resulting double heterozygous F1 plants after self-pollination produced F2 seeds. F2 seeds were sown and screened by PCR to identify double mutant homozygous plants. F2 homozygous double mutant plants were allowed to self-pollinate, and F3 seeds were obtained (Ch.II-Fig. 5). The resulting homozygous double-mutant F3 seeds were harvested and used for seeds multiplication.

5.5.3. Generation of multiple triple mutants *atesl*

Several strategies were adopted in order to generate multiple triple mutant lines. The three homozygous double mutants *esl1.02esl3.07*, *esl3.03esl3.05*, and *esl1.02esl3.03* were crossed to the four homozygous single mutants *esl3.07*, *esl1.02*, *esl3.03*, and *esl3.05* in all possible combinations. The parental plants were allowed to self-pollinate, and then the F1 seeds were collected.

The searching of *esl1.02esl3.03esl3.05esl3.07* quadruple homozygous mutant, using PCR genotyping, led to finding two homozygous triple mutants: *esl1.02esl3.03esl3.05* and *esl1.02esl3.03esl3.07*.

5.5.4. Generation of the *esl1.02esl3.03esl3.05esl3.07* quadruple mutant

To generate the quadruple mutant *esl1.02esl3.03esl3.05esl3.07*, the homozygous double mutant *esl1.02esl3.07* was crossed with the homozygous double mutant *esl3.03esl3.05*. The resultant F1 quadruple heterozygous plants were allowed to self-pollinate to produce F2 seeds. F2 seeds were sown and screened using PCR to identify homozygous quadruple mutant plants. F2 heterozygous quadruple mutant plants were allowed to self-pollinated, and F3 seeds were obtained for screening of the homozygous quadruple mutant.

6. Cloning of *AtESL1.02*, *AtESL3.03*, *AtESL3.05* and *AtESL3.07* by Gateway® technology for heterologous expression in yeast

6.1. Amplification of *AtESL* gene via PCR

Specific primers were designed to the full-length coding region (CDS) of the four *AtESL* adding 4 nucleotides, CACC, at the 5' end of the forward primer to enable directional cloning using the pENTR™-D-TOPO® cloning kit (Invitrogen) (Annex V; Table 3). The 4 AtESLs were amplified from *Arabidopsis* Col 0 cDNA derived from a water-deprived leaf

sample by PCR using Q5® High-Fidelity DNA Polymerase (New England Biolabs). A 25 µl PCR amplification was performed using 8 µl of diluted cDNA (1:10), 12.5 µl of Q5® High-Fidelity 2X Master Mix (New England Biolabs), 1.25 µl of 10 µM of each forward and reverse primer. The volume was filled up to 25 µl with distilled water. The PCR program was 98°C for 30 s followed by 35 cycles of 98°C for 10 s, 62°C for 30 s, 72°C for 1 min and a final extension at 72°C for 2 min. The annealing temperature was calculated according to the NEB $_{Tm}$ calculator. The Amplified PCR products were loaded on an agarose gel (1%).

6.2. Cloning AtESLs PCR products via the TOPO cloning reaction

After PCR, unpurified PCR products were directionally cloned into the pENTR/D-TOPO entry vector using pENTR Directional TOPO Cloning Kit, Invitrogen. Directional TOPO cloning works in a way that the overhang (GTGG) in the vector anneals to the added bases (CACC) at the 5'of the PCR product. In the TOPO cloning reaction, 0.5 to 4 µl of PCR reaction was added to 1 µl of pENTR/D-TOPO vector and 1 µl of salt solution. Water was added to a final reaction volume of 8 µl, then the reaction was incubated at room temperature (23°C) for 30 min. Subsequently, 2 µl of each reaction was transformed into TOP10 chemically competent *E. coli* cells (see section 4.5) and eight bacteria containing entry clones were picked on LB kanamycin medium and checked by colony PCR analysis (see section 4.8), positive clones were selected for plasmid isolation using the QIAprep Spin Miniprep Kit from Qiagen, following the manufacturer's instructions (see section 4.9). The presence of the insert in the plasmids was confirmed by restriction analysis (see section 4.11) and sequencing. The plasmid was sequenced using the M13 forward and T7 reverse primers by the Eurofins Genomics (Germany) (Annex V; Table 3).

6.3. LR reaction

After having checked that the AtESLs were correctly inserted into the pENTR/D-TOPO plasmid, LR recombination reactions were performed. The AtESLs flanked by attL sequences in the entry vector were recombined with attR sequences in the destination pDRf1-GW vectors. This recombination was performed using 1U LR Clonase™ II enzyme. The LR reaction was set up by combining 1.5 µl entry vector (pENTR/D-TOPO –AtESLs), 0.5 µl destination vector (pDRf1-GW), and 1 µl of LR Clonase™ II enzyme (Invitrogen). The reaction volume was adjusted to 5 µl with TE buffer (pH 8.0). After incubation (1 h, 25 °C), 2 µl of each reaction was transformed into TOP10 chemically competent *E. coli* cells and bacteria-containing expression clones were picked on LB ampicillin medium and checked by colony PCR analysis, positive clones (pDRf1-GW-AtESL) were selected for plasmid isolation

using the QIAprep Spin Miniprep Kit from Qiagen, following the manufacturer's instructions. The presence of the insert in the plasmids was confirmed by restriction analysis and sequencing. The plasmid was sequenced using the PMA forward and ADH close reverse primers by the Eurofins Genomics (Germany) (Annex V; Table 3).

7. Cloning of the AtESL3.05 and AtESL3.03 using restriction enzymes for heterologous expression in yeast

7.1. PCR amplification

The full-length coding region (CDS) of the 2 AtESL was amplified with specific primers to add XhoI and BamHI as flanking restriction sites before being cloned into the multiple cloning sites (MCS) of the pDR195 yeast expression vector. To that aim AtESLs were amplified by PCR from *Arabidopsis* Col 0 cDNA derived from a water-stressed leaf sample using Q5® High-Fidelity DNA Polymerase (#M0492S, NEB). The AtESL3 was amplified with the ESL3.5-XhoI-F and ESL3.5-BamHI-R primer pair harboring the XhoI and BamHI restriction sites, respectively. The AtESL3.03 was amplified with the ESL3.3 -XhoI-F and ESL3.3-BamHI-R harboring the XhoI and BamHI restriction sites, respectively. In addition, three bases were added upstream of the restriction sites to improve cutting performance. The cDNA of AtESL3.05 and AtESL3.03 was amplified using the primers listed in Annex V; Table 4.

The PCR conditions were as follows: 25 µl of Q5® High-Fidelity 2X Master Mix (#M0492S, NEB), 2.5 µl of 10 µM of each forward and reverse primer and distilled water to a final volume of 50 µl. The PCR program was 98°C for 30 s, then 7 cycles of 98°C for 10 s, 65°C for 30 (+2°C every 7 cycles) s, 72°C for 1 min with the final extension at 72°C for 2 min. The 7-cycle loop was repeated five times (35 cycles). Subsequently, the PCR products were loaded on a 1% gel agarose. Afterward, an A-tailing with the Taq-Polymerase (5U/ 1 µl, Promega) for 20 min at 72°C was performed, followed by cloning into the pGEM®-T Easy Vector (Promega) and in a second step into the pDR195 yeast expression vector.

7.2. Cloning of AtESLs coding region into pGemT-easy vector

The unpurified PCR products were followed by an A-tailing using the Taq-Polymerase (5U/ 1 µl, Promega). For dA-tailing, the reaction mixture was consisted of: 4 µl of PCR products, 2 µl of Go Taq buffer, 0.4 µl of 10 µM of dATP and 1 µl of Taq polymerase (5U/ µl). The final volume was made up to 10 µl with water and the mixture was then incubated at 72 °C for 20 min.

The dA-tailed PCR products were ligated to pGEM®-T Easy Vector using T4 DNA ligase. The reaction mix was consisted of: 2 µl of dA-tailed PCR products mixed with 1 µl of pGEM®-T Easy vector (Promega), 5 µl of 2X rapid ligation buffer and 1 µl of T4 DNA ligase (3U/µl). The final volume was adjusted to 10 µl with water and the mixture was then incubated at 16°C overnight. 2 µl of each ligation product was transformed into TOP10 chemically competent *E. coli* cells and eight bacteria colonies were picked on LB agar plates containing the appropriate antibiotic for selection (ampicillin, X-Gal, and IPTG) and checked by colony PCR analysis, positive clones were selected for plasmid isolation using the QIAprep Spin Miniprep Kit from Qiagen, following the manufacturer's instructions. The presence of the insert in the plasmids was confirmed by restriction analysis and sequencing. The plasmid was sequenced using the SP6 and T7 vector primers by the Eurofins Genomics (Germany) (Annex V; Table 4).

7.3.Digestion and cloning of AtESLs coding region into PDR195 vector

After checking the correct integration of AtESLs flanked by XhoI and BamHI restriction sites in the pGEM®-T Easy vector, the vector was then digested with XhoI and BamHI, and the cleaved insert was inserted into the XhoI and BamHI sites of the pDR195 vector, which was prepared by digestion with the same enzymes to generate the pDR195-AtESL3.05 and pDR195-AtESL3.03 vectors. The digestion was performed in two steps because XhoI and BamHI have 100% activity in the different buffer. The first digestion reaction consisted of 1 µg of DNA plasmid was digested with 1 µl of BamHI (40–80 u/µl), 2 µl of buffer E (Promega), 1 µl of bovine serum albumin (BSA) and MilliQ water to a final volume of 20 µl, the reaction mixture was then incubated during 3 h at 37°C. The second step of digestion was performed by adding to the same reaction mixture 1 µl of XhoI (40–80u/µl), 2 µl of buffer D (Promega), 4 µl of BSA, 1 µl of NaCl and water to a final volume of 100 µl. Unpurified digested vector and AtESLs insert were ligated using T4 DNA ligase and transformed into TOP10 chemically competent E. coli cells. Transformants were screened by colony PCR and positives colonies were sequenced with the PMA forward and ADH close reverse primers by the Eurofins Genomics (Ebersberg, Germany) (Annex V; Table 3).

8. Functional analysis of AtESLs in yeast: Drop test yeast complementation assay

Respective AtESLs cloned in pDRf1-GW or pDR195 vector and the corresponding empty control vectors pDRf1 and pDR195 were transformed into *S. cerevisiae* strain

BYW4000. Transformants were prepared as described above in section 4.6. The positive transformants were grown in 5 ml of liquid selective medium (YNB) with maltose (2%) and supplemented with appropriate auxotrophic requirements to an DO_{600} of 0.6 -1.0. The next day, 1.5 ml of culture was centrifuged (3000 g, 5 min), and the cell pellets were resuspended 4 times with 1.5 ml of sterile water to an OD_{600} of 0.5. Four serial dilutions (1:10) of cell suspensions were done. Diluted cell suspensions were plated by pipetting 10-µl drops of dilutions containing respectively 10^5,10^4,10^3, and 10^2 yeast cells/µl on YNB selective medium without uracil and containing as a carbon source either 2% maltose (as a positive control), or 2% fructose, 2% glucose, 2% galactose, 2% mannose. The plates were incubated for 5 days at 28°C.

9. Subcellular localization of *AtESL3.05*

9.1. Plasmid construction using Gateway® technology

The AtESL3.05-GFP and AtESL3.07-GFP fusion constructs used for localization studies were derived from the destination vector pB7FWG2, which enables the C-terminal fusion of AtESLs protein with GFP. The full-length coding region (CDS) of the 2 AtESL is amplified without a stop codon using a pair of specific primers. The amplified AtESLs CDS were cloned into the pENTR/D-TOPO vector using the pENTR Directional TOPO Cloning kit (Invitrogen). The products were transferred into the pB7FWG2 vector by LR recombination reaction (Invitrogen), to generate the pB7FWG2-AtESL3.05-GFP and pB7FWG2-AtESL3.07-GFP vectors. The presence of the insert in the plasmids was confirmed by DNA sequencing using the p35S and t35S by the Eurofins Genomics (Germany) (Annex V; Table 3).

All PCR amplifications were performed using Q5® High-Fidelity DNA Polymerase (NEB) and Arabidopsis Col0 cDNA derived from a water-stressed leaf sample was used. All recombinant DNA plasmids were transformed into TOP10 chemically competent E. coli cells as described above. PB7FWG2-AtESL3.05-GFP and pB7FWG2-AtESL3.07-GFP vectors were transformed into *A. tumefaciens* strain GV3101 by heat shock.

For transient co-expression of the GFP fusion constructs with the tonoplast marker constructs, the pGreen0179 harboring the p35::TIP1;1-mCherry construct was used. This plasmid was provided by Doan Trung LUU (BPMP laboratory, Montpellier University). This construct was introduced into *A. tumefaciens* strain EHA105 by electroporation.

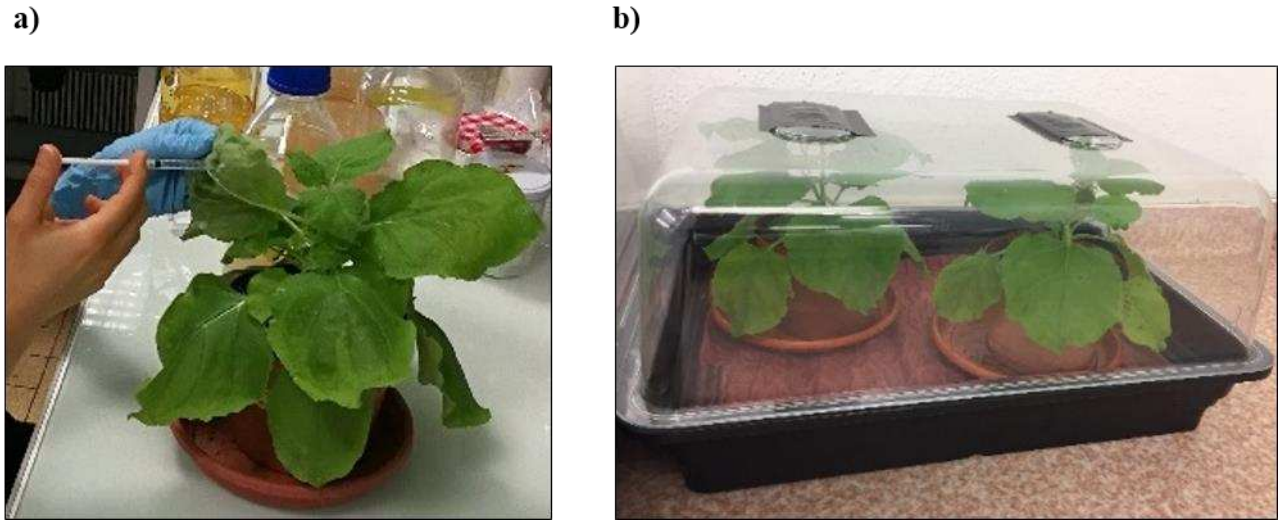

Ch.II-Fig. 6: a) Agroinfiltration of the tobacco leaves (abaxial side) using a syringe without a needle. b) Agroinfiltrated tobacco plants placed in mini greenhouse to maintain humidity.

9.2. Transient expression in *Nicotiana benthamiana* leaves by agroinfiltration

To determine the subcellular localization of AtESL3.05 in tobacco protoplasts, the transient expression of AtESL3.05-GFP, AtESL3.07-GFP (as positive control) fusion constructs in the abaxial surface of the leaf of *N. benthamiana* was performed by agroinfiltration using *A. tumefaciens* strain GV3101. In parallel, transient co-expression of the GFP fusion constructs with the tonoplast marker Tonoplast Intrinsic Protein TIP-mCherry (provided by Doan Trung LUU, BPMP laboratory –Montpellier) was performed by agroinfiltration using *A. tumefaciens* strain EHA105. Two days before agroinfiltration, a single colony derived from each recombinant *A. tumefaciens* (strain GV3101 and EHA105) was inoculated in 3 ml of LB or YEB with antibiotics. The bacterial cultures were incubated overnight at 28°C with shaking at 200 rpm, and 1 ml of the culture was inoculated into 20 ml of LB or YEB medium with antibiotics and incubated overnight at 28°C and 200 rpm. After centrifugation (2000 g, 10 min) the pellets were resuspended and adjusted to 0.2-0.6 arbitrary units of DO_{600} in the induction medium (Annex IV). In a next step acetosyringone was added to final concentration of 100 µM, and the suspension was incubated on a shaking platform for 6 h at 28°C and 200 rpm. The bacterial suspensions were centrifuged for 10 min at 4000 rpm. The resulting cell pellet was resuspended in the infiltration medium (Annex IV), adjusted to 0.2-0.6 arbitrary units of DO_{600}, and supplemented with acetosyringone at final concentration of 100 µM. The bacterial suspensions were infiltrated into abaxial leaves of 4-5-week-old *N. benthamiana* plants using a syringe without a needle (Ch.II-Fig.6a). The edge of the infiltration region was immediately marked with a black marker. After infiltration, the plants were placed in a mini-greenhouse and transferred into a culture chamber of 16 h/8 h day/night photoperiod and at temperatures of 22 - 24°C (Ch.II-Fig.6b). After 3 days of infiltration, the GFP or mCherry fluorescence appeared, and the isolation of tobacco protoplasts was performed following the steps outlined below in the next section. Upon protoplast isolation, the localization of fluorescent fusion proteins, GFP or mCherry in tobacco protoplasts was visualized through using confocal microscope.

9.3.Isolation of protoplasts from agroinfiltrated tobacco leaves

The agroinfiltrated tobacco leaves were cut into small pieces, excluding the main veins and the damaged regions, using a sharp razor blade. Immediately, the lower surface of the leaf was put facing down in a Petri dish of 9 mm-diameter filled with 9 ml of freshly prepared enzyme solution containing 1 % cellulase (w/v) and 0.25 % macerozyme (w/v) in TEX

medium (3 mM NH_4NO_3, 5 mM $CaCl_2.2H_2O$, 2.4 mM MES, 0.4 M sucrose) in Gamborg B5 medium (#G02209, Duchefa). The leaf tissue strips were incubated in the dark at 28°C for 16 h to perform digestion. After incubation, the released protoplasts were harvested by gently shaking the plates; in this way the suspension became greener. The protoplasts-containing enzymatic suspension was overlaid using a Pasteur pipette onto a steel sieve of 149 µm pore size and filtered. Additional 1mL of TEX medium was added to the same plates to release the remaining protoplast.

The filtrated suspension of protoplasts was mixed with 1 ml of Mannitol/W5 (4:1, v/v), i.e. 400 mM Mannitol in W5 medium (154 mM NaCl, 125 mM $CaCl_2$, 5 mM KCl, 5 mM glucose, 1.4 mM MES, pH 5.6), and centrifuged for 15 min at 100 *g* and 20ºC. After centrifugation, the supernatants containing the intact protoplasts were transferred into 1 ml of Mannitol/W5 at a different ratio (2:3, v/v), gently mixed, and centrifuged for 15 min at 100 *g*. The protoplast pellets were carefully resuspended in 1 ml of Mannitol/W5 (2:3, v/v) and centrifuged for 15 min at 100 *g* and 20ºC. The pellets were resuspended into Mannitol /W5 (2:3, v/v) and kept on ice until used for protoplast imaging.

9.4. Confocal microscopy

Confocal images were acquired with a laser scanning confocal microscope (Olympus FV1000, France). Argon laser with 488 nm line was used for excitation of GFP and emission fluorescence was recorded through spectral detection channel between 500-530 nm (green fluorescence emission). Red fluorescence (mCherry) was obtained sequentially with a 543 nm line of a HeNe laser and detected between 555-625 nm. The chlorophyll auto-fluorescence was detected with 633 nm excitation and >680 nm emission. Images of 800x800 pixels were acquired with planApo N x60 oil 1.4 NA objective lens. Numerical zooming at 0.13 µm pixel size was done in respect to oversampling Nyquist cryteria.

3D optical sectioning of 0.2 to 0.4µm was driven with step Z-axis motor. 3D images were analyzed with Imaris software (Bitplane, Switzerland). Images are maximum intensity projection resulting from optical sectioning of the specimen (20-60 sections, 1µm step).

10. Stable transformation in *A. thaliana*: transgenic plants overexpressing *AtESL3.05* gene

The stable transformation of *A. thaliana*, ecotype Col 0 using the floral dip method took place just after plants have formed multiple floral buds and flowers. The *Agrobacterium* strain GV3101 was transformed with binary vector pB7FWG2 containing the AtESL3.05:: GFP

construct under the control of the constitutively active 35S promoter of the cauliflower mosaic virus. A single colony from the recombinant *Agrobacterium* strain GV3101 was inoculated in 3 ml of YEB medium supplemented with antibiotics (20 mg of Gentamycin, 50 mg of Rifampicin, 50 mg of Spectinomycin), and incubated overnight at 28 °C with shaking at 200 rpm. The 3 ml culture was used to inoculate 20 ml of YEB medium with antibiotics and incubated overnight at 28°C and 200 rpm. After 24 h, *Agrobacterium* cells were centrifuged for 10 min at 2000 g, and the pellets were resuspended in infiltration medium (5% sucrose, 2.2 g MS, 300 µl Silwet L-77, 20 µl BAP, 1 ml of Gamborg B5 vitamins, 100 µM acetosyringone), and their concentration adjusted to 2.4 arbitrary units at DO_{600}. The floral meristems were dipped into the *Agrobacterium* infiltration medium for 5 min. The transformed plants were protected from light for 24 h before returning to the phytotron and grown until seeds were harvested. The selection of primary transformants T1 (seeds collected from transformed plants) was carried out by spraying Basta (Bayer) herbicide at 0.1% (v/v).

11. Isolation of vacuoles

11.1. Plant material and growth conditions

A. thaliana Col 0 and Arabidopsis T-DNA insertion lines, *atesl3.05* (SALK_047351) were grown in the same conditions as stated in section 2.1, the sole difference is that the seedlings were individually transplanted into pots (15 plants per tray) after 13 days of growth. Before the vacuoles isolation experiment, seven-week-old *A. thaliana* plants (Col 0 and the mutant *esl3.05*) were exposed to a low light intensity level (30 $\mu mol.m^{-2}.s^{-1}$) four days prior to the experiment. The plants were subsequently placed in darkness two days before the vacuoles isolation.

Vacuoles' isolation - solutions

- *Protoplast medium*: 500 mM sorbitol, 1 mM $CaCl_2.2H_2O$, 10 mM MES, pH 5.6 (adjusted with KOH, autoclaved and stored at 4°C)
- *Betaine buffer*: 400 mM betaine.H_2O, 30 mM potassium gluconate, 20 mM HEPES, pH 7.2 (adjusted with 1M imidazole, autoclaved and stored at 4°C)
- *Sorbitol buffer*: 400 mM sorbitol, 30 mM potassium gluconate, 20 mM HEPES, pH 7.2 (adjusted with 1M imidazole)
- *Lysis buffer*: 200 mM sorbitol, 20 mM EDTA, 10 mM HEPES, pH 8.0 adjusted with KOH before adding Ficoll™ PM400 (GE Healthcare 17-0300-10) at 10% final concentration. Ficoll is better dissolved in solution precooled to 4°C.

- *Percoll, pH 6*: 500 mM sorbitol, 1 mM $CaCl_2.2H_2O$, 20 mM MES in 100% Percoll (GE Healthcare 17-0891-02). pH, usually 5.9-63
- *Percoll, pH 7.2*: 500 mM sorbitol, 20 mM HEPES in 100% Percoll (GE Healthcare 17-0891-02).

11.2. Vacuoles' isolation - methods

All experimental steps were performed on ice and all centrifugations were carried out without brake.

Isolation of *Arabidopsis* rosette leaves was performed as previously described (Burla et al., 2013). In order to remove epidermis, *Arabidopsis* rosette leaves from 6-7-week-old plants were scratched with fine sandpaper (P400 granules) on their abaxial side. Scratched leaves were immediately placed in 15 ml of protoplast media supplemented with 1 mg/ml BSA. It should be noted that before the addition of enzymes containing medium, the protoplast media has to be well aspirated, because BSA inhibits enzymes. The leaves were further incubated in 10 ml of protoplast media supplemented with 1% Cellulase R10 (Duchefa Biochimie), 0.5% Macerozyme R10 (Duchefa Biochimie), for 2 h at 30°C. After incubation, the protoplasts were carefully collected and filtered through a stainless steel sieve of pore size 149 µm. Filtered protoplast suspensions were underlayered with 2 ml of 100% Percoll, pH 6 as a cushion. After centrifugation for 8 min at 470 g and 4°C, the upper layer containing the concentrated protoplasts was removed and protoplasts were mixed in the remaining solution. Additional volume of 100% Percoll, pH 6 was added to a final concentration of 40% before purification by density gradient centrifugation**.** To that aim protoplast suspension was overlaid with Percoll pH 7, 30% 1:1 (v/v) and 0.7 volume of sorbitol supplemented with 1 mg/ml BSA and 1 mM DTT. After centrifugation for 8 min at 250 *g* and 4°C, the purified protoplasts were collected from the interface between 30% Percoll, pH 7 (middle phase) and sorbitol (upper phase), and were mixed with equal volume of fresh lysis buffer pre-warmed at 42°C. The suspension was incubated for 10 min at room temperature and under gentle hand shaking by inversion. The vacuoles' release from protoplasts was controlled under microscope after 2 and 8 min of incubation. At the end of incubation, the reaction was immediately stopped by placing the tubes on ice. Lysed protoplast solution of each sample (10 ml) was divided into two equal volumes in 14 ml ice-cold glass Corex tubes. Vacuoles were further purified and concentrated by step density gradient, i.e. 5 ml of lysate initially overlaid with 5 ml of mixture

containing lysis buffer and betaine buffer at a ratio of 1:1 (v/v), and, as a next step, additional overlay with 1 ml of betaine buffer containing 1 mg/ml BSA and 1 mM DTT. After centrifugation for 8 min at 1310 *g* and 4°C, the purified vacuoles were carefully recovered from the interface between lysis buffer/fresh betaine (middle phase) and betaine buffer (upper phase). The purity and density of vacuoles were controlled under microscope. Eventually, before vacuoles were used for the transport activity experiment, the vacuoles-enriched suspension was supplemented with 100 % Percoll, pH 7.2, at final concentration of 30 %.

12. In *silico* analysis

The 1000 bp long promoter sequences of the nineteen *AtESL* genes were retrieved from TAIR (The *Arabidopsis* Information Resource) database. These sequences were then analyzed for the presence of *cis*-regulatory elements using PLACE (Plant Cis-acting Regulatory DNA Elements) database (http://www.dna.affrc.go.jp/htdocs/PLACE/).

CHAPTER III

Early-response-to-dehydration Six-Like (ESL) transporter family: emergence in Charophytes and evolution in the land plants

1. Introduction

La gestion du carbone par les plantes implique l'activité de nombreux transporteurs de sucre, qui jouent un rôle dans la partition et la re-allocation des sucres subcellulaires à l'échelle de tout l'organisme. Parmi ces transporteurs, les transporteurs de monosaccharide ESL (Early response to dehydration Six-Like) sont encore mal caractérisés bien qu'ils représentent l'une des plus grandes sous-familles de transporteurs de sucre. Cette étude fait appel à une approche génomique évolutive pour reconstruire l'histoire évolutive de cette famille multigénique. Aucune ESL n'a pu être identifiée dans le génome des rhodophytes, des chlorophytes et de l'algue brune *Ectocarpus siliculosus*, tandis qu'une ESL a été identifiée dans le génome de *Klebsormidium nitens* fournissant la preuve de l'émergence de ces transporteurs avec les Charophytes. Une analyse phylogénétique sur 519 protéines ESL putatives identifiées dans le génome de 47 espèces d'Embryophyta, espèces représentatives du règne végétal, a révélé que les séquences de protéines ESL peuvent être divisées en trois groupes, suggérant au moins trois événements majeurs de duplication liés à l'ensemble du génome, événements de duplication déjà décrits pour les plantes terrestres. Le premier s'est produit chez les ancêtres communs de tous les spermaphytes (ζ : il y a 340 millions d'années), le second chez l'ancêtre commun des Angiospermes (ε : il y a 170-235 millions d'années) et le troisième avant la séparation des rosidées et les astéridées (γ / 1R: 117 MYA). Chez certaines Eudicots (Vitales, Malpighiales, Myrtales, Sapindales, Brassicales, Malvales et Solanales), la famille ESL présente une expansion remarquable en relation avec la duplication en tandem. L'analyse des mutations non synonymes et synonymes par le rapport moyen dN / dS des copies ESL du genre *Arabidopsis* a révélé que les gènes ESL sont soumis à une sélection purifiante, même si l'augmentation progressive de ce rapport à travers les trois groupes agit en faveur des phénomènes de sous-diversification. La recherche de nouvelles fonctions des transporteurs de monosaccharide ESL a abouti à une identification et caractérisation approfondie de la structure de leurs gènes, des éléments *cis*-régulateurs de régions promotrices, ainsi que des motifs spécifiques des protéines codées.

Le profilage d'expression des ESL de *Arabidopsis* a conduit à l'identification des gènes constitutivement exprimés, ainsi que d'autres présentant d'expression préférentielle dans les différents organes. Ces résultats cooroborent l'émergence des premiers ESLs chez les Charophytes, ainsi que leur remarquable expansion chez les Eudicots.

2. Article 1

Early-response-to-dehydration Six-Like (ESL) transporter family: emergence in Charophytes and evolution in the land plants

Lucie Slawinski, Abir Israel, Caroline Paillot, Florence Thibault, Richard Cordeaux, Rossitza Atanassova, Fabienne Dédaldéchamp, Maryse Laloi*

Laboratoire Ecologie et Biologie des Interactions, Equipe "SEVE-Sucres et Echanges Végétaux-Environnement," UMR Centre National de la Recherche Scientifique 7267, Université de Poitiers, Poitiers, France

Correspondence

Dr. Maryse LALOI

maryse.laloi@univ-poitiers.fr

Abstract

Carbon management by plants involves the activity of many sugar transporters, which play roles in sugar subcellular partitioning and re-allocation at the scale of the whole organism. Among these transporters, the ESL (Early response to dehydration Six-Like) monosaccharide transporters are still poorly characterised although they represent one of the largest sugar transporter subfamilies. In this study, we used an evolutionary genomic approach to rebuild the evolutionary history of this multigenic family. No ESL could be identified in the genomes of rhodophytes, chlorophytes and the brown algae *Ectocarpus siliculosus* while one ESL was identified in the genome of *Klebsormidium nitens* providing evidence for the emergence of these transporters in Charophytes. A phylogenetic analysis using 519 putative ESL proteins identified in the genomes of 47 Embryophyta species, representative of the plant kingdom, has revealed that ESL proteins sequences can be divided into three groups. The latter suggests at least three major duplication events which are related to the whole genome duplication events already described for terrestrial plants. The first has occurred in the common ancestors of all spermaphytes (ζ :340 million years ago), the second in the common ancestor of Angiosperms (ε :170-235 million years ago) and the third before the separation of rosids and asterids (γ /1R: 117 MYA). In some Eudicots (Vitales, Malpighiales, Myrtales, Sapindales, Brassicales, Malvales and Solanales), the ESL family presents remarkable expansion in relation with tandem duplication. The analysis of non-synonymous and synonymous mutations by the dN/dS mean ratio of the *ESL* copies of the genus *Arabidopsis* has revealed that *ESL* genes are submitted to a purifying selection even if the progressive increase of dN/dS ratio trough the three groups acts in favour of sub-diversification phenomena. In order to further explore the possible acquisition of novel functions by ESL monosaccharide transporters, we identified their gene structure, and promoter cis-acting elements. The expression profiling of the *Arabidopsis ESL,* unraveled copies that are almost constitutively expressed and others displaying organ-preferential expression patterns. Our results strongly support the idea for the emergence of the first *ESL* copies in Charophytes, as well as their remarkable expansion in Eudicots.

Keywords: Sugar transporters, monosaccharides carriers, ERD6-like, ESL, evolution, gene duplication, Arabidopsis

Introduction

In higher plants, sugars display numerous important roles. They constitute sources of cellular energy and carbon skeletons, necessary for different biosynthesis pathways such as starch and cellulose biosynthesis. Acting as compatible osmolytes, they can prevent cellular damages caused by various abiotic stresses. Sugars represent also important signal molecules. They are distributed through the plant *via* sugar transporters, which are involved not only in sugar long-distance transport *via* loading and unloading of the conducting complex, but also in sugar allocation into source and sink cells. Sugar carriers belong to three different multigenic families: SWEET (Sugar will be Eventually Exported Transporter) (Chen et al., 2010a), di-saccharides transporters (SUC/SUT) (Sauer, 2007; Reinders et al., 2012) and monosaccharides transporters (MST) (Büttner, 2007). The MST family can be divided into seven subfamilies, among which that of the ESL (Early response to dehydration Six-Like). The latter represents in many species the largest subfamily, encompassing 19 members in *Arabidopsis* (Büttner, 2007) and 22 in *Vitis vinifera* (Afoufa-Bastien et al., 2010). The lineage *Brassica* present a very large ESL sub-family, between 24 to 30 ESL copies are present in *B. rapa*, *B. oleracea* and the allotetraploid *B. napus* (A and C sub-genomes)(Zhang et al., 2020). In Fabaceae, ESL family seems to be smaller as Medicago (*Medicago truncatula*) and pea (*Pisum sativum*) comprised 10 MtESL and 9 PsESL, respectively (Doidy et al., 2019). Similarly, the genome of *Malus domestica* (Wei et al., 2014), *Solanum lycopersicum* (Reuscher et al., 2014), *Ricinus communis* (Mao et al., 2017) and *Oryza sativa*(Deng et al., 2019) contains 11, 10, 9 and 6 *ESL* genes, respectively. The genome of root parasitic angiosperm weeds such as *Striga hermonthica*, *Triphysaria versicolor*, *Mimulus guttatus* and *Phelipanche aegyptiaca* are described to contain 8, 6, 6 and 5 *ESL*, respectively (Misra et al., 2019). By searching EST databases of various species representing all terrestrial plants, Johnson et al., (2006) could detect one ESL in genomes of *Selaginella* and *P. patens*, 4 in *Pinus taeda* and *Zea Maize*. Few years after, (Lalonde and Frommer, 2012) identified also 1 *ESL* in the genome of *Selaginell*a but no *ESL* in *P. patens* genome. These findings demonstrate that ESL are also present in ancient embryophyte lineages. The comparison of *Arabidopsis* and rice revealed that in rice, the STP (Sugar Transport Protein) and PLT (Polyol Transporter) subfamilies were greatly expanded, while the ESL subfamily was much larger in *Arabidopsis* (Johnson and Thomas, 2007). This difference might be due to the number of tandem duplication events during their evolutionary histories and it has been proposed that the expansion of the ESL subfamily is due to two segmental duplications and six tandem

duplications (Johnson et al., 2006). Finally, in Grapevine (*Vitis vinifera*) 14 ORFs VvESL were found to be located in tandem on chromosome 14 (Afoufa-Bastien et al., 2010). Altogether, these results put into question the biological necessity of so many duplicated *ESL* genes in some plant genomes.

Despite this high number of genes, only few *ESL* genes have been studied until now and their biological function remains largely unknown. The first ESL, named ERD6 (*At1g08930*), has been identified by differential screening of cDNA library from *Arabidopsis thaliana* plants exposed to dehydration stress (Kiyosue et al., 1994). *AtERD6* expression is up-regulated by drought (Kiyosue et al., 1998; Seki et al., 2002; Yamada et al., 2010), low temperature (Kiyosue et al., 1998), high salinity (Yamada et al., 2010) and is induced by ABA (Yamada et al., 2010). AtESL1 (for ERD six-like 1 – *At1g08920*) is a low affinity facilitator able to transport different hexoses (glucose, fructose, galactose, mannose and xylose) across the tonoplast. Its expression is up-regulated by drought, high salinity and (Yamada et al., 2010). *AtSFP1* and *AtSFP2* (Sugar-porter family protein 1 and 2 – *At5g27350* and *At5g27360*) are two tandem duplicated genes located on chromosome 5. These two genes displayed different expression patterns during leaf development. *AtSFP1* was detected in seedlings nine days after germination, but not in mature plant organs (leaves, flowers, flower buds, stem, and roots), while *AtSFP2* was expressed in all tested plants organs, and in seedlings. Further analysis showed that only *SFP1* is induced during leaf senescence but the expression of *AtSFP2* remains stable during this process (Quirino et al., 2001). AtZIF2 (Zinc-induced Facilitator – At2g48020) is a tonoplastic transporter, which is expressed in different organs, mainly in roots where it promotes the sequestration of zinc into the vacuole (Remy et al., 2014). AtERDL6 (Early Responsive to Dehydration-Like six – At1g75220) is a tonoplastic H^+/glucose symporter involved in the export of glucose from the vacuole in conditions that require the mobilization of vacuolar carbohydrate reserves. Indeed, the expression of *AtERDL6* was induced in conditions of darkness, heat stress, and wounding leaves. On the other hand, the *AtERDL6* expression was dropped under cold stress and external glucose supply during which glucose accumulates in the vacuole (Poschet et al., 2011). Furthermore, *atesl1.2* mutant showed a raise of vacuolar glucose content (more than 90 %) compared to the wild type (86%) (Poschet et al., 2011) while *Arabidopsis* lines overexpressing *AtERDL6* had lower glucose levels than wild-type plants (Klemens et al., 2014). Only 3 ESL from other species have been characterized. The apple MdERDL6-1, an orthologue of AtERDL6 in *Arabidopsis*, was recently identified. It is highly expressed in fruits; its encoded protein seems to be localized at the tonoplast and acts as an H^+/glucose symporter with a low affinity

glucose. In contrary to AtERDL6 the overexpression of MdERDL6-1 leads to an increase rather than a decrease in the sugar levels in apple and tomato leaves and fruits (Zhu et al., 2021). In Pineapple (*Ananas comosus*) the cDNA screening of a leaf cDNA library by degenerated PCR lead to the identification of AcMST1, an ESL which is demonstrated to be localized to the tonoplast (Antony et al., 2008). Breia et al., 2020 showed that the grapevine *VvERD6l13* was induced in the grape berries upon infection by a necrotrophic or biotrophic pathogen such as *Botrytis cinerea* and *Erysiphe necator*, respectively. VvERD6l13 is the first ESL described to be localized at the plasma membrane, as demonstrated in tobacco epidermal cells and even more surprisingly, using yeast as a heterologous system, it has been characterised as an low affinity H^+/sucrose symporter (Breia et al., 2020). Moreover, Desrut et al., 2020 showed that six *AtESL* genes were differentially regulated in the presence of plant growth-promoting rhizobacteria (PGPR). Indeed, *ERD6-like7*, *ERD6-like12*, and *ERD6-like16*, as well as *ERD6-like18*, were down-regulated in shoots and roots, respectively while *ERD6-like13* and *ERD6-like15* were up-regulated in roots in the response of PGPR (Desrut et al., 2020).

Altogether, these data highlight the high diversity of ESL transporters: they can transport monosaccharides and also sucrose, they are localized to the tonoplast or to the plasma membrane, and they might be involved in many plant responses to abiotic and biotic environmental cues. Furthermore, one may ask the biological necessity of so many duplicated *ESL* genes in some plant genomes. In this context, we thought interesting to deepen our comprehension of the evolutionary history of the ESL subfamily and therefore we report, in this study, a complete phylogenetic analysis of the ESL subfamily.

Materials and methods

Plant materials and growth conditions

Arabidopsis thaliana plants (ecotype Columbia: Col-0) were grown in Arasystem™ (BETATECH bvba, Belgium) containing an autoclaved mix of compost/vermiculite (3/1) into a growth chamber under a 10 h light (22°C)/14 h dark (18°C) photoperiod, with 50% (light) to 90% (dark) relative humidity. Fully expanded leaves, roots, flower buds, flowers and siliques were used for sampling. Roots were separated from soil by multiple careful washings with water before sampling.

ERD6-like sequence identification

Previously identified ESL protein of *Arabidopsis thaliana, Brachypodium distachyon, Cucumis melo, Musa acuminata, Oryza sativa, Populus trichocarpa, Solanum lycopericum Vitis vinifera* and *Zea mays* were collected from Aramemnon online database (http://aramemnon.uni-koeln.de). ESL sequences from other species were identified through Blastp analysis (Altschul et al., 1997) using the 18 full-length *V. vinifera* ESL protein sequences as queries (Afoufa-Bastien et al., 2010) and an E-value of 10^{-60} against the online server Phytozome v10.0 (https://phytozome.jgi.doe.gov/pz/portal.html) with the exceptions of *Pinus taeda* (http://congenie.org), *Galdieria sulphuraria, Chondrus crispus, Pyropia yezoensis, Chlorella vulgaris, Phoenix dactylifera, Nelumbo nucifera, Cicer arietinum, Genlisea aurea et Ectocarpus siliculosus* (https://www.ncbi.nlm.nih.gov), *Lotus japonicus* (http://www.kazusa.or.jp/lotus/) and *Klebsormidium nitens* (https://phycocosm.jgi.doe.gov/Klenit1/Klenit1.home.html). Only full-length sequences were collected and potential isoforms sequences were eliminated from the study. The species and the identified sequences are summarized in the Supplementary Table 1.

Phylogenetic analysis

Alignments of identified ESL protein sequences were performed using BioEdit software (Ibis Therapeutics, Canada) and ClustalW method. Phylogenetic analysis was performed using MEGA v.6.0 software (Tamura et al., 2013) and the Maximum Likelihood method (PhyML) with 1000 bootstrap replicates. The prior alignment performed by MEGA v.6.0 followed the JTT (Jones-Taylor Thornton) amino acid model. The sucrose transporter AtSUC2 protein sequence and one referent of each monosaccharide transporter subfamily (AtPLT5, AtINT1, AtSTP13, AtVGT1, AtTMT1, and AtpGlt) were used as out-group in order to root the phylogenetic tree. For phylogenetic tree inference, all date, periods and evolutionary data used to rebuild the evolutionary history of ESL family trough the evolution of land plants were obtained from Time Tree of Life (http://www.timetree.org, (Hedges et al., 2006; Kumar et al., 2017).

Estimation of selection pressure

ESL CDS sequences from *Arabidopsis thaliana*, *Arabidopsis lyrata*, *Arabidopsis halleri* and *Capsella rubella* were aligned with MEGA 6.0, using Neighbor-Joining method, 1000 bootstrap and the JTT amino acid substitutions model. This led to the definition of 18 monophyletic groups of *ESL* sequences, each containing at least one *A. thaliana ESL* sequence

as well as a sequence of *C. rubella* (when possible: 16 of 18 groups). For each group a second alignment was performed, using BioEdit free software (Ibis Therapeutics, Canada) and ClustalW method and was manually re-aligned in order to keep the same open reading frame for all the aligned CDS. In total, four sequences (Ah04425s02, Cr10000845, Cr10015811 and Cr10021344) were removed from the study, as it was not possible to align them correctly. The dN/dS (KaKs) ratio of *ESL* sequences was calculated using Datamonkey online server (http://www.datamonkey.org), with GA-Branch method(Kosakovsky Pond and Frost, 2005; Delport et al., 2010) following HKY85 model. The user tree set was (Ah ; Al), (At ; Cr), reflecting the evolution of these four species.

Gene structure design

ESL gene structures were determined using GSDS v.2.0 online server (Gen Structure Display Server : http://gsds.cbi.pku.edu.cn/) developed by Beijing University's Bio-Informatics center (Hu et al., 2015). Gene structures were determined *via* alignment of gDNA and CDS sequences. Each sequence was designed with all exons represented at the same scale and the same size for all introns. *Lotus japonicus* sequences were not designed.

Promoter analysis

The 1000bp long promoter sequences of the 19 *AtESL* genes were retrieved from TAIR (The *Arabidopsis* Information Resource) database. These sequences were then scanned for the presence of *cis*-regulatory elements using PLACE (Plant Cis-acting Regulatory DNA Elements) database (https://www.dna.affrc.go.jp/PLACE/?action=newplace) (Higo et al., 1999).

RNA extraction and real-time quantitative PCR (RT-qPCR) analysis

Total RNA was extracted from frozen ground *A. thaliana* tissues according to Kay et al., (1987). RNA quantity and quality were verified using a Microdrop (Thermo Fischer) and an agarose gel. Total RNA was treated with DNAse I (Sigma-Aldrich) and reverse transcription was performed using M-MLV reverse transcriptase (Promega). Real-time quantitative PCR was carried out using the GoTaq qPCR Master Mix (Promega) with a Mastercycler *realplex*^{2} instrument (Eppendorf). Target gene expression results were normalized with the average of the Ct value of the reference gene, *AtPP2a* (*At1g13320*) (Czechowski et al., 2005). The results were expressed as relative gene expression according to the $2^{-\Delta Ct}$ method. Primers have been designed using Oligo 7 and tested for their specificity and efficiency (≥90%).

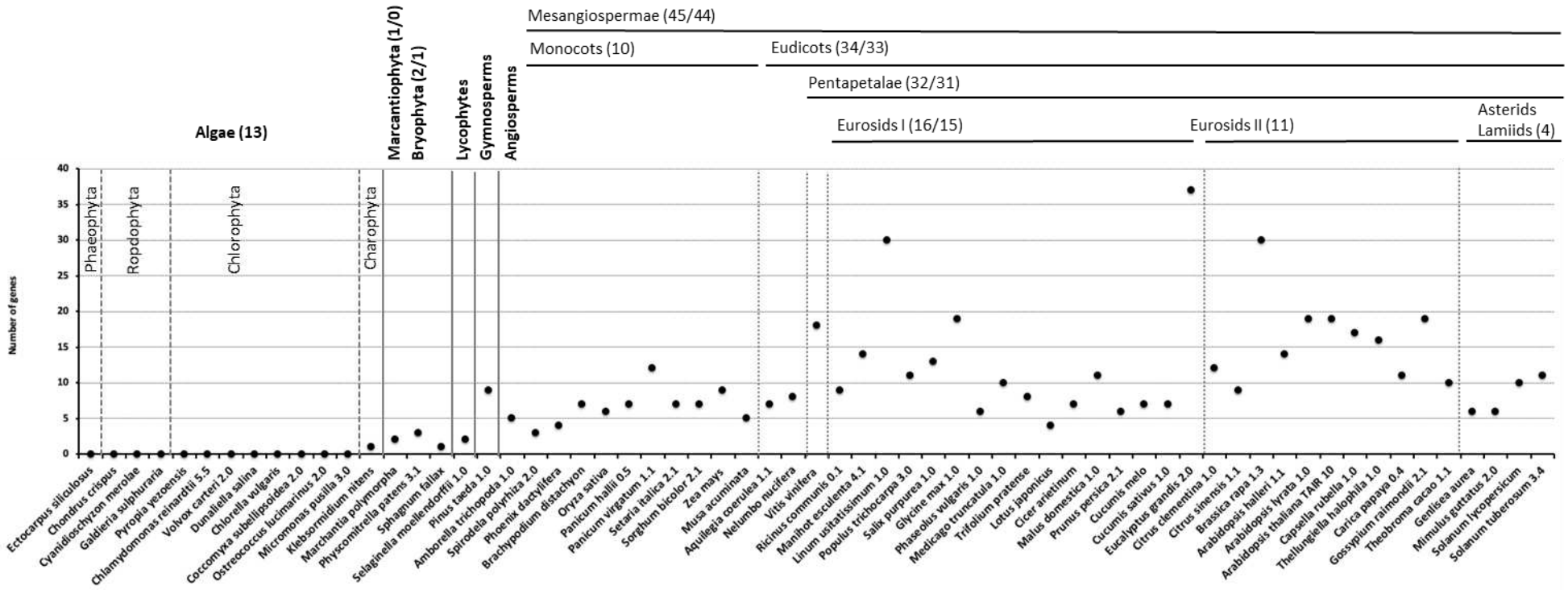

Ch.III-Fig. 1 : Number of ESL proteins identified in each species. The classification of the species is indicated on the top of the graph. Numbers into bracket indicate (total sequences number/ number of sequences included in the phylogenetic analysis)

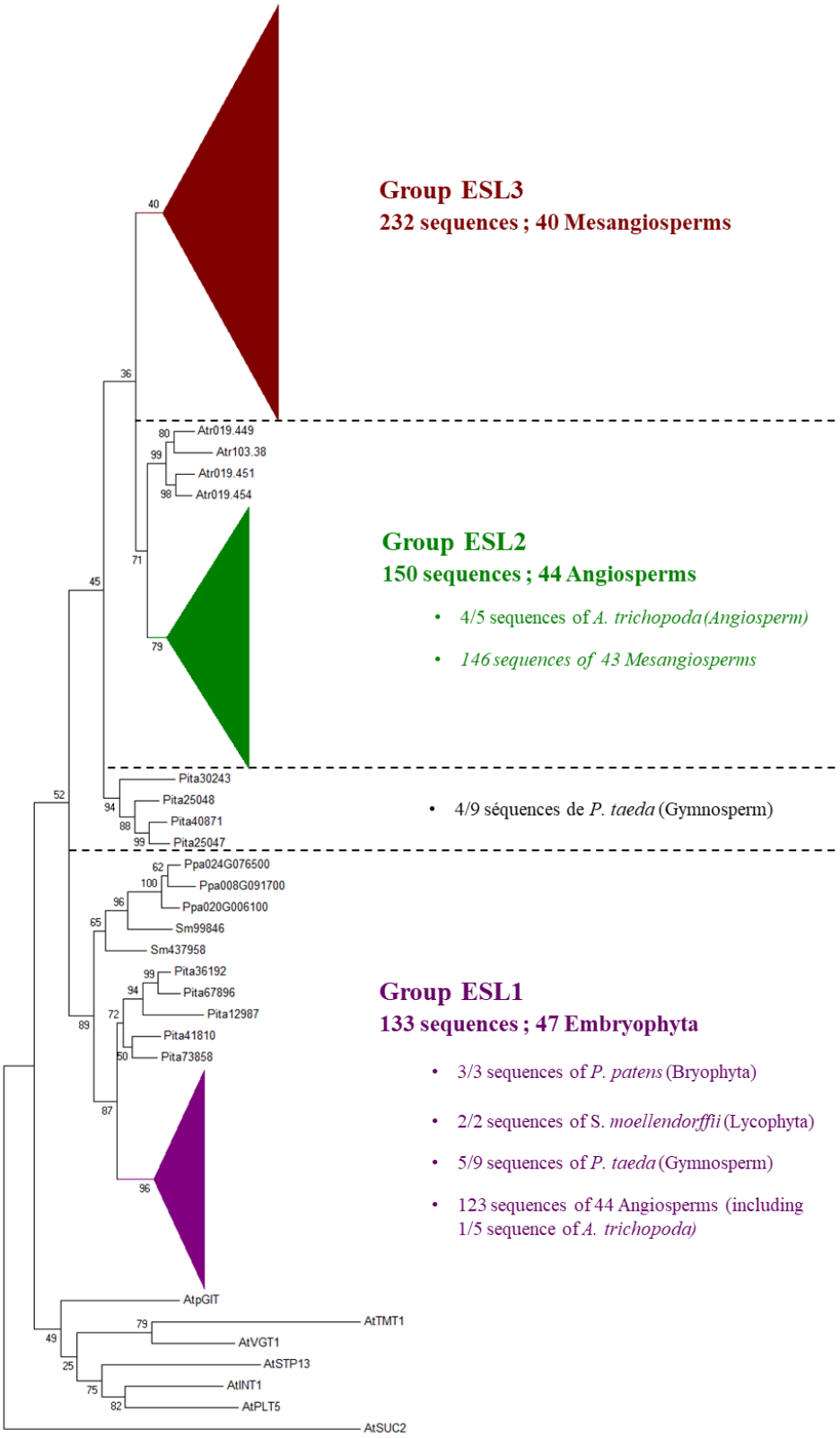

Ch.III-Fig. 2 : Maximum Likelihood phylogeny of ESL sugar transporter proteins. The tree was produced by aligning 519 amino acid ESL sequences identified in 47 Embryophyta using ClustalW and then build using the software Molecular Evolutionary Genetics Analysis (MEGAv6, Tamura et al., 2013). JTT amino acid substitution model was used and the bootstrap consensus tree was inferred from 1000 replicates. The percentage of replicate trees in which the associated taxa clustered together in the bootstrap test is shown next to the branches. The tree is drawn to scale, with branch lengths measured in the number of substitutions per site. AtSUC2 (*A. thaliana* Sucrose Carrier 2), AtPLT5 (*A. thaliana* Polyol Transporter 5), AtINT1 (*A. thaliana* Inositol Transporter 1), AtSTP13 (*A. thaliana* Sugar Transport Protein 13), AtVGT1 (*A. thaliana* Vacuolar Glucose Transporter 1), AtTMT1 (*A. thaliana* Tonoplastic Monosaccharides Transporter 1) and AtpGlT (*A. thaliana* Plastidic Glucose Transporter 1). For other sequences annotation see supplementary data 1.

Primer sequences used in this study are listed in Supplementary Table 2.

Statistical analyses

Statistical analyses were performed using XLStats 2011 (Addinsoft, France)

Results

ESL transporters have emerged with Streptophyta and have separated into three distinct groups in terrestrial plants

In order to study ESL transporter evolution, we performed a BLASTp analysis, using 18 *Vitis vinifera* ESL protein sequences as template, of 63 proteomes from photosynthetic organisms representing the main groups of algae and plant kingdom. Blastp analysis of 13 algae genomes including stramenopiles (*Ectocarpus siliculosus*), rhodophytes (*Chondrus crispus, Cyanidioschyzon merolae, Galdieria sulphuraria, Pyropia yezoensis*), chlorophytes (*Chlamydomonas reinhardtii, Volvox carteri, Chlorella vulgaris, Dunaliella salina, Coccomyxa subtellipsoidea, Ostreococcus lucimarinus, Micromonas pusilla*) and streptophytes (*Klebsormidium nitens*) led to the identification of only 1 ESL protein in the genome of *Klebsormidium nitens*. A total of 526 sequences could be identified in the genome of 50 embryophytes, among which those of mosses and lycophytes have less than 5 ESL copies (2 for *Marchantia polymorpha*, 3 for *Physcomitrella patens*, 1 for *Sphagnum fallax* and 2 for *Selaginella moellendorffii*). Genomes of gymnosperms and angiosperms have from 5 to 19 ESL, with few exceptions having either less ESL (*Spirodela polyrhiza*: 3, *Phoenix dactylifera*: 4 and *Trifolium pratense*: 4) or in contrary, a very high number of copies (*Brassica rapa*: 30, *Linum usitatissimum*: 30 and *Eucalyptus grandis*: 37). These data suggest that the ESL could have appeared with charophyta and have considerably evolved in embryophyta (Ch.III-Fig. 1 and Supplementary Table 1).

A phylogenetic analysis performed on 519 protein sequences isolated from 47 Embryophyta (sequences from *K. nitens*, *M. marchantia, S. fallax* and *T. pratense* being identified afterwards) shows that identified ESL proteins form a unique group, clearly distinct from the six other MST subfamilies and from the sucrose carrier family, as demonstrated by the presence of AtpGLT, AtTMT1, AtVGT1, AtTNT1, AtSTP13, AtINT1, AtPLT5 and AtSUC2 at the root of the tree (Ch.III-Fig. 2). The ESL of angiosperms can be divided into three main groups, named Group ESL1, ESL2 and ESL3. Group ESL1 (Ch.III-Fig. 2) is supported by a high bootstrap value (96%) and contains 123 sequences of the 44 angiosperms,

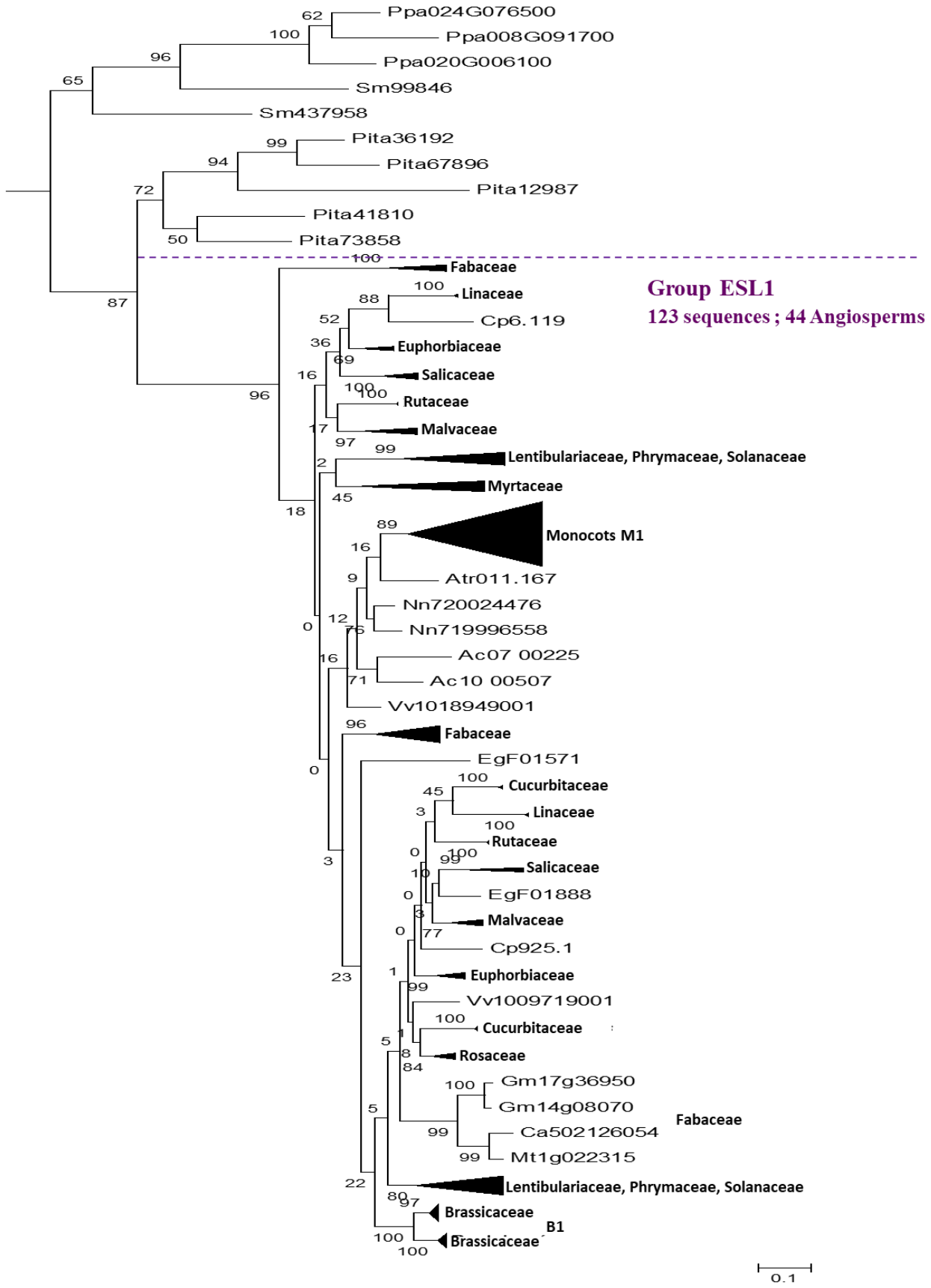

Ch.III-Fig. 3: Maximum likelihood phylogeny of ESL sugar transporter proteins: Details of Group ESL1. Same legend as that of Figure 2. For annotation of other sequences, see supplementary data 1.

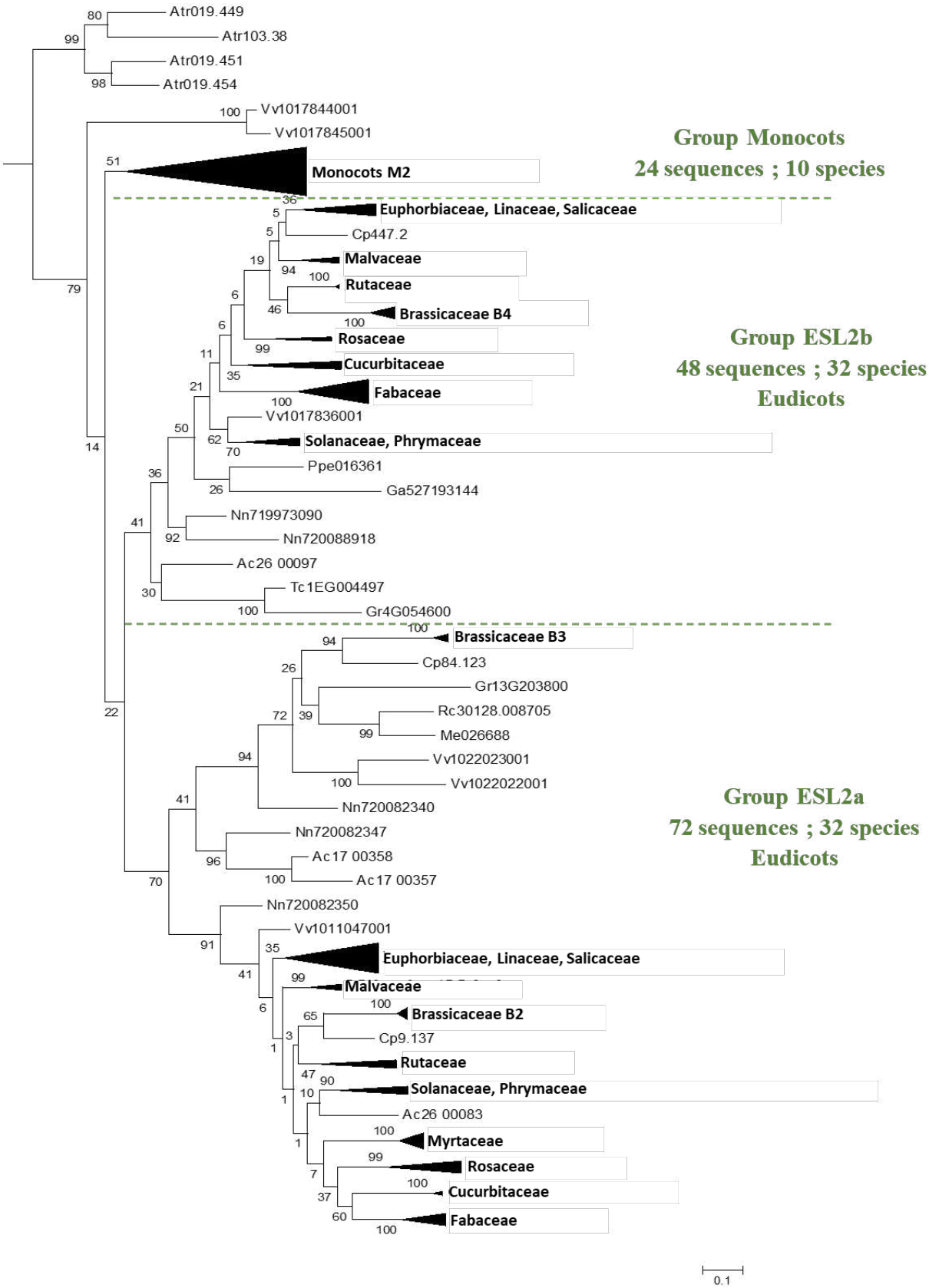

Ch.III-Fig. 4: Maximum likelihood phylogeny of ESL sugar transporter proteins: Details of Group ESL2. Same legend as that of Figure 2. For other sequences annotation see supplementary data 1.

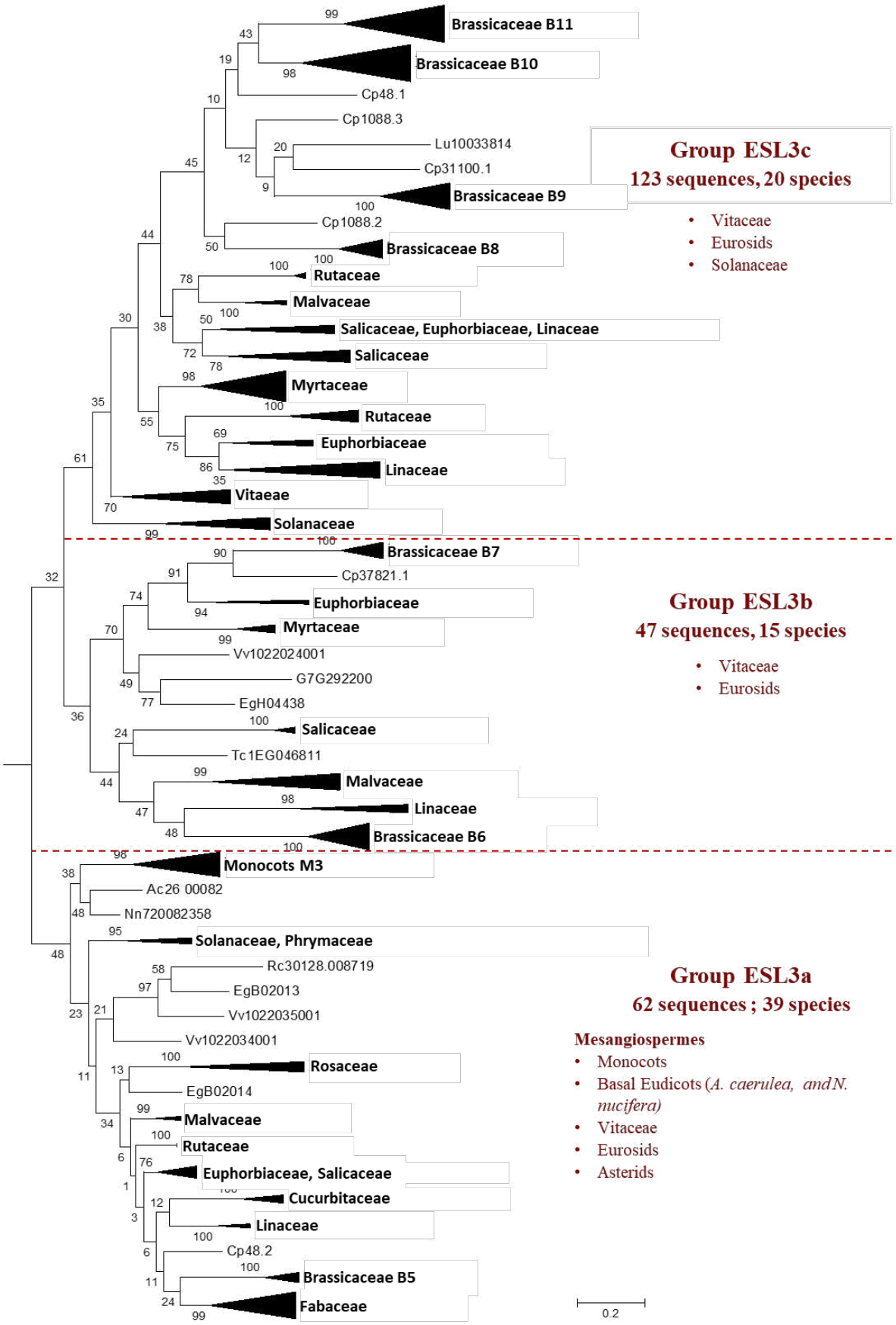

Ch.III-Fig. 5: Maximum likelihood phylogeny of ESL sugar transporter proteins: Details of Group ESL3. Same legend as that of Figure 2. For other sequences annotation see supplementary data 1.

including 1 of the 5 sequences of *A. trichopoda*. At the basis of this group are located all the sequences identified in the moss and fern (3 sequences of *P. patens*, 2 sequences of *S. moellendorffii*) and 5 of the 9 sequences of the gymnosperm *P. taeda.* All together the 133 ESL protein sequences (25, 6% of sequences) form a single group in which the 47 analysed species are represented by at least one protein sequence. Moss and fern sequences form a common group suggesting a higher similarity between them than with those of *P. taeda* and angiosperms. In group ESL1 (Ch.III-Fig. 3), monocots sequences form a single group supported by a bootstrap value of 89% at the basis of which are found 1 sequence of *A. trichopoda*, 2 sequences of *N. nucifera*, 2 of *A. caerulea* and 1 of *V. vinifera.* This suggests an ESL specific group for monocots (monocots G1) related to ESL of basal angiosperms, basal eudicots and vitales. On the contrary, asterids sequences split into two distinct groups including both solanaceae, phrymaceae and lentibulariaceae, while for eurosids sequences, at least, two separated groups for most botanical families can be observed and most of them are supported by high bootstrap values. Fabaceae sequences split into 3 groups and a single group is observed for rosaceae and myrtaceae. At the basis of Group ESL2 and Group ESL3 (Ch.III-Fig. 2) are located the 4 other sequences of the Gymnosperm *P. taeda* and no sequences of moss and fern are present. This suggests a first duplication event in the common ancestor of seed plants. The Group ESL2 (Ch.III-Fig. 2) is formed by 150 sequences of angiosperms (28, 9% of sequences). It is interesting to note that 4 sequences of *A. trichopoda* are located at the basis of a mesangiosperms group (bootstrap value = 79%) which contains 146 sequences identified in the genome of 43 species. In this group (Ch.III-Fig. 4), monocots and eudicots separate clearly in two specific groups. The monocots group (monocots G2) contains 24 sequences (10 species). The eudicots group can be divided into two main sub-groups: Groups ESL2a (72 sequences, 32 species, excluding *L. japonicus*) and ESL2b (48 sequences, 32 species, *excluding E. grandis*). In each group, protein sequences separate mainly according to the botanical families. There are two groups of ESL for fabaceae, rosaceae, cucurbitaceae, rutaceae, malvaceae, malpighiales and asterids and 3 groups for brassicaceae. The group ESL3 (Ch.III-Fig. 2) is specific for mesangiosperms as no sequences of *A. trichopoda* (one of the earliest divergent lineages within angiosperms) are present. This group contains 232 sequences of 40 species (44.7% of all sequences), *S. polyrhiza* (one of the earliest divergent lineages within monocots), *O. sativa* and *G. aurea* are not represented in this group. The group ESL3 can be divided into three sub-groups named ESL3a, ESL3b and ESL3c (Ch.III-Fig. 5). The sub-group ESL3a contains 62 sequences (11.95% of all sequences) from 39 mesangiosperms. One monocots specific group (monocots G3) is related to a sequence of two

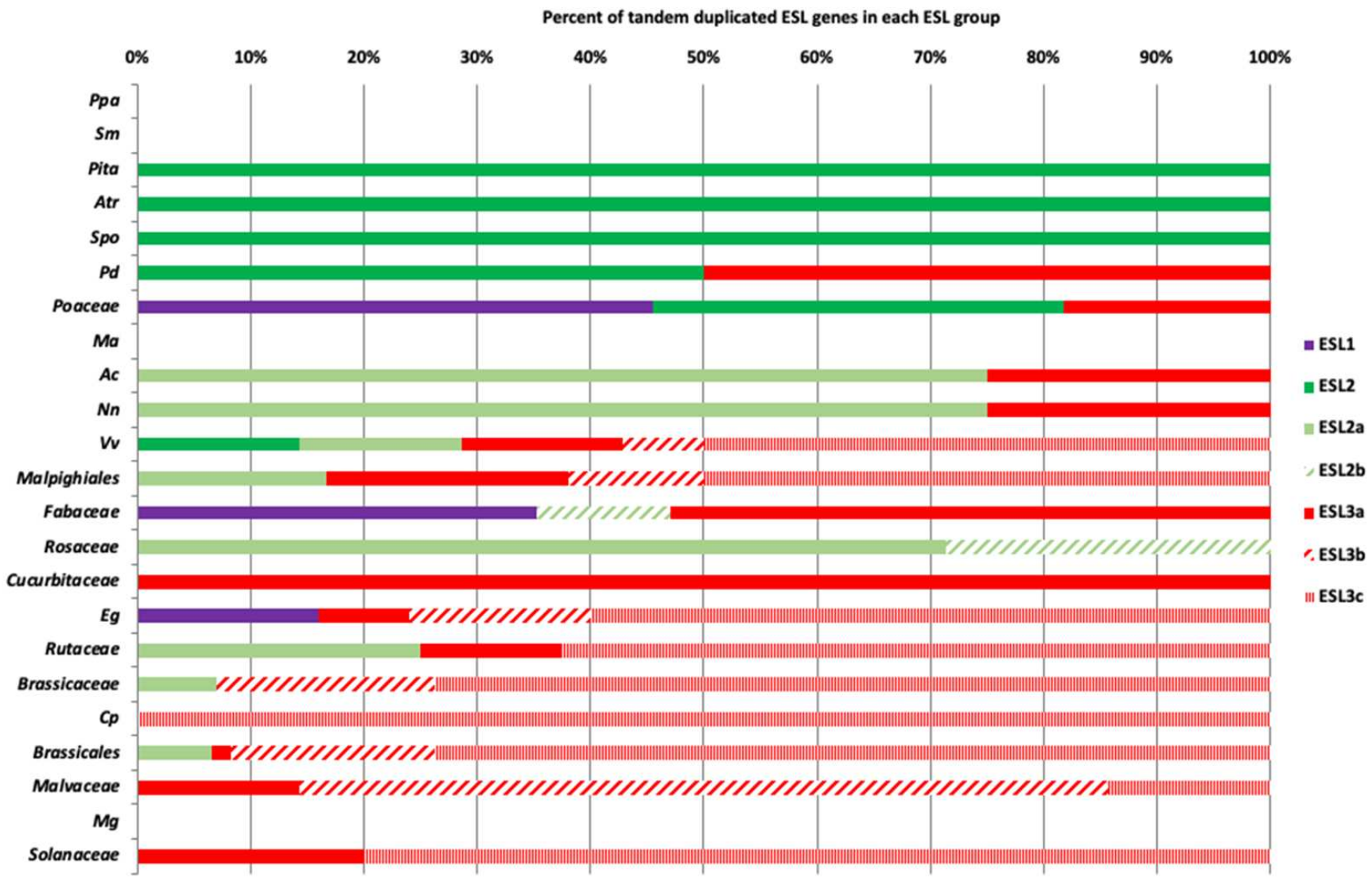

Ch.III-Fig. 6: Distribution of tandem duplicated *ESL* genes in the different ESL groups. % indicates the percentage of tandem duplicated genes relative to the total number of *ESL* per species or botanical group. Purple - for *ESL1*, green - for *ESL2* and red for *ESL3*. For abbreviations see supplementary data 1.

basal eudicots: *A. caerulea* and of *N. nucifera*. All pentapetalae (vitaceae, eurosids and asterids) form a single group in which sequences are separated according to botanical families. The sub-group ESL3b contains 47 sequences (9.05% of all sequences) identified in *V. vinifera* and 14 Eurosids and the sub-group ESL3c contains 123 sequences (23.7% of all sequences) from *V. vinifera*, Solanaceae (*S. lycopersicum*, *S. tuberosum*) and 17 eurosids.

In conclusion, the distribution of ESL sequences in the 3 main ESL groups varies according to botanical groups and four distribution types can be observed (Supplementary Table 3) *i*: The group ESL1 contains most of the poaceae (49%) and lamiales (58%) sequences and is closely related to half of sequences of *P. taeda* (56%) and to all of the sequences of *P. patens* and *S. moellendorffii ii*: The group ESL2 contains the highest number of ESL of *A. trichopoda* (amborellaceae, 80%), *A. corulea* (ranunculaceae, 57%), *N. nucifera* (nelumbonaceae, 63%), most of the fabaceae (39%), all rosaceae (53%) and cucurbitaceae (43%) *iii*: For *V. vinifera* (vitaceae 56%), all malpighiales (52%), *E. grandis* (myrtaceae, 59%), rutaceae (52%), brassicales (71%) and malvaceae (48%), the highest number of proteins is found in group ESL3. This high number is generally correlated with the presence of a high number of sequences in the group ESL3c (55 to 81% of ESL3 sequences) except for malvales for which 71% of the ESL3 sequences belong to the group ESL3b and euphorbiaceae. *iv*: For solanales, the groups ESL1 and ESL3 contain the same number of sequences (38% each) which is more than the group ESL2 (24%). In monocots and fabaceae, this distribution varies according to the species.

Tandem duplications are at the origin of the expansion of the ESL family in some Monocots and Eudicots

The genome analysis has revealed the presence of tandem duplicated genes for many species and those could explain the heterogeneous distribution of ESL into the three ESL groups. To confirm this hypothesis, we have determined the number of tandem duplicated *ESL* genes for each species and studied their distribution. *L. japonicus* and *G. aurea* were not included into this analysis (Ch.III-Fig. 6 and Supplementary Table 3). For few species, including the moss *P. patens*, the fern *S. moellendorffii,* the monocot *M. acuminate* and the asterid *M. guttatus*, no tandem duplicated genes have been identified. This could be in agreement, at least for the moss and the fern, with few numbers of *ESL* genes found in their genomes. The gymnosperm *P. taeda,* the basal angiosperm *A. trichopoda* and the basal monocot *S. polyrhiza* (alismatales) have only two duplicated *ESL2* genes. For monocots, *P. dactylifera* (arecales) contains 2 duplicated genes (1 *ESL2* and 1 *ESL3a*) while in poaceae, all

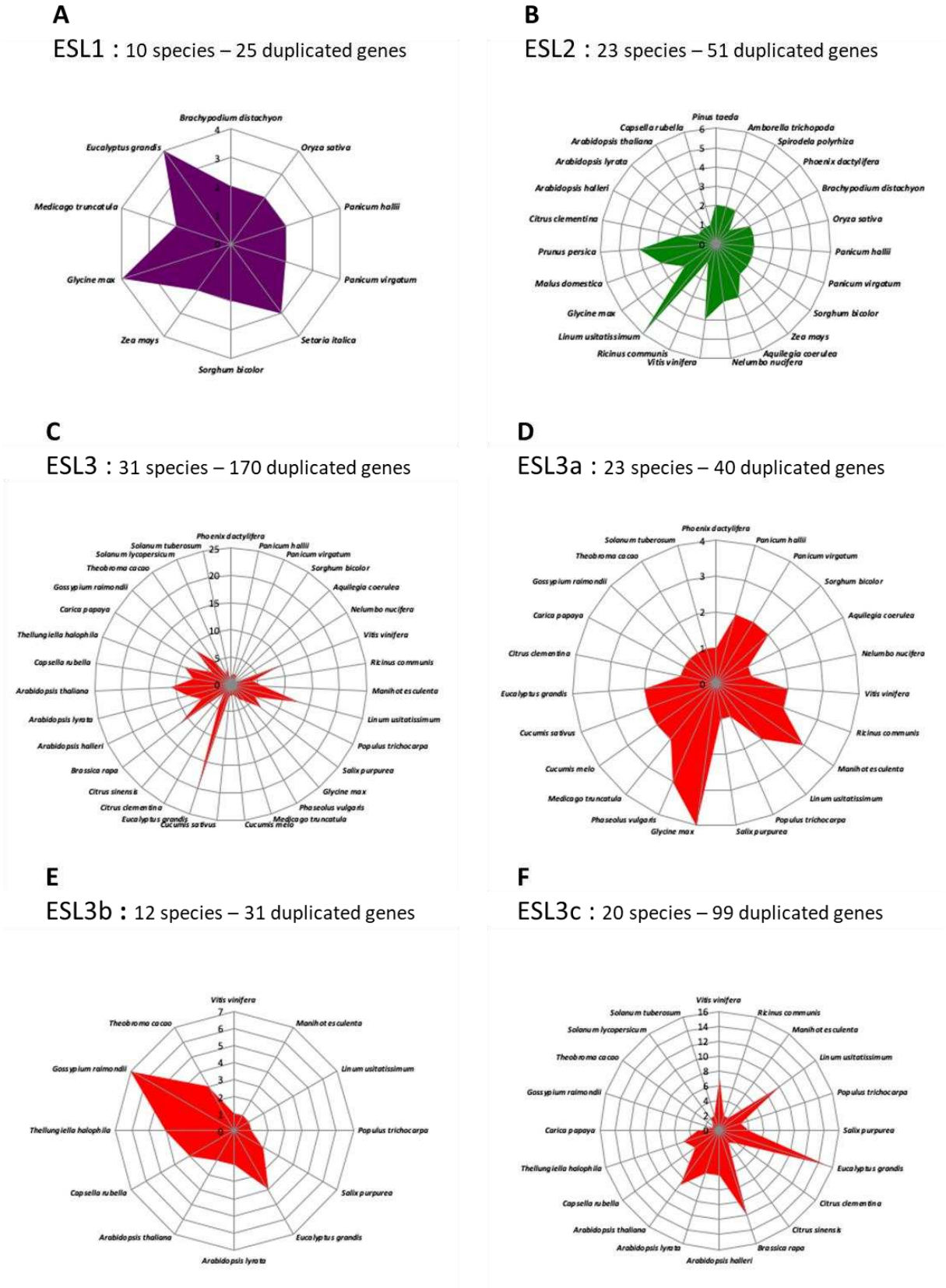

Ch.III-Fig. 7: Distribution of tandem duplicated *ESL* genes in the different ESL groups. Values correspond to the number of tandem duplicated genes for each species. Purple is for *ESL1*, green for *ESL2* and red for *ESL3*.

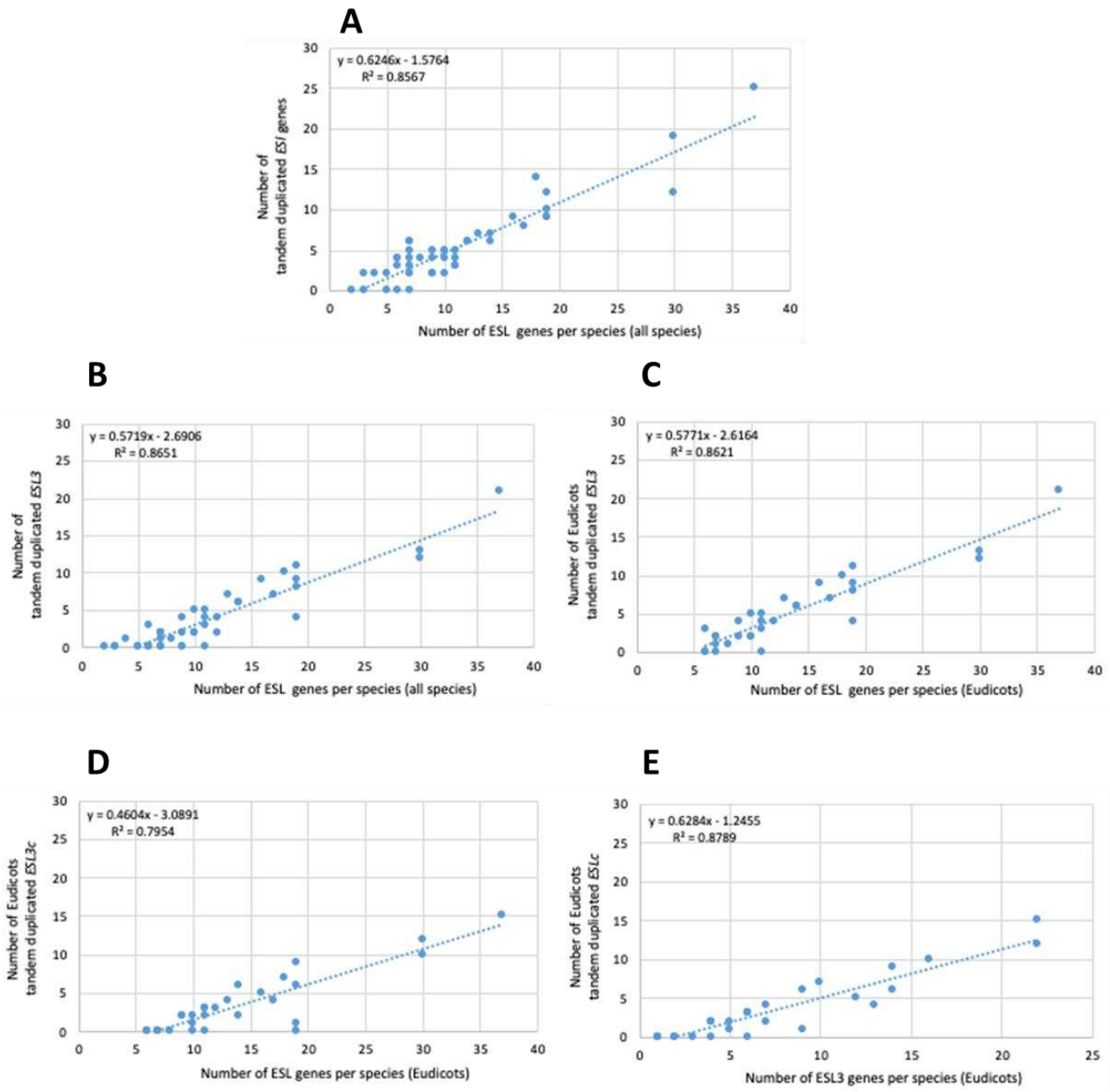

Ch.III-Fig. 8: Linear correlation of the number of tandem duplicated ESL. A: total number of duplicated *ESL* with total number of *ESL* in each species. **B:** total number of duplicated *ESL3* with total number of *ESL* in each species. **C:** total number of Eudicots duplicated *ESL3* with total number of *ESL* in each Eudicots species. **D:** total number of Eudicots duplicated *ESL3c* with total number of *ESL* in each Eudicots species. **E:** total number of Eudicots duplicated *ESL3c* with total number of *ESL3* in each Eudicots species.

A

Nb Exons	Nb gènes	%
6	1	0.19%
8	3	0.58%
9	1	0.19%
10	6	1.17%
11	6	1.17%
12	11	2.14%
13	9	1.75%
14	14	2.72%
15	19	3.69%
16 exons	**43**	**8.35%**
17 exons	**124**	**24.08%**
18 exons	**260**	**50.49%**
19	13	2.52%
20	2	0.39%
24	1	0.19%
31	1	0.19%
35	1	0.19%
Total	**515**	

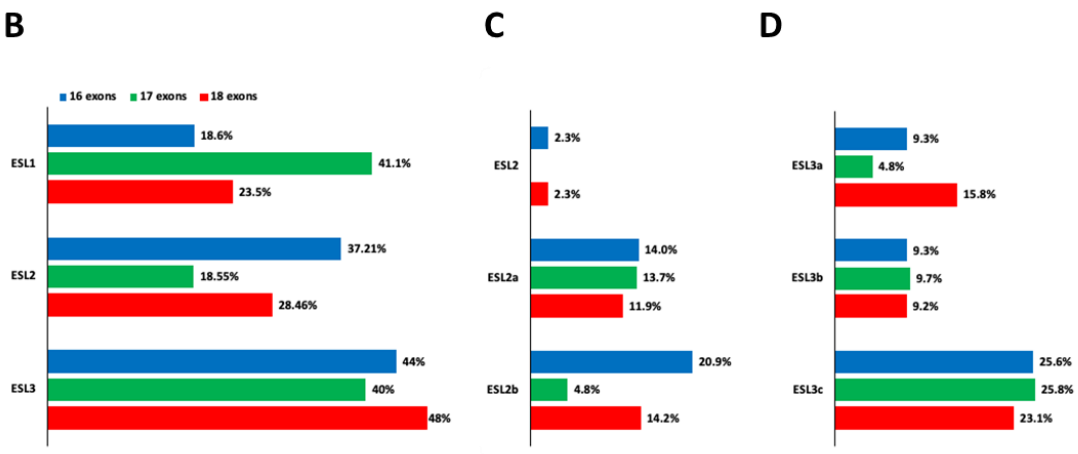

E

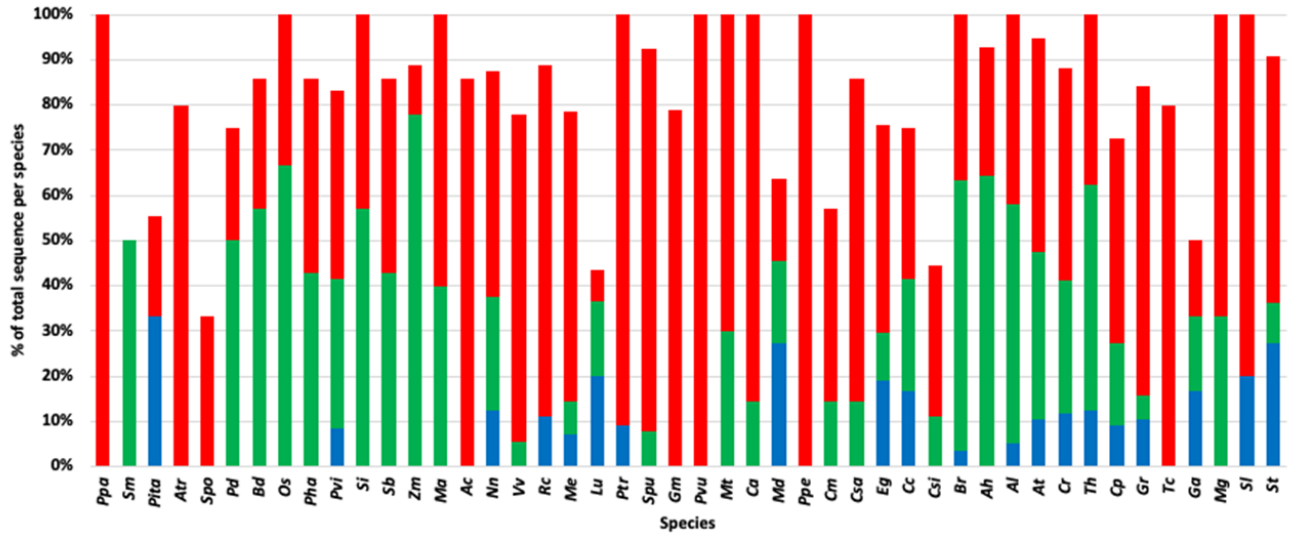

Ch.III-Fig. 9: Percentage and distribution of the different *ESL* gene structure (exons-introns). A: gene number per structure and percentage of total *ESL*. **B:** Distribution of the three main structure in the three ESL groups (% is related to the number of *ESL* having the same type of structure). **C:** Distribution amount the *ESL2* group. **D:** Distribution amount the *ESL3* group. **E:** Percentage of each type of structure per species.

species have 3 to 6 tandem duplicated *ESL* belonging to *ESL1* and/or *ESL2*. *P. hallii*, *P. panicum* and *S. bicolor* have, in addition, 2 duplicated *ESL3*. Therefore, poaceae have mainly *ESL1* (45%) and *ESL2* (36%) duplicated genes. For eudicots, only three species have duplicated ESL1: *E. grandis* (myrtales) with 4 duplicated *ESL1* (16% of the *EgESL*) and two fabaceae, *G. max* and *M. truncatula* which have 2 and 4 tandem duplicated *ESL1,* respectively, representing 35% of total fabaceae sequences. The basal eudicots, *A. coerulea* and *N. nucifera* have more than 70% of duplicated *ESL2* genes and both rosaceae only *ESL2* tandem genes. *V. vinifera*, *E. grandis*, rutaceae, and brassicaceae have more than 85% duplicated *ESL3* while cucurbitaceae, *C. papaya* and solanaceae have only duplicated *ESL3*. All in all, among the 509 analysed *ESL*, 246 are tandem duplicated genes, including 25 *ESL1* from 10 species (poaceae: 60% and eudicots: 40%), 51 *ESL2* from 23 species (eudicots: 63% and monocots: 29%) and 170 *ESL3* mostly from eudicots (96%). Furthermore, duplicated *ESL3* are not distributed homogeneously among the ESL3 subgroups. The subgroup ESL3a contains 33 duplicated eudicots genes (82.5%) and only 7 monocots genes (17.5%) identified in 23 species. The subgroups ESL3b and ESL3c have 31 and 99 eudicots duplicated genes, respectively, all from pentapetalae species including *V. vinifera*, malpighiales, *E. grandis*, brassicales and malvales. ESL3c contains also duplicated genes from rutaceae and solanaceae (Ch.III-Fig. 7; Supplementary Table 3). The group ESL3 which contains the higher number of sequences is also that which contains the most tandem duplicated genes. In fact, we observed a good correlation between the number of duplicated genes and the number of *ESL* genes per species (Ch.III-Fig. 8), which is not surprising. A similar correlation is present between the number of duplicated *ESL3* and the number of *ESL* genes per species as well as the number of eudicots *ESL* (Ch.III-Fig. 8C), which can make sense as eudicots species are more represented in this study. However, this correlation is also clearly present between the number of duplicated *ESL3c* and the number of *ESL3* genes per species (Ch.III-Fig. 8D and E), indicating that the high number of *ESL3c* (123 genes) is presumably due to numerous eudicots tandem gene duplications which have occurred in 20 species.

***ESL* genes from Monocots and Brassicaceae present specific gene structures**

In order to identify potential structural specificities for the *ESL* genes, we realized a comparative analysis of the intron/exon arrangement of 515 sequences from 46 species (*L. japonicus* was excluded from this analysis as no CDS sequences could be recovered on the *Lotus* genome website). As shown on (Ch.III-Fig. 9A), the number of exons present in the *ESL* genes varies from 6 to 35. However, 14 exon/intron arrangements, each representing

N° structure	Number of exons	Number of sequences	%	Plant orders or families				Structures
1	18	260	50,5	all species	ESL1	ESL2	ESL3	1 2 3 4 5 6 7 8 9 10 11 12 13 14 15 16 17 18
2	17	28	5,4	28 Monocots (3Bd, 2Ma, 3Os, 3Ph, 4Pvi, 1Pd, 3Si, 3Sb, 6Zm)	ESL1			1 + 2
3	17	22	4,3	20 Brassicaceae (3At, 2Ah, 4Al, 5Br, 3Cr, 3Th) 2 Fabaceae (1Ca, 1Mt)	ESL1	ESL2a	ESL3b	12 + 13
4	17	7	1,4	7 Brassicaceae (1At, 1Ah, 1Al, 2Br, 1Cr, 1Th)	ESL1			17+18
5	17	14	2,7	14 Brassicaceae (1At, 3Ah, 3Al, 4Br, 3Th)		ESL2a	ESL3c	14 + 15
6	17	5	1,0	4 Brassiceae (1At, 1Ah, 1Al, 1Br) 1 rutaceae (1Spu)			ESL3c	15 + 16
7	17	9	1,7	8 Brassicaeae (1At, 1Ah, 1Al, 3Br, 1Cr, 1Th) 1 vitaceae			ESL3c	4 + 5
8	17	3	0,6	3 Rutaceae (2Cc, 1Csi)		ESL2a		5 + 6
9	16	6	1,2	6 Brassicaceae (1At, 1Al, 1Br, 1Cr, 1Th)		ESL2b		6 + 7 9 + 10
10	16	3	0,6	3 Solanaceae (1Sl, 2St)		ESL2b		9 + 10 15 + 16

Ch.III-Fig. 10: Major types of introns/exons structure identified in *ESL* genes. The blue rectangles represent the exons and the lines the introns. The introns are represented with a scale that does not take into account their real length. Red numbers indicate the exons and the red rectangles highlight the differences. For each structure, the number of exons, of sequences are indicated as well as the percentage of total ESL sequences and the botanical groups in which, they have been detected.

less than 4% of the total sequences, might arise from incomplete sequences or erroneous CDS, or represent exceptional structures that would only concern a small number of ESL. On the contrary, arrangements with 16, 17 and 18 exons have been identified in 8.35%, 24.08% and 50.49% of *ESL* sequences.

The structure with 18 exons, named structure 1 (Ch.III-Fig. 10) is the most widespread structure and is present in 260 embryophyte sequences (50.49%). It is found in all species at the exception of the fern *S. moellendorffii*. It is the only one found in the moss *P. patens*, *P. vulgaris* (fabaceae) and in *P. persica* (rosaceae) sequences. It is present in more than 80% of the sequences of the basal angiosperm *A. trichopoda*, the basal eudicot *A. coerulea*, the salicaceae *P. trichopoda* and *S. purpurea*, the fabaceae *C. arietinum*, the malvaceae *T. cacao* and the solanaceae *S. lycopersicum*. For the other species, it represents between 20% to 80% of the *ESL* except for the monocot *Z. maize*, the linaceae *L. usitatissimun* and the lentibulatiaceae *G. aurea* for which less than 20% of the sequences have this structure (Ch.III-Fig. 9E). Forty-eight percent of *ESL* having this 18-exons structure are *ESL3* genes among which, 23.1% are *ESL3c* (Ch.III-Fig. 9B, C and D).

The arrangements with 17 exons are less widespread, they have been identified in 124 embryophyte sequences (24.08%). They are present in more than 35% of the sequences of the fern *S. moellendorffii*, the poaceae and the brassicacea with the exception of *P. virgatum* (33.3%), *and C. rubella* (29.4%). For *M. trucatula* and *M. Guttatus*, they represent 30 and 33%, respectively, and for all the others species, between 5.6 to 25% of the sequences. The genes with 17-exons arrangements split equally in *ESL1* (41.1%) and *ESL3* (40%) groups while only 18.55% are *ESL2* genes. In *ESL3* group, a quarter of them are *ESL3c* (Ch.III-Fig. 9A, B, C and D). In fact, 7 different structures with 17 exons (named structure 2 to 8) have been identified (Ch.III-Fig. 10). The structure 2 should result from the merge of exons 1 and 2 in comparison with structure 1. It is specific to monocots *ESL1* as it was identified in 28 monocots sequences from 9 poaceae and from *P. dactilyfera* (arecaceae) and *M. acuminata* (musaceae). Only the *ESL* from basal monocot *S. polyrhiza* does not have such structure. Five 17-exons structures are more or less brassicaceae specific. The structure 3 (merge of exons 12 and 13) was identified in 22 sequences essentially from brassicaceae (20 sequences) and fabaceae (2 sequences) and concerns *ESL1*, *ESL2a* and *ESL3b* genes. The structure 4 (merge of exons 17 and 18) is brassicaceae *ESL1* specific as it is found in only 7 *ESL1*. The structure 5 (merge of exons 14 and 15) is brassicaceae specific and concerns 14 *ESL2a* and *ESL3c* genes. The structure 6 (merge of exons 15 and 16) is *ESL3c* specific and was identified in 4 brassicaceae and in 1 *S. purpurea* (rutaceae) genes. The structure 7 (merge of exons 4 and 5)

is *ESL3c* specific and was identified in 8 brassicaceae and in 1 *V. vinifera* genes. Finally, the structure 8 (merge of exons 5 and 6) is *ESL2a* specific and was identified in 3 rutaceae genes.

The arrangements with 16 exons are less abundant. They have been identified in 43 sequences (8.35%) from 20 species (Ch.III-Fig. 9A, B, C and D). They are more present in *ESL2* (37.21%) and in *ESL3* (44%), especially in *ESL2b* (20.9%) and *ESL3c* (25.6%). They represent 33% of the *ESL* of *P. taeda*, 27% of those of *M. domestica* and *S. lycopersicum*, 20% of *S. tuberosum* and *L. usitatissimum* and 3 to 12.5% of the *ESL* of brassicaceae. In contrary to the 17- and 18-exons structures, the 16-exons structures are highly diverse and only two types could be identified (Ch.III-Fig. 10). The structure 9 (merge of exons 6 and 7 as well as exons 9 and 10) is *ESL2b* brassicaceae specific and concerns 6 sequences in brassicaceae. The structure 10 (merge of exons 9 and 10 as well as exons 15 and 16) is observed for 3 sequences of *ESL2b* of solanaceae.

A striking result is that *ESL1* from monocots have a 17-exons structure (structure 2) while *ESL2* and *ESL3* have mainly 18-exons structure (structure 1). Furthermore, the 17-exons structures are highly represented in brassicaceae for which 5 structures have been identified including one specific to *ESL1* (structure 4), one specific to *ESL2a* (structure 8), two specific to the *ESL3c* (structures 6 and 7), two others with less specificity (structures 5 and 3), to which is added a 16-exons structure specific to *ESL2b* (structure 9). Thus, it seemed interesting to determine whether there is a correlation between the observed structures and the different sub-groups of monocots and brassicaceae identified in the phylogenetic analysis as such a correlation could reflect the *ESL* evolution and highlight functional differences. In the phylogenetic analysis, 3 monocots (named Mx) and 11 brassicaceae (named Bx) monophyletic groups have been identified (Ch.III-Fig. 2, 3, 4, 5 and supplementary data 4). The groups M1, M2, M3 encompass 31, 24 and 12 sequences, respectively. For *ESL1* of brassicaceae, the group B1 contains 15 sequences and can be divided into two sub-groups each of them containing at least one sequence of the 6 species and characterized either by the 17-exons structure 3 or the 17-exons structure 4. Brassicaceae *ESL2a* genes are divided into two sub-groups B2 and B3 having 6 *ESL* with 17-exons structure 5 and 4 *ESL* with the 17-exons structure 3, respectively. For *ESL2b* genes, the group B4 contains 6 sequences having the 16-exons structure 9. For *ESL3a*, the group B5 contains 5 sequences with the 18-exons structure 1. *ESL3b* genes are divided into 2 sub-groups B6, containing 13 sequences with the 18-exons structure 1 and B7 containing 8 sequences with a 17-exons structure 3. *ESL3c* genes split into 4 sub-groups: B8 containing 9 sequences with an 18-exons structure 1, B9 may be subdivided

A

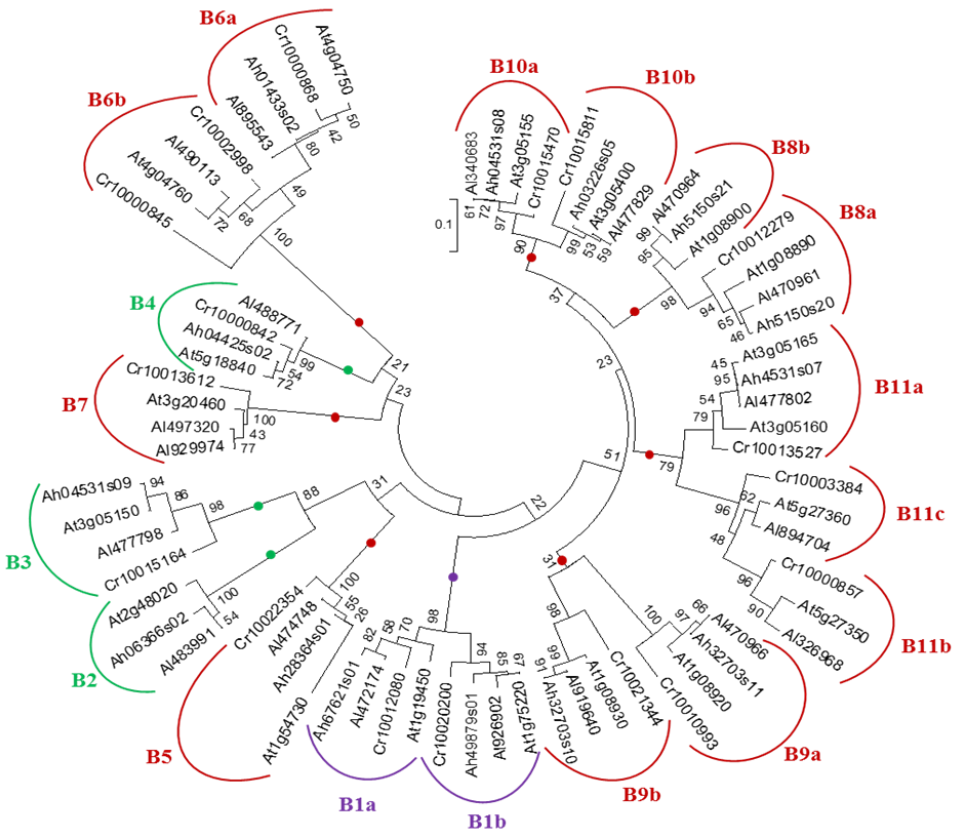

B

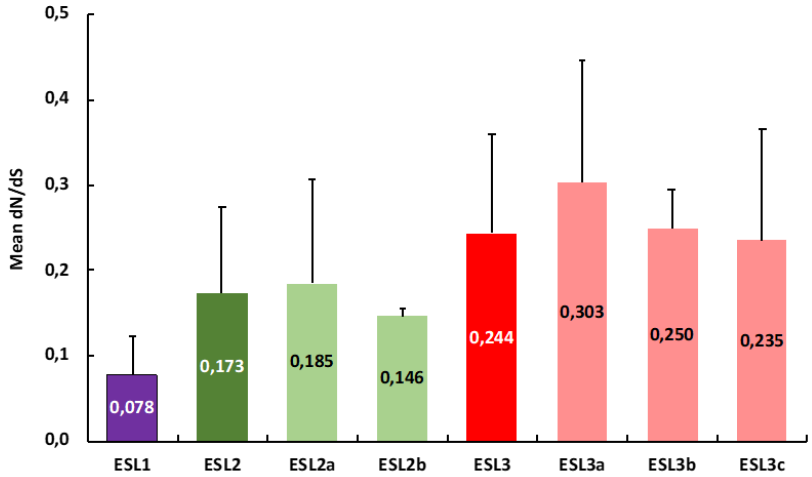

Ch.III-Fig. 11: Nucleotide substitution analysis *(dN/dS)* for *Arabidopsis ESL*. A: phylogenetic tree produced via the alignment, using ClustalW, of 69 nucleotide ESL sequences from *A. halleri*, *A. lyrate*, *A. thaliana* and *C. rubella* used as outgroup. The tree was build using the software Molecular Evolutionary Genetics Analysis (MEGAv7, Tamura et al., 2013). JTT amino acid substitution model was used and the bootstrap consensus tree was inferred from 1000 replicates. Purple is for *ESL1*, green for *ESL2* and red for *ESL3*. **B:** Means of the dN/dS values in each ESL group. Group ESL1 = 8 sequences, Group ESL2 = 10 sequences, Group ESL2a = 7 sequences, Group ESL2b = 3 sequences, Group ESL3 = 48 sequences, Group ESL3a = 4 sequences, Group ESL3b = 11 sequences, Group ESL3c =33.

into two parts one characterized by the 17-exons structure 7 and the other containing two different structures, the 17-exons structure 7 and the 18-exons structure 1, B10 is constituted by 13 sequences with the 17-exons structure 5 and B11 contains 18 sequences characterized by the 18-exons structure 1. In summary, *ESL* genes that belong to the same Brassicaceae group present the same gene structure at the exception of groups B1 and B9 for which, two or three structures are present certainly because they could be divided into sub-groups. This result shows that more the sequences have high homology, the more are similar their structures.

***ESL* transporters genes in *Arabidopsis* genus are under negative selection pressure.**

For brassicaceae, we have identified 11 groups of ESL proteins (B1 to B11), the presence of 68 tandem duplicated genes and seven different intron/exon structures. To better understand the evolutionary mechanisms involved in the genesis of *ESL* brassicaceae family we attempted to determine the selection type which is under way in the family. For this, we performed an analysis of nucleotide substitutions or dN/dS ratio for the *Arabidopsis* genus, the only one for which, in our study, the *ESL* genes have been identified in 3 different species (*A. thaliana, A. halleri* and *A. lyrata*). Since the genomes of these 3 species are highly related, the *ESL* sequences identified in *C. rubella* (another Brassicaceae) were added as an outgroup. To determine the number of alignments to be performed before calculating dN/dS ratio, a tree was built with the 65 coding sequences of the 3 *Arabidopsis* and *Capsella rubella* (Ch.III-Fig. 11A). Eighteen groups, named B1 to B11c, could be defined. They correspond to the 11 groups of brassicaceae identified on the phylogenetic tree of protein sequences (Ch.III-Fig. 2, 3, 4 and 5). Considering all sequences, the average dN/dS ratio is 0.205, with values always lower than 1 and ranging from 0.021 to 0.677. This indicates that the rate of non-synonymous mutations is lower than that of synonymous mutations. The latter means that the *ESL* sequences are under a strong selection pressure which tends to preserve the integrity of the sequences and thus potentially to conserve their functions. The 65 sequences are therefore under purifying (negative) selection. However, small differences can be detected between the means of the dN/dS ratio relative to each *ESL* group (Ch.III-Fig. 11B). The value of the dN/dS ratio for the group *ESL1* (0.078) is the lowest one, while that of *ESL3* group is the highest (0.244) and those of the sub-groups *ESL2a* (0.185) and *ESL2b* (0.146) are intermediate. Among the *ESL3* sub-groups, the group *ESL3a* shows the highest value (0.303). This suggests

Ch.III-Table 1 : Nomenclature of *A. thaliana ESL* genes

ESL Groups	Brassicaceae groups	Gene ID	New names
ESL1	B1a	At1g19450	ESL1.01
ESL1	B1b	At1g75220	ESL1.02/ERDL6
ESL2a	B2	At2g48020	ESL2.01/ZIF2
ESL2a	B3	At3g05150	ESL2.02
ESL2b	B4	At5g18840	ESL2.03
ESL3a	B5	At1g54730	ESL3.01
ESL3b	B6a	At4g04750	ESL3.02
ESL3b	B6b	At4g04760	ESL3.03
ESL3b	B7	At3g20460	ESL3.04
ESL3c	B8a	At1g08890	ESL3.05/ESL3
ESL3c	B8b	At1g08900	ESL3.06/ESL2
ESL3c	B9a	At1g08920	ESL3.07/ESL1
ESL3c	B9b	At1g08930	ESL3.08/ERD6
ESL3c	B10b	At3g05400	ESL3.09
ESL3c	B10a	At3g05155	ESL3.10
ESL3c	B11a	At3g05160	ESL3.11
ESL3c	B11a	At3g05165	ESL3.12
ESL3c	B11b	At5g27350	ESL3.13/SFP1
ESL3c	B11c	At5g27360	ESL3.14/SFP2

that even though the *ESL* genes are under purifying selection, the selection pressure might be less stringent for *ESL3* genes than that for the other *ESL*, especially the *ESL1*.

Expression Tandem duplication genes present different expression patterns in *Arabidopsis* plant

To further highlight evolution of the *ESL* genes, and especially to determine whether some of their functions are conserved or in contrary diverge, we analysed the expression of the *ESL* genes from *Arabidopsis thaliana*. First and foremost, we propose a new nomenclature for those genes, according to the 3 main ESL groups we have identified in the present phylogenetic analysis. This nomenclature (*AtESL1.xx*, *AtESL2.xx*, *AtESL3.xx*) summarized in (Ch.III-Table 1), emphasises the *ESL name of,* the group they belong to. As two tandem duplicated genes *AtESL3.09* (*At5g05155*) and *AtESL3.12* (*At5g05165*) could not be analysed because no specific primers could be designed, the expression level of 17 genes was measured in leaves, roots, buds, flowers and siliques, using qRT-PCR (Ch.III-Fig.12). The 2 *AtESL1* genes have a median expression level in the 5 tested organs, which range from 0.47 in roots and siliques to 0.82 in leaves for *AtESL1.01* and from 0.68 in siliques to 1.06 in buds for *AtESL1.02. AtESL1.02* seems to be more slightly expressed than *AtESL1.01* in all organs. The 3 *AtESL2* genes present a lower expression level. *AtESL2.01/ZIF2* and *AtESL02.2* are expressed constantly in all organs while *AtESL2.03* is more expressed in roots (1.72 ± 0.94) than in the other organs (0.11 ± 0.81). *AtESL3* genes present very diverse expression levels. *AtESL3.02*, *AtESL3.03*, *AtESL3.4,* and *AtESL3.13/SFP1* are, in all organs, the least expressed *ESL3* genes and their expression level is equivalent to that of *AtESL2* genes. On the contrary, *AtESL3.08/ERD6* is the most expressed gene in all tested organs. Its expression level is 3.5 and 11 times more important in leaves and roots than the mean of the expression values for all *ESL* in the corresponding organs. *AtESL3.01* is expressed in all organs but shows a weaker expression in roots. The other *AtESL3c* present clear organs specificities: *AtESL3.05/ESL3* expression level is 3.5 times higher in leaves (1.74 ± 1.04) than in other organs (0.37 ± 0.34). *AtESL3.06/ESL2* is more expressed in leaves (1.33 ± 0.45) as well as in siliques (0.74 ± 0.31). *AtESL3.07/ESL1* is more expressed in roots, in flowers and in siliques than in leaves and buds. *AtESL3.10* is more expressed in siliques (1.16 ± 0.63), *AtESL3.11* is more expressed in leaves (1.09 ± 0.26) and *AtESL3.14/SFP2* is more expressed in buds (1.12 ± 0.46). The normalization of the expression with the mean of the total expression in each organ, highlight that 6 ESL are highly expressed in leaves (*ESL3.08*, *ESL3.05*, *ESL3.06*, *ESL3.11*, *ESL1.02*

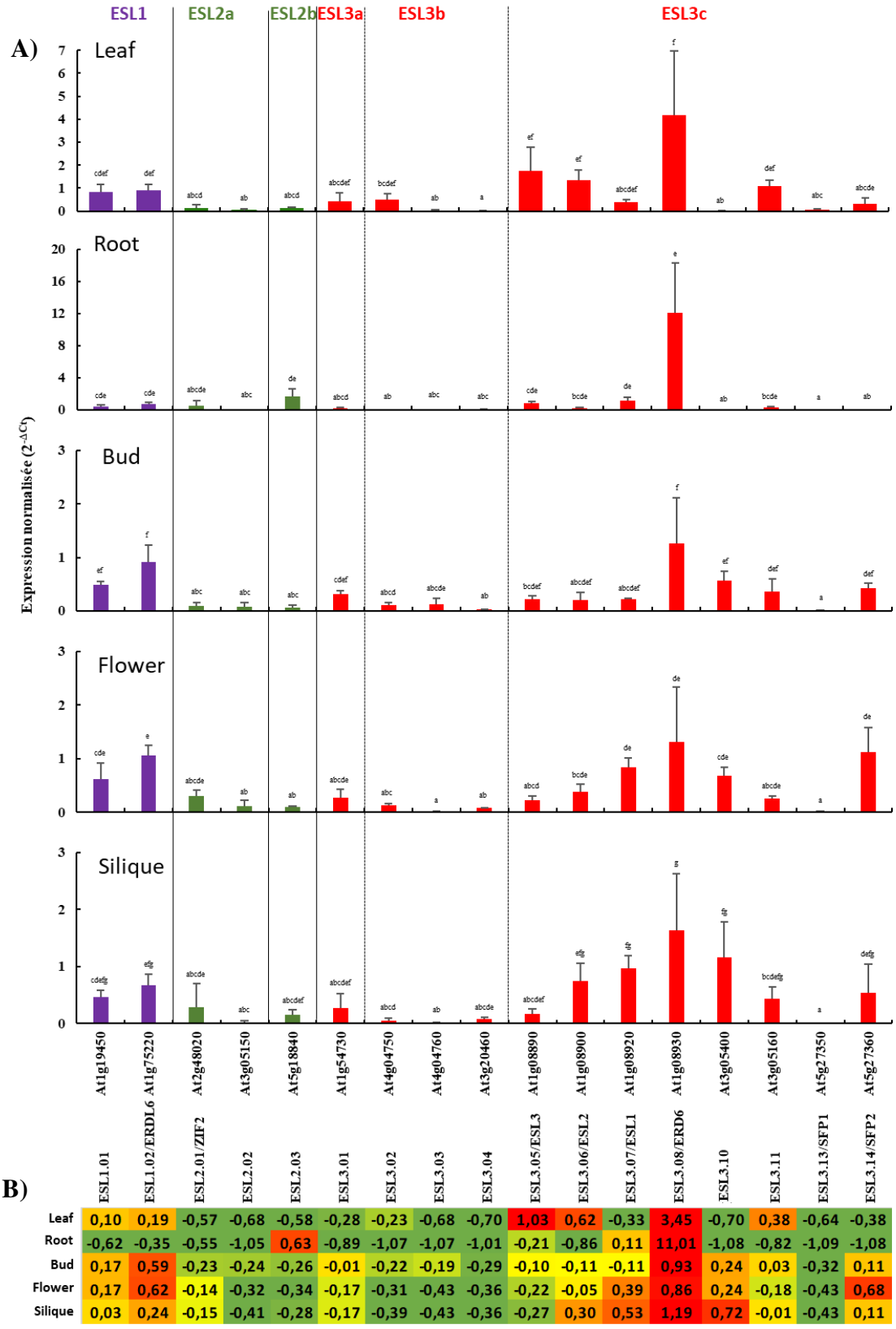

	ESL1.01	ESL1.02/ERDL6	ESL2.01/ZIF2	ESL2.02	ESL2.03	ESL3.01	ESL3.02	ESL3.03	ESL3.04	ESL3.05/ESL3	ESL3.06/ESL2	ESL3.07/ESL1	ESL3.08/ERD6	ESL3.10	ESL3.11	ESL3.13/SFP1	ESL3.14/SFP2
Leaf	0,10	0,19	-0,57	-0,68	-0,58	-0,28	-0,23	-0,68	-0,70	1,03	0,62	-0,33	3,45	-0,70	0,38	-0,64	-0,38
Root	-0,62	-0,35	-0,55	-1,05	0,63	-0,89	-1,07	-1,07	-1,01	-0,21	-0,86	0,11	11,01	-1,08	-0,82	-1,09	-1,08
Bud	0,17	0,59	-0,23	-0,24	-0,26	-0,01	-0,22	-0,19	-0,29	-0,10	-0,11	-0,11	0,93	0,24	0,03	-0,32	0,11
Flower	0,17	0,62	-0,14	-0,32	-0,34	-0,17	-0,31	-0,43	-0,36	-0,22	-0,05	0,39	0,86	0,24	-0,18	-0,43	0,68
Silique	0,03	0,24	-0,15	-0,41	-0,28	-0,17	-0,39	-0,43	-0,36	-0,27	0,30	0,53	1,19	0,72	-0,01	-0,43	0,11

Ch.III-Fig. 12: Relative expression of 17 *A. thaliana ESL* genes in different organs measured by qRT-PCR. A) $2^{-\Delta Ct}$ values are normalized according to AtPP2a expression and represent the mean of 3 biological repeats (± SD). Statistical analysis was performed using the Kruskal-Wallis test and multiple comparisons of Dunn corrected by Bonferroni. Significantly different values are indicated by different letters. Purple stands for ESL1, green for ESL2, and red for ESL3. **B)** ESL gene expression relative to the average expression of all ESL in each tested organ. The values indicated for each gene corresponds to the variation from the mean of $2^{-\Delta Ct}$ values determined for all ESL genes expressed in the considered organ. These means are equal to 0.71 in leaf, 1.09 in the root, 0.32 in flower bud, 0.44 in flower, and 0.45 in silique. The relative expression values on a red, yellow, or green background indicate that the expression of the considered gene is higher, equal, or lower than the average of the mean expression of all ESL, in the indicated organ.

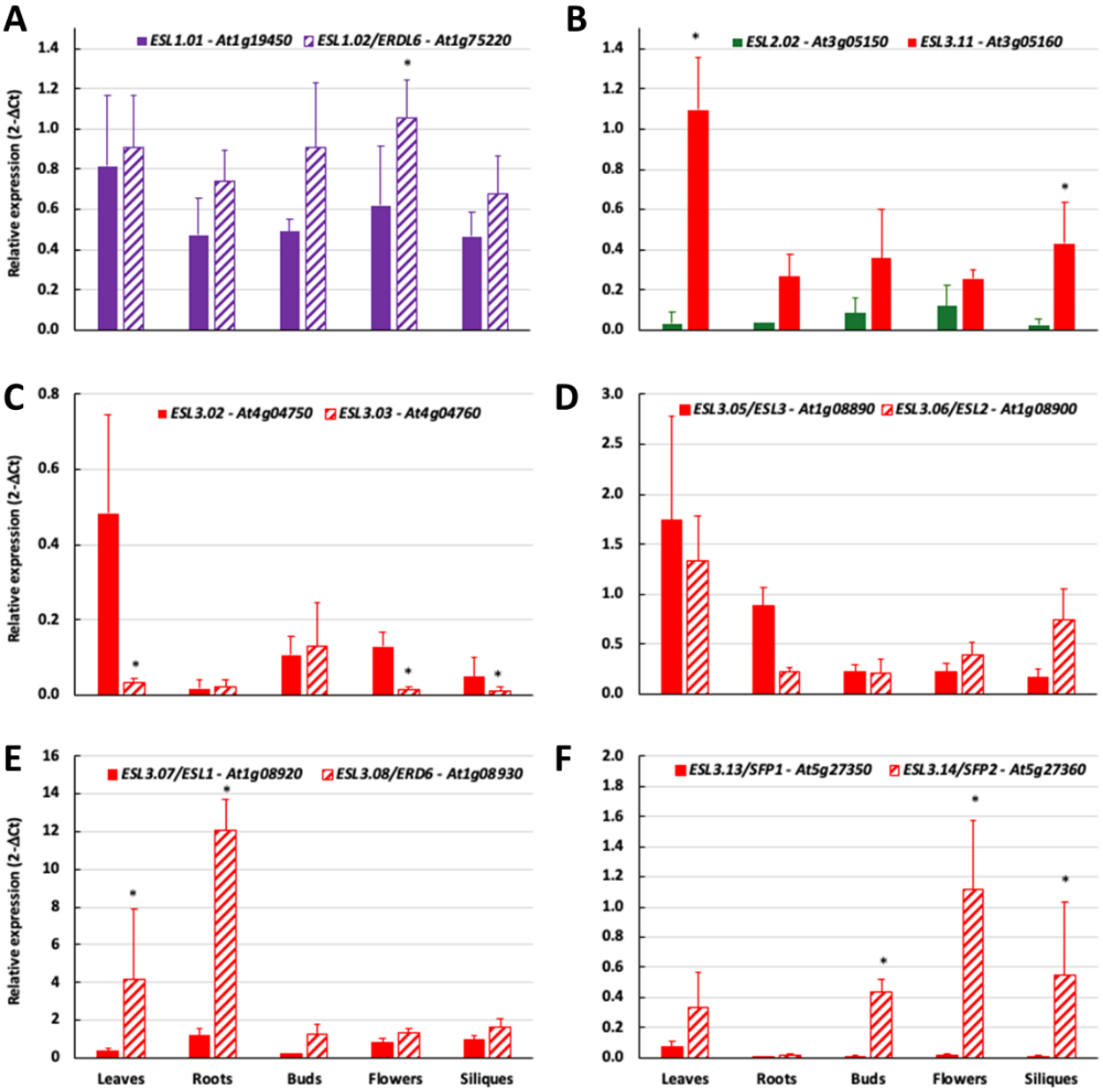

Ch.III-Fig. 12: Comparison of the relative expression of tandem duplicated *ESL* genes in different organs measured by qRT-PCR. $2^{-\Delta Ct}$ values are normalized according to *AtPP2a* expression and represent the mean of 3 biological repeats (± ecartype). Statistical analysis was performed using Kruskal-Wallis test and multiple comparison of Dunn corrected by Bonferroni. Sgnificantly different values are indicated by different letters. Purple stands for *ESL1*, green for *ESL2* and red for *ESL3*.

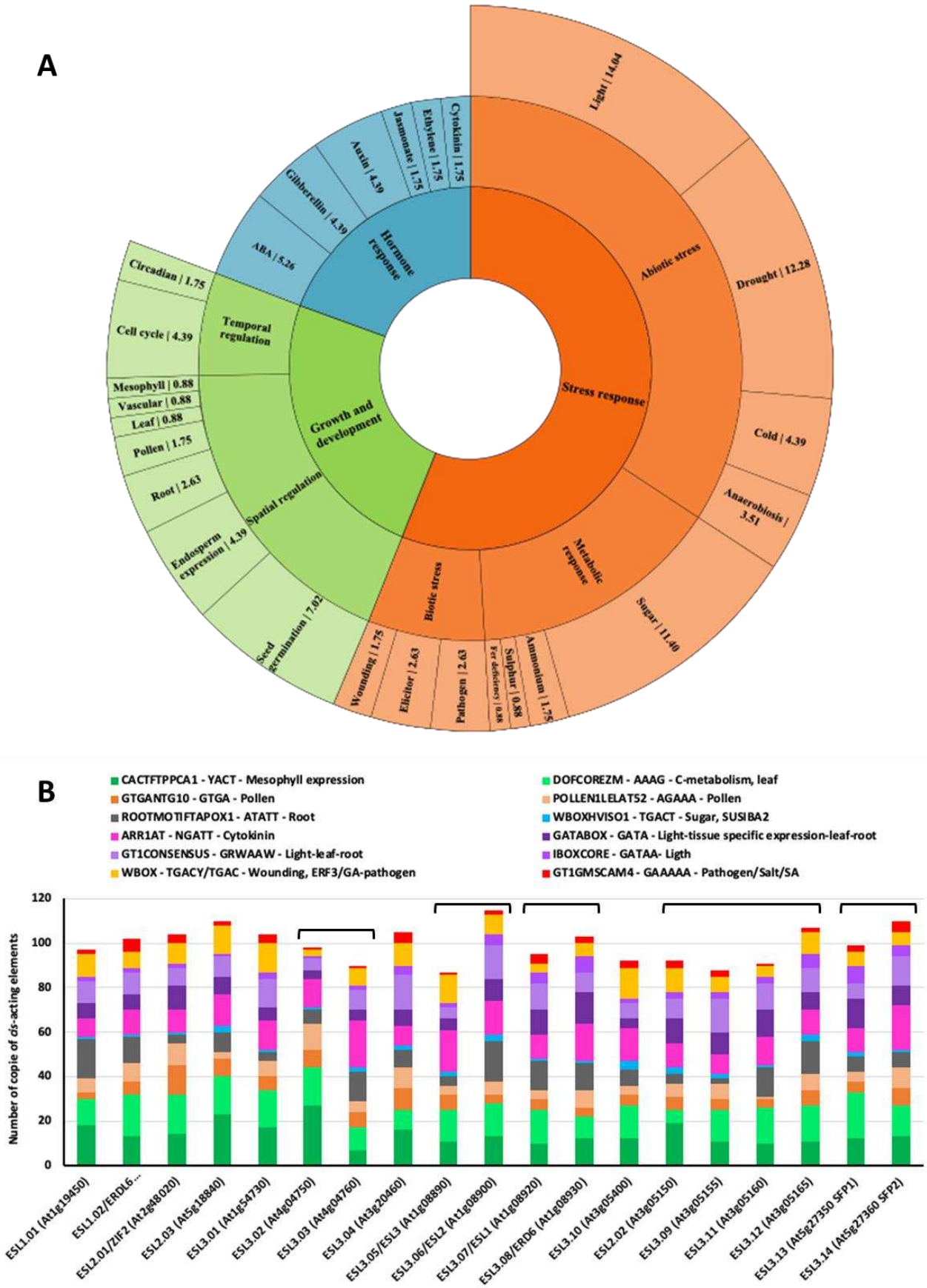

Ch.III-Fig. 13: *Cis*-regulatory elements found in the 1kb promoter of *A. thaliana ESL* genes. A: Distribution of *cis*-elements according to their specificity. **B:** Common motifs found in all analyzed *ESL* genes.

and *ESL1.01*), 3 are highly expressed in roots (*ESL3.8*, *ESL2.03*, *ESL3.07*), 5 in Buds (*ESL3.08*, *ESL1.02*, *ESL3.10*, *ESL1.01*, *ESL3.14*), 6 in flowers (*ESL3.08*, *ESL3.14*, *ESL1.02*, *ESL3.07*, *ESL3.10* and *ESL1.01*) and 5 in siliques (*ESL3.08*, *ESL3.10*, *ESL3.07*, *ESL3.06*, and *ESL1.02*).

The bioinformatic analysis lead to the identification of 5 tandem duplications (ESL2.02/ESL3.11, ESL3.02/ESL3.03, ESL3.05/ESL3.06, ESL3.07/ESL3.08, ESL3.13 /ESL3.14). We therefore compared the expression pattern of tandem genes, and included also in this analysis the two ESL1 (Ch.III-Fig. 12). The expression level of *ESL1.01* and *ESL1.02* is similar in all organs, even if ESL1.01 seems a little bit more expressed in flowers (Ch.III-Fig. 12A). *ESL3.11* is higher expressed in most organs and especially in leaves (36x) and siliques (14x) than *ESL2.02* (Ch.III-Fig. 12B). *ESL3.02* is significantly more expressed in leaves (16x), in flowers (10.7x) and siliques (5x) than *ESL3.03* (Ch.III-Fig. 12C), even if the expression level of both gene is weak. No significantly differences can be observed between *ESL3.05* and *ESL3.06* which are expressed at the same level in all the tested organs (Ch.III-Fig. 12D). *ESL3.07* and *ESL3.08* have highly different expression level in vegetative organs: *ESL3.08* is more 10.6 and 10 time more highly expressed in leaves and roots than *ESL3.07* while in reproductive organs this difference disappears as they both weakly expressed. On the opposite way, *ESL3.13* and *ESL3.14* present more different expression level in reproductive organs than in vegetative organs. *ESL3.14* is 71.6x, 111x and 91.6x time more expressed than *ESL3.13* in buds, flowers and siliques.

Cis-acting elements putatively involved in transcriptional regulation of _AtESL_ transporters

We have identified a 1kb promoter region for each of the 19 *AtESL*, performed a PLACE analysis and found 186 cis-acting elements that have been classified in three main categories: Growth and development, Hormone response and stress response, the latter ones being the most numerous (Ch.III-Fig. 13A). Twelve common motifs were found in all analyzed *ESL* genes (Ch.III-Fig. 13B). These motifs are highly repetitive (up to 27 copies) and this might be due to their limited length (4 to 6 bases). Among the Twelve *cis*-acting elements, some are able to confer expression in different plant organs such as leaves, pollen, and roots, others are involved in hormonal signaling (cytokinin and salicylic acid) or in response to biotic and abiotic environmental factors such as light and salinity. Interestingly, one motif involved in sugar regulation, WBOXHVISO1 (sequence TGACT) is present in all *ESL* promoters, in few copies. *Cis*-elements conferring expression in leaves or

Ch.III-Table 2: Unique *cis*-acting elements identified only in the promoter sequence of a single *Arabidopsis thaliana* ESL transporter gene

Gene	Cis-element name	Sequence	Response	Position	Copy number
At1g19450	AUXREPSIAA4	KGTCCCAT	Auxin	919(-)	1
	BOXCPSAS1	CTCCCAC	Light	507(+)	1
At2g48020 ZIF2	ANAERO2CONSENSUS	AGCAGC	Anaerobic	205(+)	1
At5g18840	AMMORESIIUDCRNIA1	GGWAGGGT	Ammonium response	427(-)	1
At1g54730	ATHB2ATCONSENSUS	CAATSATTG	Recognition site of Ahb-2 protein	30(-), 30(+)	2
	UP1ATMSD	GGCCCAWWW	Auxillary bud out growth	262(+)	1
	BBOXSITE1STPAT	GCTAAACAAT	Tuber specific ans sucrose induction	10(+)	1
	CEREGLUBOX2PSLEGA	TGAAAACT	Cereal glutenin box	425(+)	1
At4g04750	ABREATCONSENSUS	YACGTGGC	ABA	438(-)	1
	ACGTOSGLUB1	GTACGTG	Seed development (endosperm)	447(+)	1
	EMBP1TAEM	CACGTGGC	ABA	438(-)	1
	IRO2OS	CACGTGG	Fe deficiency	439(-)	1
At1g08890 ESL3	ABREMOTIFAOSOSEM	TACGTGTC	ABA	170(+)	1
	GCCCORE	GCCGCC	Ethylène-JA(defense)	328(-)	1
	LTREATLTI78	ACCGACA	Cold	376(+)	1
	ZDNAFORMINGATCAB1 (Z-box)	ATACGTGT	Light, leaf, shoot	169(+)	1
At1g08920 ESL1	PALINDROMICCBOXGM	TGACGTCA	Hypocotyl elongation	247(-), 247(+)	2
At1g08930 ERD6	ANAERO4CONSENSUS	GTTTHGCAA	Anaerobic	359(+)	1
	CRTDREHVCBF2	GTCGAC	Cold-drought	545(-), 545(+)	2
	SPHCOREZMC1	TCCATGCAT	seed-specific hormone (ABA)	491(-)	1
	RYREPEATVFLEB4	CATGCATG	Seed-specifique regulation	490(-)	1
	UPRMOTIFIIAT	CCNNNNNNNNNNNNCCACG	Unfolded protein response	991(+)	1
At3g05400	AMMORESIVDCRNIA1	CGAACTT	Ammonium response	896(-)	1
At3g05155	AUXRETGA1GMGH3	TGACGTAA	Auxin	726(-)	1
	PALBOXAPC	CCGTCC	Light-elicitor	495(-)	1
At3g05160	AGATCONSENSUS	TTWCCWWWWNNGGWW	Binding of Agamous	697(+)	1
At3g05165	BS1EGCCR	AGCGGG	Vascular expression	173(-)	1
	ATHB1ATCONSENSUS	CAATWATTG	Binding site of ATHB1	525(-), 525(+)	2
At5g27350 SFP1	CEREGLUBOX3PSLEGA	TGTAAAAGT	Cereal glutenin box	387(+)	1
At5g27360 SFP2	TGTCACACMCUCUMISIN	TGTCACA	Fruit-specific expression (cucumisin gene)	975(-)	1

Hormonal regulation
Abiotic stresses
Cellular development
Nutrition
Plant growth and development

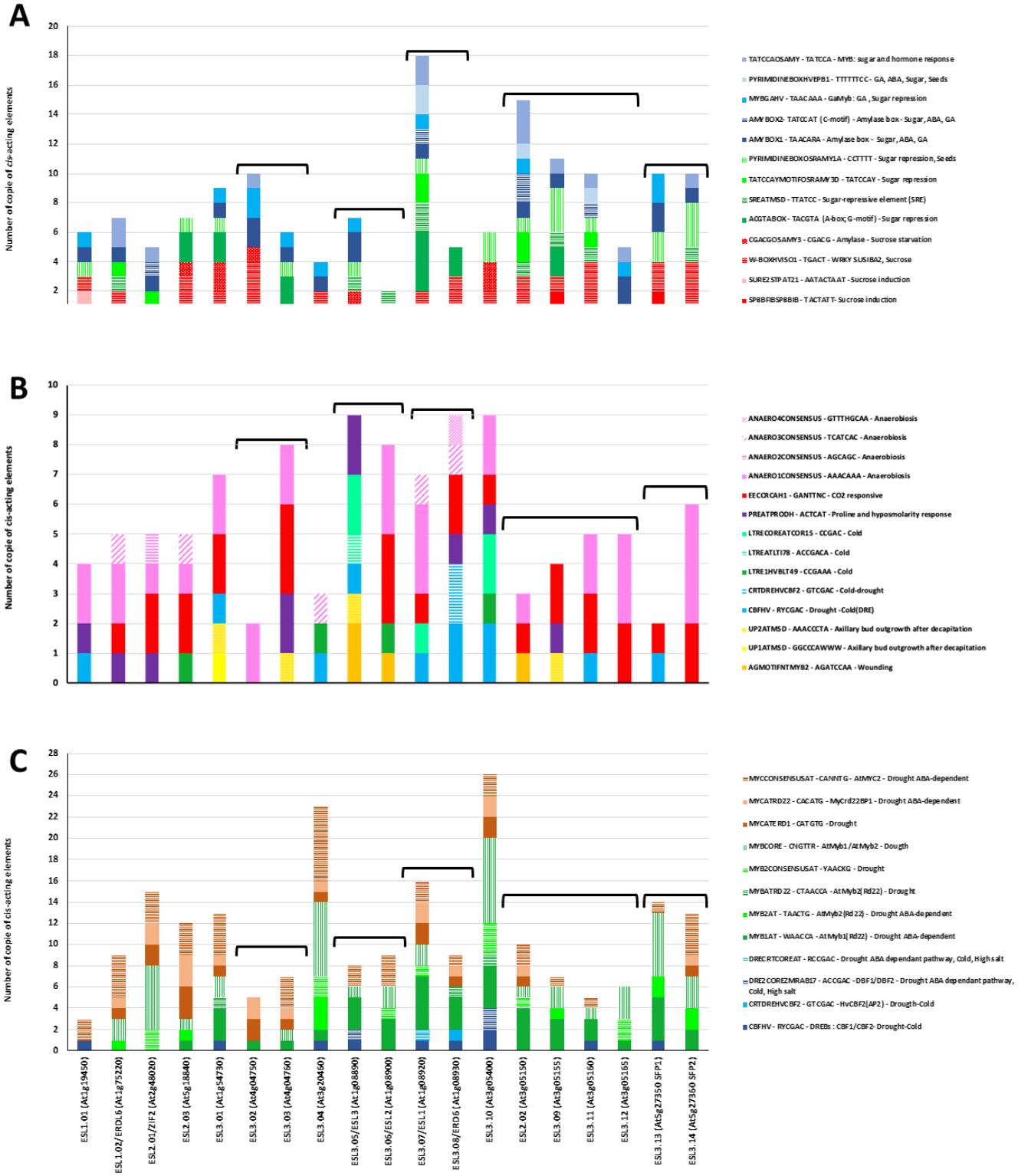

Ch.III-Fig. 14: Sugar and stress *cis*-regulatory elements found in the 1kb promoter of *A. thaliana* *ESL genes*. A: *Cis*-elements involved in sugar regulation. **B:** *Cis*-elements involved in abiotic stresses response. **C:** *Cis*-elements involved in drought response.

mesophyll cells are the more represented ones. Beside the common *cis*-regulatory elements, we identified 30 *cis*-acting elements which, were only found in a single promoter, thereby implying some expression specificity (Ch.III-Table 2). Their length varied from 6 to 19 bp. Interestingly, among the 30 identified gene-specific motifs, 5 are present only in the *ESL3.08/ERD6* promoter, 4 in *ESL3.01* and *ESL3.05/ESL3*. *ESL1.02/ERDL6*, *ESL2.02*, *ESL3.03, ESL3.04* and *ESL3.06/ESL2* do not have specific elements. These motifs can be grouped into different functional categories, which are related to hormonal regulation (6), abiotic stresses (5), cellular development (6), nutrition (3) and plant growth and development (1).

In silico analysis of *AtESL* promoters resulted in the identification 13 motifs, that are potentially involved in sugar-regulated transcription (Ch.III-Fig. 14A). We found, *cis*-acting elements involved in sucrose induction, such as SP8 and WBOXHVISO1 (sequences enabling the binding of some WRKY-type proteins, at the example of SPF and SUSIBA2), SURE boxes (SURE2STPAT21), and the CGACGOSAMY3. Four other elements are involved in sugar repression (ACGTABOX, SREATMSD, TATCCAYMOTIFOSRAMY3D and PYRIMIDINEBOXOSRAMY1A), and 5 cis-elements involved in common hormonal and metabolic (sugar) signals perception, e.g. the GARC complex consisting of the AMYBOX1 and 2, the MYBGAHV for gibberellines (GAs) induction and sugar repression, the PYRIMIDINE boxes for GAs, ABA and TATCCOSAMY a sequence enabling the binding of MYB proteins. And it is interesting to note that the number and the distribution of those sugar-elements are really different between tandem duplicated copies, at the exception of *ESL3.13/SFP1* and *ESL3.14/SFP2* and the two *ESL1*. We found also numerous *cis*-acting elements involved in diverse stress responses (Ch.III-Fig. 14B). The two more abundant are elements involved in anarebiosis (ANAEROxCONCENSUS) found in all *AtESL* except *ESL3.05/ESL2, ESL3.09* and *ESL3.13*, and a CO_2 responsive element (EECCRAH1) found in most all *AtESL* at the exception of *ESL1.01, ESL3.02* and *ESL3.05/ESL2*. Five elements involved in cold response are mainly present in promoter of ELS3 genes, as well as three other involved in wounding and axillary bud outgrowth after decapitation. The number and the distribution of those elements are really different between *ESL1.01* and *ESL1.02*, as well as between the two tandem genes *ESL3.07/ESL1* and *ESL3.08/ERD6*. Differences could be nice observed between two pairs of tandem genes: *ESL3.02* has only ANAERO1CONSENSUS element while *ESL3.03* has, in addition, *cis*-elements for hypoosmolarity, CO_2 and wounding responses.

ESL3.13/SPF1 has cis-elements involved in cold response while *ES13.14/SFP2* elements for CO_2 response. We detected in all AtESL promoters numerous drought responsive *cis*-elements (Ch.III-Fig. 14C), such as DREB or element enabling either the binding of MYB or MYC transduction factors. The cis-elements that seem the most abundant are MYB-elements. Some differences can be observed between *ESL1.01* and *ESL1.02* which does not have *cis*-acting elements for MYB but instead DREB elements and the number of cis-acting elements in ESL3.07/ESL1 is high than that found in ESL3.07/ERD6. This analysis suggests that AtESL might be differentially regulated by sugar, hormones and diverse abiotic stresses such as drought and opens perspectives for future research.

Discussion

The present study on the evolutionary history of ESL monosaccharide transporters provides arguments in favour of the hypothesis of their emergence in charophytes. This hypothesis is built on the fact that no ESLs were identified in any of the chlorophytes (8 species) and rhodophytes (3 species) genomes, as well as in that of the brown algae *E. siliculosus*, while a single ESL was identified in the genome of *K. nitens* (Ch.III-Fig. 1). It is noteworthy that the high stringency imposed in the search of ESL proteins could be restrictive for the identification of monosaccharide transporters in algae displaying low level of homology to embryophyta ESL. However, the veracity of our hypothesis is reinforced by the fact that carriers similar to sucrose and other monosaccharide transporters have been identified in algae. Sucrose transporter homologs have been identified in the genome of the characean algae *Chlorokybus atmosphyticus* (Reinders et al., 2012), of rhodophytes (*C. merolae and G. sulphuraria*) and chlorophytes (*O. lucimarinus and O. tauri*) (Peng et al., 2014), even some chlorophytes do not have sucrose transporter homologs, at the example of *C. reinhardtii* and *V. carterii* (Reinders et al., 2012). Close homologs of monosaccharides transporters (HUP1, HUP2, HUP3) have been found in the green algae *Chlorella* (Sauer and Tanner, 1989; Caspari et al., 1994; Stadler et al., 1995; Johnson et al., 2006). However, these are more closely related to the STP monosaccharide's transporters sub-family than to the ESL. Taken together, these data suggest the existence of some hexose and sucrose transporters in algae and support the idea that ESL carriers have arisen after the sucrose and the STP transporters.

The identification of an ESL transporter in *K. nitens* is in agreement with the generally accepted hypothesis that the ancestors of terrestrial plants are closely related to the

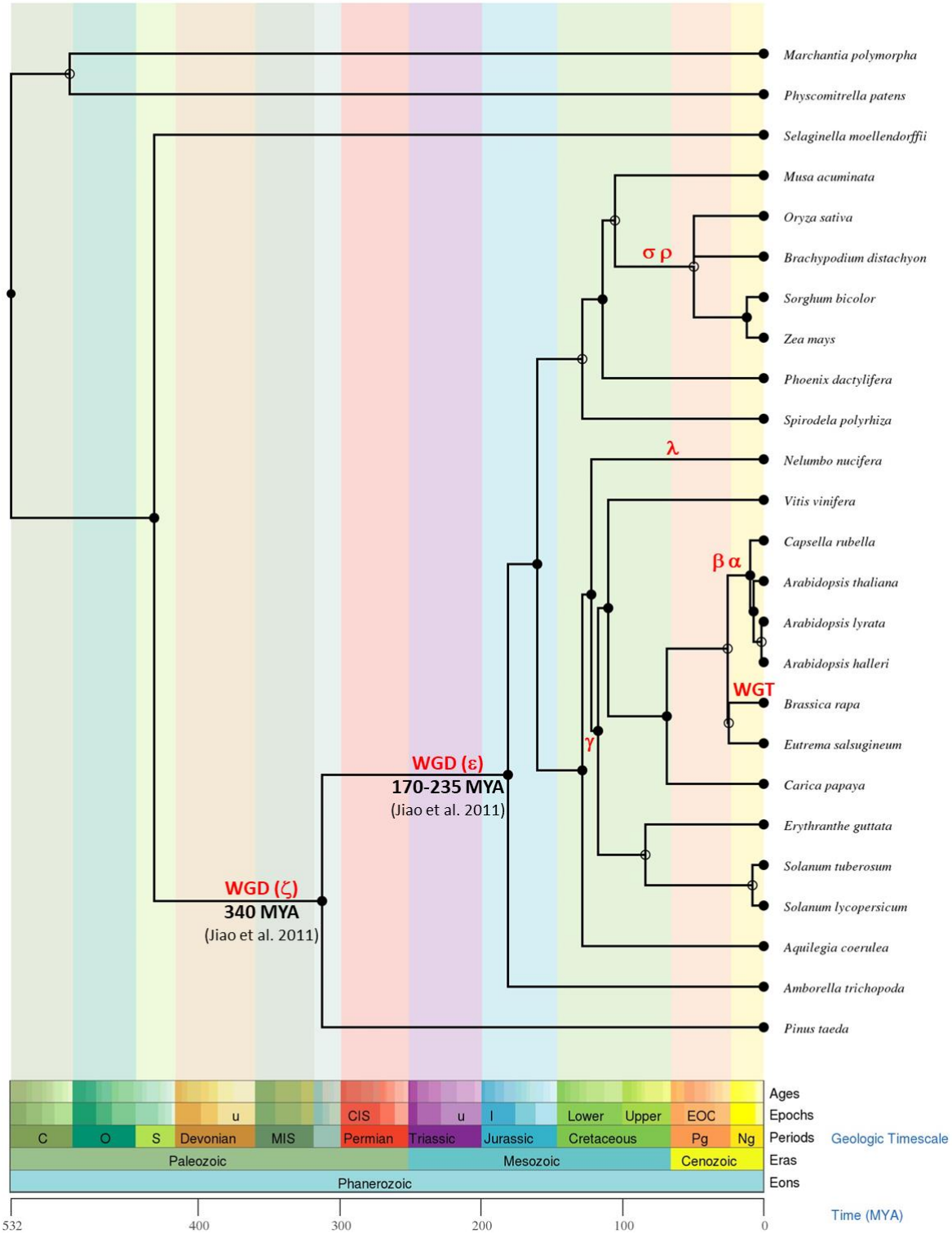

Ch.III-Fig. 15: Phylogenetic tree inference of the evolution of *ESL* genes in the plant kingdom. All date, periods and evolutionary data used to rebuild the evolutionary history of ESL family trough the evolution of land plants were obtained from Time Tree of Life (http://www.timetree.org, Hedges et al., 2006; Kumar et al., 2017). For readability reasons, only the most striking species have been considered. Major duplication events are indicated according to the literature.

charophytes (Lewis and McCourt, 2004; Leliaert et al., 2012; Timme et al., 2012). The analysis of the genomes of *K. flaccidum* (Hori et al., 2014) and *C. braunii* reveals that both organisms have acquired several plant genes, involved in phytohormones' production, tolerance to high-intensity light and to reactive oxygen species, as well as transcription factors (Hori et al., 2014; Nishiyama et al., 2018). This suggests that charophytes have already acquired necessary features required for adaptation to terrestrial live, such as tolerance to drought and freezing, as demonstrated for some *Klebsormidium* species (Morison and Sheath, 1985; Elster et al., 2008; Nagao et al., 2008; Karsten and Holzinger, 2011). As the few characterized ESL carriers have been described to be regulated in response to environmental constraints (cold, drought, high salinity, temperature, wounding and heavy metals), one can imagine that they have been acquired in charophytes also for adaptation to terrestrial environments.

The undeniable presence of ESL in each analysed embryophytes genomes, with a lower number of copies in bryophytes, and lycophytes (1 for *S. fallax*, 2 for *M. polymorpha* and *S. moellendorffii*, 3 for *P. patens*) than in seed plants (3 to 37 copies) suggests that ESL carriers have undergone significant expansion and have become a large multigenic family in angiosperms, in particular in eudicots. Our phylogenetic analysis of 519 ESL proteins identified in the proteomes of 47 Embryophytes provides evidence for the existence of three ESL monophyletic groups named Group ESL1, Group ESL2 and Group ESL3 (Ch.III-Fig. 2). The Group ESL1 encompasses sequences from each studied embryophyte including all copies, present in the genomes of *P. patens* (bryophyte), *S. moellendorffii* (lycophyte), and half of those of *P. taeda* (gymnosperm) (Ch.III-Fig. 3). Thus, *ESL1* genes might probably represent the most ancient copies. The fact that the sequences of gymnosperms and angiosperms are the only one to split into two distinct groups and that the sequences of *P. taeda* are located at the basis of both ESL2 and ESL3 groups (Ch.III-Fig. 2 and 3) highly suggests a first event of duplication in the common ancestor of seed plants (Ch.III-Fig. 15). This duplication event corresponds certainly to the most ancient whole genome duplication (WGD) named paleopolyploidy (or ζ), which has occurred approximately 340 million years ago (MYA) in the common ancestors of all spermaphytes (Jiao et al., 2011). Similarly, in the second ESL group, mesangiosperms sequences split to form ESL2 and ESL3 groups, while the ESL sequences of the basal angiosperm *A. trichopoda* are present only at the basis of group ESL2 (4 sequences), and are absent in group ESL3, which is therefore specific to mesangiosperms. These observations argue in favour for a second duplication event in the common ancestor of the mesangiosperms (Ch.III-Fig. 15), which could be related to the WGD ε described in the

angiosperm lineage that have occurred 170-235 MYA (Jiao et al., 2011). Our phylogenetic analysis suggests that this event might not have occurred for the basal angiosperm *A. trichopoda*. The ESL3 group can be clearly divided into three sub-groups named ESL3a, ESL3b and ESL3c. Sequences of monocots and of the basal eudicots: *A. coerulea* and *N. nucifera* belong only to the ESL3a and are excluded from the ESL3b and c groups, which thus represent pentapetalae (rosids and asterids) specific sub-groups. This suggests a third duplication event in the common ancestor of the pentapetalae (Ch.III-Fig. 15), probably the whole genome triplication event (WGT) γ/1R, which has taken place early in the evolution of eudicots evolution, around 117 MYA, before the separation of rosids and asterids and after the split of monocots and dicots (Jiao et al., 2012). This event witnesses the existence of an ancient hexaploidy in eudicots. The absence of sequences of the basal eudicots in group ESL3b and c is in total agreement with the fact that the γ/1R triplication event has been placed after the divergence of the ranunculales and core eudicots (Jiao et al., 2012), and that the genome of *N. nucifera* has undergone another duplication event named λ (Ming et al., 2013). The fact that monocots are also not present in ESL3b and ESL3c groups is in agreement with the description of two important WGD, named ρ and σ, that have occurred before the divergence of poaceae and are independent of the γ/1R event (Blanc and Wolfe, 2004; Paterson et al., 2004; Tang et al., 2010; D'Hont et al., 2012). Thus, we can suggest that the ESL3b and ESL3c sequences, the only sequences from vitaceae, eurosids and asterids, are the outcomes of the γ/1R triplication event (Ch.III-Fig. 15). However, ESL3b and c copies may also be marks of more recent duplication events. Such events have been described for salicaceae (Tuskan et al., 2006), for fabaceae (Cannon et al., 2005; Cannon et al., 2006; Sato et al., 2008; Varshney et al., 2013) for *M. domestica* (Velasco et al., 2010) and malvaceae (Argout et al., 2011; Wang et al., 2012). For brassicaceae, in addition to the γ/1R, 2 WGD, named α/3R and β/2R (Bowers et al., 2003; Jiao et al., 2011) have been described to occur after the divergence of brassicaceae and caricaceae around 47 and 124 MYA, respectively (Kagale et al., 2014). The 6 brassicaceae ESL groups observed in ESL3b and ESL3c groups might, therefore represent the marks of these three WGD events. In addition, the genus *Brassica* underwent a triplication (WGT) event around 7.9 and 14.6 MYA (Lysak et al., 2005; Beilstein et al., 2010), which could explain the high number of ESL genes (30 genes) identified in *B. rapa* genome. Segmental duplications may also explain the ESL diversification. It might be the case for *L. usitatissimum,* for which a specific WGD event detected around 5 to 9 MYA has been described, as well as numerous segmental duplications

(Wang et al., 2012). The high number of ESL found in this species is probably related to those events. An interesting result is the observation of a high number of tandem duplications in the ESL subfamily. We identified 246 duplicated genes representing 47% out of the 519 analysed ESL. Their proportion varies with ESL groups (10.2 % are *ESL1*, 20.7% are *ESL2* and 69.1% are *ESL3*). Furthermore, tandem duplicated genes are more present in the *ESL3c* group (40.2%) than in *ESL3a* (16.3%) and *ESL3b* (12.6%). In this latter regard, we could show a good correlation between the numbers of tandems duplicated *ESL3c* genes and the total number of *ESL3* per species (Ch.III-Fig. 7, 8 and Supplementary Table 3). *ESL3c* tandem duplications are dominant in *Vitis*, Eurosids and solanales but they were not detected in fabales, rosaceae, cucurbitales and phrymaceae. For fabales, this is certainly correlated to a weaker expansion of *ESL* genes than those observed for other monosaccharide carrier sub-families such as STP, PLT and INT (Johnson et al., 2006; Doidy et al., 2019). *E. grandis* presents a remarkable expansion with 37 *ESL* genes among which 25 are genes in tandem repeats (67.6%). The observation is in agreement with the study of Myburg et al. (2014), who have described in this species the largest number of genes in tandem repeats (34% of total genes). These results suggest that tandem duplications are also involved in the expansion of ESL family, in particular for *ESL3c* genes. It has been reported that tandem duplicated genes, which are retained in a lineage-specific manner, are mostly responsive to environmental biotic (Hanada et al., 2008) or abiotic (Zhang et al., 2016) stimuli. Therefore, the high number of tandem duplications observed for ESL emphasises the involvement of these transporters in response to environmental cues, such as already demonstrated for some of them either for abiotic (Kiyosue et al., 1998; Quirino et al., 2001; Yamada et al., 2010; Poschet et al., 2011; Remy et al., 2014) or biotic stresses (Breia et al., 2020).

The analysis of non-synonymous and synonymous mutations by the dN/dS mean ratio of the ESL copies of the genus *Arabidopsis* (*A. halleri, A. lyrata, A. thaliana*) using *C. rubella* as outgroup revealed that all these recently diverged genes have been submitted to purifying selection acting in favour of protein structural and functional conservation, as sugar transporters. It is noteworthy that the dN/dS value increases progressively from the group ESL1 (dN/dS = 0.081), throughout the group ESL2 (dN/dS = 0.172) to the group ESL3 (dN/dS = 0.233), suggesting a slow decrease of the selection pressure. Even though the threshold of 1 corresponding to a diversifying selection is not yet reached, we may speculate that the progressive increase of dN/dS ratio acts in favour of sub-diversification phenomena, towards a possible acquisition of novel functions by ESL monosaccharide transporters.

As structural changes in protein coding regions are a phenomenon that can lead to subfunctionalization or neofunctionalization following gene duplication, we analyzed the gene structure of the 519 identified *ESL.* We found at least 10 different types of structure including 1 specific to *ESL1* of monocots, 1 specific to *ESL2a* of Rutaceae, 1 specific to *ESL2b* of Solanaceae and 6 specific to Brassicaceae. The first one, named structure 1, is 18-exon structure, found in more than 50% of the *ESL* sequences including those from ancestral species. Thus, it seems likely to be the ancestral type that has been preserved throughout evolution. The nine other 17-exon and 16-exon structures have probably appeared in the course of evolution by intron loss. This hypothesis is in agreement with already reported data for Arabidopsis and rice, which show that after gene duplication, the intron loss rate is higher than that of the intron gain rate (Roy and Gilbert, 2005; Lin et al., 2006). However, it is surprising that *ESL1* for Monocots and Brassicaceae, which might represent ancient copies, has 17-exon structure, which implies more complex evolutionary mechanisms (structures 2 and 4; Figure 10).

Although *AtESL* expression levels are variable from gene to gene in *A. thaliana* organs, our expression analysis has shown that the expression of 17 genes could be detected in five organs, demonstrating that they are all expressed. On the contrary, *ESL3.09 (At3g05155)* and *ESL3.12 (At3g05165)* could not be amplified nor analyzed because no specific primers could be correctly designed for them. This is in agreement with the fact that no expression data are available in the Genevestator and BAR databases, suggesting that they are pseudogenes. At least for *ESL3.09 (At3g05155),* this is corroborated by its very short sequence presenting 13 exons only. *ESL1.01* and *ESL1.02* are expressed more or less constitutively in all tested organs and at the same level. The lack of organ-preferential expression for these *ESL1* genes potentially allows them to respond to a wide range of developmental and/or environmental signals. This is consistent with the hypothesis that *ESL1 gene*s are derived from ancestral copies, present in the genomes of *P. patens* (moss) and *S. moellendorffii* (fern). ESL2 genes are rather weakly expressed and only *ESL2.03* shows preferential expression in roots. In our experimental conditions, E*SL2.01/ZIF2,* is a weakly expressed gene, maybe slightly more expressed in roots, flowers and siliques. This is in agreement with Remy et al. (2014), who have shown higher expression in roots and flowers. However, they have identified differences in the expression levels of two splice variants, which were not taken into account in our study. For ESL3 gene, we observed low level of expression for *ESL3.03, ESL3.04* and *ESL3.13/SFP1*. Our results highlight a preferential expression pattern of

ESL3.08/ERD6 in vegetative organs compared to reproductive organs, and conversely, highest expression of *ESL3.10* in reproductive organs compared to the vegetative ones, especially in siliques. The *AtESL3c* genes, whose dN/dS within the genus *Arabidopsis,* suggests less selection pressure than that for *ESL1* and *ESL2*, show different expression patterns in the five tested organs. This implies more rapid evolution and some sub-functionalization of their copies. Among the *ESL* tandem pairs, no or weak differences in the expression between the two copies could be detected for the two pairs *ESL1.01/ESL1.01* and *ESL3.05/ESL3.06*. Inversely, highly significant differential expression was clearly demonstrated for the following tandems: *ESL2.02/ESL3.11* in leaves and siliques; *ESL3.02/ESL3.03* in leaves, flowers and siliques; *ESL3.13/ESL3.14* in the reproductive organs; *ESL3.07/ESL3.08* in the vegetative organs. *ESL3.13/SFP1* was the most weakly expressed of the *ESL3c*. The latter is corroborated by Northern blot results demonstrating that *ESL3.13/SFP1* has been undetectable in young and fully expanded leaves, stems and roots, while *ESL3.14/SFP2* expression has been observed in these organs (Quirino et al., 2001). *ESL3.13/SFP1* has strongly been expressed in seedlings and highly induced in senescent leaves, while *ESL3.14/SFP2* that has been not detectable (Quirino et al., 2001). *ESL3.08/ERD6* has been more expressed than *ESL2.08/ESL* at least in leaves, roots and buds. This result is in perfect accordance with the results of Yamada et al. (2010) who have also shown that *ESL3.08/ERD6* is more expressed than *ESL2.08/ESL1* in leaves from plants grown under normal conditions. They have also determined that transcriptional activity conferred by the promoters of *ESL3.08/ERD6* and *ESL3.07/ESL1* is preferentially located in the same organs, i.e. shoots, sepals and roots. In roots *ESL3.08/ERD6* is specifically expressed in epidermal and cortical cells, while *ESL3.07/ESL1* - in endoderm, pericycle and xylem parenchyma cells (Yamada et al., 2010). The latter data and our own results of their differential and organ-preferential expression highlight possible mechanisms of sub-functionalization for most of the tandem duplicated *AtESL*.

Conclusion

Evolutionary analysis of plant ESL transporters using protein sequences from various species representive for the main groups of the plant kingdom demonstrated that these genes have emerged in Charophytes and expanded through whole genome duplications in Embryophytes. Although the most recently diverged *AtESL* genes still remain under purifying selection, their increasing dN/dS ratios, highly variable gene structure and organ-preferential expression emphasize the onset of a plausible diversification. The remarkable plethora of

promoter *cis*-acting elements, tightly related to developmental and environmental cues, opens novel perspectives to further elucaditon the ESLs' biological functions.

Supplementary data

Supplementary data 1: ESL genes identified in this study

Supplementary data 2. Primers used for the expression analysis of *AtESL* par qRT-PCR.

Supplementary data 3: Number of ESL genes and Tandem duplicated ESL identified in this study

Supplementary data 2. Primers used for the expression analysis of *AtESL* par qRT-PCR.

Genes	Sequences	Tm (°C)	Length (nt)	Taille de l'amplicon (bp)	Efficacité	Observations
At1g19450	F : TAAGCCTCGTGATTGTAGCA	58	20	121	90	-
	R : CAAGAAATAACCATAGCCACA	58	21			
At1g75220	F : GTGGAGGAACTTTCACTCTGTA	64	22	99	90	-
	R : GTTCTTCAAGAGTTTTGCCTT	58	21			
At2g48020	F : CTGAGATATTTCCCATAAACAT	58	21	139	93	-
	R : AAGATTGCAATTTATGTCCCAG	58	21			
At3g05150	F : TTCTTTTGAAGGCTCATGGTT	58	21	200	-	-
	R : GACAAGCCATGAACTTAGCCA	62	19			
At5g18840	F : CTGAGATATTTCCGATAAACGTA	62	23	177	114	-
	R : TCTTCGCCACAAATATTATCGTC	64	23			
At1g54730	F : AATCCGGCAGGAACGTTTTATG	64	22	179	100	-
	R : CGTTATAATTAGGGACTGATAT	58	22			
At4g04750	F : TACAGGAACGTTTATGATGTTT	58	22	203	90	-
	R : CATGAAATATAAAGAGATCTGA	56	22			
At4g04760	F : CAGAGATTTATCCAGTAGATGT	60	22	174	100	-
	R : TGGCTATGAACACAAATCCAA	58	21			
At3g05400	F : CTTCTTATGACTTCAGCGTTGG	64	22	148	100	-
	R : CAATTGCGAACATCATCGT	54	19			
At1g08890	F : TGGAGTGCTTTCGGAACATATT	60	22	150	109	-
	R : GAGTAAAGAATCAACTTTGGAT	58	22			
At1g08900	F : GTAGCCTTGTAACGATGTCA	58	20	99	97	-
	R : ATATGAAATATGTTCCGGAAGC	60	22			
At3g20460	F: ACGCTATGCAATTTAACTAGCTG	64	23	89	97	-
	R : AACACACCAGAAGAGCTCCACT	66	22			
At1g08920	F : TCGGTCTCATTCCATGTGCG	62	20	131	97	-
	R : TGCATCATCTCCGCGAAGAC	62	20			
At1g08930	F : ATAATGGCTGAGATATTTCCG	58	21	176	95	-
	R : ATAAATACGATCGAACTGGC	60	20			
At3g05155	F : GTGGTACCAAAAGCTATATTGG	62	22	164	-	No amplification
	R : CCGATGCCTGCAAATTTGTACA	64	22			
At3g05160	F : GCACAAGGAACCTTTTACATAT	60	22	101	90	-
	R : AATTCTTCAAGCGACTGTCC	58	20			
At3g05165	F : AAGGAACATTTTACATATTTGC	56	22	167	-	Not enougth specificity
	R : TTTATTATTTGCAATGCGACT	54	21			
At5g27350	F : TATGTCGGAGATATTTCCAATA	58	22	269	97	-
	R : CAAATTAAGTTTGATTTCTTTC	54	22			
At5g27360	F : AGTGGAGCACTCAAGGAACATT	64	22	149	95	-
	R : TTGATTTATTCTATCGGGCTC	60	22			

CHAPTER IV

Responsiveness of ESL (Early-response-to-dehydration Six-Like) transporter genes to water deficit in *Arabidopsis thaliana* plants

1. Introduction

La sécheresse est considérée comme l'un des principaux stress abiotiques, qui affecte la croissance, le développement et le rendement des plantes. Les plantes réagissent à la sécheresse par des modifications de l'expression génique, par l'accumulation de protéines hydrophyles et d'osmolytes compatibles, dont les sucres. La répartition des sucres dans la plante entre les organes-sources et les organes-puits et au niveau subcellulaire nécessite l'implication de transporteurs de sucre. Bien que les ESL (Early response to dehydration Six-Like) représentent en termes de nombre de séquences identifiées l'une des plus grandes sous-familles de transporteurs de monosaccharides, ils restent encore mal caractérisés. Un trait commun de ces gènes concerne leur réponse à divers stress abiotiques, dont le déficit hydrique. Chez *Arabidopsis thaliana*, dix-neuf gènes ESL ont été identifiés. Dans ce contexte, l'expression des *AtESL* dans la rosette de plantes cultivées en condition de contrainte hydrique a été étudiée. Afin d'avoir une vision plus globale sur les échanges de sucre entre la vacuole et le cytosol lors d'un déficit hydrique, le profil d'expression d'autres transporteurs de sucre localisés sur le tonoplaste (*AtTMT1*, *AtTMT2*, *AtVGT2*, *AtSUC4*, *AtSWEET16* et *SWEET17*) a été défini. Les résultats les plus marquants sont que trois *AtESL* (*AtESL1.02*, *AtESL3.02* et *AtESL3.03*) ont un niveau d'expression modifié au cours de la phase végétative du développement des plantes en condition de bonne alimentation hydrique, que quatre *AtESL* (*AtESL2.03*, *AtESL3.06*, *AtESL3.11* et *AtESL3.14*) ne sont pas affectés par la contrainte hydrique, alors que d'autres réponses précocement à un déficit hydrique (*AtESL1.01*, *AtESL3.03*, *AtESL3.05*, *AtESL3.07*, *AtESL3.08* et *AtESL3.09*) ou tardivement lors d'un déficit hydrique plus sévère (*AtESL2.01, AtESL2.02*, *AtESL3.04* et *AtESL1.02*, *AtESL3.01, AtESL3.02* et *AtESL3.13*). De plus, les copies de gènes *AtESL* dupliqués en tandem présentent des réponses différentielles à la contrainte hydrique, ce qui plaide en faveur de la divergence fonctionnelle de ces transporteurs de monosaccharides. Le gène *AtTMT2* est induit, alors que les gènes *AtTMT1*, *AtSUC4*, *AtSWEET16* et *AtSWEET17* sont réprimés lors d'un stress hydrique sévère allant jusqu'au flétrissement des feuilles.

2. Article 2

Responsiveness of ESL (Early-response-to-dehydration Six-Like) transporter genes to water deficit in *Arabidopsis thaliana* plants

Lucie Slawinski*, Abir Israel*, Caroline Paillot, Florence Thibault, Rossitza Atanassova, Maryse Laloi**, Fabienne Dédaldéchamp**

Laboratoire Écologie et Biologie des Interactions, Équipe "SÉVE-Sucres et Échanges Végétaux-Environnement", UMR Centre National de la Recherche Scientifique 7267, Université de Poitiers, Poitiers, France

* Both first authors contributed equally

** Both last authors contributed equally

Corresponding author: Fabienne Dédaldéchamp

Running title: *A. thaliana ESL*s coping with water deficit

Abstract

Drought is considered as one of the main abiotic stresses, which affects plant growth, development and crop yield. Plant response to drought implies redistribution of carbone reserves. Sugar allocation between source- and sink-organs and sugar partitionning between different cell compartments require the involvement of sugar transporters. Among them, the ESLs (Early response to dehydration Six-Like) represent the largest family of monosaccharide transporters. Although this family encompasses 19 genes in *A. thaliana*, it remains poorly characterized. A common feature of these genes is their involvement in the plant response to abiotic stresses including water deficit. In this context, we carried out morphological and physiological phenotyping of plants grown under normal and water-deficit conditions, together with expression profiling of seventeen *AtESL* genes in rosette leaves. The drought responsiveness of twelve ESL genes, four up-regulated and eight down-regulated, was correlated to different water status of the rosette leaves. The differential expression of each of the tandem duplicated *AtESL* genes in response to water stress argues in favor of their plausible functional diversity. Furthermore, T-DNA insertional mutants for eact of four *ESL* genes up-regulated in response to water deprivation were identified and characterized under normal and water-deficit conditions. To gain insight into global sugar exchanges between the vacuole and the cytosol under water deficit, gene expression of other vacuolar sugar transporters and invertases (AtTMT, AtSUC, AtSWEETs and *AtβFRUCT*) was analyzed and discussed.

Key words: sugar transporters, water deficit, ESL, Arabidopsis, *atesl* mutants

Introduction

One of the present societal challenges concerns the increase of crops productivity face to climate changes. Yield losses due to abiotic constraints, at the example of water deficit range from 50% to 80%, and even exceeded those caused by the biotic stresses. In terms of fundamental research, drought responses of model plants and crops have long been studied in the purpose of improvement and/or survival under conditions of severe water deficit. However, this tolerance/survival predicts neither better growth capacity, nor enhancement of productivity. During the last decade, the global vision of research focused on genes, which allow elevation of biomass and seeds' yield under conditions of moderate water stress (Rhodes and Nadolska-Orczyk, 2001; Skirycz et al., 2011; Raza et al., 2019; Zhao et al., 2020).

To cope with water deficit, plants have developed different strategies such as escape, avoidance, osmotic adjustment, etc. (Arve et al., 2011; Fang and Xiong, 2015). The escape strategy consists in completion of the plant life cycle at the onset of drought, which reflects high degree of developmental plasticity (Chaves et al., 2003; Lawlor, 2013). Avoidance is the ability of plants to grow during periods of drought and to maintain their water status by: *i)* limitation of water loss through reducing leaf surface area and stomatal conductance, and by consequence transpiration; *ii)* optimization of water supply with deeper roots, which requires reallocation of photoassimilates in favor of root growth, thereby increasing their water absorption capacity; *iii)* storage of water in specialized organs (Jackson et al., 2000; Chaves et al., 2003; Lawlor, 2013; Rosa et al., 2019; Ilyas et al., 2020). Osmotic adjustment is used by plants to cope with water deficit by accumulating compatible osmolites (proline, sucrose, polyols…) to maintain the water potential of the cells, and the turgor pressure to support their growth (Hare and Cress, 1997; Hare et al., 1998; Munns, 2002; Xiong and Zhu, 2002; Moore et al., 2008; Hummel et al., 2010; Lawlor, 2013; Ilyas et al., 2020). In the latter context, accumulation of soluble sugars has been observed in the leaves of *Arabidopsis thaliana* during water deficit (Taji et al., 2002; Hummel et al., 2010; Mewis et al., 2012; Sperdouli and Moustakas, 2012). Under mild and moderate water deficit, stomatal conductance decreases, but the partial closure of stomata does not prevent photosynthesis to be effective. However, the efficiency of photosynthesis is reduced under more severe water stress stress (Lawlor and Cornic, 2002; Muller et al., 2011; Zhao et al., 2020). In plants, subcellular sugar partitioning requires the activity of transporters located in the membranes. In *Arabidopsis*, sugar transporters are represented by several families, among which the sucrose transporters (SUC)

localized on the plasma membrane (Stadler and Sauer, 1996; Meyer et al., 2004; Sauer, 2007; Sivitz et al., 2007; Rottmann et al., 2016; Rottmann et al., 2018a; Rottmann et al., 2018b), except SUC4, which is targeted to the (Endler et al., 2006, the STP (sugar transport proteins), ESL (Early response to dehydration Six-Like), TMT (tonoplastic monosaccharide transporters) and VGT (vacuolar glucose transporters) (Büttner, 2007; Slewinski, 2011; Reddy et al., 2012; Yan, 2013). *AtTMT1* and *AtTMT2* have been identified as H^+/sucrose antiporters (Schulz et al., 2011), and *AtTMT1* expression has been reported to increase in response to stresses such as drought or cold (Wormit et al., 2006). *AtVGT1,* the sole characterized member of this family, has been localized on the tonoplast and involved in transport of hexoses (Aluri and Büttner, 2007). More recently, "Sugar Will Eventually be Exported Transporters" family (SWEET) has been identified and its members characterized as uniporters involved in the flux of sucrose, glucose and fructose (Doidy et al., 2019; Wipf et al., 2021). Klemens et al. (2013) have reported that *AtSWEET16* activity has to be tightly regulated, in order to allow optimal development of *Arabidopis* under favorable or non-favorable conditions. Chardon et al., (2013) and Guo et al., (2014) have demonstrated that *AtSWEET17* acts as fructose uniporter across tonoplast. Nineteen ESL transporters have been identified in *A. thaliana*. Although they constitute the largest MST subfamily in *Arabidopsis*, their role is poorly understood. In order to get insight in this issue, Slawinski (2017) applied evolutionary genomics approach to study ERD6 transporters in the genome of 60 species representative of the plant kingdom, from algae to angiosperms. Based on their elucidated phylogenetic position, a new nomenclature has been suggested to rename them from ERD6 in ESL (Early response to dehydration Six-Like) transporters belonging to the ESL subfamily. Phylogenetic analysis of 520 identified protein sequences showed that these ESL transporters belong to three subgroups - ESL1, ESL2 and ESL3. Expression profiling of the *Arabidopsis ESL* genes resulted in the identification, on the one hand, of tandem copies expressed at comparable level in all tested organs (leaves, roots, flower buds, flowers and siliques), and on the other hand, of tandem copies with organ-preferential expression. In all organs, the *ESL1* and *ESL2* genes were, respectively, moderately and weakly expressed, while *ESL3* displayed organ-preferential expression (Slawinski et al., 2021, in preparation, see Chapter III).

As the first experiments have been carried out under dehydration conditions (Kiyosue et al., 1994) the ERD/ESL have been classified from ERD1 to ERD16. Only five of these have been characterized: *ESL3.08/ERD6* (Kiyosue et al., 1998), *ESL3.07/ESL1* (Yamada et al., 2010), *ESL3.13/ SFP1* (Quirino et al., 2001), *ESL2.01/ ZIF2* (Remy et al., 2014) and

ESL1.02/ERDL6 (Poschet et al., 2011; Klemens et al., 2014). These transporters are involved in plant development and responses to various abiotic stresses. In *A. thaliana* seedlings, the level of *ERD6/AtESL3.08* mRNA has been demonstrated to be very low, and transiently increased in response to dehydration and cold (4°C) or under high salinity (250 mM NaCl) conditions, while it decreases after five-hours treatment with 100 µM ABA leaves (Kiyosue et al., 1998; Yamada et al., 2010). A qRT-PCR analysis has revealed that the expression level of *AtESL3.08 /ERD6* is the same in leaves and roots, and that, under high salinity (125 mM NaCl) or ABA (100 µM), its expression decreases in leaves (Yamada et al., 2010). At present, *AtESL3.08 /ERD6* is considered to take part in the redistribution of sugars thereby protecting plant cells from the detrimental effects of dehydration (Kiyosue et al., 1998). *AtESL3.13/AtSFP1* and *AtESL3.14/AtSFP2* (Sugar-porter Family Protein) are two genes duplicated in tandem on chromosome 5. *AtESL3.13/AtSFP1* is expressed only in seedlings, while AtESL3.14 is also expressed in all tested plants organs (Quirino et al., 2001). AtESL3.07/ *ESL1* and its homologous *AtESL3.08/ERD6* are duplicated in tandem and localized on chromosome 1. In seedlings, *ESL1*/AtESL3.07 expression is induced after one-hour treatment by drought, high salinity (250 mM NaCl) and ABA (100 µM). Without stress, its expression is higher in roots than in leaves, as well as under high salinity and ABA supplementation (Yamada et al., 2010). The latter authors have suggested that the *ESL3.07/ESL1* protein could be a low-affinity glucose transporter (Km = 102.2 mM) acting as a facilitator on the tonoplast. During plant development, *AtESL1.02/ERDL6* is particularly expressed during the developmental phases with high metabolic turnover, such as seed germination, abscission zones and wound responses (Poschet et al., 2011). AtESL1.02/AtERDL6 is localized at the tonoplast and the expression of gene is regulated during the triggering of the mobilization of vacuolar carbohydrate reserves: induction by darkness, heat stress and wooding, and decreased under cold stress and glucose supply. The *atesl1.02* mutant has a higher vacuolar glucose content (> 90%) than the wild-type (86%), and the cell lines overexpressing *ESL1.02/ERDL6* have glucose levels lower than those of wild plants. These data indicate that ESL1.02/ERDL6 would act as an exporter of vacuolar glucose (Poschet et al., 2011). Klemens et al., (2014) have proposed that ESL1.02/ERDL6 could act as H^+/glucose symporter by exporting glucose from vacuole to cytosol. The expression of *AtESL2.01/AtZIF2* has been demonstrated in leaves, floral organs, and particularly in roots' endoderm and primary roots' cortex (Remy et al., 2014). In addition, this transporter located in tonoplast responds to high concentrations of zinc (Zn). The loss of function of

AtESL2.01/AtZIF2 causes hypersensitivity to Zn, while its overexpression increases tolerance (Remy et al., 2014). AtESL2.01/AtZIF2 is considered to be involved in the vacuolar sequestration of zinc at root level, thereby preventing its translocation into the rest of the plant which confers tolerance to heavy metals (Remy et al., 2014). Recently, Zhu et al., (2021) have proposed that sugar accumulation in vacuoles is mediated by the coordinated action of two classes of tonoplast sugar transporters, *MdESL1.02*/*ERDL6* and *MdTSTs* (Tonoplast H^+/sugar antiporters).

In this study, we characterized the integrative physiological response *of A. thaliana* Col-0 plants to gradual water deprivation and established the following phases of rosette leaves' water status, i.e. "Early mild water deficit" (EM), "Moderate water deficit" (MD), "Severe water deficit" (SD) and "Wilting" (Wi), which may be reversible or irreversible, respectively to plant rehydration capacity. To explore the involvement of *AtESL* genes in the plant response to water deficit, we evaluated growth, physiological and biochemical parameters in parallel with the levels of *AtESL* expression. Furthermore, T-DNA insertional mutants for the four *ESL* genes, up-regulated in response to water deficit were identified, and phenotyped under well-watering, water-deprivation and re-watering. In order to get global insight of the sugar exchanges during water deficit between two subcellular compartments, vacuole and cytosol, expression profiles of all sugar transporters located on the tonoplast (*AtTMT*, *AtVGT*, *AtSUC* and *AtSWEET*) were established, as well these of two vacuolar invertases (*AtβFRUCT*).

Material and methods

Plants materials

A. thaliana, ecotype Col-0 and T-DNA insertion lines, *at1g75220* (SALK_106049)/ESL1.02, *at1g08920* (SALK_025646)/ESL3.07, *at1g08890* (SALK_047351)/ESL3.05 and *at4g04760* (SALK_132009)/ESL3.03 were used in this study. The T-DNA insertion mutants were identified via SIGnAL site (SALK Institute Genomic Analysis Laboratory) and provided by NASC (the European Arabidopsis Stock Center). The presence of T-DNA inserts and the homozygosity of *at1g75220* (SALK_106049)/*atesl*1.02, *at1g08920* (SALK_025646)/ *ates3.07*, *at4g04760* (SALK_132009)/ *ates*3.03 and *at1g08890* (SALK_047351)/ *ates3.05* mutant lines were confirmed by PCR analysis. All primer sequences are shown in Ch.IV-Table S1.

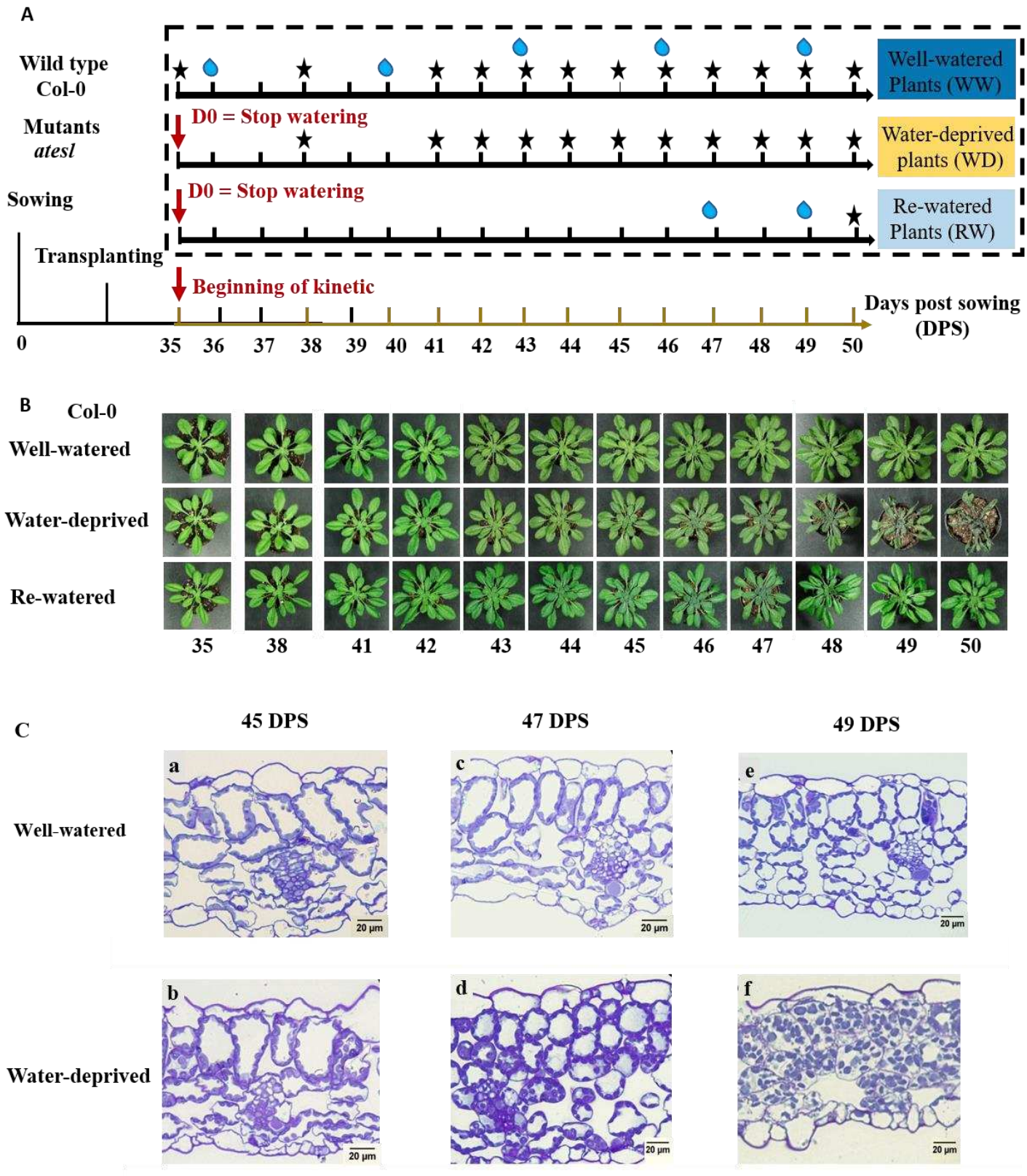

Ch.IV-Fig. 1 : Schematic representation of the different plant culture conditions for the *Arabidopsis thaliana* wild ecotype Col-0 and the four simple *atesl* mutants, in well-watered, water-deprived and re-watered condition (A), the frequency of watering is indicated by a drop of water and collection dates are expressed in days post sowing (DPS). Pictures of the development of Col 0 rosettes in well-watered, water-deprived and re-watered conditions during the 15 days of kinetics (B). Observation by light microscopy of cross sections of leaves (row 4) of Col 0 in well-watered and water-deprived conditions at the 45th (a, b), 47th (c, d) and 49th DPS (e, f) (C). The study was carried out on ten plants by culture conditions and three independent biological replicates.

Growth conditions

Seeds of Col 0 and the SALK-mutants were sown in pots containing sterile mixture of soil:vermiculite (3:1, w/w) and placed in darkness for 2 days at 4°C. Such stratification reduces residual seed dormancy and improves their germination. Afterwards, pots were placed in a growth-controlled chamber with the following parameters: 10 h-day at 100 $\mu mol.m^{-2}.S^{-1}$ of light intensity /14 h-night, 22/18℃ (day/night) and 50/90 % (day/night) relative humidity. After 13 days, the seedlings were individually transplanted into Arasystem™ (BETATECH bvba, Belgium) completed with 50 ± 2 g of soil: vermiculite mixture (3:1). Until the 35th day of growth, the plants were watered once per week and supplemented with fertilizer (PETERS (20/20/20; N/P/K).

To characterize the effect of water deficit on Col 0 and *atesl1.02*, *atesl3.03*, *atesl3.05* and *atesl3.07* mutants, the seeds were cultivated for 35 days as described above. On the 35th day post sowing (DPS), one batch of plants is well-watered (WW), a second batch of plants is not watered plants for 15 days (water-deprived, WD), a third batch of plants was not watered until the 12th day (47th DPS), and later on re-watered (RW) (Ch.IV-Fig. 1). The experiment was repeated independently six times, at 12 sampling time-points (35th, 38th DPS, 41st DPS and each next day until the 50th DPS), each time-point corresponds to the average of five plants. For each sample, half of a rosette was used to measure physiological parameters, and the other half was frozen in liquid nitrogen for RNA and sugars extractions.

Growth and physiological parameters

Leaf water status

Half-rosette of each plant sample was weighed immediately after excision to determine fresh weight (FW), and it was then placed in distilled water 24 h, at 4°C, in darkness. Afterwards turgid weight (TW) measurement, rosette material was dried for 24 h at 80°C, and eventually dry weight (DW) was determined. Based on these measurements, the relative water content (RWC) and water content (WC) were calculated as RWC = (FW – DW)/(TW – DW) and WC =(FW – DW)/ FW.

Projected rosette area and stomatal conductance

Projected rosette area (PRA) of photographed material was determined with the software ImageJ (http://imagej.nih.gov/ij/). Five plants per genotype and treatment were followed during the 15 days of experimentation. Stomatal conductance (SC, $mmol/m^2/s$) was measured using a leaf porometer (Model SC-1, Decagon Devices Inc., USA). Five plants per genotype and per condition were used. Measurements were taken daily after an illumination

period of 5 h. Two measurements were taken per plant (i.e. two leaves per plant) on 10 plants by conditions.

Soluble sugars content

Extractions of soluble sugars were carried out on previously ground in liquid nitrogen (TissueLyser II, Qiagen) and lyophilized material. Approximately 10 mg of powder were extracted by three washings (1.5 mL and twice with 0.5 mL) in methanol:chloroform:water (12:5:3, v/v/v), then the supernatants containing soluble sugars were pooled and mixed with distilled water at 0.6 final volume ratio. After centrifugation at 1200 *g* for 15 min the upper phase was collected and vacuum-dried at 50°C for 3 h in MiVac Quattro (Genevac). The soluble sugars were quantified using the Suc/Fru/D-Glc Assay Kit (Megazyme) according to the manufacturer's instructions.

Osmotic pressure

In order to determine the osmotic pressure of the cells, leaf fragments without the main vein were weighed immediately after excision. After an incubation for 24 h and 4°C and in sucrose solutions with molarity ranging from 0.01 to 1 M were weighted again. The osmotic pressure of the cells corresponds to the osmotic pressure of the solution, which does not cause a variation in mass. Three plants by genotype and by growth conditions were used at 45th, 47th and 49th DPS.

Microscopy analysis

The leaf samples were immediately fixed for1 h at 4°C in solution mixture of 2% paraformaldehyde, 0.5% glutaraldehyde and 0.05 M phosphate buffer, pH 7.2 (v/v/v). After three washes for 20 min each in 0.2 M phosphate buffer, pH 7.2 supplemented with 7.5% sucrose, a post-fixation step in 1% osmium tetroxide for 5 min followed. The dehydrated samples were embedded in LR White resin according to (Fleurat-Lessard et al., 2016). Sections were made using a microtome (EMUC6, Leica), stained with toluidine blue and observed through light microscopy (Zeiss Axioplan). Three plants by genotype and by growth conditions were used at 45th, 47th and 49th DPS.

Molecular biology

DNA extraction and amplification by PCR

The genomic DNA was extracted again using the NucleoSpin® Plant II kit (Macherey-Nagel) following the manufacturers' instructions. To determine the presence of the T-DNA insertion in homozygous and heterozygous lines, a PCR-based genotyping was used. Two

PCR reactions were performed independently to detect wild-type and mutant alleles. Two primers gene-specific LP and RP primers were used to amplify the wild type allele.
The primer pairs LP and LBb1.3 (T-DNA primer), as well as RP and LB (T-DNA primer), were used to amplify the mutant allele (Ch.IV-Table S1).

RNA extraction and cDNA synthesis

Frozen leaf samples were ground using TissueLyser II QIAGEN and subsequently, total RNA was extracted as described by Kay et al., (1987). RNA was quantified in a Nanodrop 1000 spectrophotometer (Thermo Scientific), and RNA integrity was checked by 1.5 % (w/v) agarose gel electrophoresis. cDNA was synthetized from 1 µg of total RNA after DNAse treatment (Sigma-Aldrich) using MML-V reverse transcriptase (Promega).

qPCR analysis

The expression analysis of the 17 *AtESL* (*AtESL1.01(*At1g19450) and *AtESL1.02 (*At1g75220); *AtESL2.02* (At5g18840)*, AtESL2.01 (*At2g48020) and *AtESL20.3 (*At3g05150); *AtESL3.01* (At1g54730), *AtESL3.02* (At4g4750), *AtESL3.03* (At4g04760), *AtESL3.05* (At1g08890), *AtESL3.06* (At1g08900), *AtESL3.07* (At1g08920)*, AtESL3.08* (At1g08930)*, AtESL3.10* (At3g05400), *AtESL3.11* (At3g05160), *AtESL3.13* (At5g27350) and *AtESL3.14* (At5g27360)), *AtSWEET16, AtSWEET17, AtTMT1 (At1g20840), AtTMT2 (At4g35300), AtSUC4, AtVGT2, AtβFruct3* (At1g62660) and *Atfruct4* (At1g12240) was performed in rosette of Col0 and in mutants growing in well-watered, water-deprived and re-watered conditions. The qPCR assays were performed with the Master Cycler Realplex2 (Eppendorf), in a reaction of 15 µl: 5 µl of diluted cDNA as template, 7.5 µl of SYBRGREEN® GoTaq qPCR Master Mix (Promega), 0.5 µl of each gene-specific primer (10 mM) and 1.5 µl of water. The qPCR program was set at 95°C for 2 min, then 40 cycles of 15 s at 95°C, 1 min at 60°C. At the end of amplification, a melting curve was generated to check the specificity of the primers (95°C, 15s; 60 to 95°C, 20 min; 95°C 15s). The *AtPP2a* (At1g13320) (Czechowski et al., 2005) was used as a reference gene to normalize the expression of *AtESL* genes. The relative expression was determined according to the $2^{-\Delta Ct}$ method. Each biological replicate was tested in three technical repetitions. The primers' sequences used are presented on Table S1.

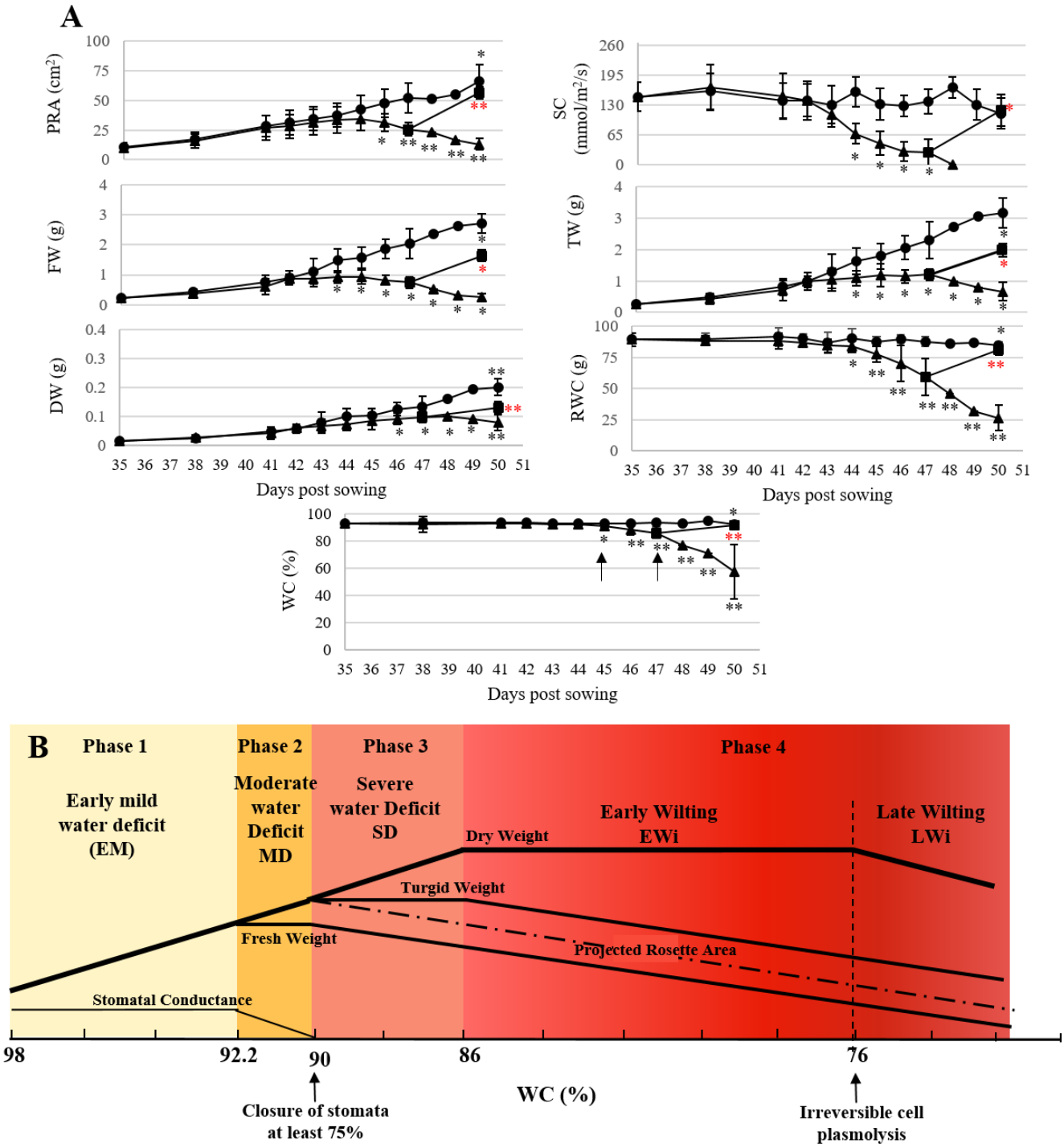

Ch.IV-Fig. 2: Characterization of the effect of water deficiency on the wild *Arabidopsis thaliana* Col 0 ecotype. The projected rosette area (PRA), the fresh weight (FW), the dry weight (DW), the stomatal conductance (SC), the turgid weight (TW), the relative water content (RWC) and water content (WC) are measured under well-watered (●), water-deprived (▲) and re-watered (■) growing conditions during 15 days of kinetic (A). Determination of four phases of water deficit intensity as a function of the physiological state of Col 0 plants (B). Phase 1, Early mild water Deficit (EM); phase 2, Moderate water Deficit (MD); phase 3, Severe water Deficit (SD) and phase 4, Wiling phase (Wi) which was subdivided into Early Wilting (EWi) and Late Wilting (LWi) respectively. The study was carried out on five plants by condition and three independent biological replicates. The asterisks represent statistically different values determined by Mann-Whitney test (*p<0.05, ** p <0.001).

Statistical analysis

Non-parametric Mann-Whitney test was used for two groups of variables. For three or more than three groups of variables Kruskall-Wallis test and Dunn test were applied using XLStats 2011 software (Addinsoft, France).

Results

Phenotype and growth parameters

Phytotron-grown 35-day-old *A. thaliana* plants were subjected either to water deficit by totally withholding water supply during 15 days (referred to as "water-deprived", WD), or to initial twelve days of water deprivation followed by watering on the last three days (referred to as "re-watered", RW). In parallel, control plants are normally watered during the same period of 15 days (referred to as "well-watered, WW") (Ch.IV-Fig. 1A). Growth and physiological parameters of plants under the above-mentioned conditions were compared between the 35th and the 50th days post sowing (DPS), initially every three days (35th, 38th and 41th DPS), and later on daily, until the 50th DPS.

For WD plants, wilting was observed as early as on the 12th day (47th DPS) after water withholding, and re-watering on the 47th DPS restored the WW phenotype of the control plants (Ch.IV-Fig. 1B). However, none of the attempts to rehydrate plants after the 48th DPS was successful, because of late wilting and cell death. These observations were confirmed by microscopy on thin sections of leaves performed on the 45th, 47th and 49th DPS (Ch.IV-Fig. 1C). In control WW plants with normal macroscopic phenotypes no histological alterations were found during the entire experimental period from the 35th to the 50th DPS. Epidermal and mesophyll cells were turgid, as demonstrated by chloroplasts positioning close to plasma membrane and cell wall. Moreover, intercellular areas were visible and well delimited (Ch.IV-Fig. 1C a, c, e). It is worth to be noted that the same observations were valid for water-deprived plants at 45th and 47th DPS. Remarkably, on the 49th DPS, chloroplasts were scattered into the cells, due to the reduced volume of vacuoles, on the onset of cell plasmolysis (Ch.IV-Fig. 1C f). The loss of turgor pressure led to reduction of intercellular areas, as well as plasma membrane retraction and enhanced cell wall rigidity of epidermal and mesophyll cells, which reflected the advanced stage of leaves' wilting (Ch.IV-Fig. 1B).

Several physiological parameters were measured in the WW, WD and RW plants, with the aim of correlating phenotype and microscopy observations to plant growth and water status. For WW plants, PRA was increased six-fold from the 35th to the 50th

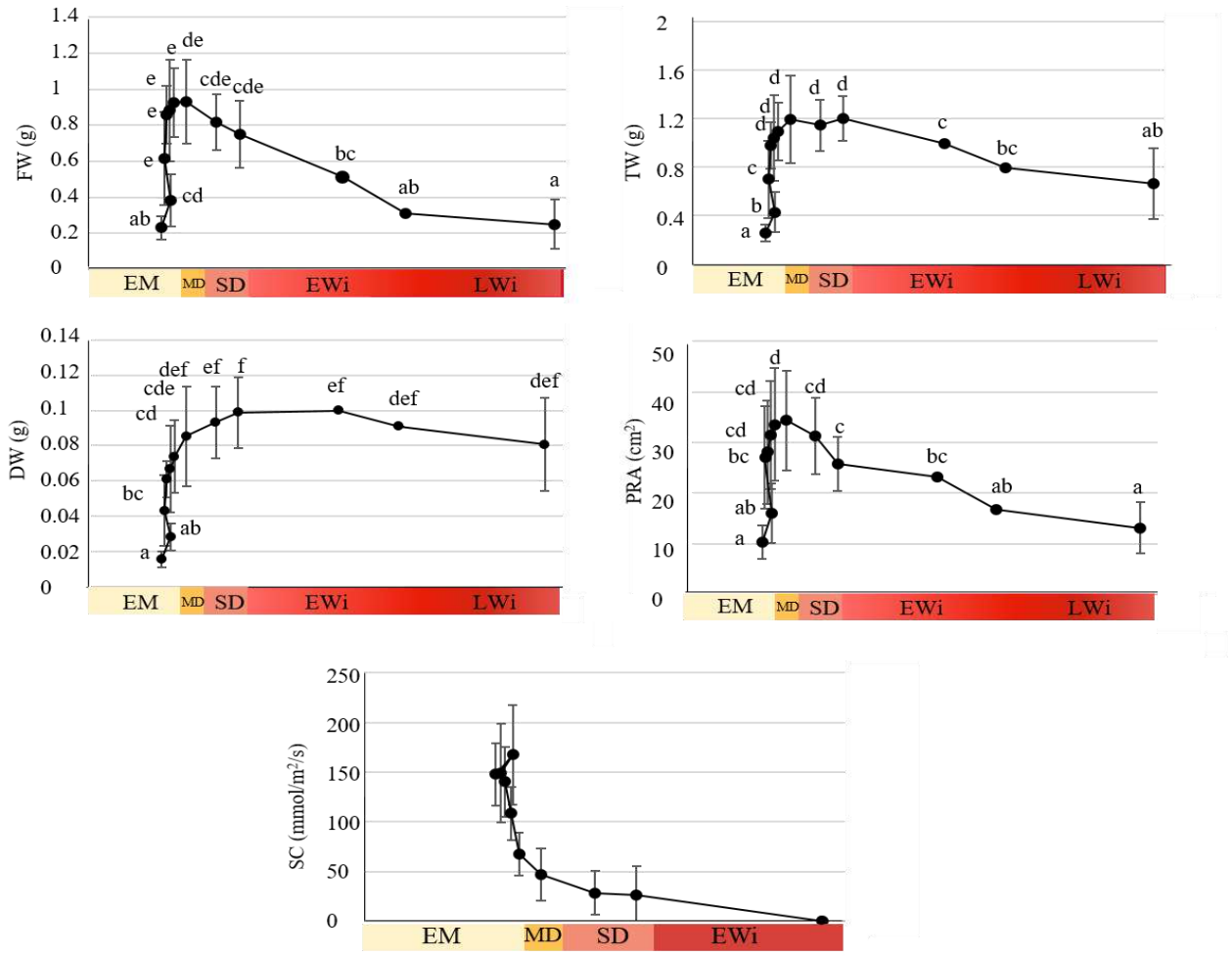

Ch.IV-Fig. 3: Analysis of the fresh weight (FW), the dry weight (DW), the turgid weight (TW), the projected rosette area (PRA), and the stomatal conductance (SC) in water-deprived *Arabidopsis thaliana* Col 0 ecotype during the four water deficit phases defined by the leaf water content. Early mild water Deficit (EM); Moderate water Deficit (MD); Severe water Deficit (SD) and Wiling phase (Wi) which was subdivided into Early Wilting (EWi) and Late Wilting (LW) respectively. The study was carried out on five plants by culture conditions and three independent biological replicates. Application of Kruskal-Wallis test, followed by Dunn's multiple comparisons test ($p < 0.05$) with Bonferroni correction resulted in significantly different groups, as indicated by different letters.

Ch.IV-Table 1 : Osmotic pressure (Mpa) in the leaves of *Arabidopsis thaliana* wild ecotype Col 0 grown under well-watered and non-watered culture conditions on 45th, 47th and 49th days after sowing

Day post sowing	Osmotic pressure (Mpa)				Water content and associated phases
	Well-watered plants		Watered-deprived plants		
	Col0	*atesl1.2* mutant	Col0	*atesl1.2* mutant	
45	1.1 – 1.2	1.1 – 1.2	1.2 – 1.4	1.1 – 1.2	90% > WC > 86% , phase 3 - SD
47	0.9 – 1.1	0.8 – 0.9	1.5 – 1.7	1.2– 1.4	
49	1.1 – 1.2	0.8 – 0.9	2.4 (for 33% of plants/ND	1.5 – 1.7	WC < 76% phase 4 - LWi

ND : not determined

DPS (Ch.IV-Fig. 2A), leading to rosette expansion rate of 3.7 ± 0.8 cm^2 per day. On the 50th DPS, FW and DW turned out increased 10.4-fold and 13.4-fold respectively (Ch.IV-Fig. 2A). FW (10.4-fold) was markedly greater than that of PRA (6-fold). Such markedly greater increase of FW than that of PRA may be explained by superimposition of most of the mature leaves occurring until the 47th DPS, which hinders PRA measurement and results in underestimated values. FW of well-watered plants displayed a two-phase curve characterized by a slow progression from the 35th to the 41th DPS and a more marked increase from the 41th to the 50th DPS (Ch.IV-Fig. 2A).

In WD plants, PRA decreased after ten days of water arrest (i.e. 45th DPS), as a first mark of growth reduction on the onset of the wilting (Ch.IV-Fig. 2A). The FW was significantly different from that of the well-watered plants until the 44th DPS corresponding to nine days of water withholding, while the DW gradually increased until the 47th DPS (Ch.IV-Fig. 2A), thereby demonstrating accumulation of organic matter. After a period of stagnation, a loss of DW is recorded on the 48th DPS. In RW plants, PRA was significantly higher on the 50th DPS than that in water-deprived plants (ca. 4.3-fold increase), and also remained significantly different from that of the WW plants. A similar profile of water-deficit response was observed for both FW and DW.

Regulation of water loss in plants can be evaluated by measurements of stomatal conductance (SC) and the degree of stomatal opening. SC was stable in well-watered plants, with a natural variation for a batch of ten plants between 160.0 ± 47.5 and 106.0 ± 46.0 mmol/m^2/s (Ch.IV-Fig. 2A). Until the 44th DPS, SC of water-deprived plants was significantly lower than that of well-watered plants with a value of 20 mmol/m^2/s corresponding to enhanced stomatal closure from 75% to 92% on the 45th DPS. It was no longer possible to measure the SC values on the 48th DPS, due to leaves' withering of the WD plants. Inversely, RW plants reached the same level of stomatal conductance as those of the well-watered plants on the 50th DPS.

Water absorption capacity of leaves was evaluated by measuring the turgid weight (TW) and the relative water content (RWC). In WW plants, TW gradually increased up to twelve-fold between the 35th and the 50th DPS. RWC was stable (87.9 ± 5.8 %), which indicated maintained water status of well-watered Col 0 plants, thereby validating them as controls for studying the impact of water stress. In comparison, TW and RWC remained significantly lower in water-deprived plants until the 44th DPS (Ch.IV-Fig. 2A).

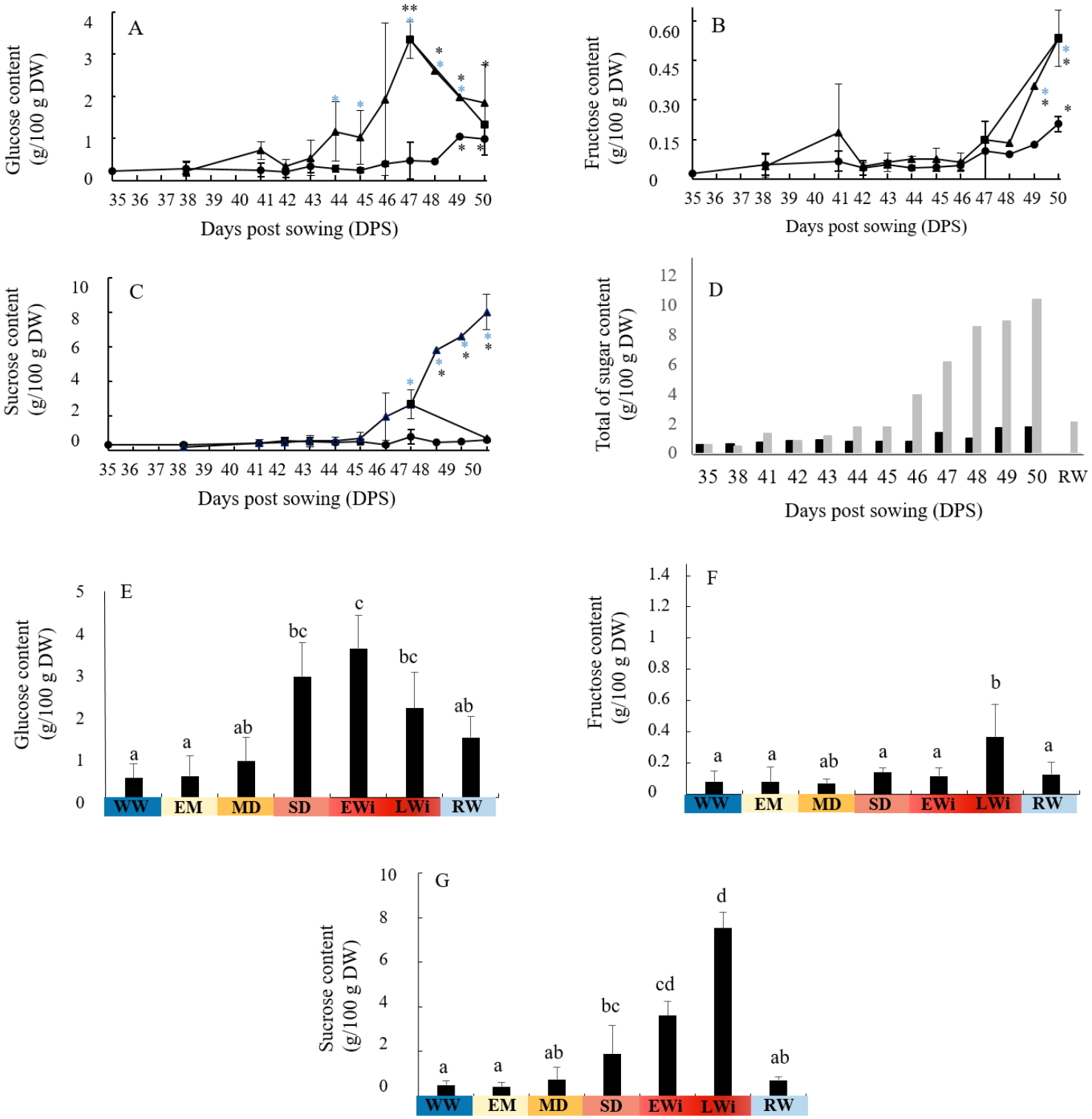

Ch.IV-Fig. 4 : Glucose, fructose, and sucrose content in the leaves of *Arabidopsis thaliana* ecotype Col 0 well-watered (●), water-deprived (▲) and re-watered (■) plant at different days post sowing. (A, B, C and D), and in the function of the four water deficit phases: Early mild water Deficit (EM); Moderate water Deficit (MD); Severe water Deficit (SD) and Wiling phase (Wi) which was subdivided into Early Wilting (EWi) and Late Wilting (LWi) respectively. The study was carried out on five plants by conditions and three independent biological replicates. (A, B, C). The blue asterisks correspond to significant differences compared to the well-watered plants at each sampling time, determined by Mann-Whitney test (p. Value <0.05). The black asterisks correspond to significant differences determined by the Kruskal-Wallis test, followed by a Dunn's test of multiple comparisons (*p<0.05; **p<0.001). (E, F, G). Application of Kruskal-Wallis test, followed by Dunn's multiple comparisons test (p-value < 0.05) with Bonferroni correction, resulted in significantly different groups, as indicated by different letters.

During the fifteen days of growth monitoring (Ch.IV-Fig. 2B), the rosettes' water content (WC) of WW plants was stable between 92.2% and 94.4 % (mean value of 93.3 ± 1.1%). For WD plants, WC slowly decreased from 92.1 ± 0.9% on the 44th DPS to 86.2 ± 4.3% on the 47th DPS, and this trend was further accelerated until 57.38 ± 19.97% on the 50th DPS. As described above, the wilting was irreversible from the 49th DPS, which corresponded to a WC below 76%, thereby triggering the death of the majority of leaf cells (Ch.IV-Fig. 1C) After final three days watering on the 48th - 50th DPS of the RW plants, their measured WC of 91.9 ± 0.54 % was found close to that of WW plants. However, the other water status parameters of the RW plants remained significantly different from those of the WW plants.

In regard with the growth and the physiological parameters of plants under water deprivation, four phases of their water status can be defined (Ch.IV-Fig. 2B and Fig.3) : *i)* Early mild water deficit (EM) characterized by WC greater than 92.2% from the 35th to the 42th DPS, increase in FW, DW, PRA and plant growth similar to those of WW plants; *ii)* Moderate water deficit (MD), with a WC decreasing from 92.2% to 90%, and also marked by a drop of stomatal conduction (from 42th to 45th DPS); *iii)* Severe water deficit (SD) characterized by a decrease in FW and PRA, the DW increase always, thus plants retain some capacity to synthesize organic matter for a WC comprise between 90% to 86% (from 45th to 47th DPS); *iv)* Wilting phase (Wi) subdivided into reversible and non-reversible wilting. Early reversible wilting (EWi) is characterized WC decrease from 90 % to 86 % on 47th-48th DPS). The irreversible wilting (LWi) on 48th-50th DPS is characterized with a much more important decrease of WC (< 76 %) corresponding to irreversible wilting, plasmolysis and cell death (Ch.IV-Fig. 2B and Fig.3).

Osmotic pressure

The osmotic pressure of the leaf cells was measured on the 45th, 47th and 49th DPS by immersing leaf fragments into solutions with increasing concentrations of sucrose. From the 45th DPS to the 49th DPS the osmotic pressure of WW plants was between 0.9 and 1.2 MPa (Ch.IV-Table 1). In water-deprived plants, the osmotic pressure increases from the 45th DPS (corresponding to the SD phase), and was 1.5-1.7 MPa over the 47th DPS corresponding to the wilting phase. At the 49th DPS, only 33% of the tested plants were with osmotic pressure of 2.4 MPa, while massive plasmolysis and cell death were observed in the remaining 67%.

Content of soluble sugars

The process of cell osmotic adjustment implies an increase of sugar content. Contents of sucrose, glucose, and fructose were determined in WW, WD, and RW plant rosettes from

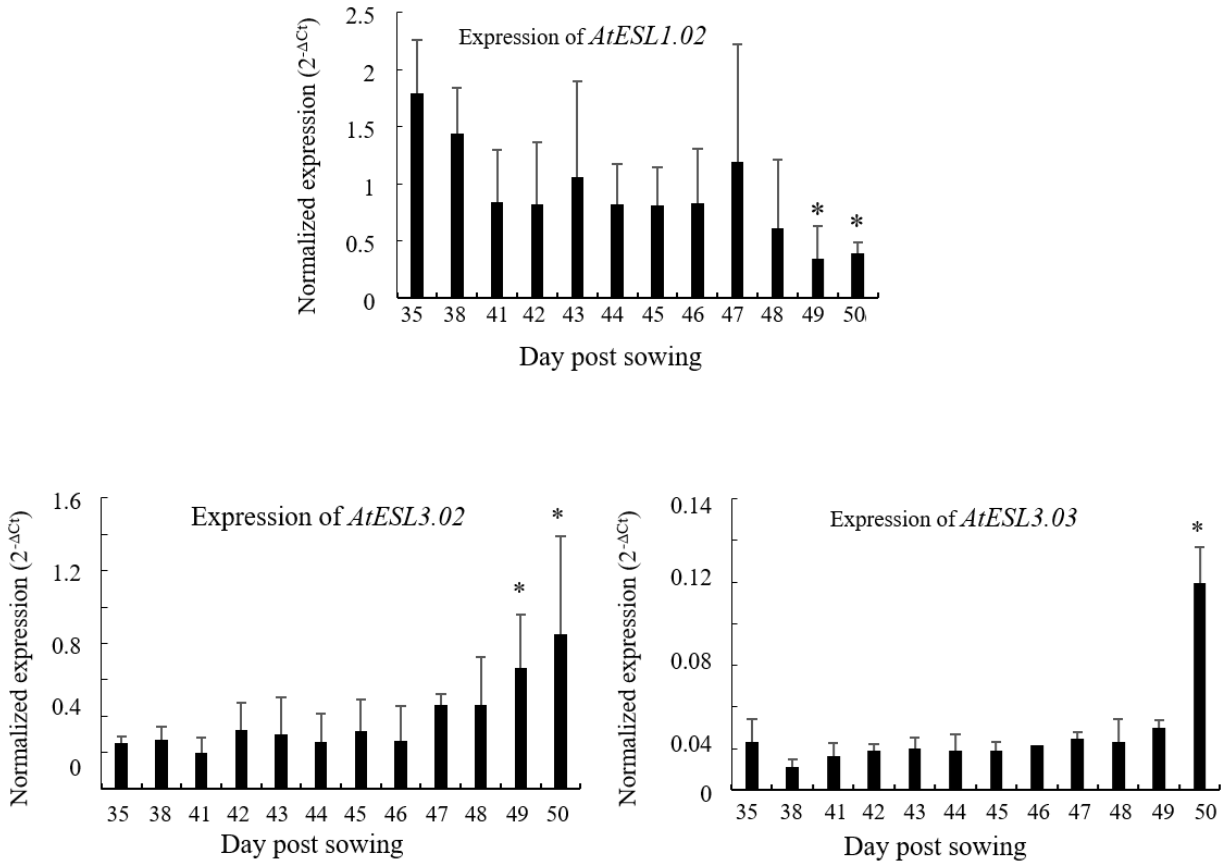

Ch.IV-Fig. 5: Relative expression *AtESL1.02*, *AtESL3.02*, and *AtESL3.03* during development of *Arabidopsis thaliana* wild type ecotype Col 0 under well-watering. The study was carried out on five plants by condition and three independent biological replicates. The asterisks represent the significantly different values determined by the Kruskal-Wallis test.

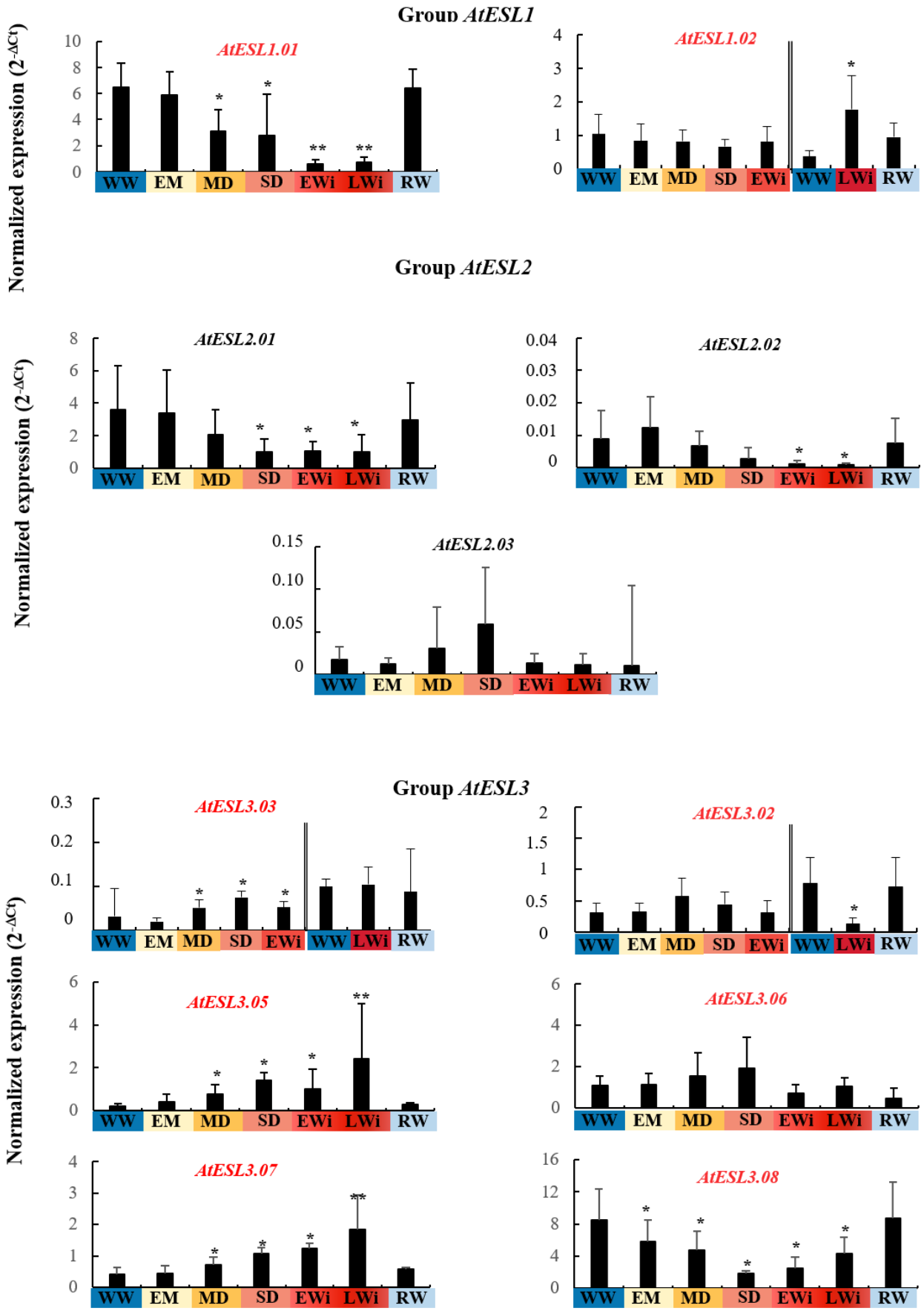
Group AtESL1
Normalized expression (2-ΔCt)
AtESL1.01
AtESL1.02
Group AtESL2
AtESL2.01
AtESL2.02
AtESL2.03
Group AtESL3
AtESL3.03
AtESL3.02
AtESL3.05
AtESL3.06
AtESL3.07
AtESL3.08
WW
EM
MD
SD
EWi
LWi
RW

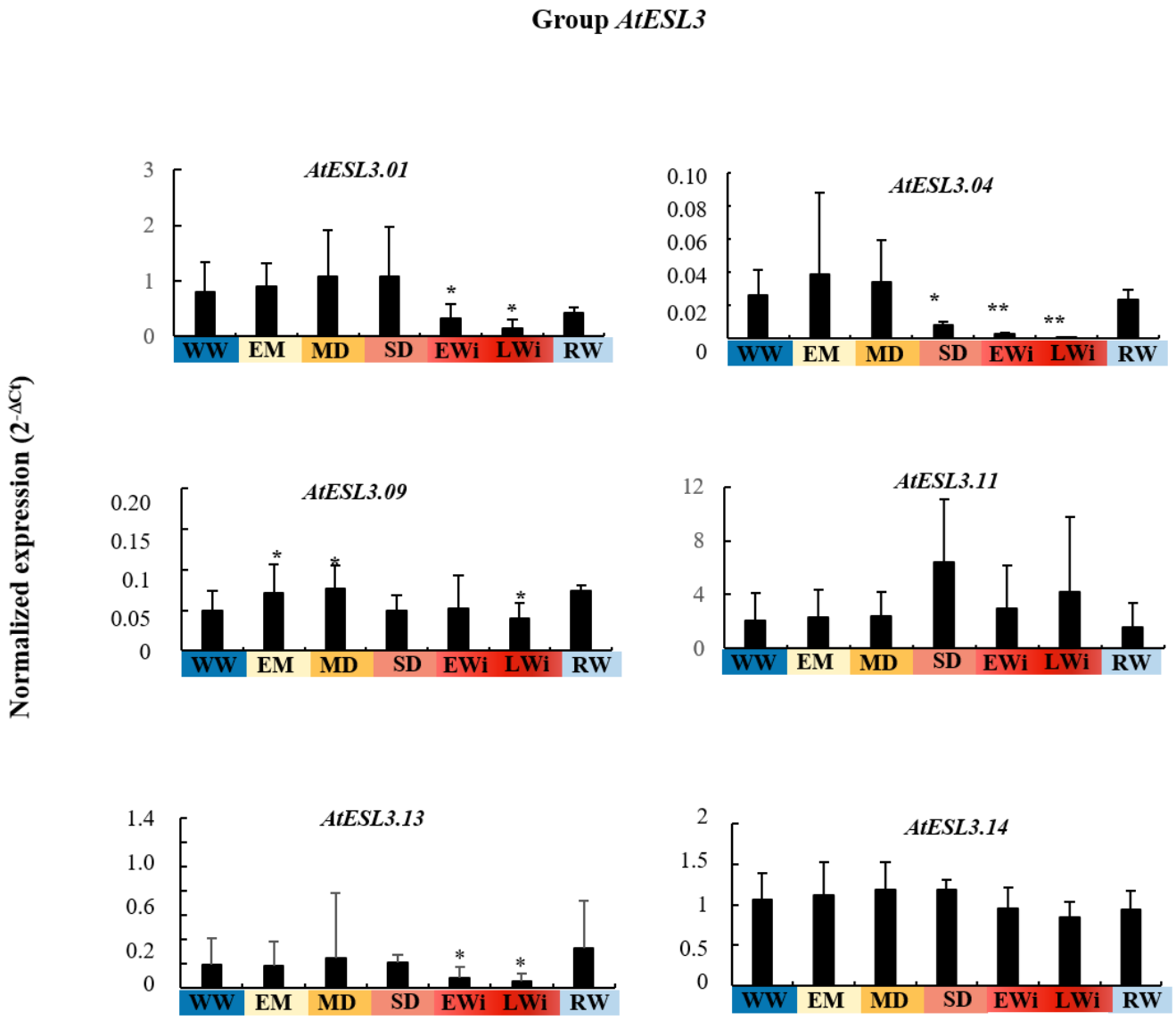

Ch.IV-Fig. 6: Relative expression of 17 *AtESL* in *Arabidopsis thaliana* wild type ecotype Col 0 in well-watered, water-deprived, and re-watered plants in function of the four phases of water deficit: Early mild water Deficit (EM); Moderate water Deficit (MD); Severe water Deficit (SD) and Wiling phase (Wi) which was subdivided into Early Wilting (EWi) and Late Wilting (LWi) respectively. The study was carried out on five plants by culture condition and three independent biological replicates. The asterisks represent the significantly different values determined by the Kruskal-Wallis test followed by Dunn's multiple comparisons tests (*p< 0.05; **p< 0.0001) with Bonferroni correction.

the 35th to the 50th DPS. In WW plants, the soluble sugars' content displayed 3.2-fold increase during the studied period (Ch.IV-Fig. 4D), while in water-deprived plants, their amount hugely increased ca. 18-fold. In WW plants, the glucose and fructose content were increased on 49th-50th DPS, while the content in sucrose remained constant. In WD plants, glucose content was higher than that in well-watered plants from 44th DPS, fructose content was increased as for WW plants from 49th DPS but with higher intensity(Ch.IV-Fig. 4A, B), and the sucrose increased three times on the 47th and the 50th DPS (Ch.IV-Fig. 4C).

Expression of the soluble sugar content in function of WC shown an increase in glucose and sucrose during the transition from MD phase (92.2% > WC > 90%) to SD phase (90% > WC > 86%), and concerning the fructose, this increase was delayed (end of the wilting phase, WC < 76%). Glucose content in re-watered plants was similar to that of water-deprived plants in MD phase (Ch.IV-Fig. 4E). During EM and MD phases similar contents were measured for the three sugars in RW, WD and WW plants (Ch.IV-Fig. 4D).

Expression of *AtESL* in leaves

The expression of seventeen *AtESL* genes was studied in plants under water deficiency in order to highlight the role of these sugar transporters in response to drought. In our experiments in the WW plants leaves, the relative expression of 14 out of the 17 *AtESL* was stable during the growth kinetic. Only the *AtESL1.02* gene was repressed from the 49th DPS, and two genes, *AtESL3.02* and its tandem *AtESL3.03*, were induced from the 49th DPS and at the 50th DPS respectively (Ch.IV-Fig. 5).

In the case of the WD plants, the relative expression of seventeen *AtESL* genes was presented in function of the four phases of water deficit (Ch.IV-Fig. 6). The genes of each of the four pairs of tandem genes, *AtESL1.01/1.02*, *AtESL3.02/3.03*, *AtESL3.05/3.06* and *AtESL3.07/3.08* were regulated differently in function of water deficit intensity. The relative expression of *AtESL1.01* decreased from the MD phase and its minimal expression was observed in the Wi phase (Ch.IV-Fig. 6). In order to evaluate the effect of the tandem gene *AtESL1.02* on development (Ch.IV-Fig. 5). We compared the average expression levels on the 49th-50th DPS of WW plants with those of WP plants, which showed 4.8-fold increase in the end of Wi phase. In the same way, *AtESL3.02* was 6-fold repressed in the LWi step and its tandem gene, and *AtESL3.03* was induced earlier in the MD phase. *AtESL3.05* and *AtESL3.07* displayed the same expression profile in water-deprived plants, marked by an induction in the MD phase (1.9 and 1.7 times respectively) and in the LWi phase (2.48 and 3.75 times respectively) compared to the EM phase (Ch.IV-Fig. 6). *AtESL3.06* gene tandem of *ESL3.05*

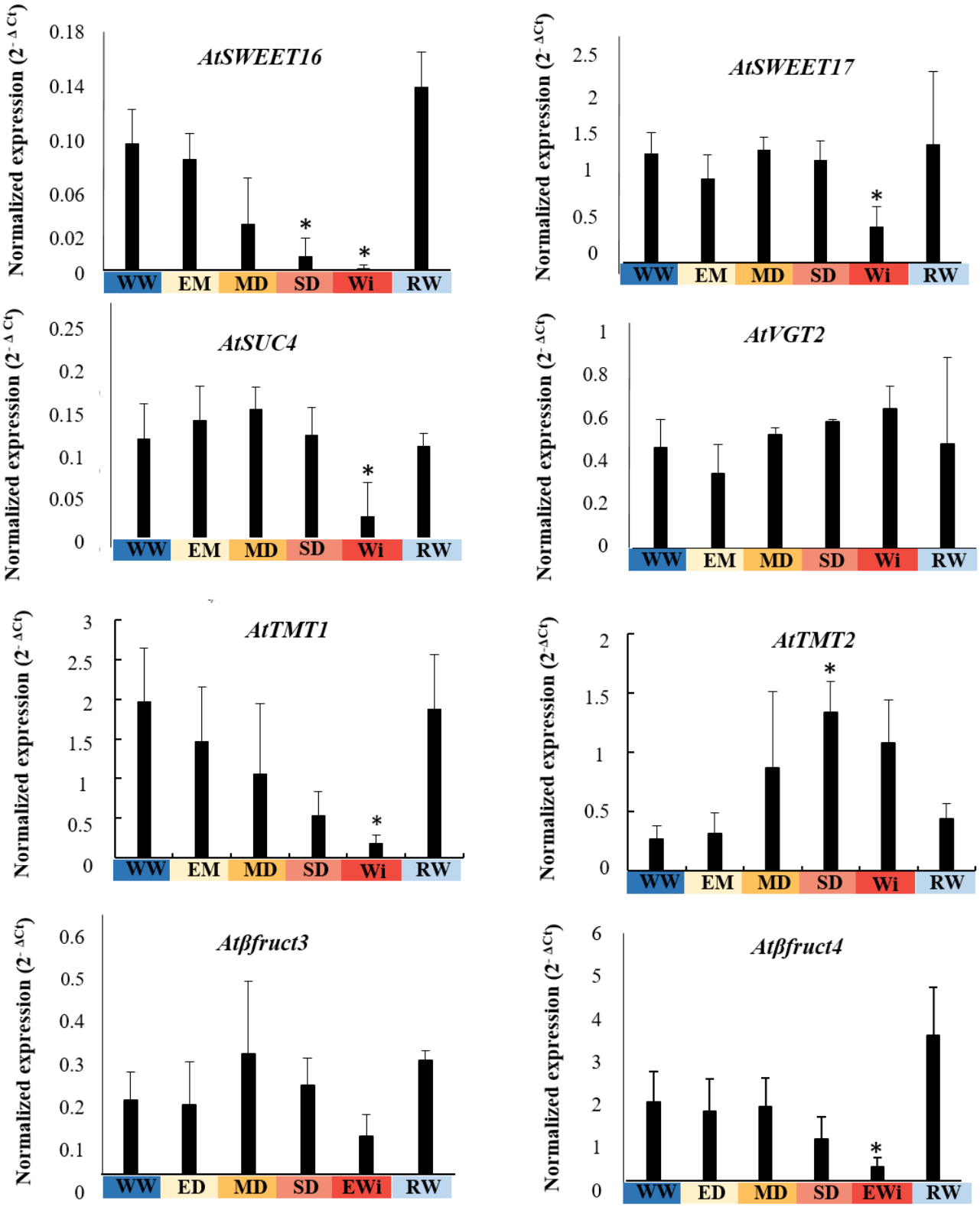

Ch.IV-Fig. 7: Gene expression of *AtSWEET16*, *AtSWEET17*, *AtSUC4*, *AtVGT2*, *AtTMT1*, *AtTMT2, Atβfruct3* and *Atβfruct4* in well-watered, water-deprived and re-watered plants in function of the four phases of water deficit: Early mild water Deficit (EM); Moderate water Deficit (MD); Severe water Deficit (SD) and Wiling phase (Wi). The blue asterisks correspond to significant differences compared to the well-watered plants at each sampling time, determined by Mann-Whitney test ($p < 0.05$). The study was carried out on five plants by condition and two independent biological replicates.

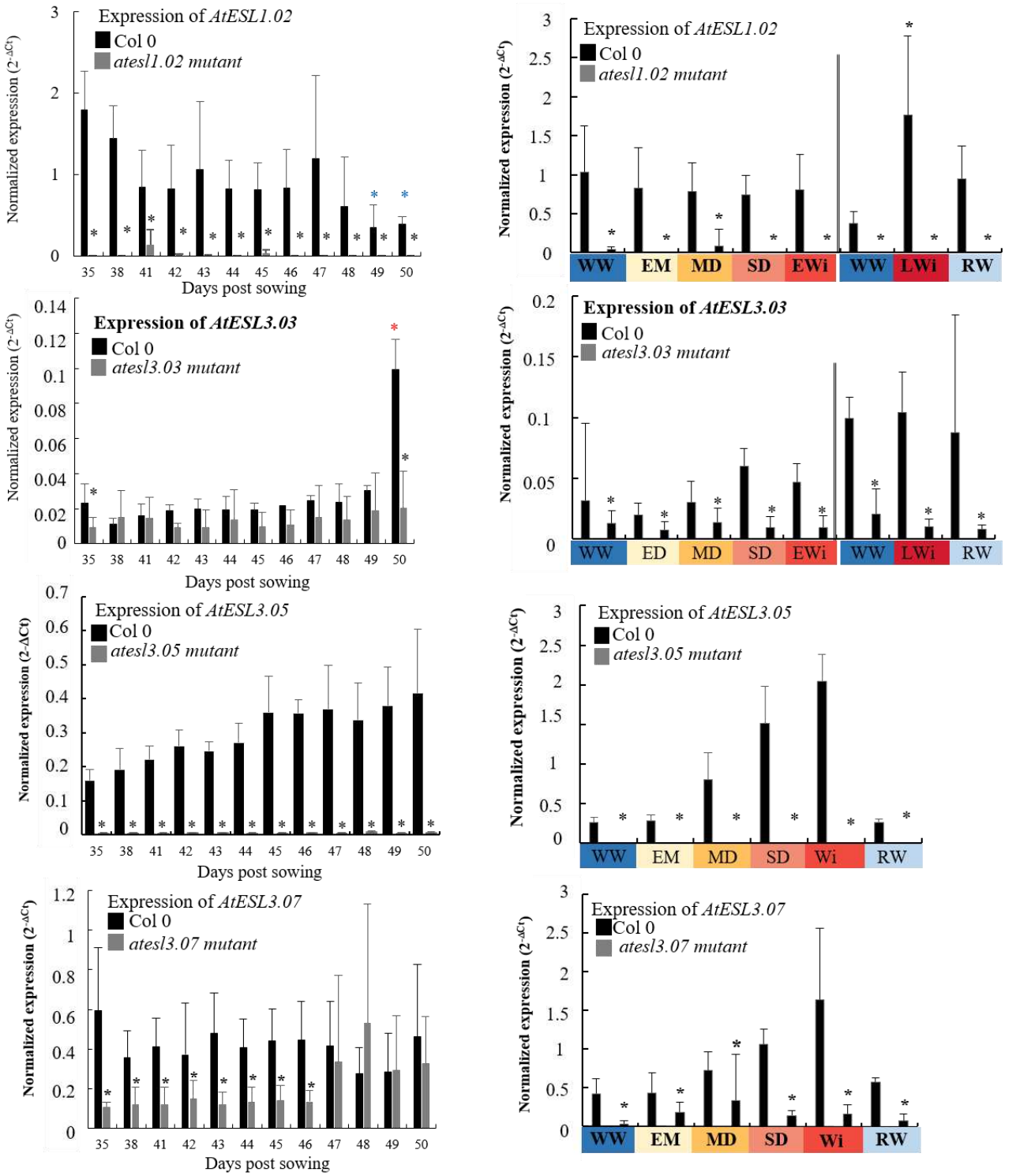

Ch.IV-Fig. 8: Characterization of four insertional T-DNA mutants *atesl1.02*, *atesl3.03*, *atesl3.05* and *atesl3.07*. Comparison of the expression level of the mutated gene in mutant corresponding and in wild-type in *Arabidopsis thaliana* Col 0 during the growth kinetic in well-watered plants. Comparison of the expression of the mutated gene in the mutant corresponding under well-watered, water-deprived and after re-watered plants in function of the four phases of water deficit: Early mild water Deficit (EM); Moderate water Deficit (MD); Severe water Deficit (SD) and Wiling phase (Wi). The values shown are the expression values normalized to *AtPP2a*. Each value represents the mean of three biological replicates (± standard deviation). Kruskal-Wallis tests was performed followed by Dunn's multiple comparisons test. Statistically different values are marked with asterisks ($p<0.05$). Blue and red asterisks indicate significant down-regulation and up-regulation respectively. Black asterisks indicate significant differences between the mutant and the wild-type Col-0.

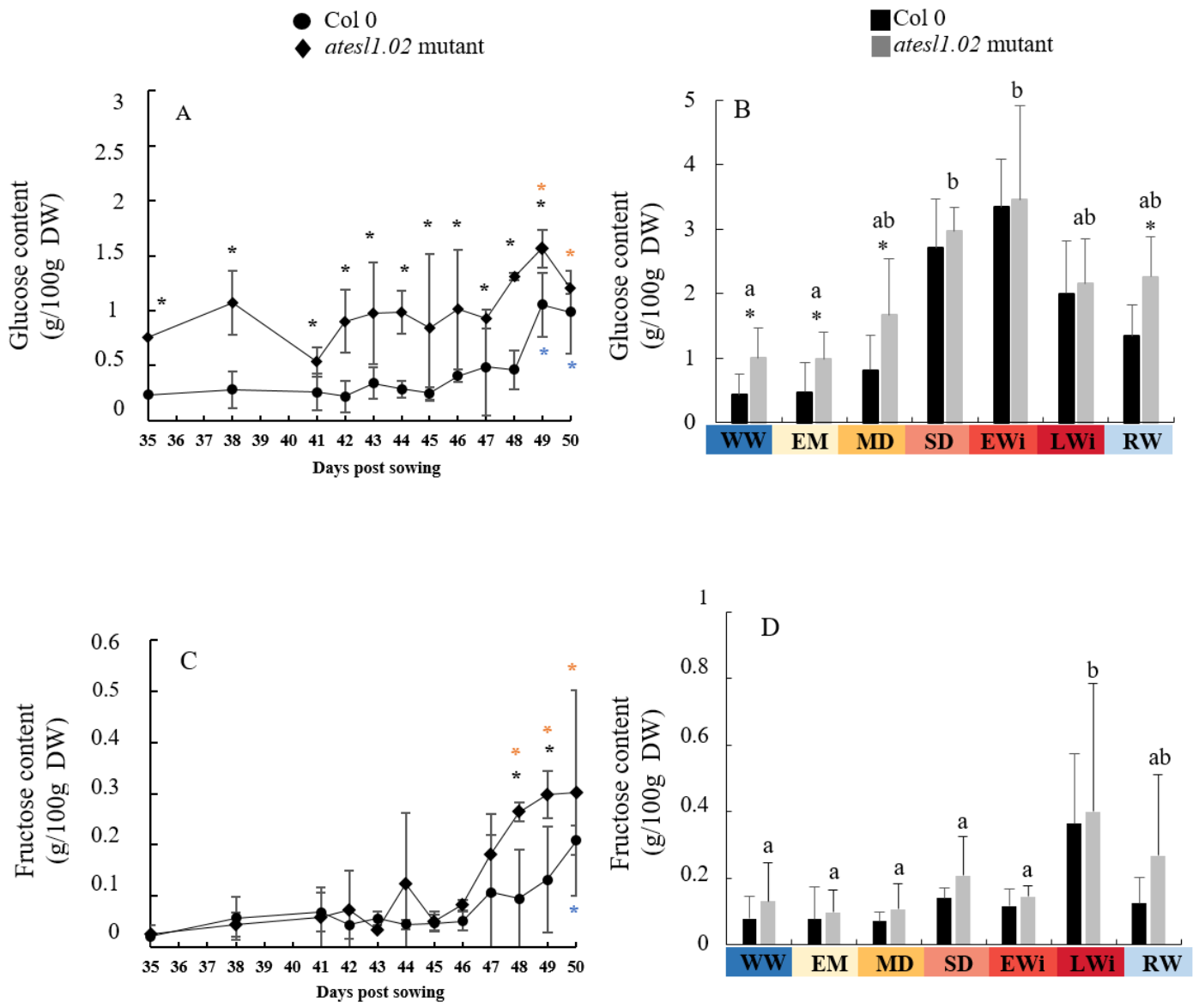

Ch.IV-Fig. 9: Glucose and fructose contents in the *Arabidopsis thaliana* wild ecotype Col 0 and in the mutant *atesl1.02* during the growth kinetics in well-watered plants, water-deprived and re-watered plants in function of the four hydric deficit phases: Early mild water Deficit (EM); Moderate water Deficit (MD); Severe water Deficit (SD) and Wiling phase (Wi) which was subdivided into Early Wilting (EWi) and Late Wilting (LWi) respectively. The values represent the mean of three biological replicates (± standard deviation). Different letters represent groups of statistically different values determined by a Kruskal-Wallis test (p.value <0.05). Kruskal-Wallis test was performed followed by Dunn's multiple comparisons test. Statistically different values are marked with asterisks (p <0.05). Blue and red asterisks indicate significant down-regulation and up-regulation respectively. Black asterisks indicate significant differences between the mutant and the wild-type Col 0.

did not respond to water deficit. For the *AtESL3.08* gene tandem of *AtESL3.07* the repression was early manifested and occurred in the EM phase. The weak expression of *AtESL3.07* persisted in all phases of the water stress. In RW plants, the relative expression of *AtESL1.01*, *AtESL1.02*, *AtESL3.02*, *AtESL3.05*, *AtESL3.06*, *AtESL3.07* and *AtESL3.08* was significantly similar to that in WW plants. Concerning the *AtESL* genes without tandem copies in WD plants, the relative expression of *AtESL2.01* and *AtESL3.04* were repressed in SD and Wi phases. *AtESL2.02*, *AtESL3.01*, and *AtESL3.13* were repressed only in Wi phases. In RW plants, the levels of expression of these *AtESL* were comparable to those in WW plants, except for *AtESL3.09*. The gene *AtESL3.09* was early induced, in the EM and MD phases. *AtESL2.03*, *AtESL3.11* and *AtESL3.14* genes did not respond to water deficit under the conditions of our study (Ch.IV-Fig. 6).

Finally, the study of the relative level of expression of seventeen *AtESL* genes showed that in WW plants only three genes (*AtESL1.02*, *AtESL3.02* and *AtESL3.03)* were affected during the growth kinetics. In WP plants four genes were not affected by water deficit (*AtESL2.03*, *AtESL3.06*, *AtESL3.11* and *AtESL3.14*), while other genes responded early (*AtESL1.01*, *AtESL3.03*, *AtESL3.04*, *AtESL3.05*, *AtESL3.07*, *AtESL3.08* and *AtESL3.10*) to water deprivation or were regulated by severe water deficit (*AtESL2.02* and *AtESL2.03),* or by wilting (*AtESL1.02*, *AtESL3.01, AtESL3.02* and *AtESL3.13*) (Ch.IV-Fig. 6).

Other vacuolar transporters and invertases

In order to further investigate the role of AtESL in sugar exchanges between the cytosol and the vacuole in response to water deficit, the relative expression of other transporter sugar genes located on the tonoplast was studied (Ch.IV-Fig. 7). *AtSWEET16* was repressed at WC of 90% during the SD phase, while the repression *AtSWEET17*, *AtSUC4*, *AtTMT1* is occurred later on, in the Wi phase. The expression of the *AtTMT2* gene increased transiently in the SD phase. There was no difference in *AtVGT2* expression depending on the WC of the leaves. The expression of *Atβfruct4* was repressed by the loss of water during the wilting phase.

Characterization of four *atesl* mutants

In order to highlight the role of ESLs in *Arabidopsis* response to water deprivation, T-DNA insertional mutants were identified for the four *AtESL* genes responsive to water deficit (*AtESL1.02*, *AtESL3.03*, *AtESL3.05* and *AtESL3.07*). When compared to Col 0 genotype three among them, *atesl1.02*, *atesl3.05* and *atesl3.07,* showed drastic repression of the disrupted gene, respectively of 98%, 98% and 87%, and were considered as knockout

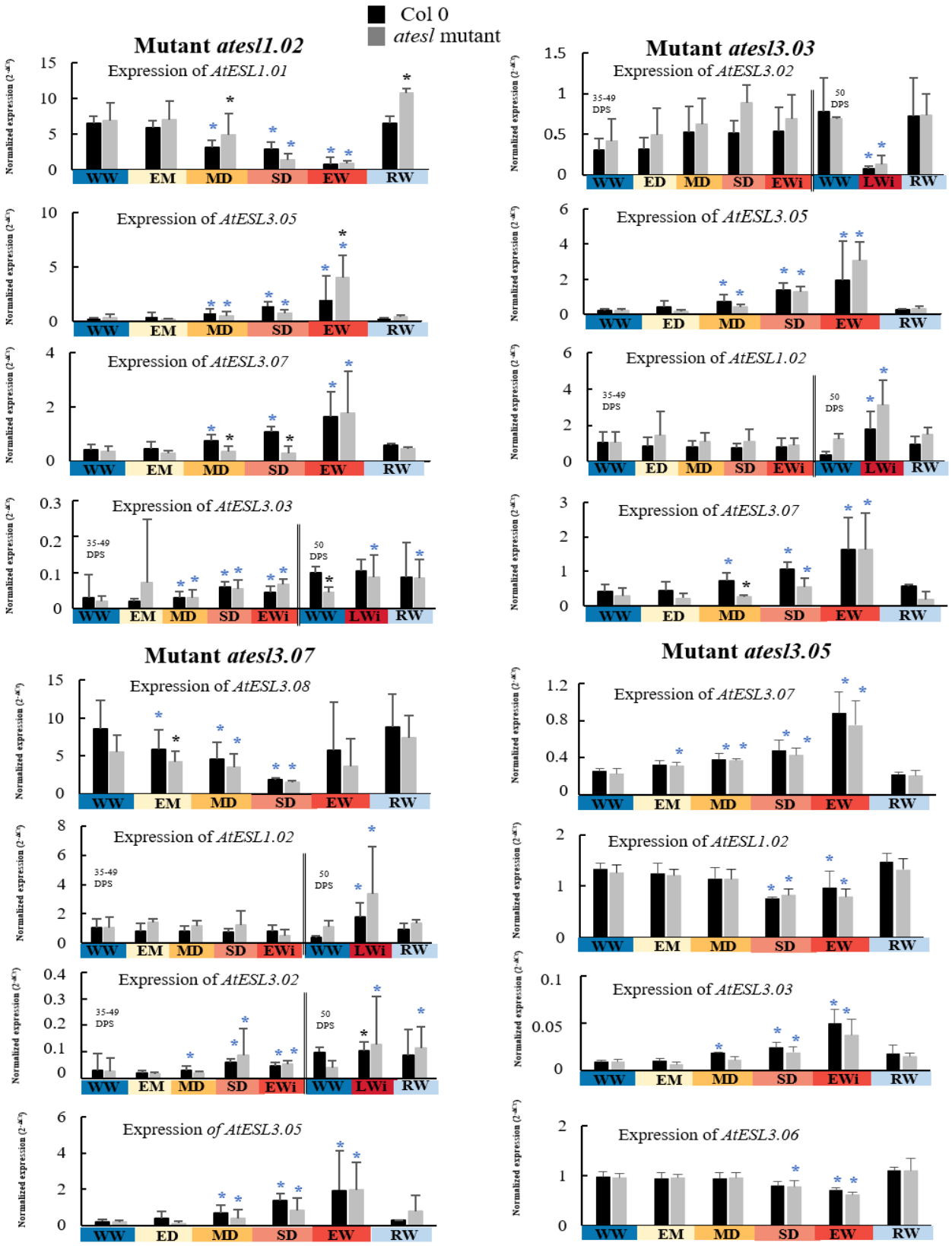

Ch.IV-Fig. 10: Level of expression of *AtESL* in the in four mutants *atest1.02*, *atesl3.03*, *atesl3.05* and *atesl3.07* in well-watered, water-deprived, and re-watered plants compared to the wild-type Col 0 plants in function of the four phases of water deficit: Early mild water Deficit (EM); Moderate water Deficit (MD); Severe water Deficit (SD) and Wiling phase (Wi) which was subdivided into Early Wilting (EWi) and Late Wilting (LWi) respectively. Data represent mean values ± SD of three biological replicates. Blue asterisks indicate significantly different values among plants watered under different conditions (Kruskal Wallis test followed by Dunn's multiple comparisons test; $p < 0.05$). Black asterisks denote values significantly different from those measured in Col-0 (Mann-Whitney tests; $p < 0.05$).

mutants. The fourth one, *atesl3.03,* was a knockdown mutant because of its 55% reduced expression (Ch.IV-Fig. 8). Furthermore, none of the four mutants demonstrated any expression increase in response to water depletion (Ch.IV-Fig. 8).

Expression profiles of four *AtESLs* (*AtESL1.02, AtESL3.03, AtESL3.05* and *AtESL3.07*) and those of their tandem genes (*AtESL1.01, AtESL3.02, AtESL3.06* and *AtESL3.08*) were studied in each of the single mutants under conditions of water arrest and after re-watering (Ch.IV-Fig. 9). In the *atesl1.02* mutant, the expression of *AtESL1.01* gene manifested five-fold decrease in the SD phase, and a further eight-fold repression during the senescence phase (Ch.IV-Fig. 10). The reduction of its expression was delayed when compared to that of the wild Col-0 genotype. In RW plants, *AtESL1.01* expression was restored and reached higher level than that of the Col-0 genotype. In the same mutant, *AtESL3.05* gene was expressed more strongly than that of Col-0 at the EWi step. The increase of *AtESL3.07* expression was delayed to that of the wild genotype, which was manifested in the Wi phase. In the *atesl3.03* mutant, the induction of *AtESL3.07* expression took place later than that of Col-0 in the SD phase. In *atesl3.07* mutant of gene the expression of its tandem gene *AtESL3.08* was reduced during the EM phase. In the *atesl3.05* mutant, no significant differences in the expression of *AtESL* genes were found when compared to those of the wild genotype (Ch.IV-Fig. 9).

As knockdown or knockout of each of the four AtESL sugar transporters might affect sugar fluxes, the content of soluble sugars (glucose, fructose and sucrose) was measured in leaves of well-watered, water-deprived and re-watered plants (Ch.IV-Fig. 9). The mutation of the *AtESL1.02* gene affected mainly the content of glucose. In the *atesl1.02* mutant the glucose content was greater than that of Col-0 not only in WW plants during EM and MD phases, but also in RW plants. In the *atesl1.02* mutant osmotic pressure in WW plants appeared slightly lower than for Col-0. In WD plants, the osmotic pressure of the *atesl1.02* mutant increased later (on the 47th DPS corresponding to the SD phase; Ch.IV-Table 1), but to a lesser extent to that of Col 0 and at the 49th DPS. In the three other mutants (*atesl3.03*, *atesl3.07* and *atesl3.05*), no significant differences with the Col-0 genotype were observed in terms of osmotic pressure and soluble sugars. In the same line, growth (PRA, DW and FW) and physiological (WC, RWC and SC) parameters of the four mutants *atesl1.02, atesl3.03, atesl3.05* and *atesl3.07* did not show significant differences in respect to those of the wild genotype under conditions of WW, WD and RW (Ch.IV-Fig. S1 and 2).

Discussion

To understand how plants cope with water deprivation and decipher the multiple faces of their drought responsiveness appeared of utmost importance for further improvement of crops resilience under constraint environment. The present study aims to correlate the response of *A. thaliana* Col-0 in terms of growth, physiological and metabolic behavior with water deficit intensity.

During the EM phase, defined by a WC of 92.2%, the studied parameters did not display any significant difference compared to those of well-watered plants. The progressive loss of water in leaves between the 35th and the 44th DPS did apparently not affect plants (Ch.IV-Fig. 2 and 3). A drastic loss of water (1.8%) in the MD phase take place within 24 h, on the 44 th- 45th DPS. This led to stomatal closure and was associated with the onset of glucose and sucrose increase in leaves. Stomatal closing is the first plant response to reduced soil water potential, which allows plants to prevent water losses (França et al., 2000; Flexas et al., 2004; Liu et al., 2005; Blouin et al., 2007; Harb et al., 2010; Arve et al., 2011; Galmés et al., 2013). ABA is the major endogenous signal inducing stomatal closure and preventing stomatal opening (Seki et al., 2007; Arve et al., 2011; Živanović et al., 2020). Glucose and sucrose content increase contributed to cells' osmotic adjustment, which maintained them turgid and metabolically active (Morgan, 1984; Kiyosue et al., 1994; Hare et al., 1998; Munns, 2002; Taji et al., 2002; Moore et al., 2008; Hummel et al., 2010; Mewis et al., 2012; Sperdouli and Moustakas, 2012; Blum, 2017). In the SD phase, corresponding in leaves to light decrease of the WC from 90% to 86% on 45th -47th DPS), the osmotic pressure (Ch.IV-Table 1) was augmented in parallel with the increase of glucose and sucrose content (Ch.IV-Fig. 4). This confirms the plant capacity to maintain basic metabolism despite the closure of stomata. Although the DW was stable, the PRA decreased as consequence of cell growth arrest and enhanced dehydration (Ch.IV-Fig. 2) (dos Santos Gouvêa and Marenco, 2018; Turner, 2018; Zhao et al., 2020; Živanović et al., 2020). When WC diminished below 90% leaf expansion was affected by the arrest of cell growth due to drop of cell water potential and respective loss of turgidity (Hsiao, 1973; Simonneau et al., 2017).Taken together our results confirm the already established concept that the arrest of cell growth responds to a milder water deficit than that required for photosynthesis rate reduction. Consequently, the limitation of carbon assimilation is not the real cause of cell growth arrest. The latter is mainly related to the cell choice to invest metabolites and energy for its osmotic adjustment, signaling of reduced water potential and cell wall stiffening in order to promote plant acclimation.

In this context Mewis et al. (2012) reported that drought stress enriched the nutritional quality of phloem sap in *A. thaliana* Col 0 plants with 93%-94% WC by increasing the amounts of free amino acids and sugars, especially sucrose. Our microscopy observations confirmed that the cells were not only viable but remained turgid until the 47th DPS (Ch.IV-Fig. 1C). When the WC shifted below 86% in the Wi phase, the soluble sugars in the leaves reached their maximum level of accumulation, which is considered as a metabolic signal to trigger senescence (Rolland et al., 2006). However, in the Wi phase re-watering allowed to restore all physiological parameters to levels observed in the MD phase. Under the conditions of our study, the water-deprived plants at the LWI step remained capable of absorbing available water even at a WC below 76%. Below the latter threshold plant wilting became irreversible and massive cell plasmolysis was observed microscopically (Ch.IV-Fig. 1C) Mewis et al., (2012) have reported that the decrease of DW started from a WC of 93%-94%, which corresponds to our experimental condition to EM phase (Ch.IV-Fig. 2B). In summary, *Arabidopsis* and other plants respond in a similar way to water deficit by decrease of WC, SC, FW, PRA and DW and concomitant increase of sugars and other compatible osmolites (Mewis et al., 2012; dos Santos Gouvêa and Marenco, 2018; Zhao et al., 2020; Živanović et al., 2020).

Although more than one thousand genes have been identified as involved in the drought response, only a few of them have characterized in terms of induced tolerance to water depletion, combined with enhanced plant productivity in model plants, as well as in agriculture important crops (Skirycz et al., 2011). In *A. thaliana* the most studied genes, whose expression was regulated in response to moderate water stress, are dehydrins, LEA, aquaporins, K^+ ionic channels and ESL sugar transporters (Kiyosue et al., 1998; Seki et al., 2002; Shinozaki and Yamaguchi-Shinozaki, 2007; Lawlor, 2013; Fang and Xiong, 2015).

Our phylogenetic analysis of ESL proteins from 60 plant taxons allowed the establishment of three groups. The ESL1 group supposedly derives from old copies already present in the Bryophyte genome, where this family would have undergone three whole genome duplication events, which resulted in their expansion in the plant kingdom (Slawinski, 2017; (Slawinski et al., 2021, in preparation, see Chapter III). The ESL2 and the ESL3 groups would result from the first and second duplication events respectively. The ESL3 group is constituted by the mostly recent copies and multiples genes tandems duplications, which have been identified in *A. thaliana* (Slawinski, 2017).

In *A. thaliana*, seventeen *AtESL* displayed various expression patterns in leaves. The *AtESL1* genes (*AtESL1.01* and *AtESL1.02*) were always moderately expressed,

the *AtESL2* genes (*AtESL2.02*, *AtESL2.01* and its tandem *AtESL2.03*) were weakly expressed, while the *AtESL3* genes showed various levels of expression (i.e. *AtESL3.01*, *AtESL3.02* and its tandem *AtESL3.03*, *AtESL3.05* and its tandem *AtESL3.06*, *AtESL3.07* and its tandem *AtESL3.08, AtESL3.10*, *AtESL3.11*, *AtESL3.13* and *AtESL3.14*). These results give ground to the hypothesis of a possible functional divergence of the ESLs (Slawinski et al., 2021, in preparation, see Chapter III). Water depletion responsiveness of these genes and their putative localization on the tonoplast, already demonstrated for a few of them, assumed the functional importance of these transporters through their involvement in subcellular sugar partitioning. In WW plants, the increase of glucose and fructose content during the growth kinetics could involve *AtESL3.02* and its tandem *AtESL3.03* gene, whose expression levels were increased from the 49th DPS, corresponding to the late vegetative plant growth (Ch.IV-Fig. 5). AtESL2.01 presents higher expression levels the days before the 49th DPS.

Expression profiling of seventeen *AtESL* genes demonstrated that twelve among them responded to water deficit, four with increased and eight with decreased expression. As *AtESL3.08* gene was inhibited at WC > 92.2%, it may be considered as early responsive to initial subtle changes of water potential, before the appearance of any significant difference of growth and physiological parameters between WW and WD *Arabidopsis* plants. These data further confirmed the already published results of *AtESL3.08* involvement in plant response only few hours after water arrest (Kiyosue et al., 1998; Seki et al., 2002; Yamada et al., 2010). The preferential expression of this gene in roots, and namely in rhizoderme (Yamada et al., 2010), might suggest a role in the perception of early signals of decreased water potential in roots.

At WC lower than 76%, all studied growth and physiological parameters dropped down, except for sugar content, whose increase mainly reflects the advanced dehydration of leaves. Remarkably, among the studied genes *AtESL1.02* was the only one with increased expression under severe water deficit. Its expression has also been increased in face to high-energy demand of the cell (Poschet et al., 2011). In mature leaves with triggered senescence due to WC below 76%, *AtESL1.02* may be involved as H^+/glucose symporter in glucose efflux from the vacuole to the cytosol, which is required for sugars' remobilization from the senescent leaves and reallocation to young sink organs organs (Poschet et al., 2011; Klemens et al., 2014).

Another important result concerns the fact that none of water deficit responsive genes and their respective tandem duplicated genes did not share the same expression profile dependent on the plant water status. *AtESL1.01* was early down-regulated (WC > 90%), while

AtESL1.02 was up-regulated at WC < 76%. *AtESL3.02* showed reduced expression at WC < 76%, while *AtESL3.03* increased in parallel to the WC lowering from 92.2% to 90%. *AtESL3.05* expression increased in phase (MD) (92.2% > WC > 90%), when *AtESL3.06* appeared insensitive to water depletion. *AtESL3.07* was up-regulated for WC comprised between 92.2 % and 90%, while *AtESL3.08* was down-regulated since the phase 1. *AtESL3.13* was repressed at WC < 86%, but *AtESL3.14* was not regulated by water depletion. These differential responses of tandem duplicated *ASL* genes issued from segmental duplications in evolution, provide arguments in favor of the diversification of AtESL roles in plant response to water deficit. Our results appear in line with the already demonstrated differential regulation of some tandem duplicated *ESL* genes under environmental constraints (Innan and Kondrashov, 2010).

In order to elucidate the roles of four *AtESL* genes up-regulated by the leaf water defict of wild genotype Col-0 plants, their respective single mutants were identified in the same genetic background and characterized under the same studied conditions. However, none of the single *atesl* mutants did display any significantly different phenotype compared to that of the wild type (Ch.IV-Fig. S1). Their expression analysis did not reveal any noticeable compensatory effect for any of the single knocked-down or knocked-out genes. These results were predictable as the ESL transporters belong to a multigenic subfamily, and in addition there exist many other sugar transporters (SWEETs, SUCs/SUTs, TMTs, VGT1) located on the tonoplast.

In WW plants, the knockout of *AtESL1.02* gene resulted in a higher glucose content in *atesl1.02* mutant than that in the wild genotype, and this difference was maintained even in water-deprived plants, with leaf WC of 90%. In re-watered plants, the glucose content was always more important in the *atesl1.02* mutant. This increase in glucose amount in *atesl1.02* mutant might be due to glucose accumulation in the vacuole (Poschet et al., 2011). *AtESL1.02* mutation might restrict glucose efflux from vacuole to cytosol. The up-regulation of *AtESL1.02* expression has been demonstrated in the transition from light to obscurity, the elevation of temperature from 23°C to 37°C, and after injury, when the changes of cell status require rapid energy mobilization through the export of vacuolar sugar reserves. Inversely, *AtESL1.02* expression has been down-regulated under conditions favorable for sugar accumulation into the vacuole, temperature decrease and high concentration of extracellular sugars. Taken together, these data and the characterization of *AtESL1.02* as H^+/glucose symporter provide evidence for the correlation between *AtESL1.02* expression and the sugar status of the cell (Poschet et al., 2011; Klemens et al., 2014). Under our experimental

conditions, AtESL1.02 may be involved in hexose remobilization in the cytosol in response to severe water deficit, because of its increased expression at WC < 76 % concomitant to glucose decrease. However, in the *atesl1.02* mutant the same curve of glucose accumulation was matching with that of Col-0 plants, and that in spite of *AtESL1.02* knockout.

At the stage of plant wilting other sugar transporters may also be required for glucose export from the vacuole. It is worth to note that the expression of *AtESL3.07* in the wild genotype was up-regulated since the phase MD, while in the *atesl1.02* mutant it was delayed at the end of phase EWi (WC < 76%). These results suggest that in in *atesl1.02* mutant the early up-regulation of *AtESL3.07* expression may be inhibited by high glucose content and only in WI phase with the decrease of glucose content, *AtESL3.07* gene expression may compensate the knockout of *AtESL1.02* (Ch.IV-Fig. 9). This hypothesis is corroborated by the characterization of AtESL3.07 as a low-affinity facilitator suitable for hexose export through facilitated diffusion (Yamada et al., 2010).

Conclusion

In summary, the expression profiling of seventeen *Arabidospsis* ESL genes revealed that twelve are responsive to water deficit, four are up-regulated and eight are down-regulated. All the twelve *AtESLs* transporter genes were differentially expressed depending on the physiologically defined phases of plant water status. The comparison of four *atesl* single mutants and the wild type Col-0, under well-watering and water-deprivation growth conditions, did not reveal any phenotypic difference**.** The latter is probably due to functional redundancy of ESLs and their synergistic actions. However, the differential expression of each of the tandem duplicated *AtESL* genes in response to water stress argues in favor of their plausible functional diversity. Our results corroborate the hypothesis of acquisition of new physiological functions by the ESLs, which favors plant plasticity to cope with environmental constraints.

Supplementary data

Table S1: Primers used in qPCR for gene expression analysis and Primers used for genotyping.

Figure S1: Characterization of the effect of water deficiency on the wild *Arabidopsis thaliana* Col-0 ecotype and the *atesl1.02*, *atesl3.03*, *atesl3.05* and *atesl3.07* mutants under well-watered, water-deprived and re-watered plants in function four hydric deficit phases

Figure S2: Glucose and sucrose content in *Arabidopsis thalian*a wild ecotype Col-0 and the *atesl1.02*, *atesl3.03*, *atesl3.05* and *atesl3.07* mutants under well-watered, water-deprived and re-watered plants.

Acknowledgments:
We thank Vincent Lebeurre for the culture of plants.

Author contributions:
AI, FD, LS, ML, RA, designed the experiments. AI, CP, FD, FT, LS, ML, RA performed the experiments. AI, FD, LS, ML, RA discussed the data and wrote the article. All authors approved the published version of the manuscript.

Funding:
This work was funded by the 2015-2020 State-Region Planning Contracts (CPER), European Regional Development Fund (FEDER), and intramural funds from the Centre National de la Recherche Scientifique (CNRS) and the University of Poitiers.

Conflict of interest:
The authors declare to not have any commercial or associative interest that represents a conflict of interest in relation with this study.

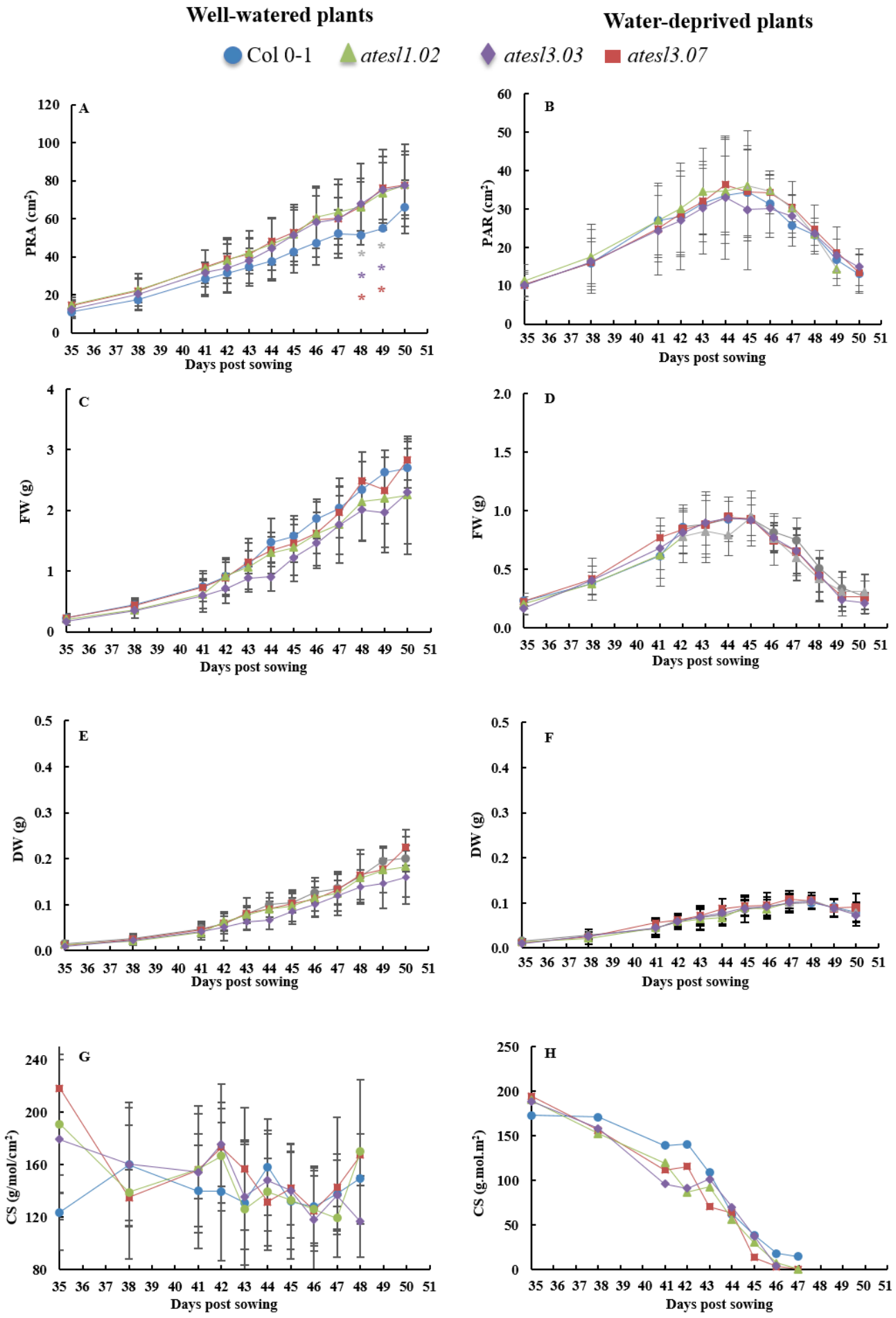
Well-watered plants
Water-deprived plants
Col 0-1
atesl1.02
atesl3.03
atesl3.07
A
PRA (cm²)
B
PAR (cm²)
C
FW (g)
D
FW (g)
E
DW (g)
F
DW (g)
G
CS (g/mol/cm²)
H
CS (g.mol.m²)
Days post sowing

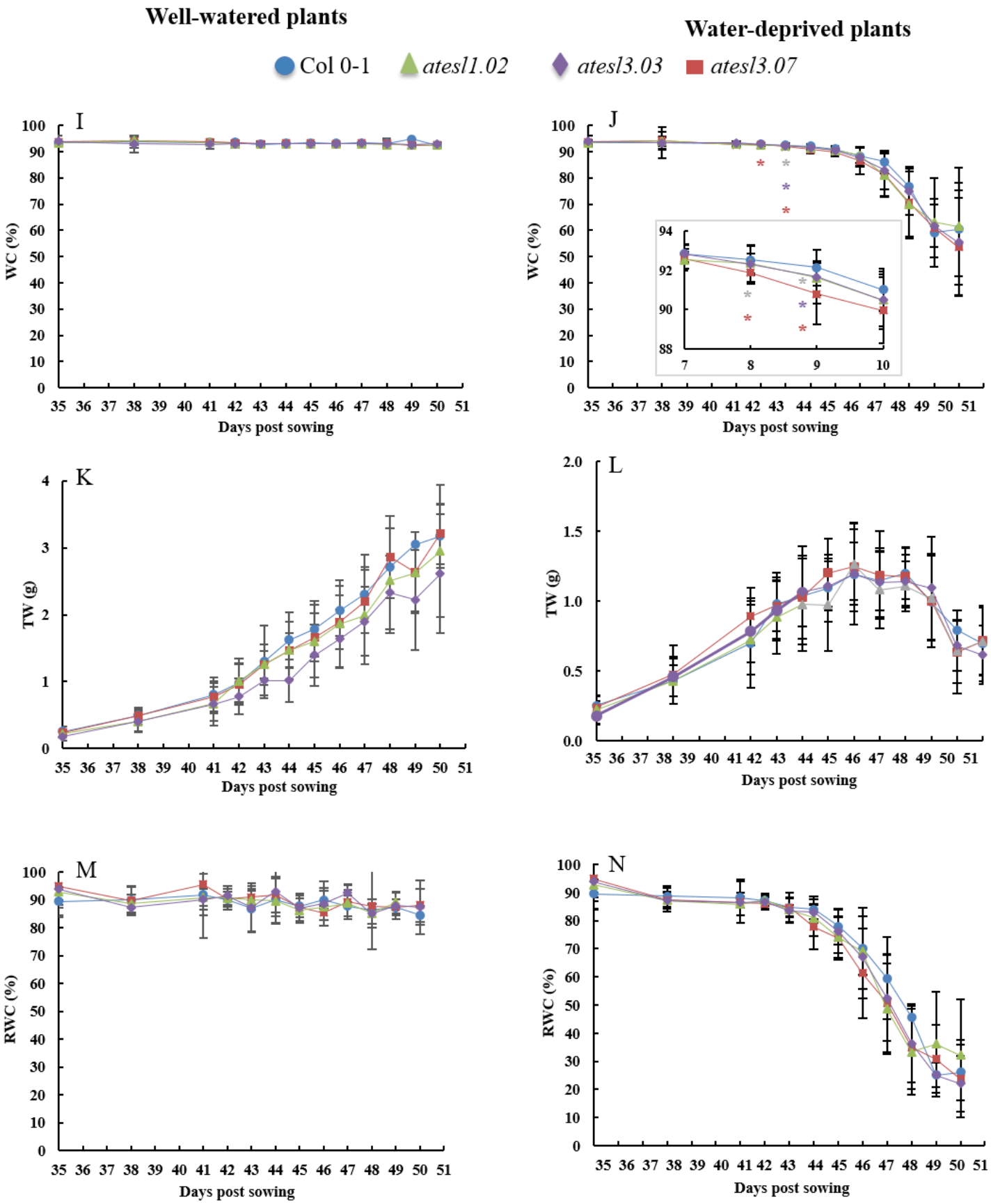
Well-watered plants
Water-deprived plants
Col 0-1
atesl1.02
atesl3.03
atesl3.07
I
J
K
L
M
N
WC (%)
TW (g)
RWC (%)
Days post sowing

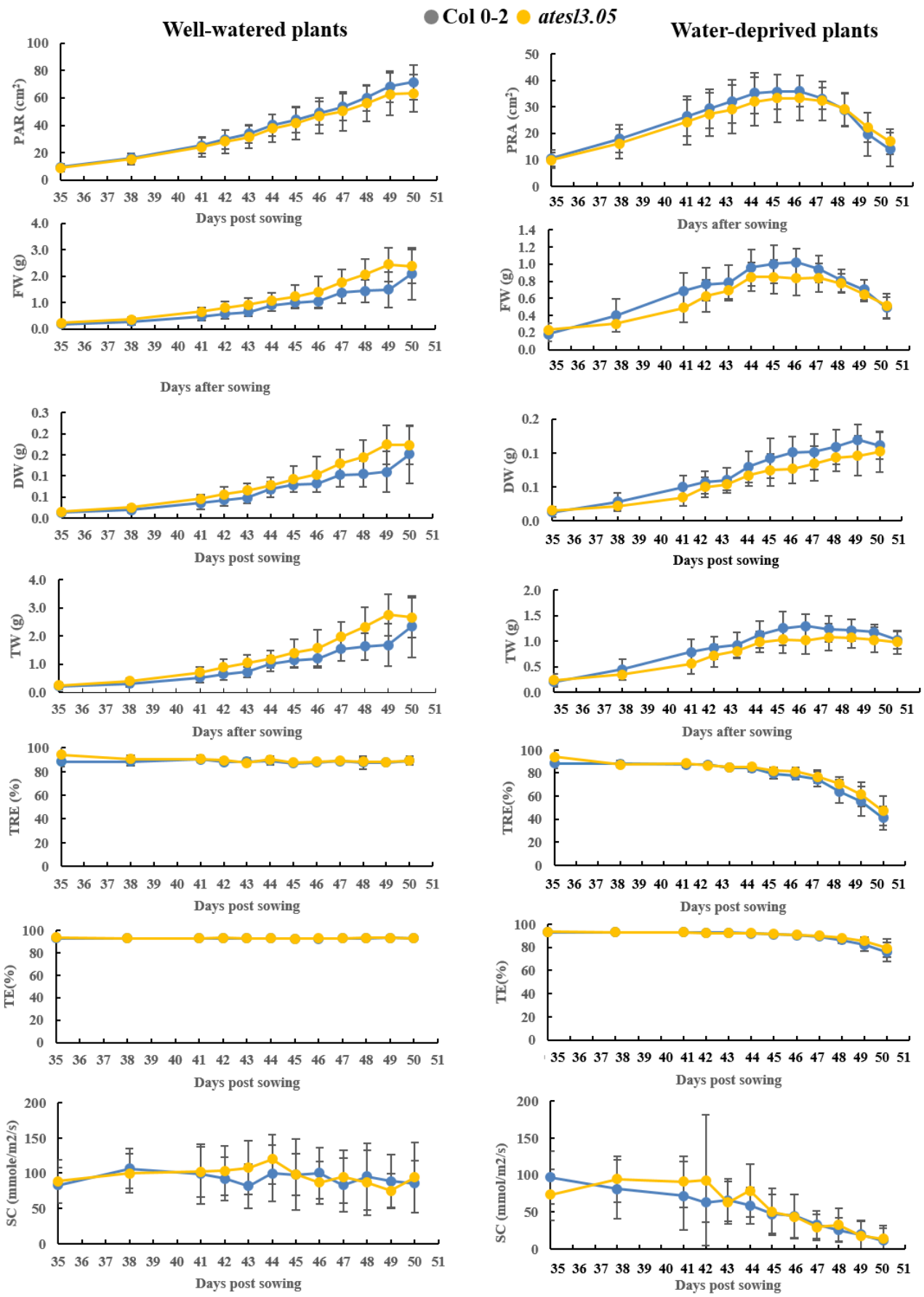
Col 0-2
atesl3.05
Well-watered plants
Water-deprived plants
PAR (cm²)
PRA (cm²)
FW (g)
DW (g)
TW (g)
TRE (%)
TRE(%)
TE(%)
SC (mmole/m2/s)
SC (mmol/m2/s)
Days post sowing
Days after sowing

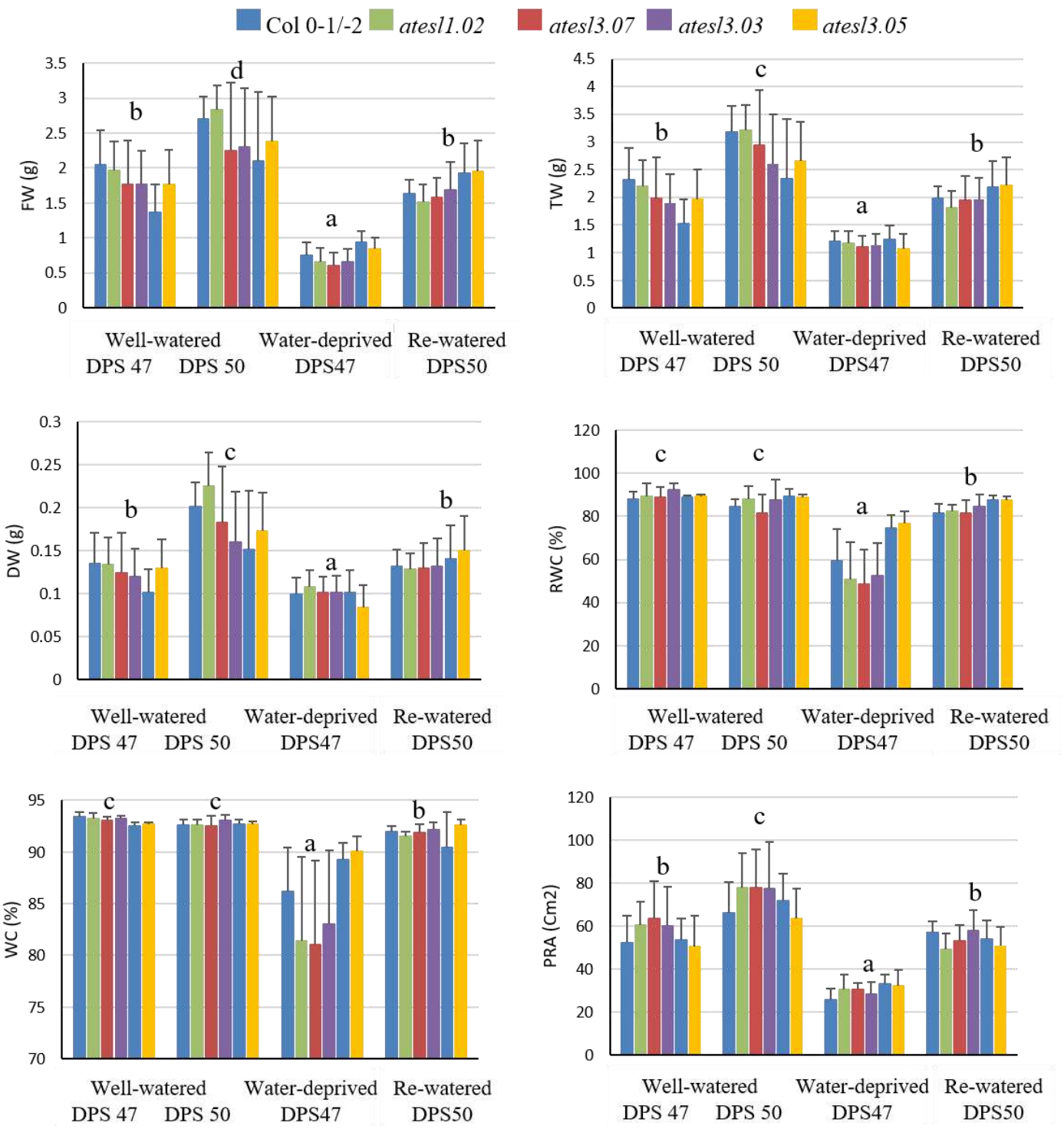

Ch.IV-Fig. S1: Characterization of the effect of water deficiency on the wild *Arabidopsis thaliana* Col-0 ecotype and the four mutants *atesl1.02*, *atesl3.03*, *atesl3.05* and *atesl3.07* under well-watered, water-deprived and re-watered plants in function four hydric deficit phases : Phase 1, Early mild water Deficit (EM); phase 2, Moderate water Deficit (MD); phase 3, Severe water Deficit (SD) and phase 4, Wiling phase (Wi) which was subdivided into Early Wilting (EWi) and Late Wilting (LWi) respectively. The projected aerea rosette (PAR), the fresh weight (FW), the dry weight (DW), the stomatal conductance (SC), the turgid weight (TW), the relative water content (RWC) and water content (WC) are measured under well-watered, water-deprived and re-watered growing conditions during 15 days of kinetic. The study was carried out on five plants by condition and in three independent biological repetitions. Kruskal-Wallis tests was performed followed by Dunn's multiple comparisons test. Asterisks in several colors indicate significant difference between kinetics time-points for any of the genotypes ($p < 0.05$). Black asterisks indicate significant differences between any of the respective mutants and the wild type Col-0.

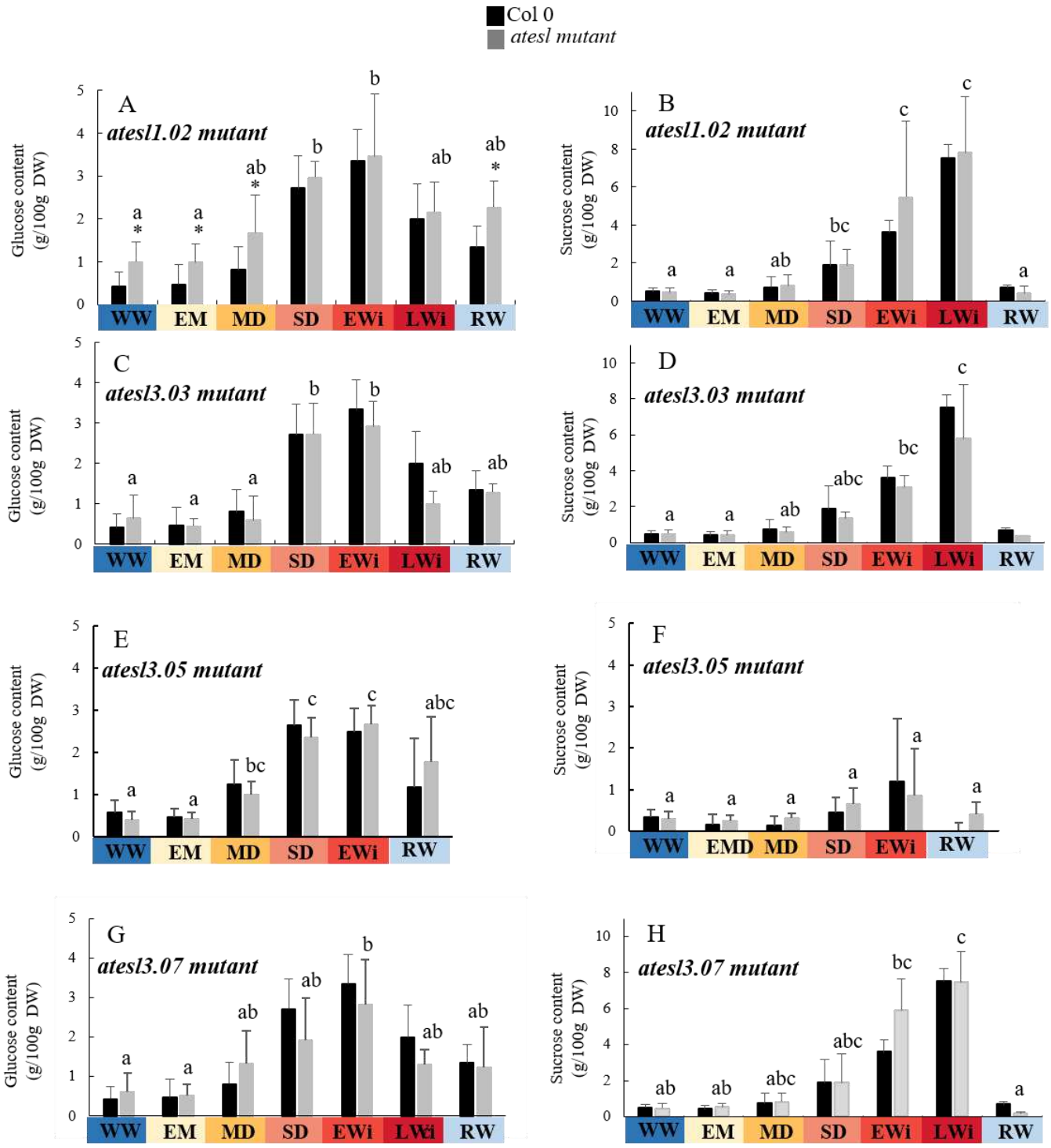

Ch.IV-Fig. S2: Glucose and sucrose content in the leaves of *Arabidopsis thaliana* wild ecotype Col-0 and the four mutants *atesl1.02*, *atesl3.03*, *atesl3.05* and *atesl3.07* under well-watered, water-deprived and re-watered plants in function four hydric deficit phases : Phase 1, Early mild water Deficit (EM); phase 2, Moderate water Deficit (MD); phase 3, Severe water Deficit (SD) and phase 4, Wiling phase (Wi) subdivided in Early Wilting (EWi) and Late Wilting (LWi) respectively. The values represent the mean of three biological replicates ± standard deviation. The letters a, b, c indicate statistically different groups, as analyzed by Kruskal-Wallis test at $p < 0.05$. Mann-Whitney pairwise comparison tests revealed statistical difference between the values for Col-0 and *atesl.02* mutant (black asterisks).

Ch.IV-Table S1 : Primers used in qPCR for gene expression analysis and Primers used for genotyping.

Gene	Accession	Gene expression Sequence 5'-3'	SALK database	Genotyping Sequence 5'-3'
ESL3.07	At1g08920	F: TCGGTCTCATTCCATGTGCG R: TGCATCATCTCCGCGAAGAC	SALK_025646	LP: AGAACCAAAACGACATCAACG RP: TCCCCATTTTCCCTATACACC
ESL1.02	At1g75220	F: GTGGAGGAACTTTCACTCTGTA R: GTTCTTCAAGAGTTTTGCCTT	SALK_106049	LP: GCAACAAATCCAAGATTCGAC RP: TATCCCCAAGTTTTGTTTCC
ESL3.05	At1g08890	F: TGGAGTGCTTTCGGAACATATT R: GAGTAAAGAATCAACTTTGGAT	SALK_047351	LP: TGCTCTTGCAACAATTTTGTG RP: TTTACCGAAAGCACTCCATTG
ESL3.03	At4g04760	F: CAGAGATTTATCCAGTAGATGT R: TGGCTATGAACACAAATCCAA	SALK_132009	LP: TTTACCGAAAGCACTCCATTG RP: ATTGATCCCATACCAGAACC LBb1.3: ATTTTGCCGATTTCGGAAC
PP2a*	At1g13320	F: TAACGTGGCCAAAATGATGC R: GTTCTCCACAACCGCTTGGT		

* Initially designed by Czechowski et al., 2005.

CHAPTER V

Arabidopsis ESL1.02, ESL3.03, ESL3.05 and ESL3.07 sugars transporters in seed germination and early seedling development in response to endogenous and exogenous cues

1. Introduction

Chez les plantes, les sucres en tant que photoassimilats sont des métabolites structurels et énergétiques indispensables pour la croissance et le développement des plantes. En effet, ils agissent comme des molécules de signalisation, à l'interconnection des voies de signalisation métabolique et hormonale (Jang et al., 1997; Moore et al., 2003; Rolland et al., 2006). Le glucose est le signal glucidique le plus étudié. Chez les plantes, un seul senseur du glucose, l'hexokinase 1 (HXK1), a été clairement identifié. Il est connu pour son rôle clé dans la perception et la transmission des signaux des sucres "sugar sensing and signaling". Chez les plantes, trois voies de signalisation du glucose ont été suggérées : une voie indépendante de HXK1, une deuxième voie dépendante de HXK1 en tant que senseur, ainsi qu'une troisième voie dépendante de l'activité catalytique de HXK1, donc de la glycolyse (Xiao et al., 2000).

De plus, les sucres peuvent moduler plusieurs processus biologiques dans les plantes tels que la germination des graines, le développement des plantules, la transition florale et la sénescence (Rolland et al., 2006). La germination des graines est une étape cruciale dans le cycle de vie des plantes, qui nécessite la maturation de l'embryon ainsi que la dessiccation des graines. La dormance des graines empêche temporairement la germination, afin que cette dernière ait lieu dans des conditions environnementales favorables garantissant la survie du semis (Finch-Savage and Leubner-Metzger, 2006; Finkelstein et al., 2008; Nonogaki, 2014; Shu et al., 2016). Chez *Arabidopsis*, deux types de dormance ont été reconnus : la dormance primaire et la dormance secondaire. Les graines libérées de la plante mère sont en état de dormance primaire. Cela suppose l'implication de la signalisation ABA pendant la maturation des graines (Baskin and Baskin, 2004; Finch-Savage and Leubner-Metzger, 2006). Des mutants d'*Arabidopsis* affectés par la synthèse ou la signalisation de l'ABA ont montré une réduction de la dormance (Koornneef et al., 1989). En revanche, quand les conditions de germination ne sont pas favorables, les graines libérées de la plante mère seront dans un état non dormant. Par la suite ces graines peuvent revenir en dormance secondaire (Baskin and Baskin, 2004; Finch-Savage and Leubner-Metzger, 2006). La germination est régulée par des facteurs externes, tels que la lumière et la température, ainsi que par des facteurs internes comme les hormones végétales. L'ABA et les gibbérellines (GAs) agissent de manière antagoniste sur la dormance. Il est largement reconnu que l'ABA est par excellence "l'hormone de la dormance" bloquant la germination, tandis que les GAs lèvent la dormance

et favorisent la germination. Lorsque le rapport ABA/GA est élevé, l'état de dormance est maintenu. Toutefois, un faible rapport ABA/GA permet de lever la dormance et par la suite le déclenchement de la germination (Ali-Rachedi et al., 2004; Finch-Savage and Leubner-Metzger, 2006). Malgré l'équilibre hormonal endogène, des facteurs exogènes tels que la post-maturation à sec (after-ripening), le traitement par le froid à l'humidité (stratification) et l'application exogène des GAs peuvent lever la dormance résiduelle des graines (Finkelstein et al., 2008). La post-maturation est définie comme une période prolongée de stockage à sec et à température ambiante des graines fraîchement récoltées. Au cours de cette phase, les graines perdent leur capacité de dormance. La stratification fait référence au traitement des graines par le froid afin de rompre la dormance. Les mécanismes de la stratification des graines sont couplés à la voie de la biosynthèse des GAs (Finkelstein et al., 2008).

Dans ce chapitre, nous présentons la génération, par croisement génétique, des mutants homozygotes simples, doubles, triples et quadruples pour les quatre gènes *ESL.* L'analyse des graines par Geneinvestigator a montré une expression élevée de gène *ESL1.02* et des niveaux d'expression modérés pour les gènes *ESL3.07*, *ESL3.05* et *ESL3.03*. De plus, nos résultats ont montré l'absence de réponse différentielle nette de ces quatre gènes *AtESL* en déficit hydrique. Dans ce contexte, nous avons généré, par croisement de quatre mutants simples dans différentes combinaisons, trois mutants double et deux mutants triple *esl*. Ensuite, nous avons procédé au phénotypage de ces différents mutants pendant la germination des graines et au cours du le développement précoce des plantules, afin de mettre en évidence leurs sensibilité/résistance au glucose et à l'acide abscissique (ABA), ainsi qu'aux stresses salin et froid.

2. Experimental results

Introduction

In plants, sugars resulting from the photosynthesis are essential structural and energy metabolites for plant growth and development. Twenty years ago, it has been demonstrated that sugars act as signal molecules at the crosstalk of plant metabolic and hormonal signaling pathways (Jang et al., 1997; Moore et al., 2003; Rolland et al., 2006). Glucose is the most studied sugar signal and its cytosolic sensor, hexokinase 1 (HXK), plays a key role in sugar sensing and signaling. In plants, three different pathways for glucose signaling have been suggested: (1) a HXK1-dependent pathway, (2) a HXK1-independent pathway, and (3) a glycolysis-dependent pathway that depends on the enzymatic activity of HXK1 (Xiao et al., 2000). Besides, sugars can modulate several japrocesses such as seed germination, seedling development, floral transition, and senescence, through the regulation of gene expression (Rolland et al., 2006). During the plant life cycle, seed germination is a crucial stage for plant survival. Even under favorable conditions for germination, a seed will not germinate if embryo maturation and seed dessication are not completed. Seed dormancy prevents temporally seed germination, which ensures that seeds germinate only when favorable conditions are suitable for both early seed germination and seedling survival (Finch-Savage and Leubner-Metzger, 2006; Finkelstein et al., 2008; Nonogaki, 2014; Shu et al., 2016). Two types of dormancy, primary and secondary dormancy, have been recognized in *Arabidopsis*. The seeds released from the mother plant are in primary dormant state, which implies involvement of ABA signaling during their maturation (Baskin and Baskin, 2004; Finch- Savage and Leubner- Metzger, 2006). *Arabidopsis* mutants affected in ABA synthesis or signaling have shown reduction of dormancy (Koornneef et al., 1989). In contrast, when seeds dispersed by mother plant are in a non-dormant state and the germination conditions are not suitable, they can re-enter in secondary dormancy (Baskin and Baskin, 2004; Finch- Savage and Leubner- Metzger, 2006). Germination is regulated by external factors, such as light and temperature, as well as by internal factors, at the example of plant hormones. ABA and gibberellins (GAs) act antagonistically on dormancy. It is widely recognized that ABA acts as “hormone of dormancy” which blocks germination, while GAs are suppress dormancy and promote germination. Under high ABA:GAs ratios, the dormant state is maintained, whereas low ABA:GAs ratios allow to overcome dormancy and induce germination (Ali-Rachedi et al., 2004; Finch-Savage and Leubner-Metzger, 2006).

Ch.V- Table 1: Number of double heterozygous mutants obtained in the F1 generation

Cross combination		No. of analyzed plants	No. of double heterozygous lines
Female	Male		
esl3.07	*esl3.05*	11	7
esl3.05	*esl3.07*	13	3
esl1.02	*esl3.03*	13	8
esl3.03	*esl1.02*	11	2
esl3.05	*esl3.03*	23	8
esl3.03	*esl3.05*	8	2
esl3.07	*esl3.03*	15	8
esl3.03	*esl3.07*	14	6
esl3.07	*esl1.02*	20	7
esl1.02	*esl3.07*	17	3
esl3.05	*esl1.02*	16	8
esl1.02	*esl3.05*	10	4

Ch.V- Table 2: Summary of mutant lines obtained in this study

Mutant line		
Single	Double	Triple
esl1.02	*esl1.02esl3.07*	*esl1.02esl3.03esl3.07*
esl3.03	*esl3.03esl3.05*	*esl1.02esl3.03esl3.05*
esl3.05	*esl1.02esl3.03*	
esl3.07		

Despite the endogenous hormonal balance, external factors such as after-ripening, cold treatment (stratification), and exogenous application of GAs can break seed dormancy (Finkelstein et al., 2008). After-ripening is defined as a prolonged period of dry storage of freshly harvested seeds at room temperature, during which seeds lose their capacity of dormancy. Cold stratification refers to seeds cold treatment to break dormancy. The mechanisms of this seeds stratification strategy are coupled to GAs biosynthesis pathway (Finkelstein et al., 2008).

In this chapter, we present the generation through genetic crossing of single homozygous mutants for the four studied *ESL* genes the successive steps of our strategy to obtain double, triple and quadruple mutants. In seeds, Geneinvestigator analysis shows high gene expression for *ESL1.02* and moderate levels for *ESL3.07*, *ESL3.05*, and *ESL3.03*. In addition, our results demonstrated the lack of a clear-cut differential response of these four *AtESL* genes to water deficit. In this context, we generated by crossing of four single mutants in different combinations three double and two triple *esl* mutants. Furthermore, we realized the phenotyping of these mutant genotypes throughout their seed germination and early seedling development sensitivity/resistance to glucose and abscisic acid, as well as to salt and cold constraints.

3. Results

Steps on the route towards *esl1.02esl3.03esl3.05esl3.07* quadruple mutant

Identification and characterization of *esl3.05* simple mutant

A first task in my thesis work consisted in the identification and the characherization of SALK_047351 mutant, the *esl3.05* homozygous line. This knockout mutant was further analyzed under normal and water deficit conditions to complete our study of ESLs functional behavior in relation with different plant water status (Chaptre Ⅳ). As we already reported the four *atesl* single mutants, *esl3.07*, *esl1.02*, *esl3.05*, and *esl3.03*, did not show any phenotypic difference compared to the wild type under normal and water deficit conditions. An approach for revealing the effect of combinatory and combined repression of these four *AtESL* genes is to generate double, triple and quadruple mutant lines. The *Arabidopsis* T-DNA insertion lines SALK_106049, SALK_025646, SALK_047351, and SALK_132009, which are designated here as *esl1.02*, *esl3.07*, *esl3.05*, and *esl3.03*, respectively, were used for the generation of doubles and triple mutants.

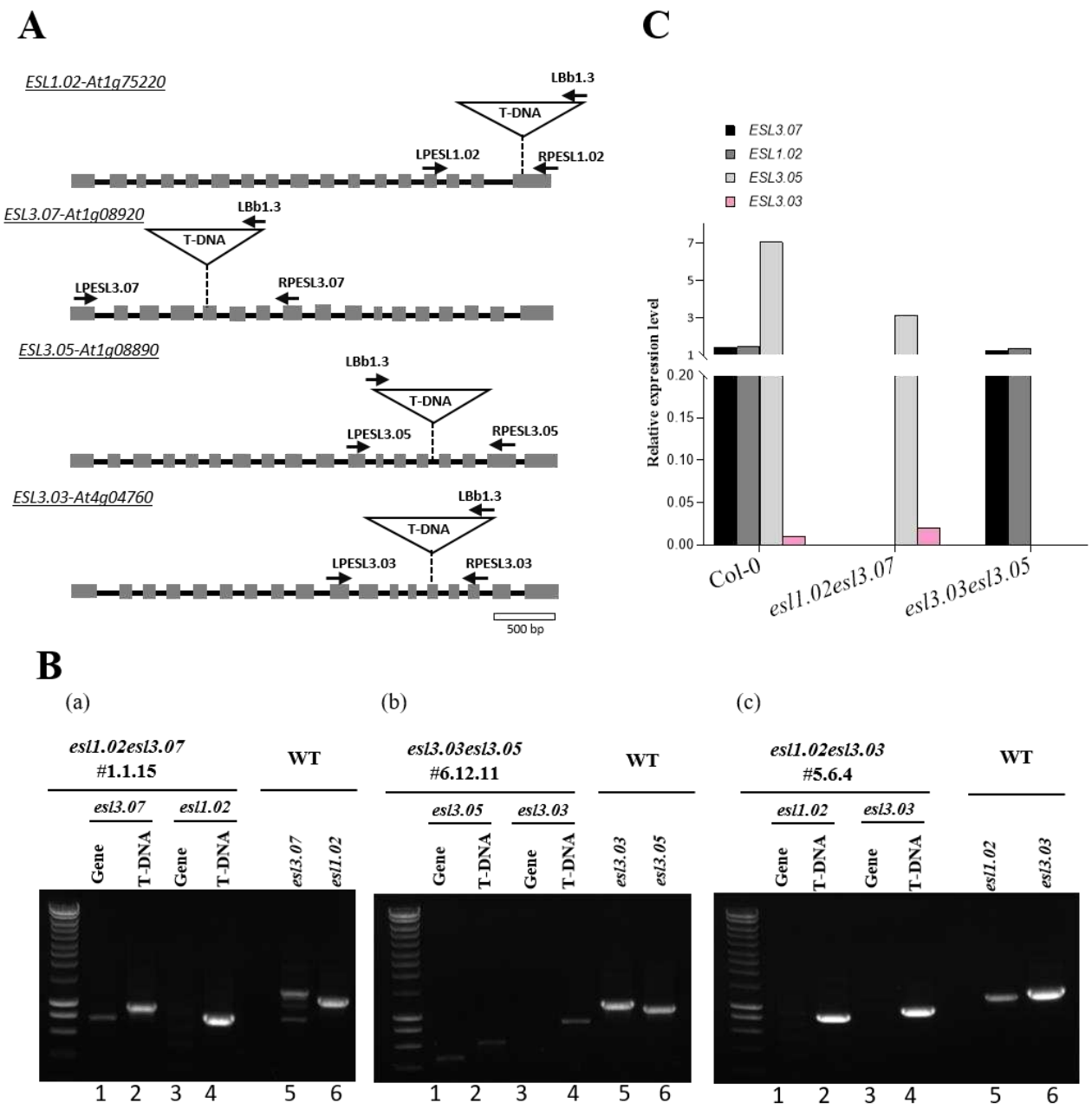

Ch.V- Fig. 1 : Genotyping of *atesls* double mutants. (A-B) *atesls* double mutants were generated by crossing the single homozygous mutants (*esl3.07*, *esl1.02*, *esl3.05*, and *esl3.03*). A) Graphical representation of the four *AtESL* genes. Exons are indicated by gray boxes, introns by solid black lines, and T-DNA insertions by white triangles. Arrows indicate primer locations used for PCR genotyping of the four *AtESL* alleles; RP, reverse primer; LP: forward primer; LBb1.3: left T-DNA border primer. B) PCR analysis on genomic DNA using the following primers: gene-specific primers LPESLs and RPESLs was used amplify the *AtESLs* genes (lanes 1, 3, 5, and 6), while T-DNA primer and gene-specific primer (LPESLs or RPESLs and LBb1.3) was used to reveal the presence of T-DNA insertions (lanes 3 and 4). The locations of the primers are indicated in A. C) Relative expression level of the four *AtESLs* genes in the leaves of wild-type, and *esl1.02esl3.07*, and *esl3.03esl3.05* double mutant lines. The data of RT-qPCR were normalized using *AtPP2a* (*At1g13320*) as a reference gene. The RT-qPCR analysis was carried out using total RNA extracted from rosette leaves of Col-0 wild type and double homozygous mutants.

Generation of double *atesl* mutant lines

To enhance the chance to rapidly find double homozygous lines, the single homozygous mutants *esl1.02*, *esl3.03*, *esl3.05* and *esl3.07*, were crossed between them in all possible combinations. We realized twelve different combinations. In the F1 generation the genotype of all hybrid lines was checked by genomic DNA analysis for the presence of the T-DNA and the genes of interest. The T-DNA has been inserted in the seventeenth exon for *esl1.02*, in the fifth exon for *esl3.07*, in the fourteenth intron for *esl3.05*, and in the fourteenth exon for *esl3.03* (Ch.V- Fig. 1A). The PCR profiles revealed a large number of heterozygous double mutants was obtained (Ch.V- Table 1). Each of these lines was self-pollinated to obtain the F2 generation. The resulting F2 seeds were sown in soil and then PCR checked for the identification of double homozygous mutants.

The next step consisted in PCR genotyping of 208 F2 plants issued from self-pollination of F1 double heterozygous mutants. This resulted in identification of F2 double heterozygous mutants clustered in six groups: (i) Forty-six *esl3.05esl3.07*; (ii) Thirty-six *esl1.02esl3.05;* (iii) Forty-two *esl3.03esl3.07*; (iv) Twenty-three *esl1.02esl3.07;* (v) Twenty-seven *esl3.03esl3.05;* (vi) Thirty-four *esl1.02esl3.03.* No F2 double homozygous mutants were found in the first three groups (*esl3.05esl3.07, esl1.02esl3.05, and esl3.03esl3.07*), while some were identified in the other groups, i.e. two out of 23 in the fourth group of *esl1.02esl3.07*, one out of 27 in the fifth group *esl3.03esl3.05*, and two out of 34 in the sixth group of *esl1.02esl3.03*.

These double mutant genotypes were further confirmed by PCR analysis of genomic DNA, using two sets of primer pairs LP_RP (Forward primer and Reverse primer of *AtESL*s) and LP_LBb1.3 or RP_LBb1.3 (Forward primer or Reverse primer of *AtESLs* and T-DNA primer) (Ch.V- Fig. 1B). For the double homozygous *esl1.02esl3.07* mutant, the T-DNA insertion within *ESL3.07* and *ESL1.02* genes were detected as specific PCR products using LP*ESL3.07*_LBb1.3 and LP*ESL1.02*_LBb1.3 (Ch.V- Fig. 1B-a), lane 2 and 4). Alldough, no PCR products were detected using gene-specific primers (LP*ESL3.07*_RP*ESL3.07* and LP*ESL1.02*_ RP*ESL1.02*) due to the large-sized T-DNA (Figure 14B (a), lane 1 and 3). Products corresponding to the *ESL3.07* and *ESL1.02* genes, 1230-bp and 1082-bp PCR respectively, were amplified for the wild genotype (Ch.V- Fig. 1B-a) , lane 5 and 6). The lack of expression of *ESL3.07* and *ESL1.02* genes was verified by qPCR (Ch.V- Fig. 1C). Compared to the wild genotype Col-0, the expression level of *ESL3.07* and *ESL1.02* was

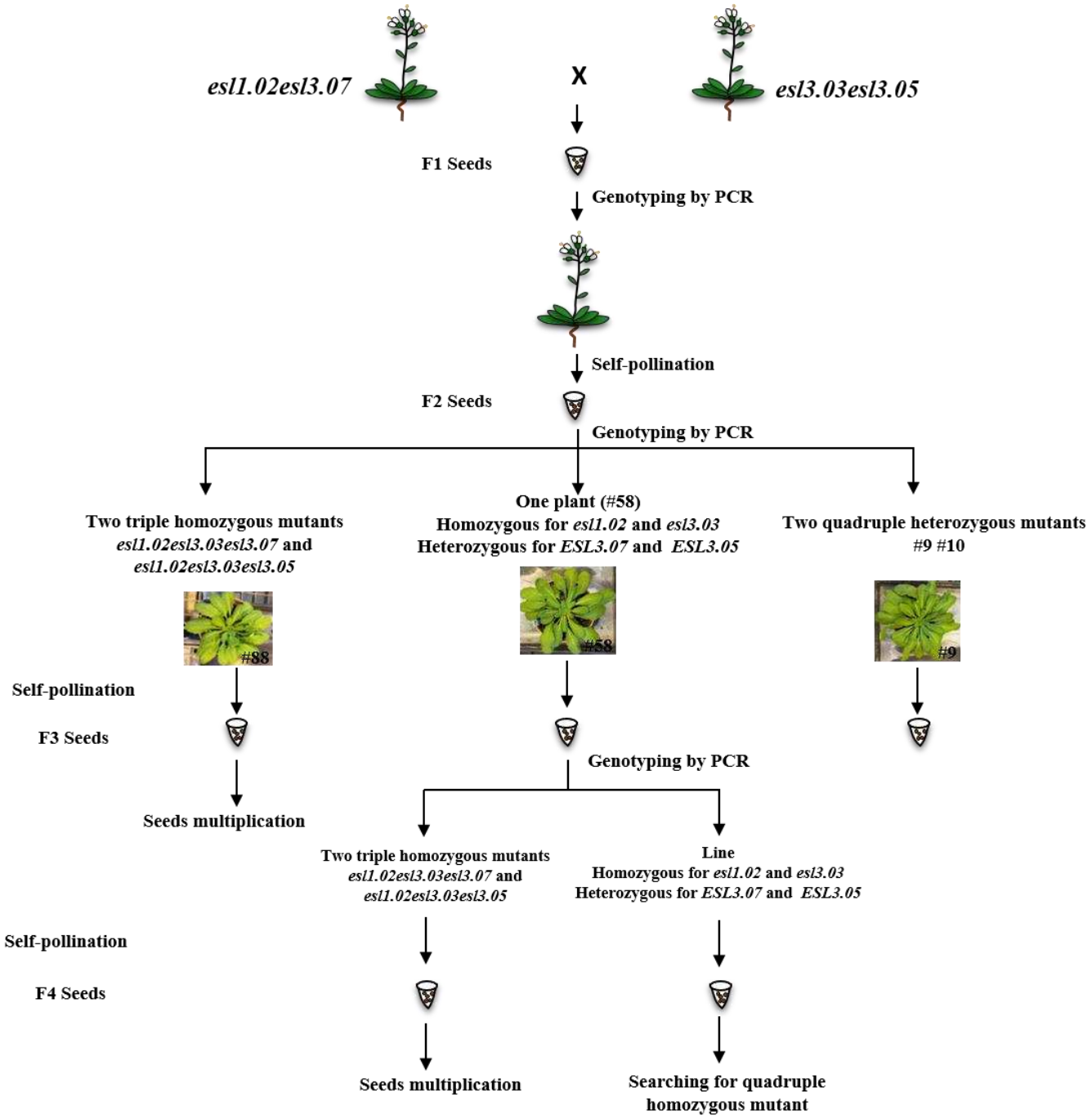

Ch.V- Fig. 2: Steps for the generation of double, triple and quadruple *esl* mutants

almost undetectable in the *esl1.02esl3.07* double mutant. Relative expression of *ESL3.07* gene in Col-0 was 1.4, while in the double mutant *esl1.02esl3.07* its level dropped down to 0.09, because *esl3.07* is a knockdown mutant. Moreover, the expression level of *ESL1.02* in Col-0 was 1.44, while in the double mutant it was undetectable as *esl1.02* is a knockout mutant (Ch.V- Fig. 1C).

For the *esl3.03esl3.05* double homozygous mutant line, PCR analysis on genomic DNA confirmed the presence of the T-DNA insertion within *ESL3.05* and *ESL3.03* genes. The presence of the T-DNA insertions was detected by specific PCR products using RP*ESL3.05*_LBb1.3 and LP*ESL3.03*_LBb1.3 primer pairs (Ch.V- Fig. 1B-b, lane 2 and 4); whereas no PCR products were amplified using the gene-specific primers (LP*ESL3.05*_ RP*ESL3.05* and LP*ESL3.03*_ RP*ESL3.03*), plausibly because of the large T-DNA size (Ch.V- Fig. 1B-b, lane 1 and 3). but 1159-bp and 1022-bp PCR products corresponding to the *ESL3.03* and *ESL3.05* genes, respectively, were amplified from wild genotype genomic DNA (Ch.V- Fig. 1B-b), lane 5 and 6). To confirm the absence of *ESL3.05* and *ESL3.03* expressions in the *esl3.03esl3.05* homozygous line, qPCR assays were performed. Compared to the wild genotype Col-0, the expression level of *ESL3.05* and *ESL3.03* was undetectable in the *esl3.03esl3.05* double mutant (Ch.V- Fig. 1C). In addition to these lines, a third double mutant was obtained, affected for both *ESL1.02* and *ESL3.03* (designated as *esl1.02esl3.03*). The homozygosity for *esl1.02esl3.03* was confirmed by the presence of the T-DNA insertions using LP*ESL1.02*_LBb1.3 and LP*ESL3.03*_LBb1.3 (Ch.V- Fig. 1B-c, lane 2 and 4), while no PCR amplicons were detected using gene-specific primers (LP*ESL1.02*_RP*ESL1.02* and LP*ESL3.03*_ RP*ESL3.03*) because of the T-DNA size (Ch.V- Fig. 1B-c, lane 1 and 3) but 1082-bp and 1159-bp PCR products corresponding to the *ESL1.02* and *ESL3.03* genes, respectively, were amplified from wild genotype genomic DNA (Ch.V- Fig. 1B-c, lane 5 and 6). Taken together, these results confirmed the homozygosity of *esl1.02esl3.07*, *esl3.03esl3.05*, and *esl1.02esl3.03* double mutants since only the T-DNA amplicons turned out amplified. It is worth to be noted that none of the obtained double homozygous mutants displayed any phenotypic difference compared to Col-0 grown under normal conditions.

Generation of triple *atesl* mutant lines

To further obtain triple and quadruple mutants the homozygous double mutant *esl1.02esl3.07* was crossed with the homozygous double mutant *esl3.03esl3.05* (Ch.V- Fig. 2). Seeds derived from the F1 generation were screened for the presence of T-DNA insertions

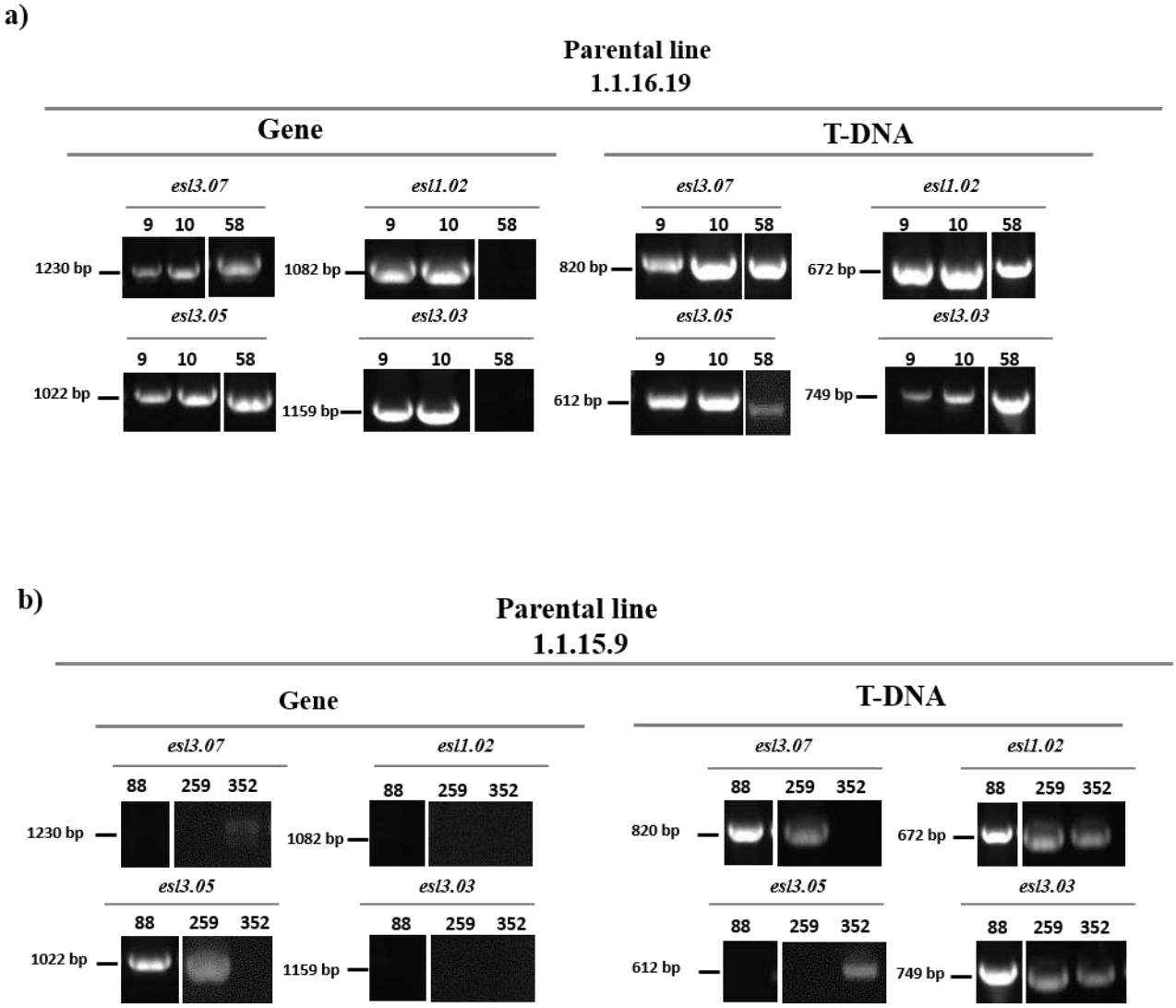

Ch.V- Fig. 3: PCR confirmation of multiple *atesls* mutants. a) Analysis of #9, #10, and #58 lines deriving from the parental line 1.1.16.19 (quadruple heterozygous mutant). PCR analysis on genomic DNA was carried out using the following primers: LPESLs and RPESLs were used to amplify the *AtESLs* genes, while T-DNA primer and gene-specific primer (LPESLs or RPESLs and LBb1.3) was used to reveal the presence of T-DNA insertions. The locations of the primers are given in Ch. V-Fig.1A. b) Analysis of #88, #259,#352 lines deriving from parental line 1.1.15.9 (quadruple heterozygous mutant). Triple homozygous lines #88 and #259 lacking *ESL1.02*, *ESL3.03*, and *ESL3.07* (designated as *esl1.02esl3.03esl3.07*). Triple homozygous lines #352 lacking *ESL1.02*, *ESL3.03*, and *ESL3.05* (designated as *esl1.02esl3.03esl3.05*). PCR analysis on genomic DNA was realized using the same primers as in Ch. V-Fig.1. The locations of the primers are given in Ch. V-Fig.1A.

and, respectively, the absence of wild-type transporter genes. Several quadruple heterozygous mutant lines were obtained. These plants were self-pollinated to obtain the F2 generation. The resulting F2 seeds were sown in soil and then genotyped by PCR (Ch.V- Fig. 2). Seventy-two F2 plants derived from the parental line #1.1.16.19 were screened for their homozygous or heterozygous states using PCR analysis of genomic DNA. Several quadruple heterozygous mutants were identified. In the two quadruple heterozygous lines #9 and #10, the T-DNA insertions were detected by specific PCR products using T-DNA and gene-specific primers (LP or RP_ LBb1.3), and the specific amplicons of four *ESLs* genes were obtained with gene-specific primers (LP_RP) (Ch.V- Fig. 3a). Line #58 which, has the genotype *esl1.02esl3.03*ESL3.05+/− ESL3.07+/− (i.e., homozygous for *esl1.02* and *esl3.03* and heterozygous for *ESL3.07* and *ESL3.05*) was identified by the presence of T-DNA insertions within the four *ESL* genes, and the absence of amplicons obtained with gene specific primers for *ESL1.02* and *ESL3.03* genes. PCR products were obtained with gene specific primers for *ESL3.07* and *ESL3.05* genes (Ch.V- Fig. 3a). These lines (#9, #10, and #58) were self-pollinated to obtain the F3 generation (Ch.V- Fig. 2).

After genotyping of more than 350 F2 #1.1.15.9 plants, two triple homozygous mutants, *esl1.02esl3.03esl3.07* and *esl1.02esl3.03esl3.05* were obtained (Ch.V- Fig. 2). The plant lines (#88 and #259) were homozygous for *esl1.02*, *esl3.03*, and *esl3.07* (designated as *esl1.02esl3.03esl3.07*) due to the presence of T-DNA insertions within these three genes, while no PCR products were amplified using gene-specific primers (Ch.V- Fig. 3b). The plant line (#352) was homozygous for *esl1.02*, *esl3.03*, and *esl3.05* (designated as *esl1.02esl3.03esl3.05*) due to the presence of T-DNA insertion within these three genes, while no amplification was obtained with gene-specific primers (Ch.V- Fig. 3b). The long systematic search for *esl1.02esl3.03esl3.05esl3.07* quadruple homozygous mutant allowed us to identify two triple homozygous mutants *esl1.02esl3.03esl3.07* and *esl1.02esl3.03esl3.05* (Ch.V- Fig. 2 and Ch.V- Table 2).

Germination of *atesl* mutant seeds in response to glucose, ABA, salt and cold

In the aim to study the impact of ABA and glucose, as well as that of salt and cold treatments on the seed germination of four *AtESL*, wild- and mutant genotypes, seed germination assays were performed. Seeds of Col-0 wild genotype and T-DNA insertion lines, four single mutants (*esl1.02*, *esl3.07*, *esl3.05* and *esl3.03)*, three double mutants

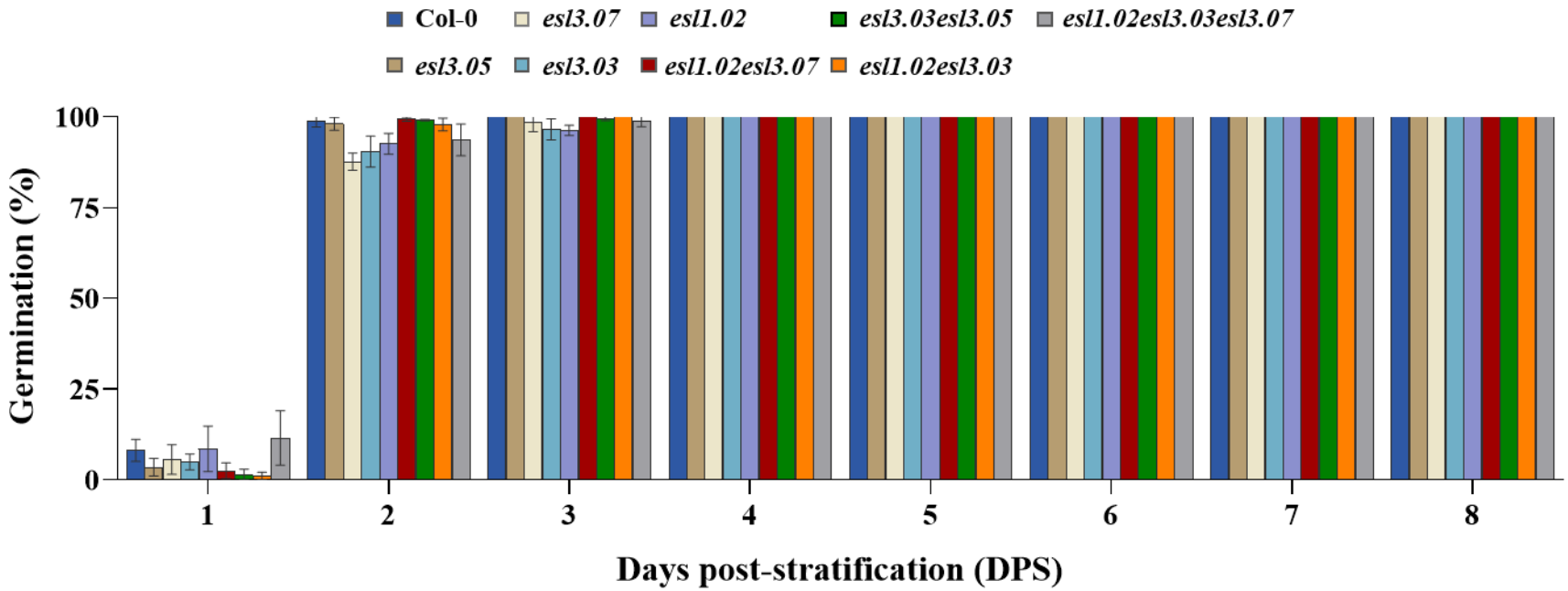

Ch.V- Fig. 4: Seed germination of Col-0, *esl3.05, esl3.07*, *esl3.03* and *esl1.02* single mutants, *esl1.02esl3.07*, *esl3.03esl3.05* and *esl1.02esl3.03* double mutants and *esl1.02esl3.03esl3.07* triple mutant on minimal MS medium without sugar (control condition). Data represent mean values ± SEM of three biological independent replicates. Each replicate contained 100 to 250 seeds per genotype.

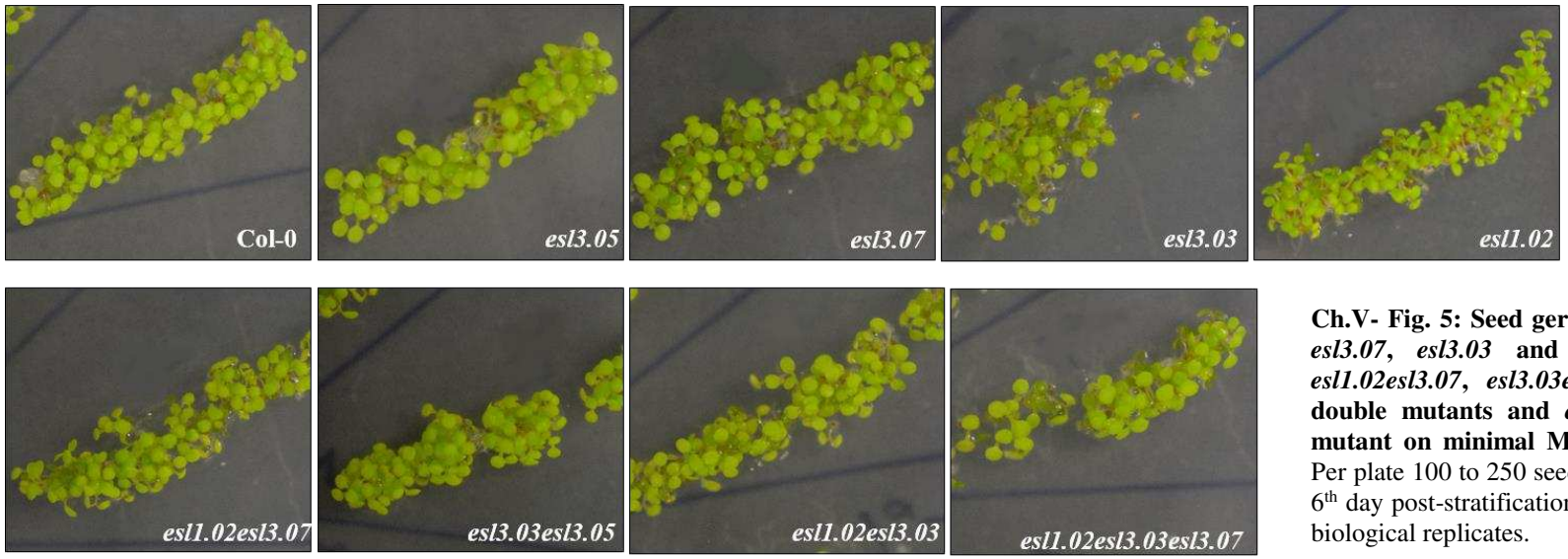

Ch.V- Fig. 5: Seed germination of Col-0, *esl3.05*, *esl3.07*, *esl3.03* and *esl1.02* single mutants, *esl1.02esl3.07*, *esl3.03esl3.05* and *esl1.02esl3.03* double mutants and *esl1.02esl3.03esl3.07* triple mutant on minimal MS medium without sugar. Per plate 100 to 250 seeds sown. Photos taken at the 6th day post-stratification and representative of three biological replicates.

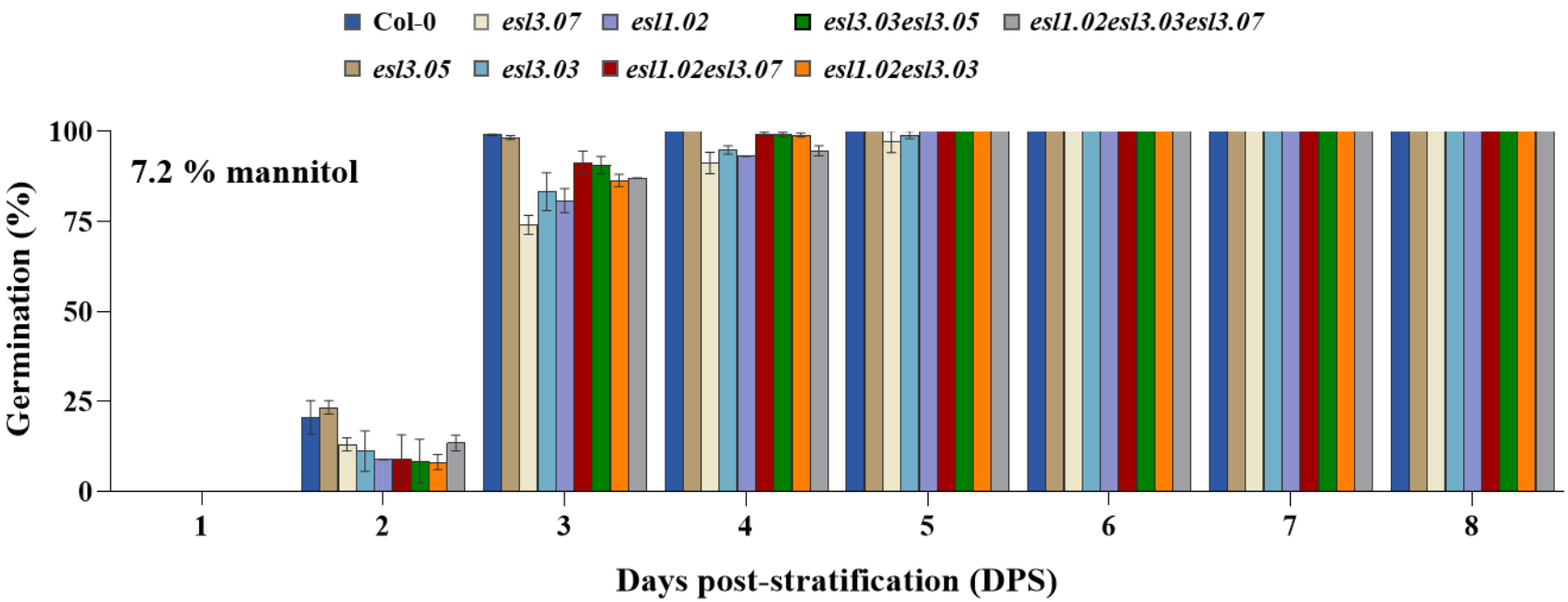

Ch.V- Fig. 6: Seed germination of Col-0, *esl3.05, esl3.07*, *esl3.03* and *esl1.02* single mutants, *esl1.02esl3.07 esl3.03esl3.05* and *esl1.02esl3.03* double mutants and *esl1.02esl3.03esl3.07* triple mutant on minimal MS medium supplemented with 7.2% of mannitol (osmotic control). Data represent mean values ± SEM of three biological replicates. Each replicate contained 100 to 250 seeds per genotype.

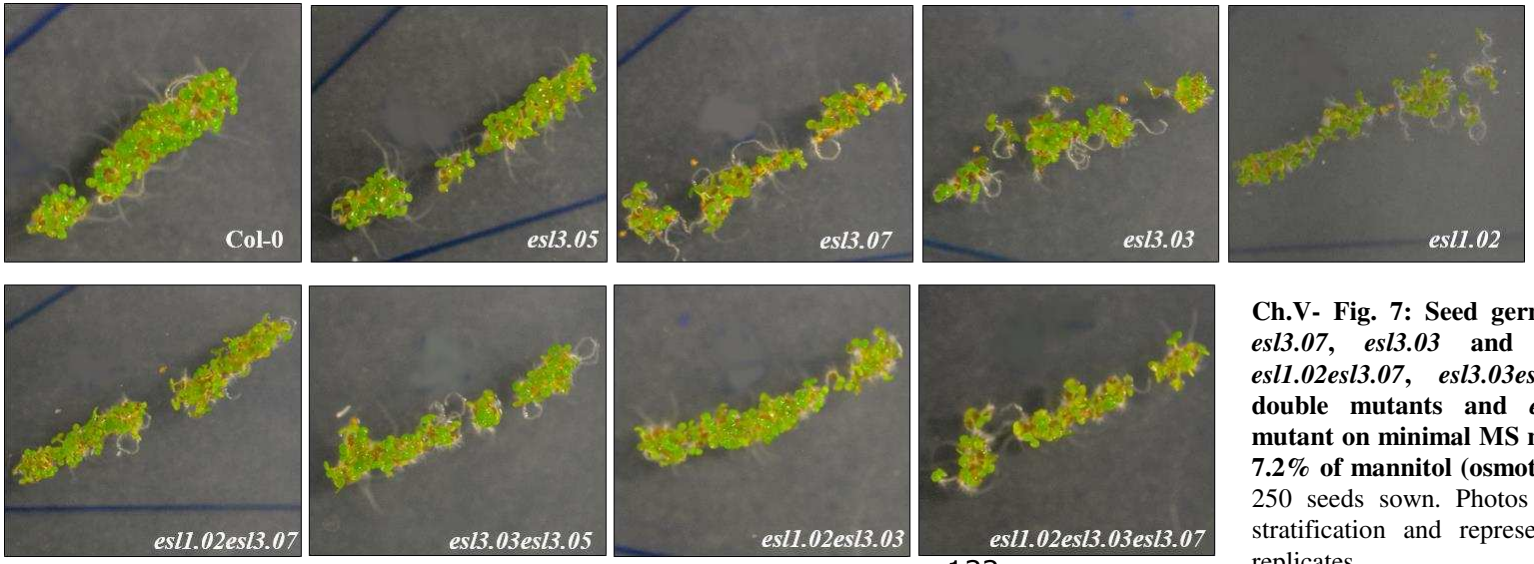

Ch.V- Fig. 7: Seed germination of Col-0, *esl3.05*, *esl3.07*, *esl3.03* and *esl1.02* single mutants, *esl1.02esl3.07*, *esl3.03esl3.05* and e*sl1.02esl3.03* double mutants and *esl1.02esl3.03esl3.07* triple mutant on minimal MS medium supplemented with 7.2% of mannitol (osmotic control). Per plate 100 to 250 seeds sown. Photos taken at the 6th day post-stratification and representative of three biological replicates.

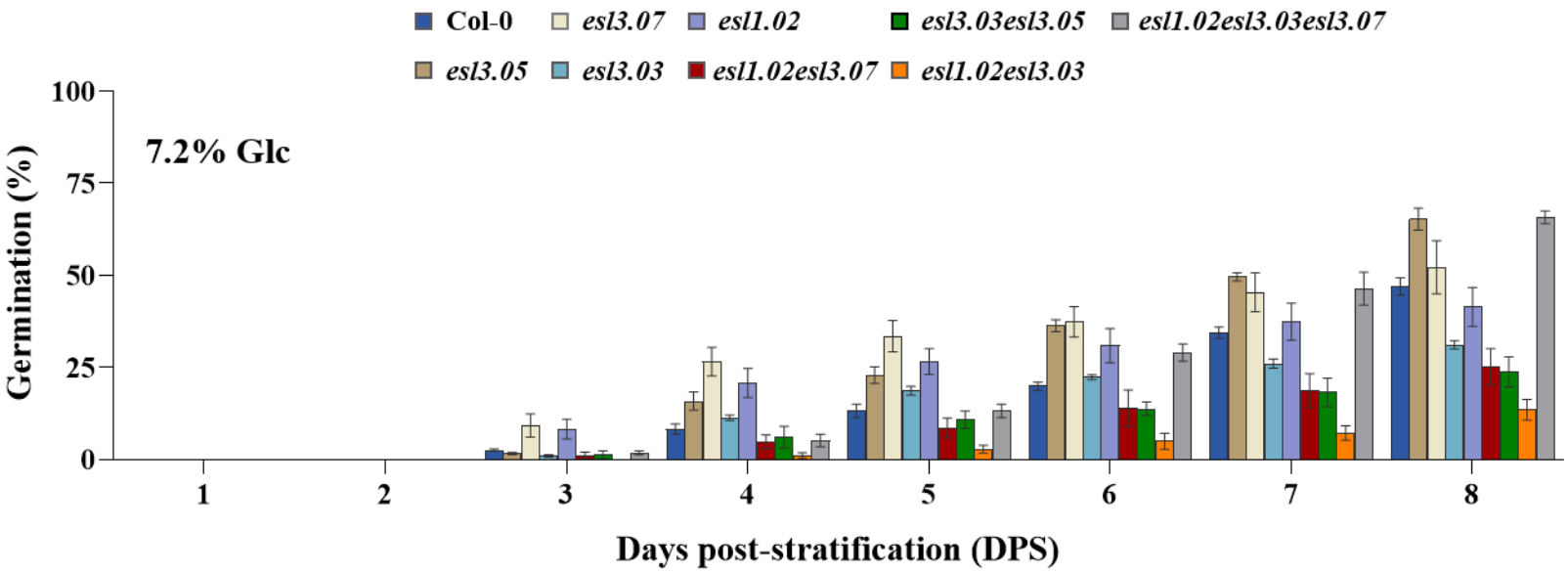

Ch.V- Fig. 8: Seed germination of Col-0, *esl3.05, esl3.07*, *esl3.03* and *esl1.02* single mutants, *esl1.02esl3.07*, *esl3.03esl3.05* and *esl1.02esl3.03* double mutants and *esl1.02esl3.03esl3.07* triple mutant on minimal MS medium supplemented with 7.2% of glucose. Data represent mean values ± SEM of three biological replicates. Each replicate contained 100 to 250 seeds per genotype.

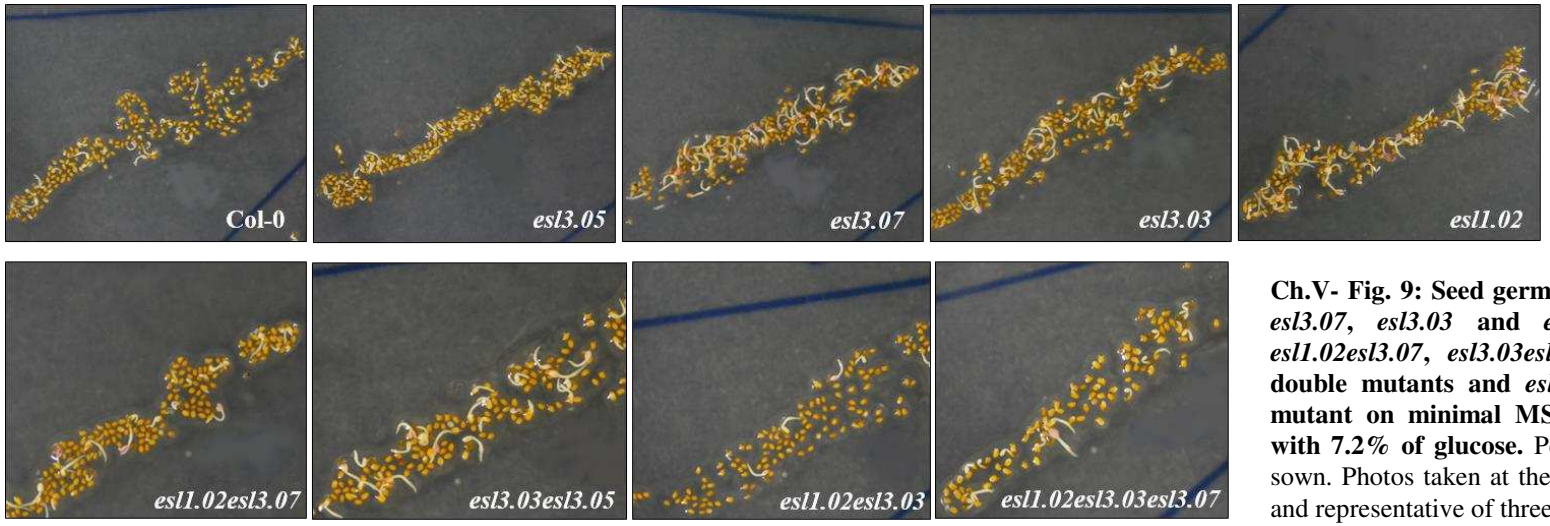

Ch.V- Fig. 9: Seed germination of Col-0, *esl3.05*, *esl3.07*, *esl3.03* and *esl1.02* single mutants, *esl1.02esl3.07*, *esl3.03esl3.05* and e*sl1.02esl3.03* double mutants and *esl1.02esl3.03esl3.07* triple mutant on minimal MS medium supplemented with 7.2% of glucose. Per plate 100 to 250 seeds sown. Photos taken at the 6th day post-stratification and representative of three biological replicates.

(*esl1.02esl3.07, esl3.03esl3.05*, *esl1.02esl3.03*), and the triple mutant *esl1.02esl3.03esl3.07*, were surface-sterilized and germination was conducted on minimal MS medium (macro- and micro-elements without sugar) or minimal MS supplemented with 7.2% glucose (Glc), or 7.2% mannitol (used as osmotic control), or 3 µM ABA, or 200 mM NaCl. Overall, seeds of nine lines (wild-type and eight mutants) were plated on five different culture media. The triple mutant *esl1.02esl3.03esl3.05* was not presented, because there were not enough seeds for the three biological replicates studied.

Dormant seeds are characterized by the inability to germinate, even under favorable conditions for germination, but dormancy can be broken by cold treatment under high relative humidity, known as stratification (Finch-Savage and Leubner-Metzger, 2006). Under conditions of *in vitro* culture, stratification is often used to promote and synchronize the germination of seeds (Yamauchi et al., 2004). To allow germination after 24h stratification of plated seeds at 4°C, in the dark, plates were transferred to continuous light at 22°C, except of those submitted to cold stress at 4°C. Seed germination at 22°C was monitored daily and for 8 days, except that under cold treatment, which was recorded for 10 days.

On MS minimal medium (control condition), no difference was observed in seed germination among all seeds tested. All nine genotypes started to germinate after one day under continuous light and reached nearly 100% germination at the 3th day post-stratification (DPS) (Ch.V- Fig. 4 and 5). These results demonstrated the high viability of seeds and allowed the comparative analysis of their sensibility/resistance to the applied treatments.

To study the effect of glucose signaling on seed germination, the seeds of nine genotypes were plated on MS minimal medium supplemented with 7.2% Glc and, in parallel, on minimal MS with 7.2% mannitol as osmotic control. Compared to the control condition, the beginning of seed germination of all genotypes in the presence of 7.2% mannitol was slightly delayed to the 2d DPS. The delay caused by 7.2% mannitol was probably due to its initial osmotic effect, but at the 3th DPS this osmotic effect was overcome since all genotypes manifested 80-100% germination, and their germination efficiency reached 100% at the 5th DPS (Ch.V- Fig. 6 and 7).

When plated at high Glc concentration (7.2%), all tested genotypes exhibited delayed germination, which started at the 3th DPS (Ch.V- Fig. 8) At the 5th DPS, seeds of *esl3.05*, *esl3.07*, and *esl1.02* single mutants demonstrated higher efficiency than that of Col-0 seeds. The reference genotype (Col-0) had 13% germination, while *esl3.05*, *esl3.07*, and *esl1.02* single mutants had 22 %, 33 % and 26 % respectively. Conversely, *esl1.02esl3.03* double mutant seeds exhibited lower germination (2%) than that of the Col-0 (13%). At the same

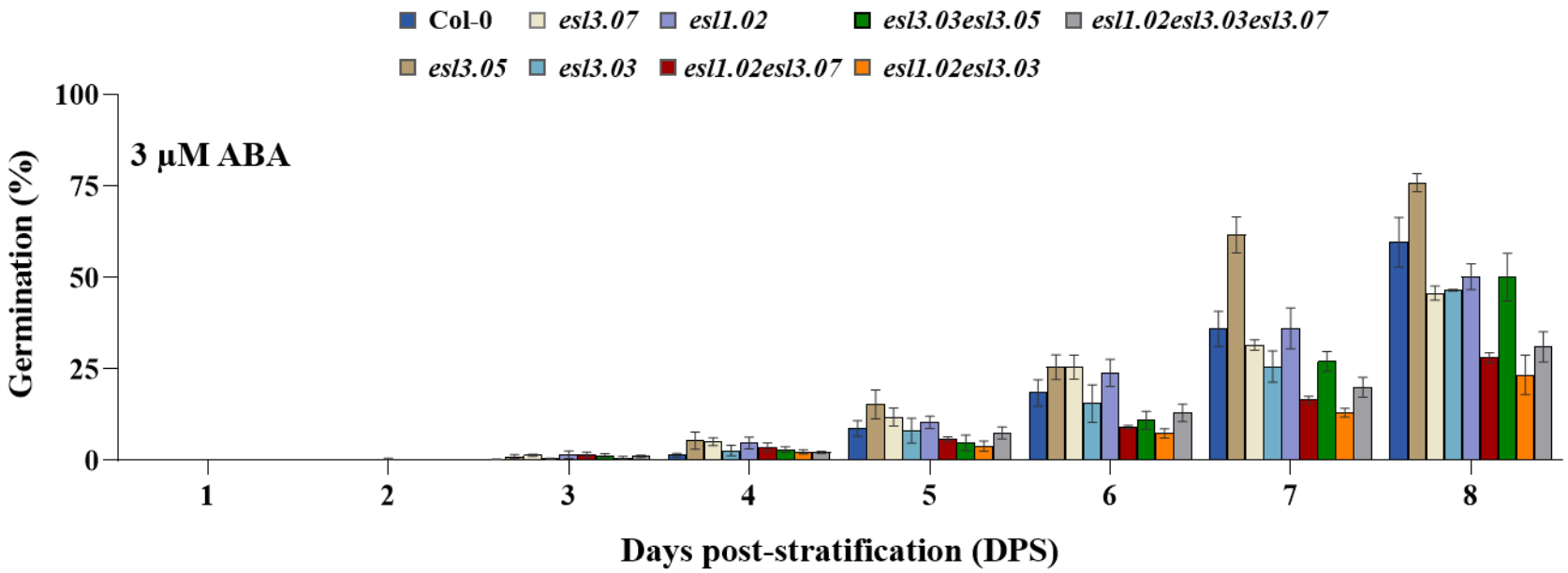

Ch.V- Fig. 11: Seed germination of Col-0, *esl3.05, esl3.07*, *esl3.03* and *esl1.02* single mutants, *esl1.02esl3.07, esl3.03esl3.05* and *esl1.02esl3.03* double mutants and *esl1.02esl3.03esl3.07* triple mutant on minimal MS medium supplemented with 3 µM ABA. Data represent mean values ± SEM of three biological replicates. Each replicate contained 100 to 250 seeds per genotype.

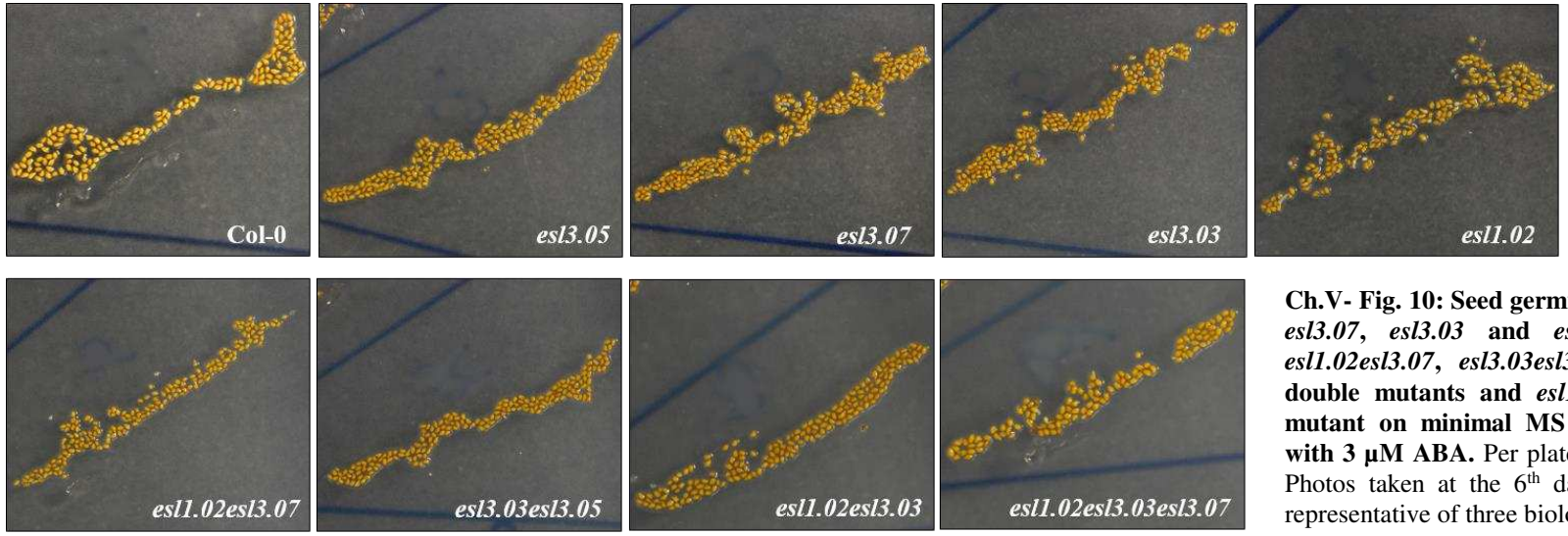

Ch.V- Fig. 10: Seed germination of Col-0, *esl3.05*, *esl3.07*, *esl3.03* and *esl1.02* single mutants, *esl1.02esl3.07*, *esl3.03esl3.05* and e*sl1.02esl3.03* double mutants and *esl1.02esl3.03esl3.07* triple mutant on minimal MS medium supplemented with 3 µM ABA. Per plate 100 to 250 seeds sown. Photos taken at the 6th day post-stratification and representative of three biological replicates

DPS, *esl3.03*, *esl1.02esl3.07*, *esl3.03esl3.05*, and *esl1.02esl3.03esl3.07*, did not display any significant difference in their germination rate compared to Col-0(Ch.V- Fig. 8). From 6th to 8th DPS, the germination efficiency of *esl3.05* single and *esl1.02esl3.03esl3.07* triple mutants remained significantly higher than that of Col-0, while this effect was abolished for *esl3.07* and *esl1.02* single mutants. At the same time point, germination of *esl1.02esl3.07* and *esl3.03esl3.05* double mutants remained lower compared to that of Col-0. The double mutant *esl1.02esl3.03* exhibited the most reduced germination efficiency, and this for all the duration of the experimental period. The latter displayed only 13% of germinated seeds at day 8th *versus* 47% for Col-0 (Ch.V- Fig. 8 and 9). Our results clearly demonstrated that the delay of germination caused by 7.2% glucose may be not attributed to osmotic effect, when compared to germination efficiency on 7.2% mannitol. Taken together, the data obtained for glucose effect on germination and those of absolute control, the minimal MS medium, and the manniol supplemented one as osmotic control, clearly demonstrated the differential responses of *atesl* mutants to glucose signaling.

The endogenous hormonal balance between ABA and GAs, both acting antagonistically, regulates seed germination process. In other terms, the optimal ABA/GAs balance triggers germination without respect to how high or low are their absolute concentrations (Finkelstein et al., 2008). In this regard, the addition of exogenous ABA can block or delay seed germination (Weitbrecht et al., 2011). An exogenous supply of 3 µM ABA to medium can suppress germination of *Arabidopsis* seeds (Finkelstein et al., 2002). After one DPS on the control medium the germination of all genotypes tested reached approximately 80-100% (Ch.V- Fig. 4). By contrast, in the presence of 3 µM ABA, the germination of all genotypes was significantly delayed. At a glance, the visual comparison of effects of 3 µM ABA and 7.2% glucose demonstrated that ABA at low concentration was more restrictive for seed germination than glucose at high concentration. Germination of all nine genotypes on 3 µM ABA reached nearly 10 % at the 5th DPS, while the same efficiency was overcome at the 4th DPS at 7.2% glucose. The three single mutants *esl3.07*, *esl1.02*, and *esl3.03* did not display any difference of germination when compared to Col-0 throughout the experiment. Only the single mutant *esl3.05* displayed a slightly higher germination efficiency (25%) compared to that of Col-0 (18%) at the 6th DPS, which reached 61% for *esl3.05* single mutant versus 35% for Col-0 seeds at the 7th DPS, but the difference between both genotypes decreased at day 8th (Ch.V- Fig. 10 and 11). The double mutant *esl3.03esl3.05* did not show any increased ABA sensitivity compared to the wild genotype. Conversely, the double mutants *esl1.02esl3.07*, *esl3.03esl3.05*, and *esl1.02esl3.03* exhibited a lower germination (9%,

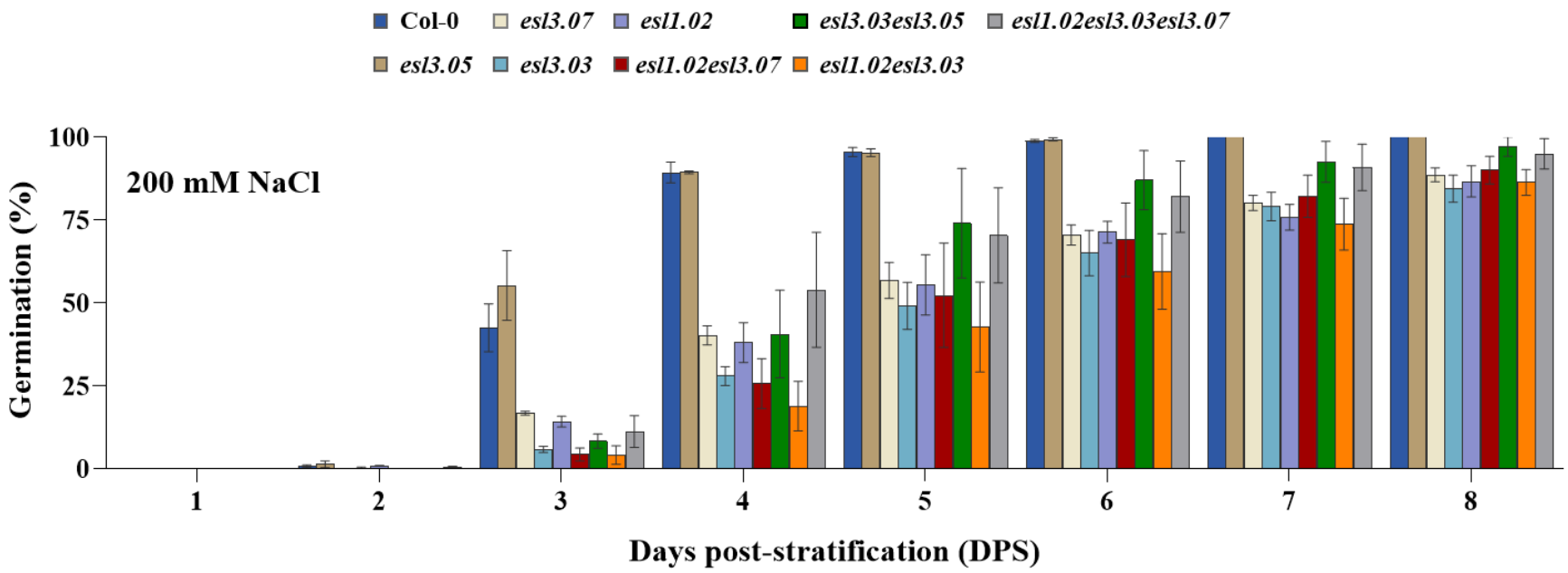

Ch.V- Fig. 12: Seed germination of Col-0, *esl3.05, esl3.07*, *esl3.03* and *esl1.02* single mutants, *esl1.02esl3.07*, *esl3.03esl3.05* and *esl1.02esl3.03* double mutants and *esl1.02esl3.03esl3.07* triple mutant on minimal MS medium supplemented with 200 mM NaCl. Data represent mean values ± SEM of three biological replicates. Each replicate contained 100 to 250 seeds per genotype.

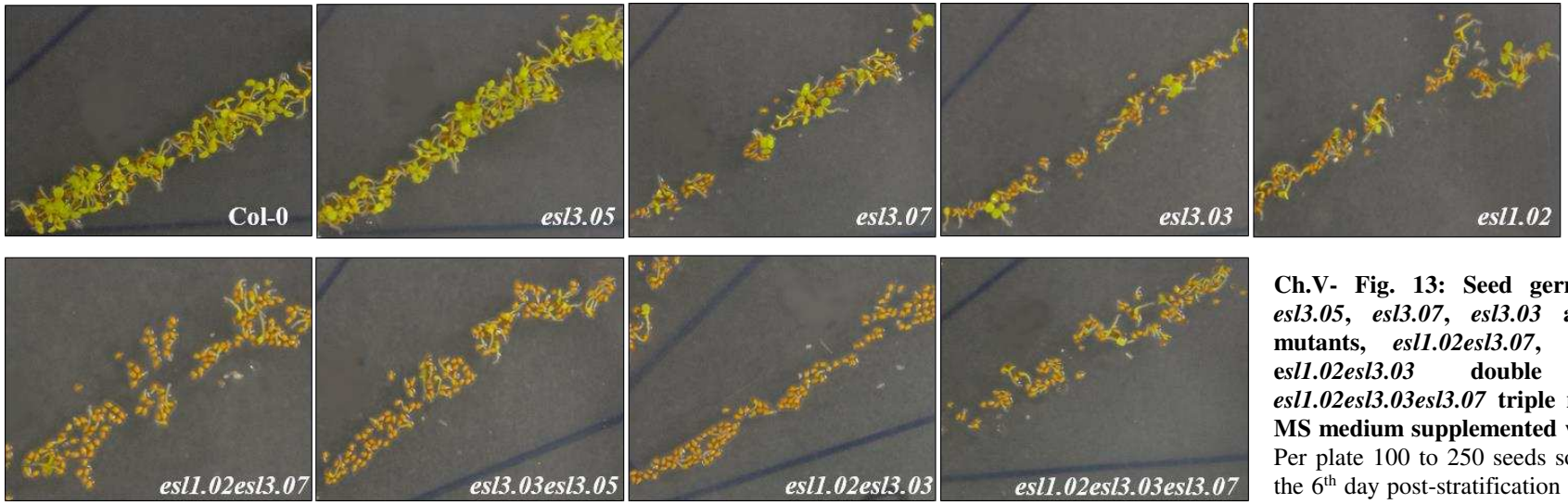

Ch.V- Fig. 13: Seed germination of Col-0, *esl3.05*, *esl3.07*, *esl3.03* and *esl1.02* single mutants, *esl1.02esl3.07*, *esl3.03esl3.05* and *esl1.02esl3.03* double mutants and *esl1.02esl3.03esl3.07* triple mutant on minimal MS medium supplemented with 200 mM NaCl. Per plate 100 to 250 seeds sown. Photos taken at the 6th day post-stratification and representative of three biological replicates.

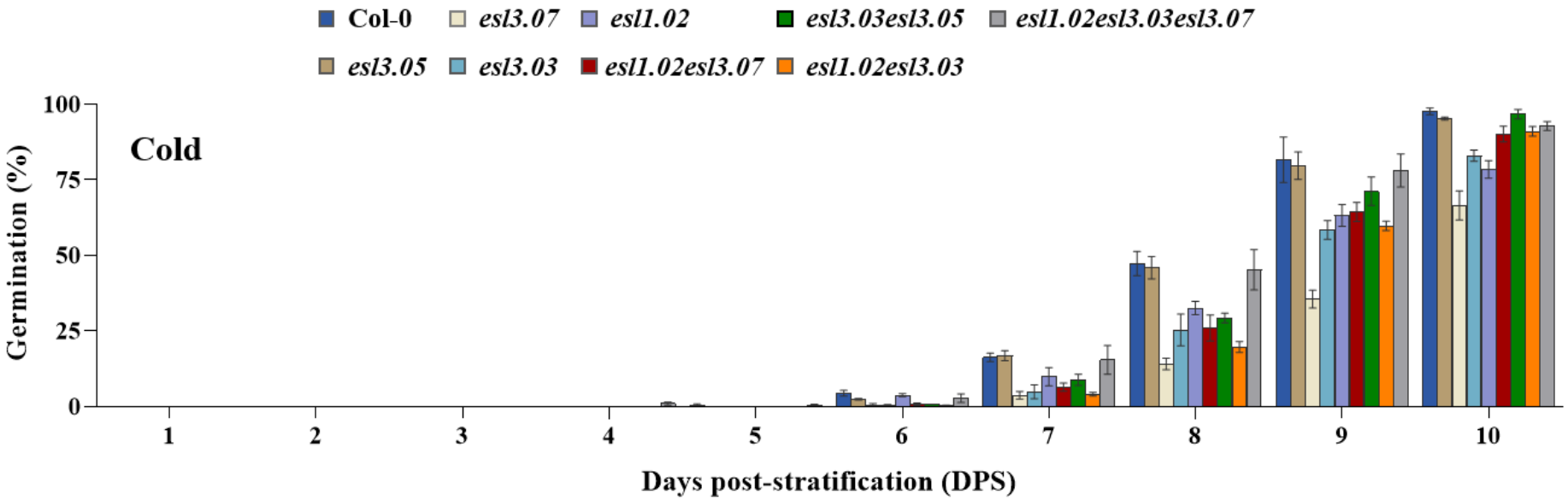

Ch.V- Fig. 14: Seed germination of Col-0, *esl3.05, esl3.07*, *esl3.03* and *esl1.02* single mutants, *esl1.02esl3.07*, *esl3.03esl3.05* and *esl1.02esl3.03* double mutants and *esl1.02esl3.03esl3.07* triple mutant on minimal MS medium without sugar. Plates subjected to cold treatment 4°C. Data represent mean values ± SEM of three biological replicates. Each replicate contained 100 to 250 seeds per genotype.

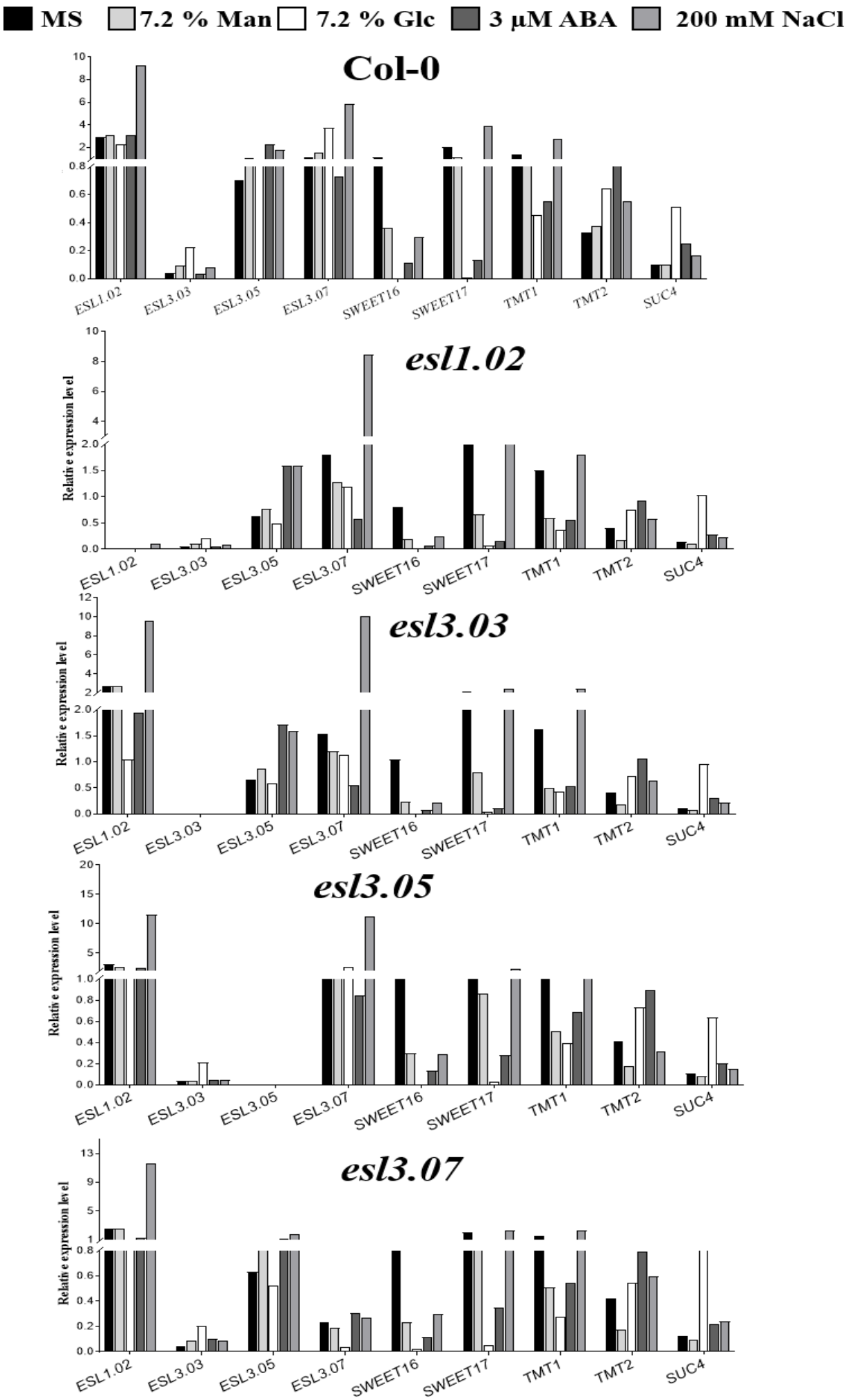
MS
7.2 % Man
7.2 % Glc
3 µM ABA
200 mM NaCl
Col-0
esl1.02
esl3.03
esl3.05
esl3.07
Relative expression level
ESL1.02
ESL3.03
ESL3.05
ESL3.07
SWEET16
SWEET17
TMT1
TMT2
SUC4

10%, and 7%, respectively) compared to Col-0 (18%), at the 6th DPS (Ch.V- Fig. 10 and 11). Their ABA sensitivity was further sustained at the 7th DPS (16% and 13% respectively *vs.* 35% for Col-0) and at the 8th DPS (28 % and 23% respectively *vs.* 59% for Col-0. Interestengly, the germination of triple *esl1.02esl3.03esl3.07* mutant did not show any significant difference in comparison with Col-0 (Ch.V- Fig. 10).

High salinity (200 mM NaCl) delayed and inhibited seed germination. At the 2th DPS, all tested genotypes displayed very low germination efficiency, less than 3% (Ch.V- Fig. 12). Since the 3th DPS, the response of *esl3.05* single mutant to salt stress was undistinguishable from that of Col-0. The double *esl3.03esl3.05* and the triple *esl1.02esl3.03esl3.07* mutants showed low germination rates at the 3th and the 4th DPS, before to subsequently restore their efficiency. Three single mutants (*esl3.07*, *esl1.02*, and *esl3.03)*, and two double mutants (*esl1.02esl3.03* and *esl1.02esl3.07*) demonstrated the most important and sustained reduction of germination, when compared with Col-0. Their efficiency of germination remained at least three-fold to two-fold lower than that of the wild type from the 3th to the 5th DPS, before to increased progressively up to 8th DPS (Ch.V- Fig. 12 and 13). For example, at the 4th DPS, the single mutant, *esl3.07* seeds exhibited 40% of germinated seeds *vs.* 89% for Col-0. On the same DPS, the double mutant *esl1.02esl3.03* showed a dramatic inhibition with only 18% of germinated seeds *vs.* 89% for Col-0 (Ch.V- Fig. 12).

Cold treatment, even under continuous light, severely delayed germination of all tested genotypes (Ch.V- Fig. 14).The onset of germination was observed only at the 6th DPS. Throughout the experiment, *esl3.05* single mutant and *esl1.02esl3.03esl3.07* triple mutant displayed the same germination response to cold as the WT. At 7th DPS, single mutants (*esl3.07*, *esl1.02*, *esl3.03*) and double mutants (*esl1.02esl3.07*, *esl3.03esl3.05*, and *esl1.02esl3.03*) had lower germination rates than those of Col-0. The strongest negative impact of cold stress on germination was observed for *esl3.07* single mutant at the 8th and 9th DPS (14% *vs.* 50%, and 35% *vs.* 85% for Col-0). At the 10th DPS, the delay was nearly abolished for *esl1.02* and *esl3.03* single and *esl1.02esl3.07*, *esl3.03esl3.05*, and *esl1.02esl3.03* double mutants. At the same time point, the germination of the *esl3.07* single mutant was reduced in comparison to that of Col-0 (Ch.V- Fig. 14).

Expression profiling of vacuolar sugars transporter and invertase genes in wild- and *esl*-mutant genotypes in response to glucose and ABA signaling, osmotic and salt stresses.

In order to highlight *ESL* gene expression under different germination conditions, we performed real time-PCR analysis on 16-day-old seedlings of the nine studied genotypes

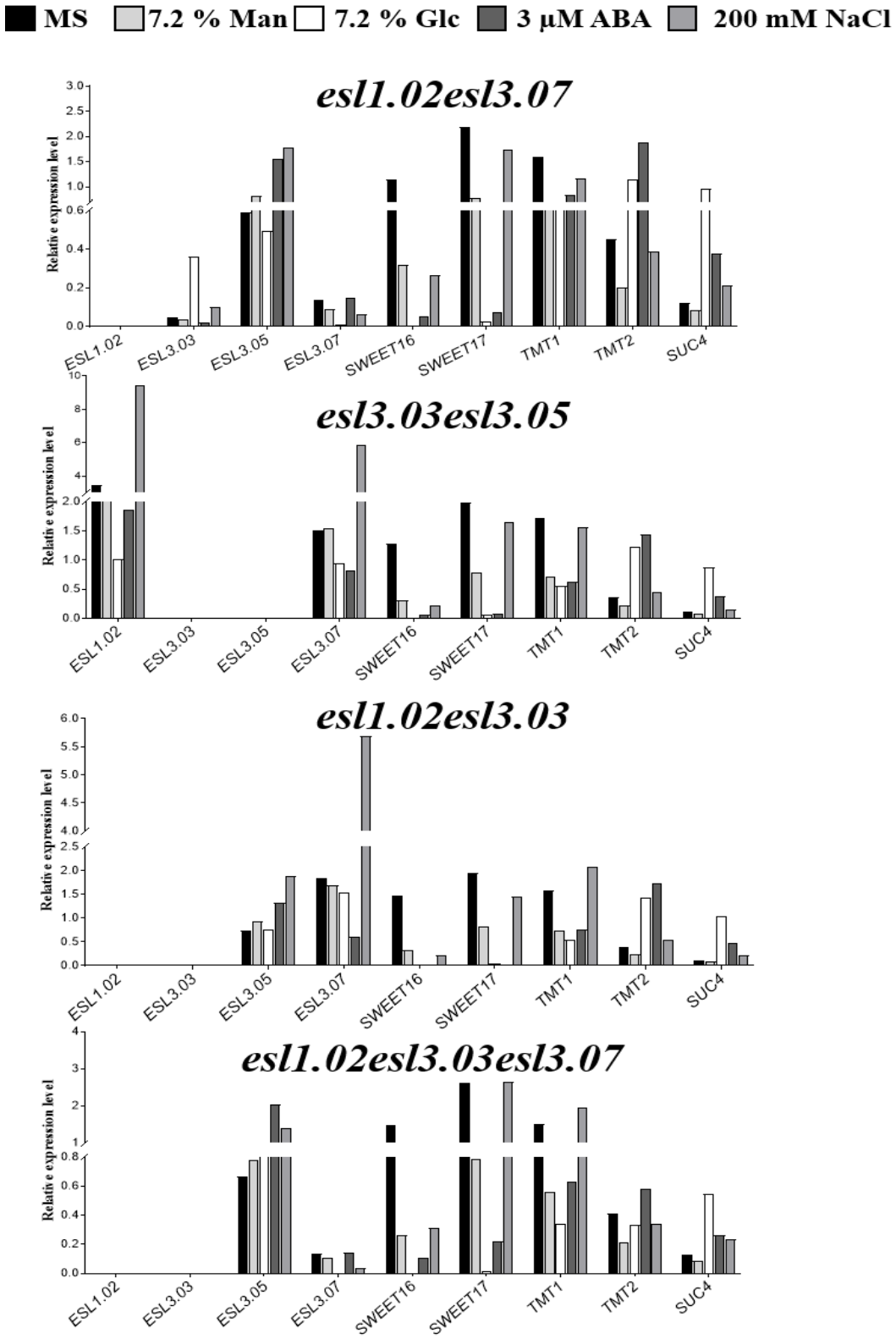

Ch.V- Fig. 15: Gene expression analysis of tonoplast sugar transporters in *Arabidopsis* (*ESL1.02, ESL3.03 ESL3.05, ESL3.07, SWEET16, SWEET17, TMT1, TMT2, SUC4*) in the reference genotype (Col-0) and the single mutants *esl1.02*, *esl3.03*, *esl3.05* and *esl3.07*, double mutants *esl1.02esl3.07*, *esl3.03esl3.05* and *esl1.02esl3.03*, and the triple mutant *esl1.02esl3.03esl3.07.* The wild-type and the *esl* mutant seeds were grown on MS medium supplemented either with 7.2 % mannitol, or 7.2% glucose, or 3 µM ABA, or 200 mM NaCl. Seedlings were collected at the 16th day post stratification. The data of qPCR were normalized using *AtPP2a* (*At1g13320*) as a reference gene. Data represent the mean of two biological replicates for all conditions except for 3 µM ABA (one biological replicate). For Col-0 under 200 mM NaCl treatment, the values represent one biological replicate. Man: Mannitol. Glc: Glucose

(Col-0, *esl3.05, esl3.07*, *esl1.02* and *esl3.03* single mutants, *esl1.02esl3.07*, *esl3.03esl3.05* and *esl1.02esl3.03* double mutants, and *esl1.02esl3.03esl3.07* triple mutant). To allow a global overview of vacuolar sugar transporters and their related invertase genes, our study also encompassed *TMT1*, *TMT*2, *SWEET16*, *SWEET17*, *SUC4*, *Atβfruct3* and *Atβfruct4* genes. The wild genotype Col-0 and the minimal MS medium were used as references. It is worth to note, that the presented results of expression analysis are issued from two independent experiments and performed in parallel in the nine studied genotypes, which may be consider as biological replicates.

In comparison to germination medium of reference, the addition of 7.2% mannitol did not change the expression profiles of the four *ESL* genes in all studied genotypes (Ch.V- Fig. 15). Conversely, the expression level of both *AtSEWEET*s was differentially inhibited by mannitol in all genotypes, with a stronger reduction for *AtSEWEET16* than that of *AtSEWEET17*. Concerning *TMT1* and *TMT2,* these genes did not respond to mannitol in seedlings of the reference genotype, but their expression decreased in all *esl* mutant genotypes. The sucrose transporter*, SUC4,* did not show any change in response to mannitol, as control of the osmotic pressure effect (Ch.V- Fig. 15). The high glucose concentration did not affect expression of *ESL3.05*, and *ESL3.07* genes in all tested genotypes. *ESL1.02* gene was down-regulated in *esl3.03* single mutant and *esl3.03esl3.05* double mutant (Ch.V- Fig. 15). Despite the very low expression of *ESL3.03* on all studied media, this gene appeared up-regulated by glucose in Col-0, *esl1.02*, *esl3.05*, and *esl3.07* single mutants, as well as in the *esl1.02esl3.07* double mutant. Conversely, glucose strongly down-regulated *AtSWEET16* and *AtSWEET17* expression in the reference and all *esl* mutant genotypes. As above mentioned for mannitol, the expression of *TMT1* and *TMT2* was differentially regulated by glucose, and only *TMT*2 was induced in the presence of 7.5% glucose in all studied genotypes. Interestingly, the sucrose carrier, *SUC4*, showed a clear-cut up-regulation by glucose in all nine genotypes (Ch.V- Fig. 15).

ESL1.02, *ESL3.03*, *ESL3.05*, and *ESL3.07* were differently responsive to exogenous ABA (Ch. V-Fig.15). While *ESL1.02*, *ESL3.03*, and *ESL3.07* transcript levels remained constant under ABA treatment for all genotypes that of *ESL3.05* slightly increased in *esl1.02* and *esl3.03* single mutants, *esl3.07esl1.02* double mutant, and the triple mutant. *AtSEWEETs* manifested a high responsiveness to exogenous ABA in the wild and mutant genetic backgrounds, and their down-regulation ressembles that caused by glucose. Once again *TMTs* genes were differentially regulated by ABA, and the expression of *TMT1* was decreased, while

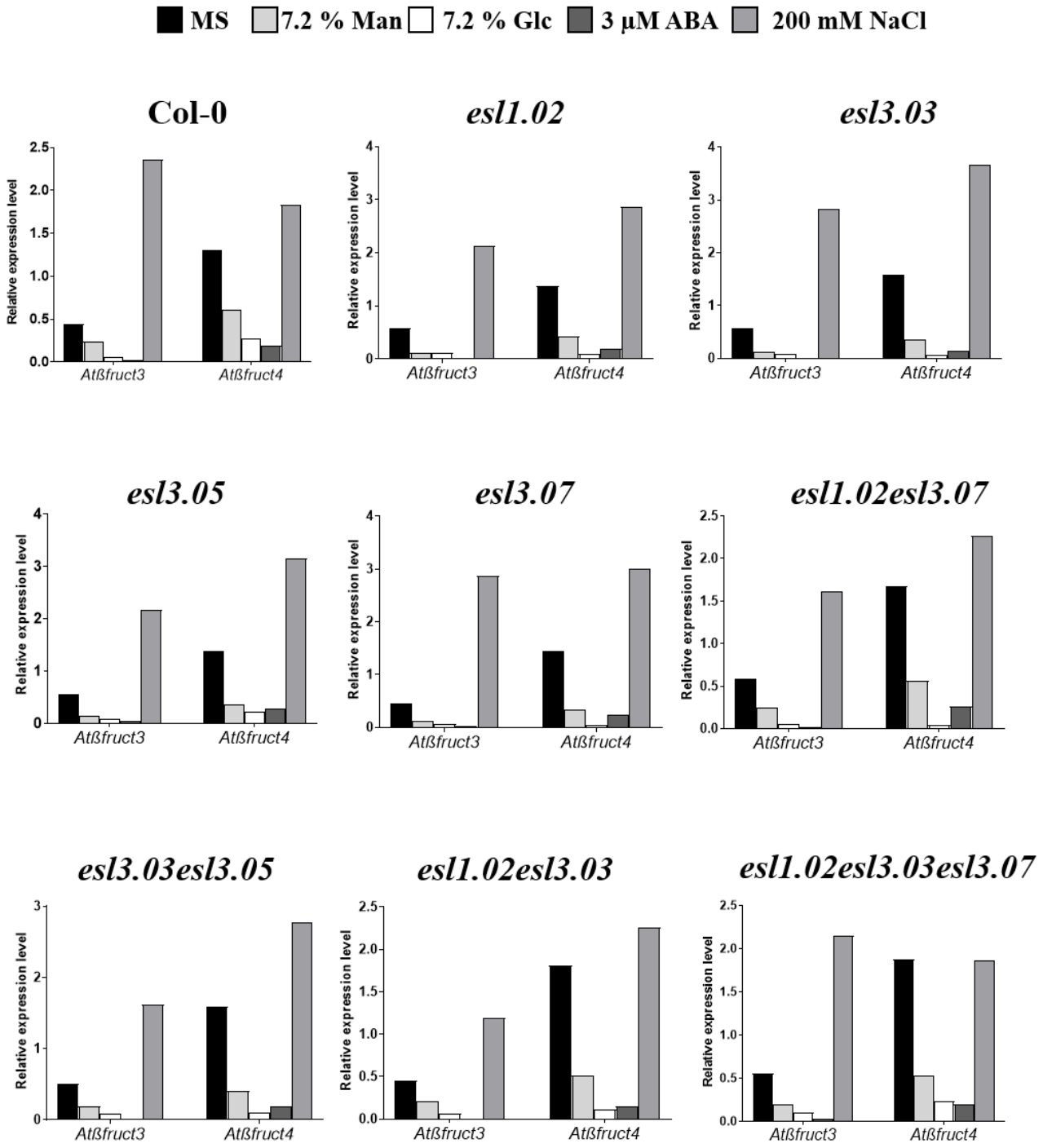

Ch.V- Fig. 16: Expression analysis of vacuolar invertase genes in *Arabidopsis* (*Atβfruct3* and *Atβfruct4*) in the reference genotype (Col-0) and the single mutants *esl1.02*, *esl3.03*, *esl3.05* and *esl3.07*, double mutants *esl1.02esl3.07*, *esl3.03esl3.05* and *esl1.02esl3.03*, and the triple mutant *esl1.02esl3.03esl3.07.* The wild-type and the *esl* mutant seeds were grown on MS medium supplemented either with 7.2 % mannitol, 7.2% glucose, 3 µM ABA or 200 mM NaCl. Seedlings were collected at the 16th day post-stratification. The data of qPCR were normalized using *AtPP2a* (*At1g13320*) as a reference gene. Data represent the mean of two biological replicates for all conditions except for 3 µM ABA (one biological replicate). For Col-0 under 200 mM NaCl treatment, the values represent one biological replicate. Man: Mannitol. Glc: Glucose

TMT2 expression was increased in all genotypes. Inversely, *SUC4* did not respond to exogenous ABA in all studied genotypes (Ch.V- Fig. 15).

Gene expression profiling under high NaCl concentration clearly revealed that the four *ESL* genes involved in the plant response to water deficit were also up-regulated by the salt stress during seed germination and early seedlings development (Ch.V- Fig. 15). It is worth to note that each of these four *ESLs* was up-regulated in the wild type and all mutant genotypes except those encompassing its proper knock-down or knockout form. Consequently, *ESL1.02* and *ESL3.07* genes displayed expression elevation in the reference genotype, as well as in the *esl3.05* single, and *esl3.03esl3.05* double mutants. The expression of *ESL1.02* and *ESL3.05* was increased in the *esl3.07* mutant, and *ESL3.05* and *ESL3.07* were up-regulated in the *esl1.02* single and *esl1.02esl3.03* double mutants. The expression of *ESL1.02*, *ESL3.03*, and *ESL3.07* was elevated in the *esl3.03* mutant, and *ESL3.05* was up-regulated in the *esl1.02esl3.07* double mutant and in the *esl1.02esl3.03esl3.07* triple mutant. As presented on Ch.V- Fig. 15, *ESL3.03* showed a very low expression under control conditions, and its level remained constantly low under salt treatment. The expression of *AtSEWEET16* was decreased in response to high NaCl concentration, while no notable changes were observed for *AtSWEET17*. Interestingly, in our experimental conditions *TMT1*, *TMT2* and *SUC4* did not respond to salt stress (Ch.V- Fig. 15).

In order to provide a global vision about vacuolar flux of sucrose and its derived hexoses (glucose and fructose), the expression profiles of two vacuolar invertases *Atβfruct3* and *Atβfruct4* (Haouazine-Takvorian et al., 1997) were analyzed (Ch.V- Fig. 16). Under control condition, the expression level of *Atβfruct4* was higher than that of *Atβfruct3* in 16-day-old seedlings of Col-0 and all *esl* mutant lines. Exogenous mannitol, glucose and ABA down-regulated the gene expression of both vacuolar invertases in all studied genotypes. Inversely, the expression of *Atβfruct3* and *Atβfruct4* was globally up-regulated by high NaCl concentration. *Atβfruct3* expression demonstrated highly significant and reproducible increase, while that of *Atβfruct4* was also sustained, but less strong, and not observed for the triple *esl* mutant (Ch.V- Fig. 16).

4. Discussion

For a first time we succeeded crossing the homozygous parental lines of the four single mutants (*esl1.02*, *esl3.07*, *esl3.05*, and *esl3.03*) to generate three double (*esl1.02esl3.07*, *esl3.03esl3.05*, *esl1.02esl3.03*) and two triple (*esl1.02esl3.03esl3.07*, *esl1.02esl3.03esl3.05*) mutants. It should be noted that when grown under normal conditions,

esl single, double, and triple mutants exhibited a phenotype similar to that of the wild genotype Col-0. In the aim to decipher the functional diversity of *Arabidopsis ESL* genes, we tried to discriminate the responsiveness of *esl* single, double, and triple mutants to ABA and glucose, as well as to salt and cold treatments, by performing seed germination assays.

Previously it has been shown that glucose delays seed germination of *Arabidopsis* (Price et al., 2003; Dekkers et al., 2004). Our preliminary essays of seed germination on three increasing glucose concentrations (2%, 6% and 7.2%) demonstrated most important and sustained effect for the highest 7.2% glucose. Indeed, in the presence of 7.2% glucose, seed germination of all tested genotypes was delayed, and that of wild-type seeds required eight DPS to reach nearly 50% efficiency (Ch.V- Fig. 8). The early osmotic effect of control 7.2% mannitol showed only one-day shift of germination beginning compared to the minimal MS medium, and this difference was overcome since the 3th DPS. By consequence, we considered the high inhibitory impact of 7.2% glucose on seed germination as mainly due to glucose signaling. As the largely studied *abi* mutants (*abi3, abi4, abi5*) have been affected in both ABA and glucose signaling pathways (Finkelstein et al., 2002), we compared germination resistance/sensitivity of *esl* mutant- and wild type seeds in response to ABA as a hormonal and glucose as a metabolic signal. In our experimental conditions, the low 3 µM ABA concentration produced the most pronounced impact on seed germination than that at high 7.2% glucose concentration, in terms of time delay and response uniformity of the genotypes. The effect of 200 mM NaCl compared to our both controls, minimal MS and minimal MS with 7.2 % mannitol, manifested a higher inhibitory impact but a clearer differential responsiveness of studied genotypes. As expected, the cold treatment was the most restrictive factor for seed germination over time, and also contributed to its relative uniformity.

Our results provided evidence that among the four single mutants, the *esl3.05* line displayed germination efficiency similar to that of the wild type under mannitol, NaCl and cold treatments. Interestingly, *esl3.05* was the only one among the studied mutants, which demonstrated less germination sensitivity to glucose and to ABA during the experiments. In a general manner, germination of single mutants was less affected than that of double mutants, remaining close to that of the wild type. Poschet et al. (2011) have shown that the germination of the *esl1.02*/*erdl6* was highly sensitive to the same concentration of glucose as that used in our study (7.2% Glc). Conversely, the overexpression of its sugar beet orthologue *Bv*IMP (Integral Membrane Protein) in *Arabidopsis* has been reported to delay seed germination in the presence of 2.5% glucose or 1.5% fructose (Klemens et al., 2014).

A plausible explanation of this data descrepency may consist in the different growth conditions: composition of culture media, light spectra and photoperiods. Our results concerning *esl1.02* mutant, namely its enhanced germination resistance to glucose under our test conditions corrobore those of Klemens et al. (2014), since the overexpression of *ESL1.02* sugar beet orthologue in *Arabidopsis* reduced seed germination resistance to glucose.

In this regard, the three double mutants (*esl1.02esl3.07, esl1.02esl3.03* and *esl3.03esl3.05*) manifested enhanced sensitivity to glucose and ABA compared to Col-0 and the single parental mutant lines (Ch.V- Fig. 10). The germination of *esl1.02esl3.03* double mutant showed higher glucose sensitivity in comparison to that of Col-0 and the two other double mutant lines (*esl1.02esl3.07* and *esl3.03esl3.05*) (Ch.V- Fig. 8). This low germination is neither due to an osmotic effect, nor to a loss of seeds' viability, because *esl1.02esl3.03* double mutant seeds could germinate nearly at 100% when sown on minimal MS medium or the same medium supplemented with 7.2% mannitol. Inversely, in the presence of 3 µM ABA, germination of *esl1.02esl3.07* and *esl1.02esl3.03* double mutants showed enhanced sensitivity to ABA, when compared to those of Col-0 and *esl3.03esl3.05* double mutant line. These findings suggest that the double mutants are more responsive to ABA and glucose than the single parental mutants. It is noteworthy that the triple mutant *esl1.02esl3.03esl3.07* manifested germination sensitivity to ABA, but not to glucose. In conclusion, our results revealed that *esl1.02esl3.03* double mutant is hypersensitive to glucose and ABA, suggesting the involvement of their metabolic and hormonal signaling pathways in the regulation of *ESL3.03* gene expression.

Common feature of the *ESL* genes is their responsiveness to various abiotic stresses. Our seed germination analysis demonstrated that all tested *esl* mutant genotypes were more sensitive to high salinity, except *esl3.05*. Under high NaCl condition (200 mM), Col-0 and *esl3.05* mutant lines were relatively insensitive to NaCl and germinated up to 100% at the 6th DPS (Ch.V- Fig. 12). The *ESL3.07/ESL1* gene is highly expressed under high salinity, as reported by Yamada et al. (2010), and our own Genevestigator analysis. Using qPCR analysis, we demonstrated that the expression of *ESL3.07* and *ESL1.02* was up-regulated by NaCl in sixteen-day-old seedlings of the wild genotype. On the other hand, *esl1.02esl3.07* and *esl1.02esl3.03* double mutants displayed enhanced sensitivity to high NaCl concentration, where their germination was lower than that of Col-0. These results indicate that the *esl1.02esl3.07* and *esl1.02esl3.03* double mutants are more sensitive to NaCl than the reference genotype.

The response of the different genotypes to cold stress was also tested. It is largely accepted that environmental factors such as light and cold strongly modulate seed germination (Bentsink and Koornneef, 2008). Indeed, the germination of all tested genotypes was delayed by cold treatment, as all seeds started to germinate only at the 6th DPS (Ch.V- Fig. 14). Our knowledge about the expression of the four *ESL* genes under cold treatment was largely based on Genevestigator database. In perfect agreement with the latter, our results showed that the single *esl3.05* mutant displayed enhanced tolerance to cold stress and similar germination efficiency as that of the reference Col-0 genotype. Conversely, the expression of *ESL3.07* gene has been induced under cold treatment (Genevestigator) and, in the same line, we observed that *esl3.07* was more sensitive to cold stress, with about 50% of germinated seeds at the 10th DPS.

To further highlight the functional relatioinship between the tonoplast sugar transporters ESL*, TMT, SUC4,* and *SWEETs*, we analyzed their expression profiles in 16-day-old seedlings of the nine studied genotypes, grown under different germination conditions. It is well known that the gene expression of sugar transporters may be regulated by sugars as their proper substrates (Williams et al., 2000; Büttner, 2007; Sauer, 2007). In this regard, DNA microarray analysis has revealed responsiveness of monosaccharide transporters to glucose (Price et al. 2004). The latter study has demonstrated that four STP monosaccharide transporter genes, *STP1, STP4*, *STP13,* and *STP14*, were down-regulated by glucose. Concerning the *ESL* genes, *ESL1.01* (*At1g19450*) was reported as re-regulated by glucose, while *ESL2.01/ZIF2* (*At2g48020*) and *ESL3.08/ERD6* (*At1g08930*) as down-regulated by glucose (Price et al., 2004). In this context, our results demonstrated that the expression levels of *ESL1.02*, *ESL3.05* and *ESL3.07* remained unchanged in the early seedling development on 7.5% glucose-containing medium. Interestingly, the *ESL3.03* gene was expressed at a very low level under all tested conditions, but its expression was significantly induced in response to 7.5% glucose concentration (Ch.V- Fig. 15). Its responsiveness to glucose signaling was confirmed under osmotic stress, when the seedlings were grown on the 7.2% mannitol-containing medium and the expression levels of the four *ESLs* were similar to those of the control condition. After germination in the presence of exogenous 3 µM ABA, we showed that the expression level of *ESL3.07* in 16-day-old seedlings was decreased compared to that of the control medium. This down-regulation of *ESL3.07* in response to 3 µM ABA was confirmed for all studied genotypes. Inversely, *ESL3.07/ESL1* was strongly up-regulated in *Arabidopsis* leaves after spray-treatment with 750 µM ABA (Slawinski, 2017). These results suggest that ABA effect on *ESL3.07* expression is dependent on the hormone concentration,

the targeted organ, the stage of plant development and its physiological status. The promoter analysis of the nineteen *AtESL* genes revealed the presence of a unique ABRE motif (TACGTGTC) in the promoter region of the *AtESL3.05* gene. The analysis of Geneinvestigator data showed that the *ESL3.05 (At1g08890)* gene is also up-regulated after 3h of ABA (concentration) treatment compared to that in mock-treated seedlings. Accordingly, we showed that *ESL3.05* expression was increased in 16-day-old seedlings germinated on 3 µM ABA of all studied genotypes.

In *Arabidopsis*, AtSWEET16 has been localized on the tonoplast, and its transport activity allows the plant to cope with unfavorable environmental conditions (Klemens et al., 2013). The authors showed that *AtSWEET16* expression was down-regulated by exogenous application of sugars (glucose, fructose, and sucrose), as well as by osmotic stress conditions such as mannitol and NaCl (Klemens et al., 2013). Similarly, in our study we observed that the expression level of *AtSWEET1*6 was decreased in the presence of mannitol, glucose, NaCl, and 3 µM ABA (Ch.V- Fig. 15). AtSWEET17 was also localized on the tonoplast and shown to transport fructose (Chardon et al., 2013; Guo et al., 2014). It has been demonstrated that the expression level of *AtSWEET17* was very low in leaves (Chardon et al., 2013; Guo et al., 2014) and its expression is induced in roots in the presence of fructose, whereas the presence of glucose or sucrose exerts no effect on *AtSWEET17* expression (Guo et al., 2014). Conversely, *DsSWEET17* from *Dianthus spiculifolius* was induced by 2% glucose, 250 mM mannitol and 150 mM NaCl (Zhou et al., 2018). Our qPCR analysis of *AtSWEET17* showed that its expression was repressed by high 7.5% glucose concentration. In addition, we showed that the expression level of *AtSWEET17* was decreased by 7.5% mannitol and 3 µM ABA, but its expression remained constant under 200 mM NaCl treatment (Ch.V- Fig. 15). Taken together, all these data suggest that, at the difference with the studied ESL monosaccharide transporters, gene expression of the sugar facilitators AtSWEET16 and AtSWEET17 is not only strongly regulated by glucose, but also by high osmotic pressure.

In *Arabidopsis*, *TMT1* and *TMT2* monosaccharide transporters are localized on the tonoplast and can import glucose and fructose from the cytosol to the vacuole (Wormit et al., 2006). These authors have reported that the expression of both *TMT* genes was regulated by abiotic stresses. Through RNA gel blot analysis, they have shown important accumulation of *TMT1* and *TMT2* transcripts in seven-day-old seedlings under high 5% glucose concentration. Interestingly, in the conditions of our study, *TMT1* and *TMT2* genes demonstrate strong differential regulation by glucose signaling. On the one hand, *TMT1* expression was

significantly decreased in 16-day-old seedlings, obtained from seeds germinated on high 7.5% glucose concentration in all studied genotypes. On the other hand, the expression level of TMT2 was significantly increased by high 7.5% glucose concentration in all studied genotypes. In the same line and for all tested genotypes, *TMT1* and *TMT2* were differentially regulated in response to exogenous ABA, and only *TMT2* was up-regulated under ABA treatment (Ch.V- Fig. 15). In conclusion, our results strongly suggest that the fine-tuning of *TMT2* gene expression is at the crosstalk of glucose and ABA signaling pathways.

The four studied *ESL* genes are known to be involved in plant responses to different abiotic stresses (Yamada et al., 2010; Genvestigator data). The same authors have reported that the expression of *ESL3.07*/*ESL1* was enhanced after 250 mM NaCl treatment. Furthemore, they have shown that *ESL1* and the vacuolar invertases, *Atβfruct3* and *Atβfruct4*, were up-regulated under abiotic stresses and they work coordinately to accumulate monosaccharides in plant cells (Yamada et al., 2010). It has been shown that *TMT1* and *TMT2* expression was enhanced in response to salinity (Wormit et al., 2006). In agreement with the above-mentioned results, our experiments demonstrated that *ESL3.07* was strongly up-regulated in response to high salinity (200 mM NaCl) in different genotypes encompassing its wild gene. Moreover, under such conditions, *ESL1.02* and *ESL3.05* expression was also enhanced in all studied genotypes (Ch.V- Fig. 15). We showed that the expression patterns of *Atβfruct3* and *Atβfruct4* were similar to those of *ESL1.02*, *ESL3.05*, and *ESL3.07* in 16-day-old seedlings, obtained from seeds germinated on high NaCl concentration (Ch.V- Fig. 16). In contrast, using qPCR analysis, we showed that the expression level of *TMT1* and *TMT2* did not differ from the control medium. Under osmotic stress, we showed that *TMT1* and *TMT2* remained constant in the reference genotype, whereas their expression levels were decreased in 16-day-old seedlings for all *esl* mutants. In conclusion, it is not unlikely that at least the three *ESL* genes, *ESL1.02*, *ESL3.05*, and *ESL3.07*, work in concert with vacuolar invertases to maintain vacuole sugar homeostasis under salt stress.

Concerning *Arabidopsis* SUC/SUT disaccharide transporters, *AtSUC2* gene has been found to be repressed by glucose (Price et al., 2004). *AtSUC2* and *AtSUC4* have also be reported as up-regulated after treatment with 10 µM ABA, 300 mM mannitol and 150 mM NaCl (Gong et al., 2015). In *Vicia faba* upon exposure to high 150 mM glucose or 150 mM sucrose, the expression level of *VfSUT1* has been decreased in cotyledons, while the expression of *VfSTP1* has been not affected by sugars. Conversely, *VfSUT1* expression remained constant at low 10 mM glucose or 10 mM sucrose concentrations (Weber et al., 1997). In *Arabidopsis*, the sucrose transporter, SUC4, has been reported as localized on the

tonoplast and involved in the sucrose transport from vacuole to cytosol (Schneider et al., 2012). In our experimental conditions using 3 µM ABA, the expression of *SUC4* remained unchanged compared to that of the control medium. Interestingly, we found that the expression level of *SUC4* was strongly up-regulated at high glucose concentration (7.2%) (Ch.V- Fig. 15). This glucose-induced increase of *SUC4* expression in 16-day-old seedlings was confirmed for Col-0 and *esl* single, double, and triple mutant genotypes. To further highlight this unexpected induction of *SUC4* by glucose, we investigated the gene expression pattern of two vacuolar invertases, *Atβfruct3* and *Atβfruct4*, in 16-day-old seedlings of all studied genotypes. Upon exogenous application of high glucose concentration (7.2%), the expression levels of *Atβfruct3* and *Atβfruct4* were decreased (Ch.V- Fig. 16). In line with this finding, our results demonstrate inverse correlation between the up-regulation of *SUC4* and the down-regulation of both invertase genes, *Atβfruct3* and *Atβfruct4*. Since the repression of vacuolar invertases might lead to an accumulation of sucrose in the vacuole, the increase of the *SUC4* expression does allow further export of sucrose into the cytosol.

CHAPTER VI

Towards the deciphering of transport activity and subcellular localization of AtESL monosaccharide transporters

1. Introduction

Dans les plantes, les sucres jouent un rôle clé en tant que nutriments ainsi que molécules de signalisation (Rolland et al., 2002). Plusieurs transporteurs de sucre sont nécessaires pour la répartition des sucres à l'échelle de la plante entière et au niveau subcellulaire (Williams et al., 2000; Lalonde et al., 2004; Büttner, 2007). Le saccharose est réparti entre les organes sources et les organes puits. Le chargement et le déchargement du phloème peut se faire de manière symplasmique ou apoplasmique. La voie apoplasmique nécessite des transporteurs actifs de saccharose sur la membrane plasmique, des SUC et des SWEET facilitateurs, ainsi que des transporteurs de monosaccharide après le clivage du saccharose par les invertases pariétales (Lemoine et al., 2013). Un grand nombre de transporteurs de sucre situés dans les différentes membranes organelles (vacuolaires et plastidiennes) sont impliqués dans la répartition subcellulaire des sucres et le maintien de l'homéostasie. Le saccharose peut être stocké temporairement dans les vacuoles et, son homéostasie est régulée au niveau de la vacuole à travers l'hydrolyse du glucose et du fructose par des invertases vacuolaires (Martinoia et al., 2012; Klemens et al., 2014; Hedrich et al., 2015). Dans les feuilles adultes, les cellules sont caractérisées par la présence de grandes vacuoles occupant plus de 80 % du volume cellulaire. Les vacuoles sont des compartiments de stockage pour les sucres, les acides inorganiques, les ions et beaucoup d'autres métabolites primaires et secondaires (Martinoia et al., 2000; Martinoia et al., 2012; Hedrich et al., 2015). Le tonoplaste, la membrane vacuolaire, possède plusieurs transporteurs de sucre, et chacun d'entre eux remplit une fonction spécifique pour maintenir l'homéostasie des sucres.

Chez *Arabidopsis*, les transporteurs vacuolaires AtTMT1 et AtTMT2 (Tonoplast Monosaccharide Transporter) peuvent importer du glucose et du fructose, ainsi que du saccharose, et AtVGT1 (Vacuolar Glucose Transporter) participe à l'import de glucose et de fructose (Wormit et al., 2006; Aluri and Büttner, 2007). De plus, les transporteurs qui exportent les sucres, sont considérés également comme indispensables pour le maintien de l'homéostasie du sucre dans la cellule végétale. Cinq transporteurs exportateurs de sucre ont été identifiés : AtSUC4, qui agit comme un symporteur saccharose/H^+ (Schneider et al., 2012), AtERDL6 qui est un symporteur glucose/H^+ (Klemens et al., 2014) et trois transporteurs d'efflux de sucres, AtSWEET16 impliqué dans l'efflux du glucose, du fructose et du saccharose, AtESL1 - du glucose et du fructose (Yamada et al., 2010) et AtSWEET17 - du fructose uniquement (Chardon et al., 2013; Klemens et al., 2013).

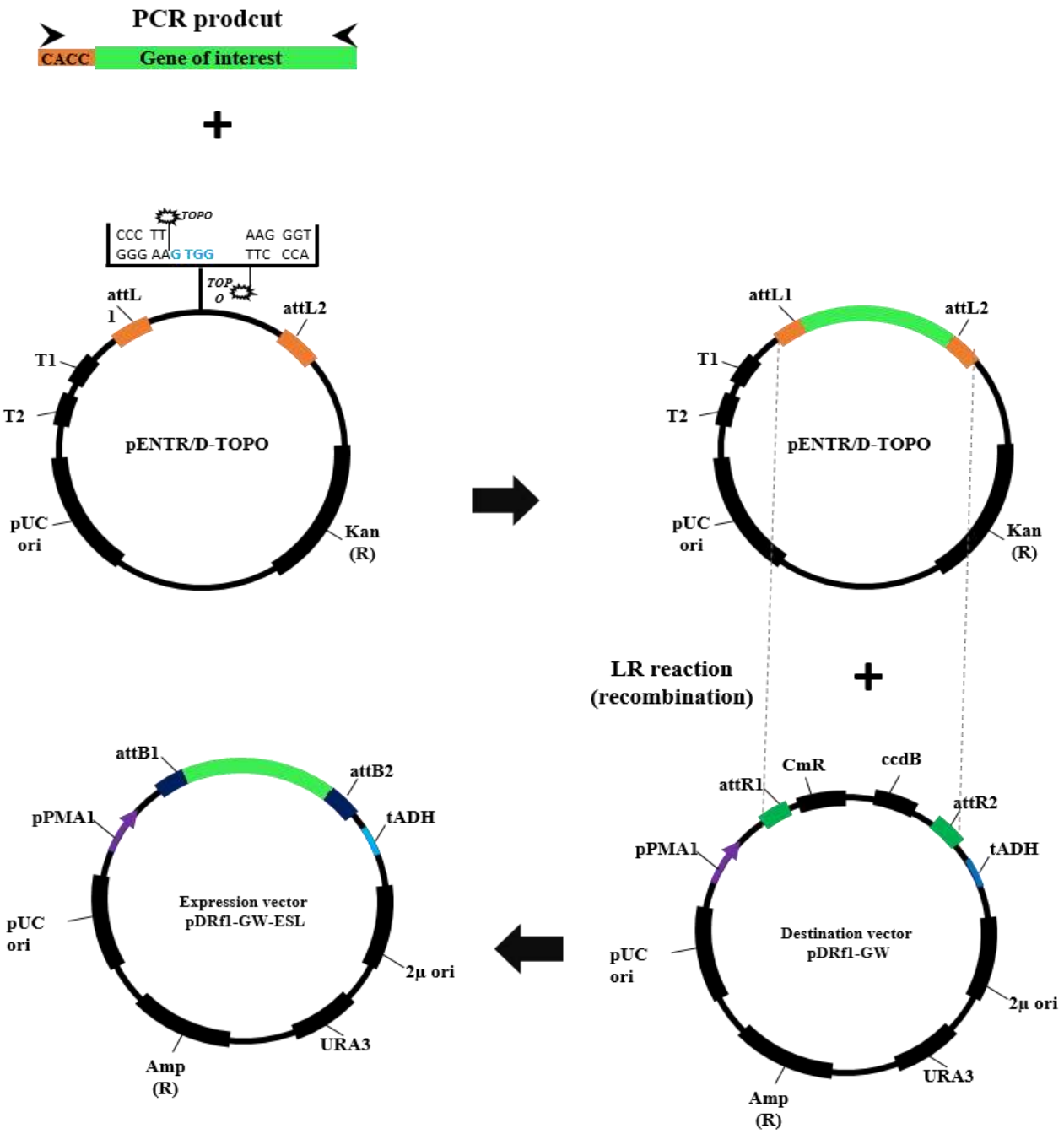

Ch.VI-Fig. 1: Schematic representation of the Gateway® cloning technology used to clone AtESLs in the yeast expression vector pDRf1-GW.

2 µ ori: yeast replication origin, *Amp*(R): confers resistance to ampicillin, attL1/attL2: Gateway® recombination sites, attR1/attR2: Gateway® recombination sites for LR reaction, *ccdB*: a bacterial toxin for negative selection of entry clone, *Cm*(R): confers resistance to chloramphenicol, *Kan*(R): confers resistance to kanamycin, pPMA1: yeast plasma membrane ATPase 1 promotor, pUC ori: bacterial replication origin, tADH: alcool-dehydrogenase terminator; transcription terminator for yeast, *URA3*: Orotidine-5'-phosphate (OMP) decarboxylase CDS needed for uracil biosynthesis and used as yeast auxotrophic marker.

Parmi les dix-sept membres de la sous-famille de transporteurs de monosaccharides AtESL, seuls trois transporteurs ont été fonctionnellement caractérisés jusqu'à présent. Dans ce contexte, il est important de comprendre le fonctionnement des transporteurs d'ESL, de définir leur localisation subcellulaire ainsi que caractériser leur activité de transport. Dans ce chapitre, nous présentons nos résultats sur la localisation et l'activité de transport de deux membres de la famille ESL qui sont le AtESL3.05, et AtESL3.03, dont les gènes sont impliqués dans la réponse des plantes au déficit hydrique.

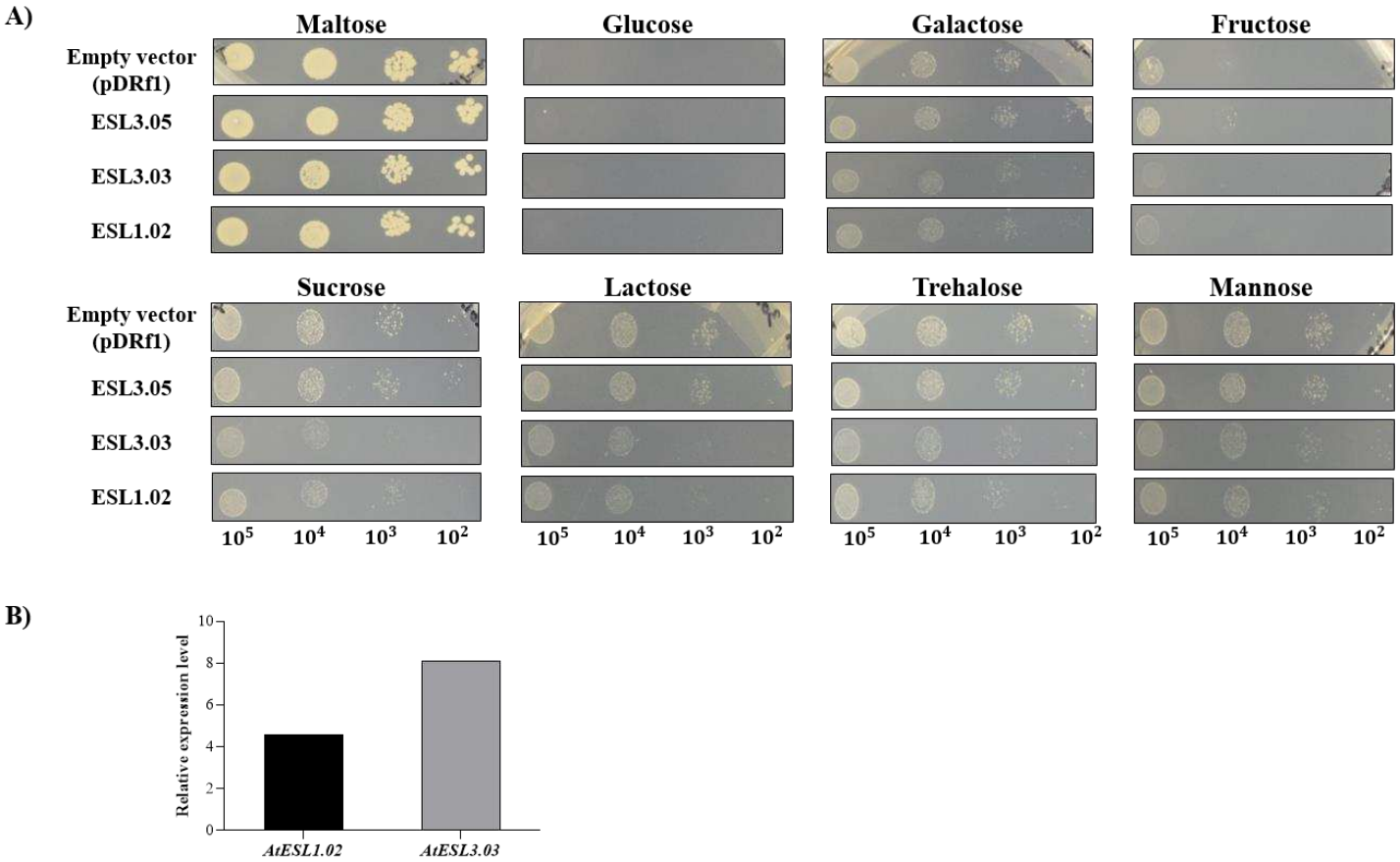

Ch.VI-Fig. 2: Functional complementation of AtESLs in *S. cerevisiae* hexose transporter deficient strain EBY.VW4000. A) Drop-test of yeast strain expressing either *AtESL3.05* or *AtESL3.03*, or *AtESL1.02* (positive control) or with the empty pDRf1 vector as a negative control. Yeast cell suspensions were ten-fold serially diluted, and 10 µl of each dilution was plated on YNB medium without uracil and supplemented with 2% of different sugars (as indicated) as the sole source of carbon. Maltose medium was used as a positive control for the growth of the EBY.VW4000 strain. Plates were incubated for 7 days at 28°C. B) The relative expression level of the *AtESL1.02* and *AtESL3.03* in the EBY.VW4000 yeast expressing either *AtESL1.02* or *AtESL3.03*. For RNA extraction, the transformed EBY.VW4000 cells were cultured in a YNB liquid medium supplemented with 2% of maltose to an OD600 of 0.6. The data of RT-qPCR were normalized using *ACT1* as a reference gene.

2. Experimental results

Introduction

In plants, sugars play a key role as nutrients as well as signaling molecules (Rolland et al., 2002). Several transporters are required for the distribution of sugars at whole plant and subcellular levels (Williams et al., 2000; Lalonde et al., 2004; Büttner, 2007). Sucrose is allocated from the source organs to the sink organs. Despite the symplastic way, apoplastic phloem loading and unloading necessitate active plasma membrane sucrose transporters SUCs and facilitators SWEETs, as well as monosaccharide transporters after sucrose cleavage by cell wall invertases (Lemoine et al., 2013). A large panel of sugar transporters located in different organelle membranes (cellular, vacuolar, plastidial) are involved in sugar subcellular partitioning and homeostasis maintaining. Sucrose can be temporarily stored and its homeostasis regulated in vacuoles through hydrolysis in glucose and fructose by vacuolar invertases (Martinoia et al., 2012; Klemens et al., 2014; Hedrich et al., 2015). In adult leaves, cells are characterized by the presence of large vacuoles occupying more than 80% of the cellular volume. Vacuoles are storage compartments for sugars, inorganic acids, ions and much other primary and secondary metabolites (Martinoia et al., 2000; Martinoia et al., 2012; Hedrich et al., 2015). Tonoplast, the vacuolar membrane, possesses several sugar transporters, and each of them fulfills specific function to maintain sugar homeostasis. The *Arabidopsis* TMT (Tonoplast Monosaccharide Transporter) and VGT (Vacuolar Glucose Transporter) are vacuolar transporters capable of mediating glucose and fructose loading. AtTMT1 and AtTMT2 can import glucose and fructose, as well as sucrose, and AtVGT1 can also assume the uptake of glucose and fructose (Wormit et al., 2006; Aluri and Büttner, 2007). To maintain sugar homeostasis, carriers that export sugars are also necessary, and actually five exporters have been identified: AtSUC4, which acts as a sucrose/H^+ symporter (Schneider et al., 2012), AtERDL6 is glucose/H^+ symporter (Klemens et al., 2014) and three facilitators, AtSWEET16 involved in the efflux of glucose, fructose and sucrose, AtESL1 - of glucose (Yamada et al., 2010) and AtSWEET17 - of fructose only (Chardon et al., 2013; Klemens et al., 2013). Among the seventeen members of the AtESL monosaccharide transporter subfamily, so far, only three have been functionally characterized. Therefore, to enhance our understanding on the biological functions of ESL transporters, their subcellular localization and transport activity must be characterized. In this chapter, we report our results on the localization and the transport activity of two members of the ESL family, AtESL3.05, and AtESL3.03, whose

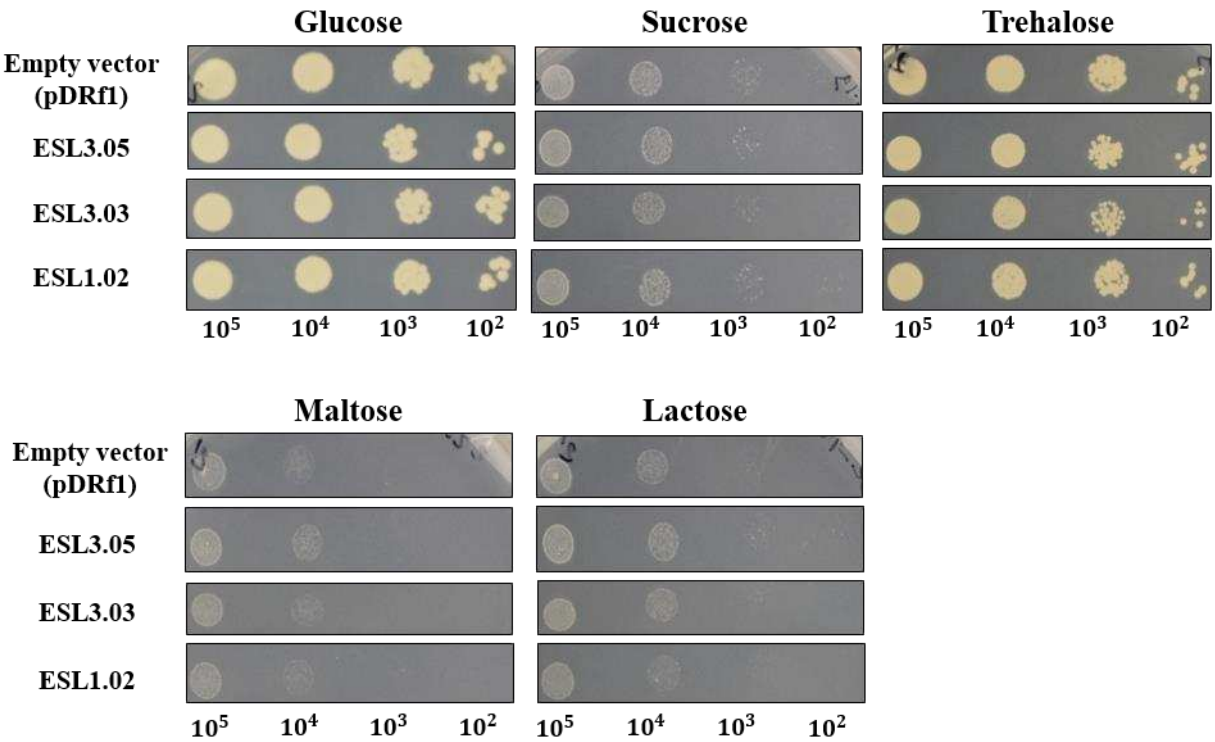

Ch.VI-Fig. 4 : Functional complementation of *AtESLs* in the *S. cerevisiae* sucrose transport deficient strain SUSY/ura3. Drop-test assays of yeast strains transformed either with *AtESL3.05 or AtESL3.03*, or *AtESL1.02* (positive control) or with the empty pDRf1 vector as a negative control. Yeast cell suspensions were serially diluted (ten-fold), and 10 µl of each dilution was plated on YNB medium without uracil and supplemented with 2% of different sugars (as indicated) as the sole source of carbon. The glucose medium was used as a positive control for the growth of the SUSY7/ura3 strain. Plates were incubated for 10 days at 28°C.

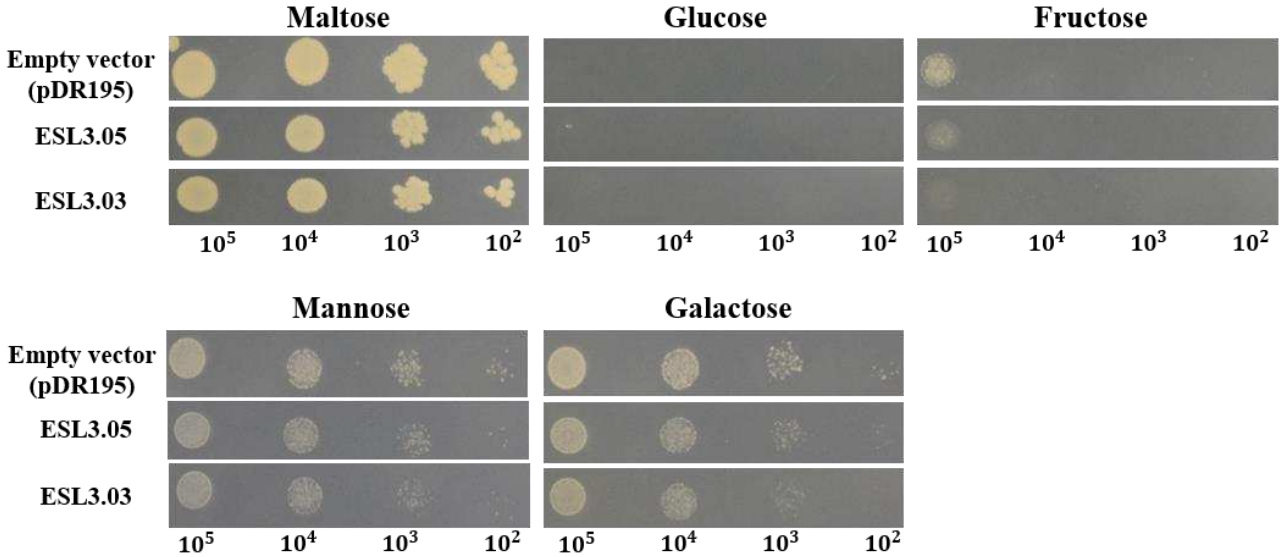

Ch.VI-Fig. 3 : Functional analysis of *AtESLs* in the *S. cerevisiae* hexose transport deficient strain EBY.VW4000. Drop-test assays of yeast strain expressing either *AtESL3.05* or *AtESL3.03* or with the empty pDR195 vector as a negative control. Yeast cell suspensions were serially diluted (10 fold) and 10 µl of each dilution was plated on YNB medium without uracil and supplemented with 2% of different sugars (as indicated) as the sole source of carbon. Maltose medium was used as a positive control for EBY.VW4000 strain. Plates were incubated for 7 days at 28°C.

genes are involved in plant response to water deficit.

3. Results

Functional characterization of AtESL3.05 and AtESL3.03 in yeast

To investigate the ability of AtESL3.05 and AtESL3.03 to transport sugars, we first explored their heterologous expression in yeast, *S. cerevisiae*, a well-established system in our lab. Genes encoding both carrier proteins were expressed in two yeast mutant strains. EBY.VW4000 mutant strain is hexose transport-deficient (Wieczorke et al., 1999), while the SUSY7/ura3 mutant strain is sucrose transport-deficient (Riesmeier et al., 1992). Using gateway technology, the full-length coding regions (CDS) of *AtESL3.05* and *AtESL3.03* were PCR-amplified and cloned into the pDRf1-GW yeast expression vector under control of the strong promoter PMA1 (Plasma membrane ATPase1) and the ADH (Alcohol-dehydrogenase) terminator (Ch.VI-Fig. 1). As a positive control, the CDS of *AtESL1.02*, already characterized for its glucose and fructose absorption activity, was also subcloned into the same pDRf1-GW yeast expression vector. As a negative control, the empty vector, pDRf1 was used. In parallel, two yeast mutant strains, EBY.VW4000 and SUSY7/ura3, were transformed with each of newly constructed vectors (pDRf1-GW-AtESL3.05, pDRf1-GW-AtESL3.03, pDRf1-GW-AtESL1.02) and the empty vector. Drop tests were realized to follow the growth of the yeast transformants. In brief, the positive colonies obtained with the transformed EBY.VW4000 and SUSY7/ura3 yeasts were grown in YNB liquid medium containing 2% maltose or 2% glucose as a sole carbon source, respectively. Thereafter, drop tests of serial dilutions were performed on a solid YNB medium containing 2% of different monosaccharides (maltose, glucose, fructose, mannose and galactose) or disaccharides (sucrose, trehalose, maltose and lactose). As expected, the drop test assay showed that the EBY.VW4000 yeast strains containing either a vector harboring AtESLs or an empty vector (negative control) grew on a medium containing maltose as sole carbon source, since maltose was used as a positive control for growth of the EBY.VW4000 yeast strain (Ch.VI-Fig. 2A). For the other sugars, no or residual growth was detected using the yeasts expressing either AtESL3.05 or AtESL3.03, or AtESL1.02 (positive control) compared with the growth of EBY.VW4000 yeast expressing the empty vector (Ch.VI-Fig. 2A). This result demonstrates that the yeast expressing AtESLs was not able to rescue the mutant yeast growth on any of the tested sugars. Moreover, using the yeast mutant strain SUSY7/ura3, both the control yeasts and the yeasts expressing either

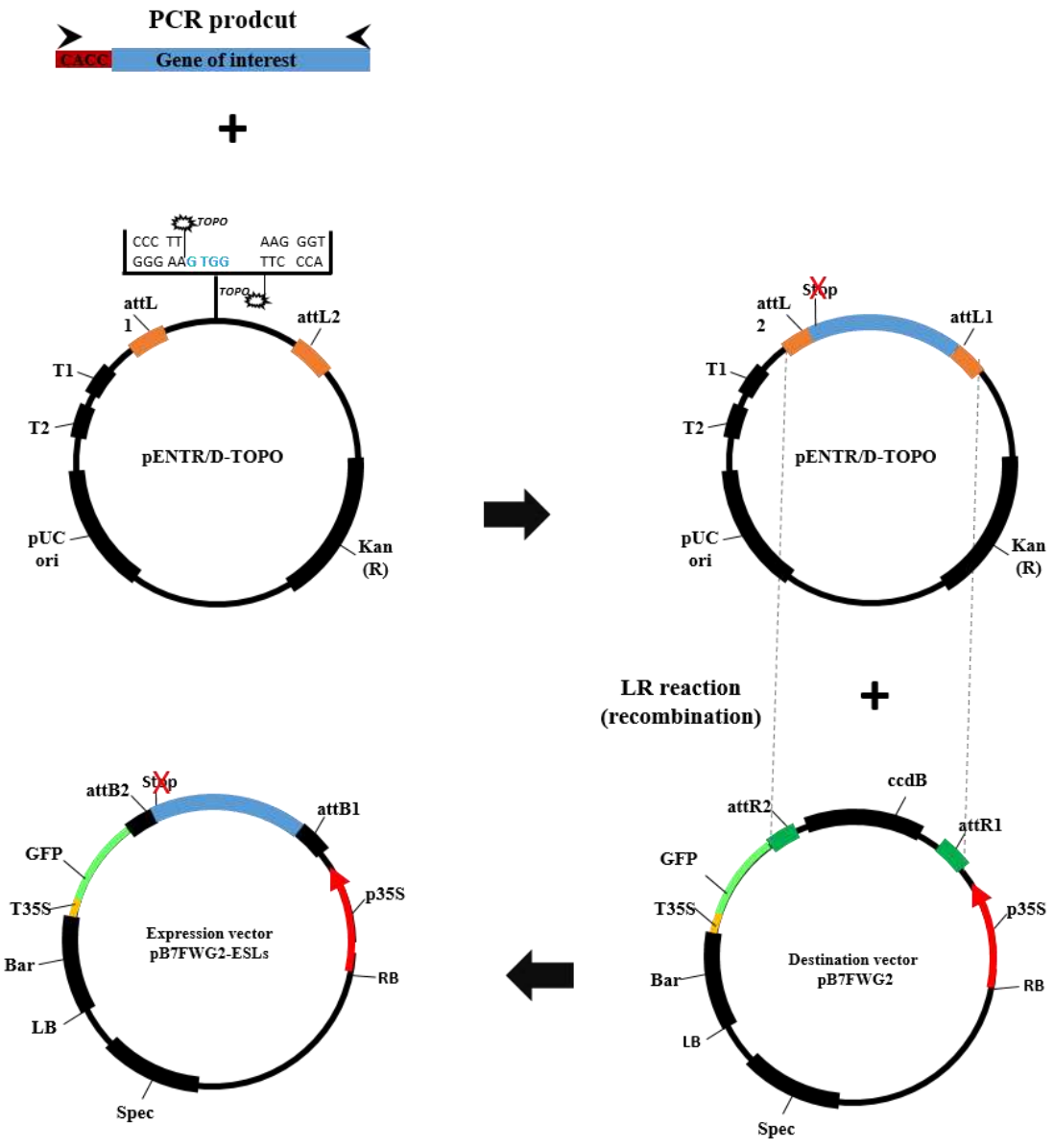

Ch.VI-Fig. 5 : Schematic of the Gateway® cloning used to clone AtESLs in the Gateway expression vector pB7FWG2.

attL1/attL2: Gateway® recombination sites, attR1/attR2: Gateway® recombination sites for LR reaction, *ccdB*: a bacterial toxin for negative selection of entry clone, *Spec*: confers resistance to Spectinomycin, p35s: Cauliflower mosaic virus promoter, t35S: Cauliflower mosaic virus terminator.

AtESL3.05 or AtESL3.03 exhibited similar growth on the YNB medium containing sucrose, trehalose, maltose, and lactose (Ch.VI-Fig. 4). These results indicate that the expression of AtESLs did not restore the growth of both transformed yeast mutant strains.

To discard any potential doubt in the veracity of our results, we also cloned the full-length coding regions (CDS) of the *AtESL3.05* and *AtESL3.03* into the classical pDR195 yeast expression vector to generate pDR195-AtESL3.05 and pDR195-AtESL3.03 vectors, respectively. Subsequently, the yeast strain EBY.VW4000 was transformed with the vectors containing AtESLs and the empty pDR195 vector (negative control). Drop tests were realized under the same conditions as described above. The yeasts were spotted on a solid YNB medium containing either 2% of maltose, glucose, fructose, mannose, or galactose. As expected, the two yeast strains expressing AtESL3.05 or AtESL3.03 and the control yeast harboring the empty vector showed similar growth on maltose-containing medium (control carbon source). Inversely, no growth was detected on the media supplemented with the other hexoses (Ch.VI-Fig. 3). These results confirmed that the expression of AtESL3.05 and AtESL3.03 did not restore growth of the yeast EBY.VW4000 mutant strain.

Yeast expression system is routinely used in our laboratory for studying absorption activity of plant sugar transporters. However, our results showed that neither AtESL3.03 and AtESL3.05, nor AtESL1.02 (positive control) were able to complement the EBY.VW4000 and SUSY7/ura3- yeast mutant strains. In this context, we additionally verified *AtESL3.03* and *AtESL1.02* expression in the EBY.VW4000 mutant strain by extracting mRNA from *AtESL3.03*, *AtESL3.05* and *AtESL1.02* yeast transformants and subsequent real-time qPCR analysis (Ch.VI-Fig. 2B). Our positive results for *AtESL* gene expression in yeast turned out in contradiction with these of the drop tests. Such discrepancy between *AtESL* gene expression and lack of activity of encoded transporter proteins might be due to AtESLs localization in the vacuolar membrane in yeast cells.

Subcellular localization of AtESL3.05

To determine the subcellular localization of AtESL3.05, we applied the strategy of fusion-proteins. We generated AtESL3.05-GFP construct using the Gateway expression vector pB7FWG2 containing the gene of the green fluorescent protein (GFP). In parallel, we created AtESL3.07-GFP fusion as a positive control because this AtESL transporter is already known to be located on the tonoplast. To construct AtESL3.05-GFP and AtES3.7-GFP fusion proteins, full-length coding regions devoid of stop codons of *AtESL3.05* and *AtESL3.07* genes

Ch.VI-Table 1 : Fusion proteins and their combinations for agroinfiltration or co-agroinfiltration of *N. benthamiana* leaves

Fusion proteins	ESL3.07-GFP	ESL3.05-GFP	AtTIP1;1-mCherry
ESL3.07-GFP	infiltration		co-infiltration
ESL3.05-GFP		infiltration	co-infiltration
AtTIP1;1-mCherry	co-infiltration	co-infiltration	infiltration

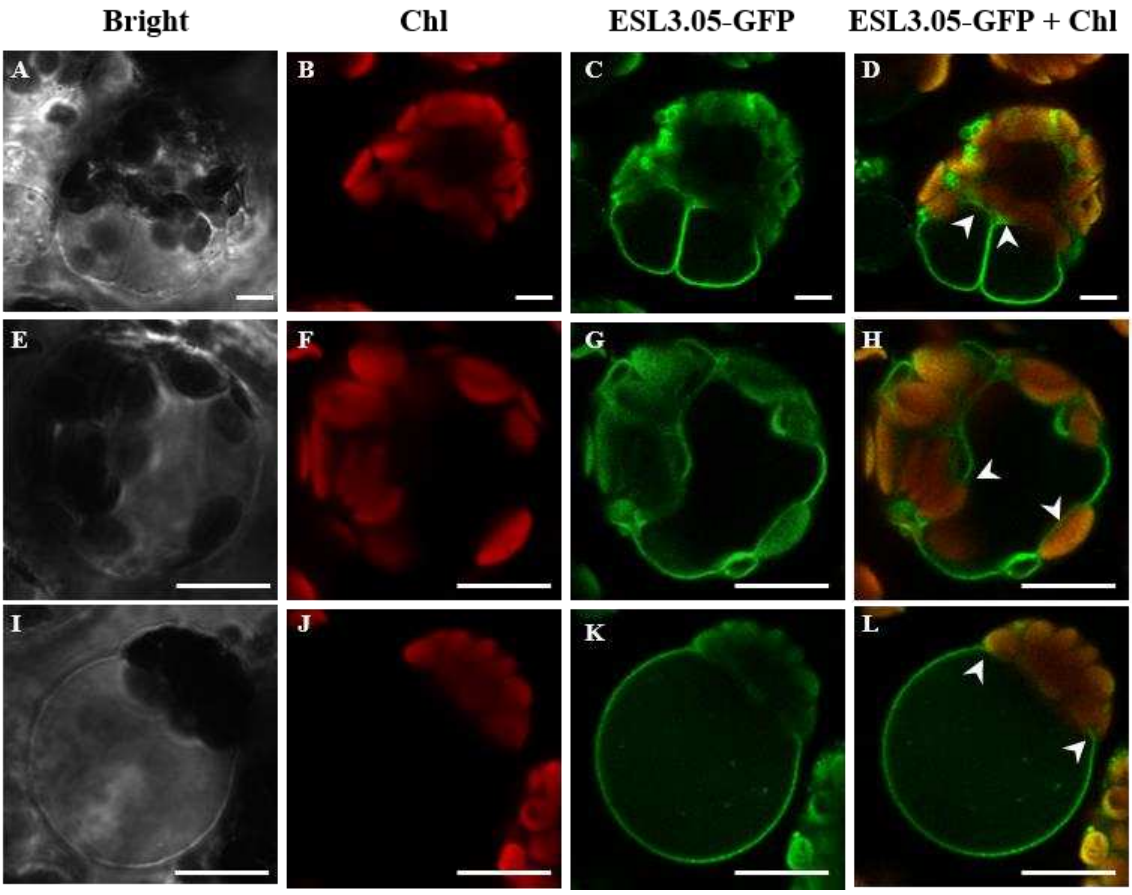

Ch.VI-Fig. 6: Subcellular localization of AtESL3.05 in protoplasts isolated from agroinfiltrated *N. benthamiana* leaves. *N. benthamiana* leaves were co-infiltrated with AtESL3.05-GFP protein fusion under the control of the 35S promoter. The protoplasts were then isolated using an enzymatic reaction and analyzed under a confocal microscope. The left panel shows the bright-field images of *N. benthamiana* protoplasts. The second panel displays the chloroplast autofluorescence (red). The third panel shows AtESL3.05-GFP localization to the tonoplast (green). The right panel shows merged fluorescence images of AtESL3.05-GFP and chloroplast autofluorescence. White arrowheads indicate that the tonoplast(s) is (are) behind the chloroplasts. Chl: chlorophyll. (Scale bar, 5 µm).

were amplified by PCR and cloned into the binary vector pB7FWG2 under the control of the constitutive promoter and terminator of the CaMV 35S RNA (Ch.VI-Fig. 5). The insertions were verified by sequencing using the primers specific for p35S and t35S (Eurofins Genomics, Germany). Eventually, the AtTIP1;1-mCherry (Tonoplast Intrinsic Protein 1) construct, as tonoplast specific marker, was kindly provided by Doan Trung LUU (BPMP Laboratory, Montpellier University). Firstly, we used AtESL3.07-GFP fusion protein as a positive control to check our transient expression system. AtESL3.05-GFP and AtESL3.07-GFP at the one hand, and AtTIP1;1-mCherry at the other hand were introducd into *A. tumefaciens* strains GV3101 and EHA105, respectively. We used two methods to perform *Agrobacterium* transformation: strain GV3101 was transformed by heat chock, while EHA105 strain was transformed by electroporation of previously prepared electrocompetent cells.

Our experimental design was conceived in the aim to cover sufficient number of agroinfiltrated plants for each individual construct and their respective combinations for co-infiltration (Ch.VI-Table 1). Leaves of four-weeks old *N. benthamiana* plants were agroinfiltrated on their abaxial face covering the full leaf area. After 72 h of transient expression, leaf mesophyll protoplasts were isolated (see section Materials and methods) and fusion protein localization was immediately analyzed by confocal microscopy. Under specific excitation, fluorescence emission revealed the expression of each distinct fusion protein and further allowed their co-expression analysis. Chloroplasts revealed by their chlorophyll autofluorescence were also used to better discriminate between the plasma membrane and the tonoplast.

Three different protoplasts isolated from *N. benthamiana* leaves infiltrated with AtESL3.05-GFP are presented on (Ch.VI-Fig. 6). The left panel allows the visualization of these protoplasts under transmission light (Ch.VI-Fig. 6A, E and I). On the second panel, the red autofluorescence of the chlorophyll corresponds to intracellular location of chloroplasts, which also suggests vacuoles' boundaries (Ch.VI-Fig. 6B, F and J). The most important observation concerns the green fluorescence of AtESL3.05-GFP fusion protein, which apparently delimits several vacuolar compartments (Ch.VI-Fig. 6C, G and K). The most significant visualization of the putative vacuoles location is obtained by merged both red chlorophyll autofluorescence and green AtESL3.05-GFP fluorescence (Ch.VI-Fig. 6D, H and L). The latter merged images present the first plausible indication for AtESL3.05-GFP localization on the tonoplast, confirmed by the chloroplast position outside the green fluorescent membrane structure.

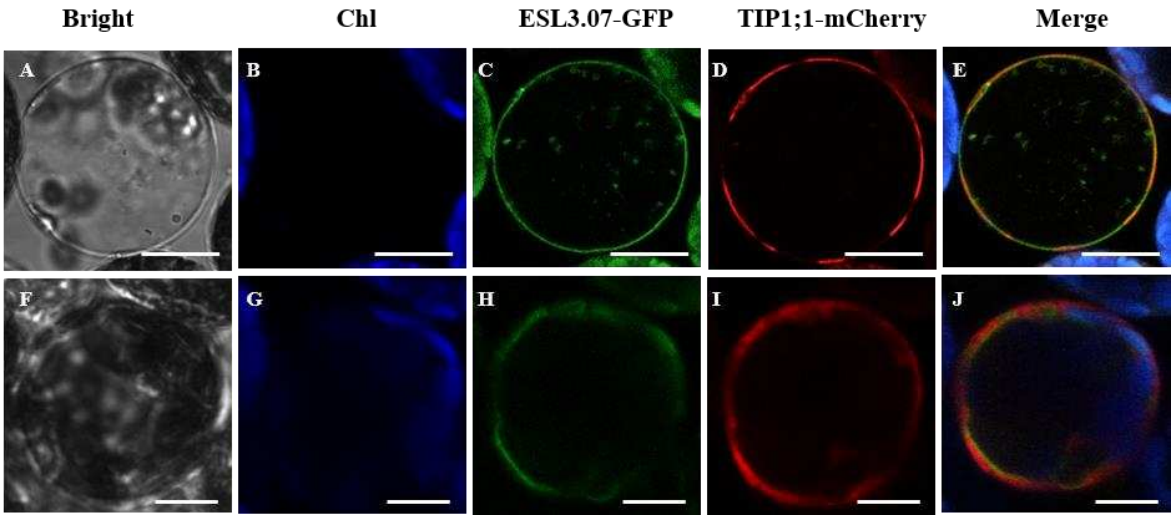

Ch.VI-Fig. 7: Co-localization of AtESL3.07 and AtTIP1;1-mcherry in protoplasts isolated from agroinfiltrated *N. benthamiana* leaves. *N. benthamiana* leaves were co-infiltrated with AtESL3.07-GFP (positive control) and AtTIP1;1-mCherry (tonoplast marker) fusions under the control of the 35S promoter. The protoplasts were then isolated using an enzymatic reaction and analyzed under a confocal microscope. The left panel shows the bright-field images of *N. benthamiana* protoplasts. Panels 2 and 5 correspond to chloroplast autofluorescence (blue), panel 3 - GFP (green), panel 4 - mCherry (red) fluorescence signals. The right panel shows merged fluorescence images of both AtESL3.07-GFP and AtTIP1;1-mCherry fusion protein, which indicates clear co-localization of AtESL3.07. Chl: chlorophyll. (Scale bars, 5 µm).

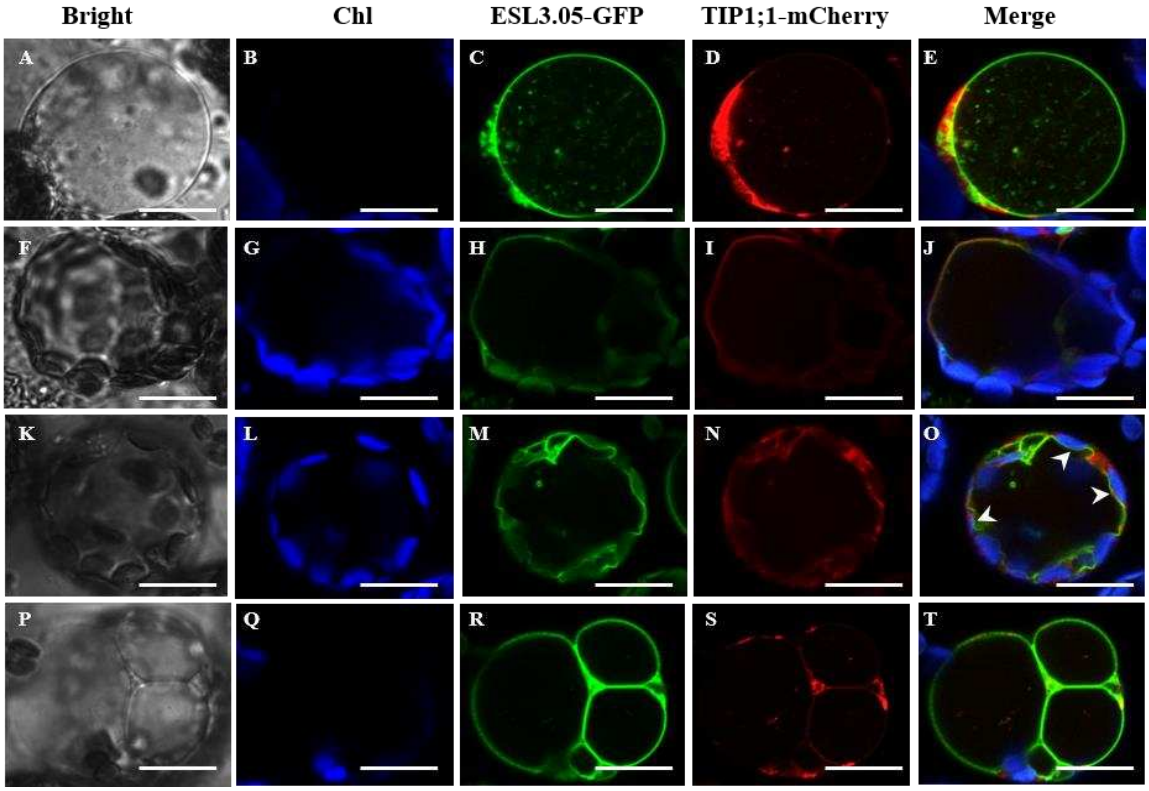

Ch.VI-Fig. 8: Co-localization of AtESL3.05 with AtTIP1;1 as tonoplast maker in protoplasts isolated from agroinfiltrated *N. Benthamiana* leaves. *N. benthamiana* leaves were co-infiltrated with AtESL3.05-GFP and AtTIP1;1-mCherry (tonoplast marker) fusions under the control of the 35S promoter. The protoplasts were then isolated using an enzymatic reaction and analyzed under a confocal microscope. The left panel shows the bright-field images of *N. benthamiana* protoplasts. Panels 2 and 5 indicate chloroplast autofluorescence (blue), panel 3-GFP (green), and panel 4- mCherry (red). The right panel shows merged fluorescence images of both AtESL3.05-GFP and AtTIP1;1-mCherry fusion protein, which indicates clear co-localization of AtESL3.05. White arrowheads indicate that the tonoplast(s) is (are) behind the chloroplasts. Chl: chlorophyll. (Scale bars, 5 µm).

To further check the veracity of this assumption, we observed the co-expression of AtESL3.07-GFP and AtTIP1;1-mCherry: AtESL3.07 as ESL transporter already identified as vacuolar membrane protein (Yamada et al., 2010) and AtTIP1;1 as specific tonoplast marker (Gattolin et al., 2010). The first two panels correspond, respectively, to protoplasts under transmission light (Ch.VI-Fig. 7A and F) and chlorophyll autoflourescence (set purposely in blue pseudocolor) to be distinguished from the red fluorescence of mCherry fluorophore (Ch.VI-Fig. 7B and G). The AtESL3.07-GFP green fluorescence on the third panel and AtTIP1;1-mCherry red fluorescence on the fourth panel share the same nearly perfect empty forms delimited by thin membrane structures (Ch.VI-Fig. 7C and H, D and I, respectively). The merged images (Ch.VI-Fig. 7E and J, white arrowheads) unambiguously confirm the co-localization of these both vacuolar proteins, and their use as positive controls for the further subcellular location of AtESL3.07.

The confocal micrographs on Ch.VI-Fig. 8 correspond to protoplasts co-expressing AtESL3.05-GFP and AtTIP1;1-mCherry, used for the identification of precise subcellular localization of AtESL3.05 transporter. The five vertical panels are as described above: bright-field (Ch.VI-Fig. 8A, F, K and P), blue chlorophyll autofluorescence (Ch.VI-Fig. 8B, G, L and Q), green AtESL3.05-GFP fluorescence (Ch.VI-Fig. 8C, H, M and R), red AtTIP1;1-mCherry fluorescence (Ch.VI-Fig. 8D, I, N and S) and these three kinds of fluorescence merged Ch.VI-Fig. 8E, J, O and T), Keeping in mind that the final spatial superposition of AtESL3.05-GFP and AtTIP1;1-mCherry fluorescence is subsequently dependent on the efficiency of their co-agroinfiltration, co-expression and mutual steric hindrance effect on the tonoplast, we observed different protoplasts expressing both fusion proteins at sufficiently high level. Merged images clearly provide evidence for the co-localization of AtESL3.05 and AtTIP1;1 proteins on the tonoplast. Moreover, the intracellular location of chloroplasts, outside of vacuoles, corroborates the AtESL3.05 position in the vacuolar membrane.

Vacuoles isolation from wild ecotype Col-0 plants

As we successfully demonstrated the localization of AtESL3.05 at the tonoplast, it appeared evident for us that the next step was to explore the glucose absorption activity on isolated vacuoles. It has already been demonstrated that sugar absorption of vacuole membrane is lower than that of plasma membrane. For that reason, the successful analysis of sugar transporters activity on the tonoplast requires highly purified and concentrated intact vacuoles. The isolation of vacuoles was performed on leaves of the Col-0 genotype and

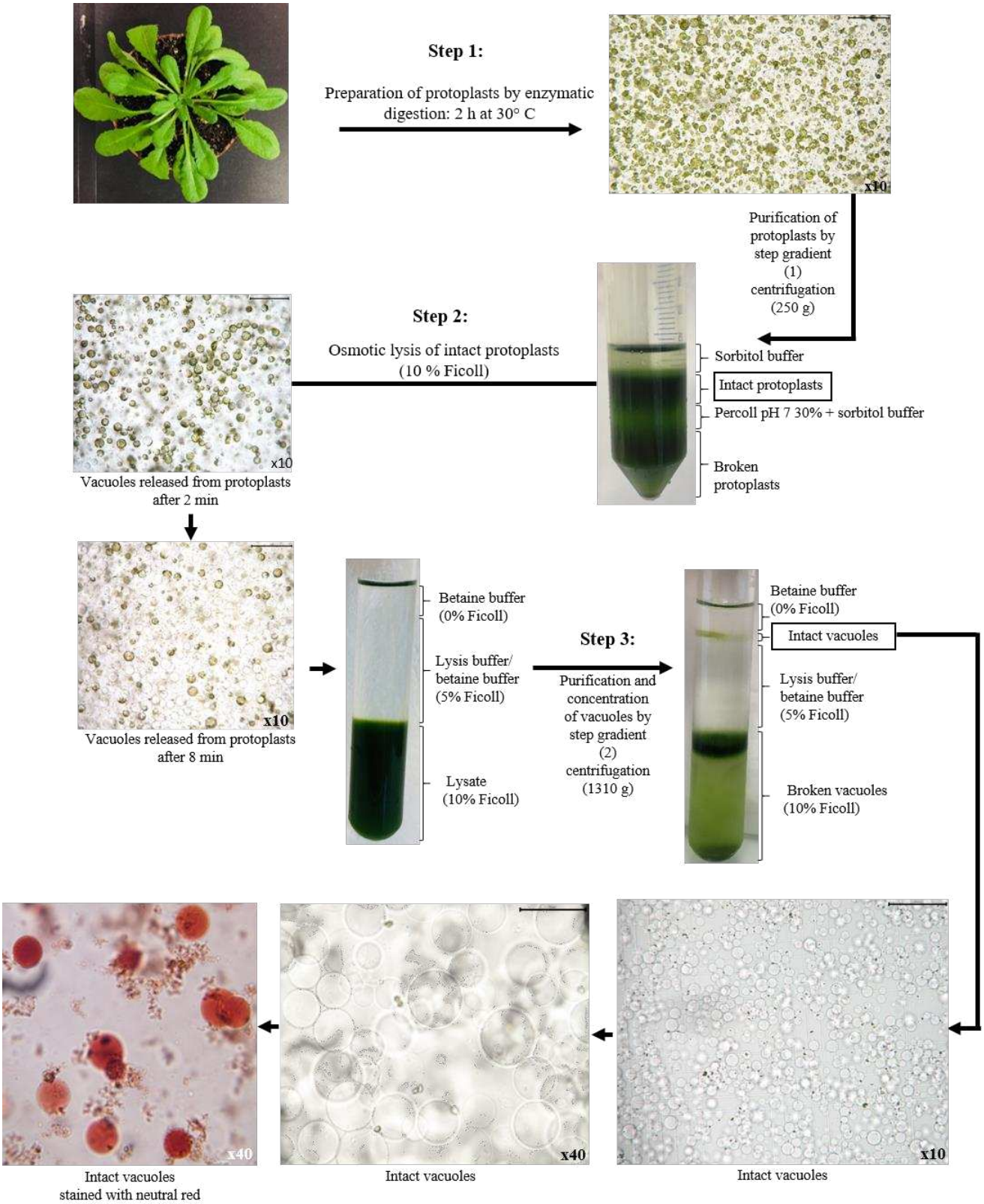

Ch.VI-Fig. 9: Isolation of intact vacuoles from *Arabidopsis* Col-0 rosette leaves. Vacuoles are isolated from mesophyll cell protoplasts, by osmotic lysis and final purification (according to Burla et al., 2013; described in detail in Materials & Methods).

knockout *atesl3.05* mutant plants, as described by (Burla et al., 2013) (more details can be found in the section "Materials and methods"). The introduction of this protocol in our laboratory was laborious and time-consuming. The complete procedure, from harvesting rosette leaves to obtaining purified vacuoles, takes ca. 8 hours, and comprises three main steps (Ch.VI-Fig. 9). The first step consists in the isolation of protoplasts by cell wall enzymatic digestion. The second step aims the isolation of intact vacuoles from purified protoplasts by gentle and finely controlled, subsequent osmotic and heat shocks. The third step concerns the purification and the concentration of the isolated vacuoles applying Ficoll step gradient (Ch.VI-Fig. 9). Eventually, the concentration of vacuoles was microscopically quantified in Malassez counting chamber. After several repetitions and multiple protocol adjustments we succeeded in setup this experiment and obtained relatively high vacuole concentration nearly 2.10^7 vacuoles/ml.

The most difficult part of our work consisted in the development of an efficient protocol for the analysis of vacuolar sugar transport. We performed six attempts to measure radiolabeled sugars in isolated vacuoles. In a first series of experiments, we used isolated vacuoles from plants grown under normal light conditions and mesured three different radiolabeled sugars, ^{14}C-glucose, ^{14}C-fructose and ^{14}C-sucrose, at 1 mM concentration and performed uptake kinetics for 5 to 30 min. Under these experimental conditions, we were not able to detect any sugar absorption. We realized that it is important to grow *Arabidopsis* plants in dark for at least two days before vacuoles' isolation in order to reduce vacuolar sugar content (i.e., to obtain vacuoles of lighter weight), thereby enhancing their absorption activity (E. Martinoia, personal communication). To that purpose we performed second series of experiments with isolated vacuoles from plants that have been cultivated under low light for two or three days plus additional two or three days in darkness. We then performed ^{14}C-glucose kinetics (3 to 30 min) using 1 mM glucose, but any glucose uptake could be detected. We then assumed that the sugar concentration was not suitable to detect a glucose absorption. Therefore, according to the results of Wormit et al., (2006), who observed glucose uptake into *Arabidospsis thaliana* isolated vacuoles at 100 µM glucose concentration, we decided to decrease the glucose concentration to 100 µM and, in parallel, to test a much higher concentration of 5 mM glucose. The performed uptake experiment with vacuoles isolated from plants cultivated under low light and in darkness did not allow to detect glucose uptake

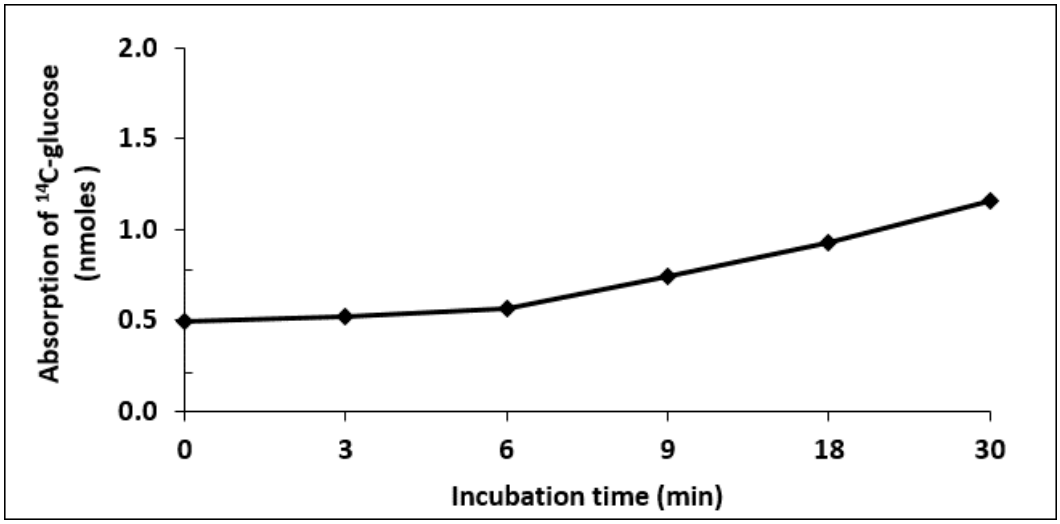

Ch.VI-Fig. 10: Absorption of ^{14}C-glucose by vacuoles isolated from rosette leaves of Col-0. The glucose concentration in this assay was 5 mM.

for glucose concentrations of 100 µM and 1 mM. However as shown on (Ch.VI-Fig. 10), after 6 min of incubation, wild-type vacuoles isolated from Col-0 started to uptake slightly ^{14}C-glucose (0.74 nmol), and after 30 min of incubation, there occurred some more increase in^{14}C-glucose absorption (1.16 nmol).

Even though this absorption remains low (maybe at the level of background noise), it is encouraging and suggests the possibility of being able to characterize certain transporters in isolated vacuoles.

4. Discussion

Functional analysis of AtESL3.05 and AtESL3.03

In this study, a heterologous system was used to investigate the transport activity of AtESL3.05 and AtESL3.03. Drop test assays showed that the expression of AtESL3.05 and AtESL3.03 in yeast cells failed to rescue the growth of the two mutant yeast strains on all monosaccharides and disaccharides tested (Ch.VI-Fig. 2, 3 and 4). In this regard, previous studies have reported that the transport activity of some of the sugar transporters in yeast cells was undetectable. The *Arabidopsis* AtESL3.08/AtERD6 protein has been expressed in yeast cells, and no transport activity of any of the substrates tested has been observed, presumably due to its intracellular localization (Kiyosue et al., 1998).

As shown by (Aluri and Büttner, 2007), the heterologous expression of AtVGT1 has also turned out unable to restore the growth of the EBY.VW4000 yeast mutant strain. This is possibly due to vacuolar localization of AtVGT1-GFP in yeast cells, and transport activity of AtVGT1 has been characterized using isolated vacuoles of yeast. Further analysis has shown that AtVGT1 transports hexoses, such as glucose (Km=3.7 mM) and fructose, in ATP-dependent manner. The conclusion is that AtVGT1 is localized on tonoplast, where it acts as glucose/H^+ antiporter to allow glucose influx into the vacuoles.

The heterologous expression of the three AtTMTs (AtTMT1, AtTMT2, and AtTMT3) in yeast mutant strain affected in hexose transporter genes has not resulted in any detectable glucose transport activity. Interestingly, despite expression in transformed yeasts of the three *AtTMT* genes at mRNA level, no corresponding proteins have been found (Wormit et al., 2006).

In our study, the expression of the *AtESL3.03* and *AtESL1.02* (positive control) was detected in transformed EBY.VW4000 mutant strain, but no functional complementation was

observed (Ch.VI-Fig. 2). The absence of detectable sugar transport activity can also be due to the localization of the AtTMTs on the vacuolar membrane in yeast. In the same idea, the AtTMTs have been localized on the tonoplast (Wormit et al., 2006). Conversely, the expression of *ERDL10-GFP* (formerly known as ESL3.11) in *S. cerevisiae* has shown partial mistargeting to the plasma membrane. Indeed, EBY.VW4000 yeast mutant expressing *ESL3.11* has shown partial complementation of yeast growth on glucose (Klemens et al., 2014). This complementation has been reported as due to protein mistargeting in yeast. In grapevine, VvERDl13 has been localized on the plasma membrane after expression in epidermal cells of tobacco leaves. Furthermore, (Breia et al., 2020) have reported sucrose/H^+ co-transport activity of VvERDl13 expressed in EBY.VW4000 yeast mutant. Taken together our results and those of others imply that AtESL3.05 and AtESL3.03 are probably localized on the vacuolar membrane in yeast cells. Indeed, we identified the subcellular localization of AtESL3.05 on the tonoplast in protoplasts, isolated from agroinfiltrated tobacco leaves.

Transport activity of AtESL3.05 and AtESL3.03 in isolated yeast vacuoles may be further investigated, but this will necessitate previous determining of the subcellular localization of AtESL3.05 and AtESL3.03.

AtESL3.05 localizes on the vacuolar membrane in tobacco protoplasts

We identified for a first time the vacuolar localization of AtESL3.05 using the approach of fusion proteins, AtESL3.05-GFP, with a powerful transient expression system, namely protoplasts isolated after agroinfiltration of *N. benthamiana* leaves (Ch.VI-Fig. 6). This result was confirmed when the AtESL3.05-GFP is co-expressed with a tonoplast marker AtTIP1;1-mCherry. AtESL3.05-GFP, fluorescence co-localized with AtTIP1;1-mCherry fluorescence (Ch.VI-Fig. 8). To date, in *Arabidopsis,* only three members of the ESL subfamily have been localized on the tonoplast. Our positive control co-localization experiment in protoplasts isolated from agroinfiltrated tobacco leaves, using the tonoplast marker the AtTIP1;1-mCherry and the AtESL3.07-GFP (formerly known as AtESL1) fusion protein confirms the vacuolar localization of the AtESL3.07 (Ch.VI-Fig. 7), previously described by Yamada et al. (2010), who showed that AtESL1 (named in our study AtESL3.07) is localized on the tonoplast of both protoplasts and transgenic *Arabidopsis* plants. It has been reported that the N-terminal part of the AtESL3.07 amino-acid sequence contains a $_{10}$LXXXLL$_{15}$ motif, responsible for the tonoplast sorting of the transporter (Yamada et al., 2010). Furthermore, the same authors have demonstrated that in the N-

terminal sequence of ESL1 the mutation of leucine at position 10 has turned out sufficient for transporter mistargeting to the endoplasm reticulum. It is worth to note that this motif was not found in the N-terminal region of the AtESL3.05, but the latter protein contains at position 10 a leucine amino acid residue, which may be important for the sorting of AtESL3.05 to the tonoplast. To elucidate whether the leucine amino acid residue at position 10 of AtESL3.05 N-terminal part is critical for its subcellular sorting, it may be mutagenized by targeted PCR. Yamada et al. (2010) have also shown that AtESL3.06 (formerly known as AtESL2) was localized on the tonoplast due to its intrinsic LXXXLL motif. The fusion AtESL1.02-GFP protein (formerly known as AtERDL6) has been transiently expressed in *Arabidopsis* protoplasts and its localization on the tonoplast has been suggested (Poschet et al., 2011). AtESL2.01 (formerly known as AtZIF2) has also been localized on the tonoplast of *Arabidopsis* protoplasts (Remy et al., 2014). More recently, the localization on the tonoplast of *Malus domestica* MdERDL6-1 transporter has been demonstrated (Zhu et al., 2021). Conversely, grapevine VvERD6l13 transporter has been detected to co-localize with AtPIP2.1-RFP, a plasma membrane aquaporin. This unexpected plasma membrane localization highlights the diversity and the complexity of the ESL family (Breia et al., 2020). This feature of vacuolar membrane intrinsic proteins is shared with other plant sugar transporters. For example, the *Arabidopsis* TMT1-GFP and TMT2-GFP fusion proteins have been transiently expressed in protoplasts isolated from tobacco leaves and *Arabidopsis* cell suspension, and their location has been observed on the tonoplast (Wormit et al., 2006). The *Arabidopsis* AtVGT1 has been also proposed to be localized on the tonoplast in *Arabidopsis* protoplasts (Aluri and Büttner, 2007). Furthermore, through fusion with GFP, the pear (*Pyrus bretschneideri*) PbTMT4 has been characterized as tonoplastic protein in *Arabidopsis* protoplasts (Cheng et al., 2018). Last but not least, type III SUTs from many species have been demonstrated to localize on the vacuole membrane (Reinders et al., 2012) The presence of all these diverse sugar transporters on the tonoplast reflects the complexity of sugar exchanges between the vacuole and the cytosol across this membrane.

We provided evidence that the AtESL3.05 localizes on tonoplast, and the vacuolar transport activity has to be further characterized using isolated mesophyll vacuoles from *Arabidopsis* lines such as wild-genotype Col-0 and our respective simple, double and triple *esl* mutants. In this context, a previous study of (Wormit et al., 2006) has shown that vacuoles isolated from *tmt1 simple* and triple *tmt1,2,3* mutants exhibit reduced glucose transport activity compared to those of vacuoles isolated from the wild-type under cold conditions. This data imply that the transporters play important function under cold stress. In order to

determine the transport mode of TMT patch-clamp approach has been performed on vacuoles prepared from plants overexpressing TMT1, which resulted in glucose increase in comparison with the wild-type vacuoles. These results gave ground for considering *Arabidopsis* TMT1 and TMT2 as glucose/H^+ antiporters (Wingenter et al., 2010). Moreover, Schulz et al. (2011) have demonstrated that these two vacuolar transporters also can function as sucrose/H^+ antiporters. A third research group using patch-clamp assays on vacuoles isolated from the double mutant *tmt1-2* and the triple mutant *aterdl6/ tmt1-2* has shown that AtERDL6 (referred to as AtESL1.02 in our study) acts as a glucose/H^+ symporter (Klemens et al., 2014).

In summary, this chapter presents functional characterization of AtESL3.05 and AtESL3.03. The successful expression *AtESLs* genes in yeast heterologous system combined with undetectable sugar transport activity for any of the studied monosaccharides and disaccharides implied their plausible vacuolar localization. In this regard and through transient expression by agroinfiltration of tobacco leaves, we demonstrated that AtESL3.05 was localized on the vacuolar membrane of isolated protoplasts. To further perform functional characterization of AtESL3.05, we opted for sugar absorption analysis of isolated vacuoles from *Arabidopsis* rosette leaves. Eventually, we succeeded to isolate vacuoles from leaf mesophyll of the wild-genotype Col-0 and started to develop the analysis of vacuolar sugar uptake. We also showed that under normal growth conditions neither single, double nor triple *atesl* mutants exhibited any remarkable phenotypic features, which is possibly due to their functional redundancy. In future, it will be necessary to obtain *AtESL3.05* overexpression lines in order to improve the performance of this system, and to characterize explicitly the sugar transport mode of AtESL3.05.

CHAPTER VII

Conclusion & Perspectives

Conclusion and perspectives

The main purpose of my thesis work is to unravel the functional diversity of AtESL sugar transporters in *A. thaliana* development and response to abiotic constraints. This challenging question relies on the evolutionary history of the ESL family of monosaccharide carriers. The phylogenetic study of 520 identified protein sequences, provides arguments in favor of the emergence of ESL genes in Charophytes, and the onset of their diversification in Bryophyta with the passage to terrestrial live (Slawinski et al., 2021, in preparation, see Chapter III). Another important contribution of the thesis of Slawniski (2017) concerns the demonstration that the ERD6-like monosaccharide transporters became a large family in Angiosperms, and in particular in Eudicots, due to multiple events of duplication (Johnson et al., 2006). The results of our group, in agreement with those of literature, argue in favor of at least two major events of genome duplication undergone by the ESL: the first one in the common ancestor of Gymnosperms and Angiosperms, and the second one in the common ancestor of Angiosperms. It should be emphasized that in certain Eudicots (Vitales, Solanales, and Eurosidae) the ESL family reaches remarkable expansion. The hexaploidization event occurred in the common ancestor of the Grapevine, as well as the segmental and the monogenic duplications are the main triggers of ESL diversification. The building of the phylogenic tree of 520 ESL, identified in the proteomes of 47 Embryophyta and 1 Streptophyta, provides evidence for the existence of three monophyletic groups (ESL1, ESL2 and ESL3).

Taken together, these data raise the question whether the so large expansion of ESL family in Eudicots might be related to the triggering of ESL transporters' functional diversity. The analysis of synonymous and non-synonymous mutations through the mean dN/dS ratio of ESL sequences of *A. hallery, A. lyrata and A. thaliana* (genus *Arabidopsis*) and *C. rubella* (as an out-group) reveals that they are under the pressure of a purifying selection for conservation of proteins and their functions. However, the progressive elevation of dN/dS values, up to three-fold from ESL1 through ESL2 to ESL3 group suggests a slow but progressive decrease of the selective pressure enabling phenomena of sub-functionalization and acquisition of novel functions.

In this regard, to enrich our knowledge on ESL genes diversity, I completed the previous phylogenic work with *in silico* functional analysis of their promoter regions. This was the first step towards understanding of ESL genes' transcriptional regulation. A search

through the tools of PLACE database for the *cis*-acting elements was performed on identified 1 kb regions upstream of the translation initiation codon of CDS of the nineteen *AtESL* sugar transporter genes. This global approach of *cis*-regulatory elements identification allowed me to compare ESL promoter sequences for the presence/absence of these motifs, as well to evaluate their relative abundance. A repertory was created according to their involvement in growth and developmental stages, in hormonal and metabolic signaling pathways, as well as in response to abiotic and biotic stresses. Our search for common specific "sequence" of ESL promoters performed by MEME tool did not reveal any unique "signature". Therefore, the identification of *cis*-acting elements such as SURE2STPAT21, Pyrimidine-box, and A-box, in the promoter region of some of the ESL genes clearly suggested that ESL genes might be regulated by sugars. This assumption was corroborated by the presence of WBOXHVISO1 motif (TGACT) previously known to be involved in sugar signaling (Sun et al., 2003), as a common sequence within the promoter region of all *ESL* genes. Conversely, the identification of promoter unique *cis*-regulatory motifs, at the example of the ABRE element found only in the promoter of *ESL3.05*, implies certain diversification of the ESL genes' responsiveness to endogenous and environmental cues that was acquired during evolution.

In *Arabidopsis*, the nineteen ESL sugar transporters are considered as the largest subfamily of the MSF superfamily, but remain still poorly characterized. Taken together data from the literature assign them the common feature of responsiveness to various abiotic stresses (Kiyosue et al., 1994; Kiyosue et al., 1998; Quirino et al., 2001; Yamada et al., 2010). To further provide arguments in favor of our working hypothesis for the functional diversity of ESLs, we further explored their behavior under water deprivation. To that aim, we performed expression profiling of seventeen *Arabidopsis ESL* genes (except the two pseudogenes), which revealed twelve among them as responsive to water deficit, four up-regulated and eight down-regulated. Interestingly, all the twelve *ESLs* transporter genes were differentially expressed depending on the four physiologically defined phases of plant water status. Indeed, the expression of *AtESL1.01* was decreased in the phase of moderate water deficit (MD), while its tandem gene *AtESL1.02* was induced in the late phase. *AtESL3.02* was down-regulated in this late phase, while its tandem gene *AtESL3.03* was up-regulated in the MD phase. *AtESL3.05* and *AtESL3.07* were up-regulated in the MD phase, whereas the *AtESL3.05* tandem gene, *AtESL3.06*, did not respond to water deficit, and the *AtESL3.07* tandem gene, *AtESL3.08*, was repressed in the early phase (ED) without significant modification of the plant water status. In addition, *AtESL3.13* was repressed in the late phase of wilting, while its tandem gene *AtESL3.14* did not respond to water deficit.

Eventually, the *AtESL* genes lacking tandem copies, *AtESL2.01*, *AtESL2.02*, *AtESL3.01* and *AtESL3.04*, displayed decreased expression levels in the late phase of plant wilting. The differential gene expression of *AtESLs* under conditions of water deficit was in agreement with their increasing dN/dS ratio, which implies acquisition propensity of new functions in the evolutionary processes of acclimation and adaptation to changing environment. We may speculate that the purifying selection acting in favor of the conservation of ESL proteins' molecular structure and role provides the necessary and sufficient functional redundancy, required for plant survival. In the evolutionary continuum from conservation to diversification, the acquisition of new ESLs physiological functions' favors the improvement of plant plasticity to cope with environmental constraints.

To better understand the individual role of *Arabidopsis* ESL transporters in response to water deficit, we successfully identified four T-DNA insertional mutants corresponding to each of the four up-regulated genes, referred to as *esl1.02*, *esl3.03*, *esl3.05*, and *esl3.07*. Our comparative in-depth phenotyping of the four *atesl* single mutants and the wild type Col-0, grown under normal watering and water-deprivation conditions, did not reveal any phenotypic difference. These results may be explained by the functional redundancy of ESLs and their plausible synergistic actions. In the aim to decipher the physiological functions of these four ESLs, we performed genetic crossings of their single mutants exploring all possible combinations. For a first time, we created three double homozygous mutants *esl1.02esl3.03*, *esl1.02esl3.07*, and *esl3.03esl3.05*, as well as two triple homozygous mutants *esl1.02esl3.03esl3.07* and *esl1.02esl3.03esl3.05*. Under normal growth conditions, no particular phenotype was observed for any of the double and triple mutants compared to that of the wild type.

To get more insight the functional diversity of *Arabidopsis ESL* genes, we tried to discriminate the responsiveness of *esl* single, double, and triple mutants to ABA and glucose, as well as to osmotic, salt and cold treatments. This was performed by seed germination assays, which allow comparing in parallel the resistance/sensitivity of nine studied genotypes after administration of four above-mentioned effectors, and cold treatment. Our results provided evidence that the *esl3.05* line was the only one among the single mutants, which demonstrated increased germination resistance to both, glucose and ABA. Conversely, the three double mutants (*esl1.02esl3.07, esl1.02esl3.03* and *esl3.03esl3.05*) manifested enhanced germination sensitivity to glucose and ABA compared to that of Col-0 and the single parental mutant lines. In general, seed germination efficiency of single mutants,

remaining close to that of the wild type, was less affected than that of double mutants arguing in favor of our strategy to create mutants affected in more than one *ESL* gene. However, as exception of this rule, the triple mutant *esl1.02esl3.03esl3.07* manifested germination sensitivity to ABA, but not to glucose.

To further highlight the functional relationship between the tonoplast sugar transporters ESL1.02, ESL3.03, ESL3.05, ESL3.07*, TMT1, TMT2, SUC4, SWEET16, SWEETA7 and two vacuolar invertases,* Atβfruct3 and Atβfruct4, we analyzed their expression profiles in 16-day-old seedlings of the nine studied genotypes, grown on the five germination media. Several interesting deductions were made:

- Among the four studied *ESL* genes and in all studied genotypes, *ESL3.03* expression strongly increased in response to high 7.5% glucose concentration, while *ESL3.05* expression was increased by 3 µM ABA. Only *TMT2* gene was strongly up-regulated by both glucose and ABA.

- Gene expression of the sugar facilitators *AtSWEET16* and *AtSWEET17* was strongly repressed by glucose, mannitol and ABA, the signaling of the latter being involved in plant response to osmotic stress.

- Interestingly, on high NaCl concentration up-regulation of *Atβfruct3* and *Atβfruct4* were similar to those of *ESL1.02*, *ESL3.05*, and *ESL3.07*. In contrast, the expression levels of *TMT1* and *TMT2* remained not affected by high salinity. It is not unlikely that at least the three ESL transporters, ESL1.02, ESL3.05, and ESL3.07, work in concert with vacuolar invertases to maintain vacuole sugar homeostasis under salt stress.

- Eventually, among the studied genes *SUC4* expression displayed remarkable glucose-dependent elevation. We provided evidence for the inverse correlation between the up-regulation of *SUC4* and the down-regulation of both invertase genes, *Atβfruct3* and *Atβfruct4*, in response to high glucose concentration. Since the repression of vacuolar invertases might lead to accumulation of sucrose in the vacuole, the induction of the *SUC4* expression does allow further export of sucrose into the cytosol.

Our first attempt to highlight the complex interplay of some vacuolar sugar transporters and their related enzymes have to be completed with sugar transporters' and enzymes' activities, as well as sugar fluxes through the tonoplast. In this regard, seed germination and early seedling development appear as a highly pertinent system for positioning of ESLs and other sugar transporters in the complex interplay of metabolic (glucose) and hormonal signaling pathways (ABA, gibberellins, ethylene, etc.).

As far as we know, only three members of the large ESL family have been functionally characterized. During my thesis work, I explored sugar transport activity of two members of the ESL family, ESL3.05 and ESL3.03. To that purpose, I prepared all needed constructs concerning these both transporters by two different approaches, the classical cloning based on restriction enzymes and the gateway system approach. The latter were used to ascertain the successful heterologous expression in two EBY.VW4000 and SUSY7/ura3 yeast mutant strains. Drop-test analysis showed that the expression of AtESL3.05, AtESL3.03, and AtESL1.02 (positive control) did not rescue growth of EBY.VW4000 and SUSY7/ura3 yeast mutant strains on all tested monosaccharides (maltose, glucose, fructose, mannose and galactose) and disaccharides (sucrose, trehalose, maltose, and lactose). Our functional complementation analysis revealed discrepancy between the drop-test results and those of *AtESL* gene expression analysis in yeast. In this regard, we hypothesized that in yeast cells the AtESLs might be targeted to the vacuolar membrane, and not to the plasma membrane. The veracity of our hypothesis is reinforced by the fact that other research groups failed to demonstrate transport activity of sugar transporters in yeast, because they have been identified not on the plasma membrane but on the vacuolar membrane (Wormit et al., 2006; Aluri and Büttner, 2007).

In this line, our major contribution consists in the determination of AtESL3.05 subcellular localizations. This finding was made by transient co-expression of AtESL3.05-GFP, AtESL3.07-GFP fusion proteins and AtTIP1;1-mCherry through agroinfiltration of *N. benthamiana* leaves. Confocal observation of specific fluorescence of each of the fusion proteins was carried out in protoplasts isolated from agroinfiltrated tobacco leaves. This analysis unambiguously demonstrates the co-localization of AtESL3.05 with each of both positive controls (AtESL3.07-GFP and AtTIP1;1-mCherry) on the tonoplast. Eventually, these results allowed us to identify the subcellular location of AtESL3.05 at the vacuolar membrane, and to further explore its transport activity. As the successful analysis of sugar absorption activity on the tonoplast requires highly purified and concentrated intact vacuoles, we succeeded the setup of this approach, which allowed performing preliminary glucose transport assays. Our strategy of further exploration of the ESL3.05 transport activity and its contribution to sugar exchanges between the vacuole and the cytosol consists in generation of *ESL3.05* overexpressor lines to compare their absorption activity with those of the wild type and the single *esl3.05* mutant.

Our arsenal of *esl* mutants (single, double, triple) together with the ongoing generation of the quadruple mutant, as well as their respective overexpressors, would serve to better elucidate the contribution of these ESL transporters to sugar storage and remobilization in the vacuole, thereby improving cell tolerance to water, osmotic, salt and cold abiotic stresses.

REFERENCES

References

Abe H, Urao T, Ito T, Seki M, Shinozaki K, Yamaguchi-Shinozaki K (2003) *Arabidopsis* AtMYC2 (bHLH) and AtMYB2 (MYB) function as transcriptional activators in abscisic acid signaling. Plant Cell **15**: 63–78

Abe H, Yamaguchi-Shinozaki K, Urao T, Iwasaki T, Hosokawa D, Shinozaki K (1997) Role of *Arabidopsis* MYC and MYB homologs in drought- and abscisic acid-regulated gene expression. Plant Cell **9**: 1859–1868

Afoufa-Bastien D, Medici A, Jeauffre J, Coutos-Thévenot P, Lemoine R, Atanassova R, Laloi M (2010) The *Vitis vinifera* sugar transporter gene family: phylogenetic overview and macroarray expression profiling. BMC Plant Biol **10**: 245

Agarwal PK, Agarwal P, Reddy MK, Sopory SK (2006) Role of DREB transcription factors in abiotic and biotic stress tolerance in plants. Plant Cell Rep **25**: 1263–1274

Aguirrezabal L, Bouchier-Combaud S, Radziejwoski A, Dauzat M, Cookson SJ, Granier C (2006) Plasticity to soil water deficit in *Arabidopsis thaliana*: dissection of leaf development into underlying growth dynamic and cellular variables reveals invisible phenotypes. Plant Cell Environ **29**: 2216–2227

Aida M, Ishida T, Fukaki H, Fujisawa H, Tasaka M (1997) Genes involved in organ separation in *Arabidopsis*: an analysis of the cup-shaped cotyledon mutant. Plant Cell **9**: 841–857

Ali-Rachedi S, Bouinot D, Wagner M-H, Bonnet M, Sotta B, Grappin P, Jullien M (2004) Changes in endogenous abscisic acid levels during dormancy release and maintenance of mature seeds: studies with the Cape Verde Islands ecotype, the dormant model of *Arabidopsis thaliana*. Planta **219**: 479–488

Altschul SF, Madden TL, Schäffer AA, Zhang J, Zhang Z, Miller W, Lipman DJ (1997) Gapped BLAST and PSI-BLAST: a new generation of protein database search programs. Nucleic Acids Res **25**: 3389–3402

Aluri S, Büttner M (2007) Identification and functional expression of the *Arabidopsis thaliana* vacuolar glucose transporter 1 and its role in seed germination and flowering. Proc Natl Acad Sci U S A **104**: 2537–2542

Ambawat S, Sharma P, Yadav NR, Yadav RC (2013) MYB transcription factor genes as regulators for plant responses: an overview. Physiol Mol Biol Plants **19**: 307–321

Antony E, Taybi T, Courbot M, Mugford ST, Smith JAC, Borland AM (2008) Cloning, localization and expression analysis of vacuolar sugar transporters in the CAM plant *Ananas comosus* (pineapple). J Exp Bot **59**: 1895–1908

Aoki N, Hirose T, Scofield GN, Whitfeld PR, Furbank RT (2003) The sucrose transporter gene family in rice. Plant Cell Physiol **44**: 223–232

Apel K, Hirt H (2004) REACTIVE OXYGEN SPECIES: Metabolism, oxidative stress, and signal transduction. Annu Rev Plant Biol **55**: 373–399

Arenas-Huertero F, Arroyo A, Zhou L, Sheen J, León P (2000) Analysis of *Arabidopsis* glucose insensitive mutants, gin5 and gin6, reveals a central role of the plant hormone ABA in the regulation of plant vegetative development by sugar. Genes Dev **14**: 2085–2096

Argout X, Salse J, Aury J-M, Guiltinan MJ, Droc G, Gouzy J, Allegre M, Chaparro C, Legavre T, Maximova SN, et al (2011) The genome of *Theobroma cacao*. Nature Genet **43**: 101–108

Arroyo A, Bossi F, Finkelstein RR, León P (2003) Three genes that affect sugar sensing (Abscisic Acid Insensitive 4, Abscisic Acid Insensitive 5, and constitutive triple Response 1) are differentially regulated by glucose in *Arabidopsis*. Plant Physiol **133**: 231–242

Arve L, Torre S, Olsen J, Tanino K (2011) Stomatal responses to drought stress and air humidity. doi: 10.5772/24661

Ayre BG (2011) Membrane-transport systems for sucrose in relation to whole-plant carbon partitioning. Mol Plant **4**: 377–394

Baena-González E, Rolland F, Thevelein JM, Sheen J (2007) A central integrator of transcription networks in plant stress and energy signalling. Nature **448**: 938–942

Baillo EH, Kimotho RN, Zhang Z, Xu P (2019) Transcription factors associated with abiotic and biotic stress tolerance and their potential for crops improvement. Genes (Basel). doi: 10.3390/genes10100771

Barberon M, Geldner N (2014) Radial transport of nutrients: the plant root as a polarized epithelium1. Plant Physiol **166**: 528–537

Barker L, Kühn C, Weise A, Schulz A, Gebhardt C, Hirner B, Hellmann H, Schulze W, Ward JM, Frommer WB (2000) SUT2, a putative sucrose sensor in sieve elements. Plant Cell **12**: 1153–1164

Baskin JM, Baskin CC (2004) A classification system for seed dormancy. Seed Science Res **14**: 1–16

Baud S, Wuillème S, Lemoine R, Kronenberger J, Caboche M, Lepiniec L, Rochat C (2005) The AtSUC5 sucrose transporter specifically expressed in the endosperm is involved in early seed development in *Arabidopsis*. Plant J **43**: 824–836

Beaudoin N, Serizet C, Gosti F, Giraudat J (2000) Interactions between Abscisic Acid and Ethylene Signaling Cascades. Plant Cell **12**: 1103–1116

Beilstein MA, Nagalingum NS, Clements MD, Manchester SR, Mathews S (2010) Dated molecular phylogenies indicate a Miocene origin for *Arabidopsis thaliana*. Proc Natl Acad Sci U S A **107**: 18724–18728

Bel AJE van (2003) Transport phloem: low profile, high impact. Plant Physiol **131**: 1509–1510

Bentsink L, Koornneef M (2008) Seed dormancy and germination. *Arabidopsis* Book. doi: 10.1199/tab.0119

Biłas R, Szafran K, Hnatuszko-Konka K, Kononowicz AK (2016) Cis-regulatory elements used to control gene expression in plants. Plant Cell Tiss Organ Cult **127**: 269–287

Blanc G, Wolfe KH (2004) Widespread paleopolyploidy in model plant species inferred from age distributions of duplicate genes. Plant Cell **16**: 1667–1678

Blatt MR (2000) Cellular signaling and volume control in stomatal movements in plants. Annu Rev Cell Dev Biol **16**: 221–241

Blouin M, Lavelle P, Laffray D (2007) Drought stress in rice (*Oryza sativa L.*) is enhanced in the presence of the compacting earthworm Millsonia anomala. Environ Exp Bot **60**: 352–359

Blum A (2017) Osmotic adjustment is a prime drought stress adaptive engine in support of plant production. Plant Cell Environ **40**: 4–10

Bowers JE, Chapman BA, Rong J, Paterson AH (2003) Unravelling angiosperm genome evolution by phylogenetic analysis of chromosomal duplication events. Nature **422**: 433–438

Boyer JS (1982) Plant Productivity and Environment. Science **218**: 443–448

Braun DM, Slewinski TL (2009) Genetic control of carbon partitioning in grasses: roles of sucrose transporters and tie-dyed loci in phloem loading. Plant Physiol **149**: 71–81

Bray EA (1997) Plant responses to water deficit. Trends Plant Science **2**: 48–54

Breia R, Conde A, Conde C, Fortes AM, Granell A, Gerós H (2020) VvERD6l13 is a grapevine sucrose transporter highly up-regulated in response to infection by *Botrytis cinerea* and *Erysiphe necator*. Plant Physiol Biochem **154**: 508–516

Burla B, Pfrunder S, Nagy R, Francisco RM, Lee Y, Martinoia E (2013) Vacuolar transport of abscisic acid glucosyl ester is mediated by ATP-Binding cassette and proton-antiport mechanisms in *Arabidopsis*. Plant Physiol **163**: 1446–1458

Bush DR (1999) Sugar transporters in plant biology. Curr Opim Plant Biol **2**: 187–191

Büttner M (2010) The *Arabidopsis* sugar transporter (AtSTP) family: an update: *Arabidopsis* sugar transporter family. Plant Biol **12**: 35–41

Büttner M (2007) The monosaccharide transporter(-like) gene family in *Arabidopsis*. FEBS Lett **581**: 2318–2324

Büttner M, Sauer N (2000) Monosaccharide transporters in plants: structure, function and physiology. Biochim Biophys Acta **1465**: 263–274

Cannon SB, Crow JA, Heuer ML, Wang X, Cannon EKS, Dwan C, Lamblin A-F, Vasdewani J, Mudge J, Cook A, et al (2005) Databases and information integration for the *Medicago truncatula* genome and transcriptome. Plant Physiol **138**: 38–46

Cannon SB, Sterck L, Rombauts S, Sato S, Cheung F, Gouzy J, Wang X, Mudge J, Vasdewani J, Schiex T, et al (2006) Legume genome evolution viewed through the *Medicago truncatula* and *Lotus japonicus* genomes. Proc Natl Acad Sci U S A **103**: 14959–14964

Caspari T, Stadler R, Sauer N, Tanner W (1994) Structure/function relationship of the *Chlorella* glucose/H+ symporter. J BiolChem **269**: 3498–3502

Chalker- Scott L (1999) Environmental Significance of Anthocyanins in Plant Stress Responses. Photochem Photobiol **70**: 1–9

Chardon F, Bedu M, Calenge F, Klemens PAW, Spinner L, Clement G, Chietera G, Léran S, Ferrand M, Lacombe B, et al (2013) Leaf Fructose Content Is Controlled by the Vacuolar Transporter SWEET17 in *Arabidopsis*. Curr Biol **23**: 697–702

Cha-um S, Charoenpanich A, Roytrakul S, Kirdmanee C (2009) Sugar accumulation, photosynthesis and growth of two indica rice varieties in response to salt stress. Acta Physiol Plant **31**: 477–486

Chavarria G, dos Santos HP (2012) Plant water relations: absorption, transport and control mechanisms. Advances in selected plant physiology aspects. doi: 10.5772/33478

Chaves M, Oliveira M (2004) Mechanisms underlying plant resilience to water deficit: Prospects for water-saving agriculture. J Expl Bot **55**: 2365–2384

Chaves MM (1991) Effects of water deficits on carbon assimilation. J Exp Bot **42**: 1–16

Chaves MM, Flexas J, Pinheiro C (2009) Photosynthesis under drought and salt stress: regulation mechanisms from whole plant to cell. Ann Bot **103**: 551–560

Chaves MM, Maroco JP, Pereira JS (2003) Understanding plant responses to drought — from genes to the whole plant. Funct Plant Biol **30**: 239

Chaves MM, Pereira JS, Maroco J, Rodrigues ML, Ricardo CPP, Osório ML, Carvalho I, Faria T, Pinheiro C (2002) How plants cope with water stress in the field. Photosynthesis and growth. Ann Bot **89** Spec No: 907–916

Chazen O, Neumann PM (1994) Hydraulic signals from the roots and rapid cell-wall hardening in growing Maize (*Zea mays* L.) leaves are primary responses to polyethylene glycol-induced water deficits. Plant Physiol **104**: 1385–1392

Chen L-Q, Hou B-H, Lalonde S, Takanaga H, Hartung ML, Qu X-Q, Guo W-J, Kim J-G, Underwood W, Chaudhuri B, et al (2010a) Sugar transporters for intercellular exchange and nutrition of pathogens. Nature **468**: 527–532

Chen L-Q, Lin IW, Qu X-Q, Sosso D, McFarlane HE, Londoño A, Samuels AL, Frommer WB (2015) A Cascade of Sequentially Expressed Sucrose Transporters in the Seed Coat and Endosperm Provides Nutrition for the *Arabidopsis* Embryo. Plant Cell **27**: 607–619

Chen L-Q, Qu X-Q, Hou B-H, Sosso D, Osorio S, Fernie AR, Frommer WB (2012) Sucrose Efflux Mediated by SWEET Proteins as a Key Step for Phloem Transport. Science **335**: 207–211

Chen L-T, Luo M, Wang Y-Y, Wu K (2010b) Involvement of Arabidopsis histone deacetylase HDA6 in ABA and salt stress response. J Exp Bot **61**: 3345–3353

Chen ZJ, Tian L (2007) Roles of dynamic and reversible histone acetylation in plant development and polyploidy. Biochimica et Biophysica Acta (BBA) - Gene Struct Exp **1769**: 295–307

Cheng R, Cheng Y, Lü J, Chen J, Wang Y, Zhang S, Zhang H (2018) The gene PbTMT4 from pear (Pyrus bretschneideri) mediates vacuolar sugar transport and strongly affects sugar accumulation in fruit. Physiologia Plantarum **164**: 307–319

Cheng W-H, Endo A, Zhou L, Penney J, Chen H-C, Arroyo A, Leon P, Nambara E, Asami T, Seo M, et al (2002) A Unique short-Chain dehydrogenase/reductase in *Arabidopsis* glucose signaling and abscisic acid biosynthesis and functions. Plant Cell **14**: 2723–2743

Cho D, Shin D, Jeon BW, Kwak JM (2009) ROS-Mediated ABA Signaling. J Plant Biol **52**: 102–113

Cho M-H, Lim H, Shin DH, Jeon J-S, Bhoo SH, Park Y-I, Hahn T-R (2011) Role of the plastidic glucose translocator in the export of starch degradation products from the chloroplasts in *Arabidopsis thaliana*. New Phytol **190**: 101–112

Cho Y-H, Yoo S-D, Sheen J (2006) Regulatory Functions of Nuclear Hexokinase1 Complex in Glucose Signaling. Cell **127**: 579–589

Cominelli E, Sala T, Calvi D, Gusmaroli G, Tonelli C (2008) Over-expression of the *Arabidopsis* AtMYB41 gene alters cell expansion and leaf surface permeability. Plant J **53**: 53–64

Conklin PL (2001) Recent advances in the role and biosynthesis of ascorbic acid in plants. Plant, Cell Environ **24**: 383–394

Cornish K, Zeevaart JAD (1986) Abscisic Acid Accumulation by in Situ and Isolated Guard Cells of *Pisum sativum* L. and Vicia faba L. in Relation to Water Stress 1. Plant Physiol **81**: 1017–1021

Corrêa LGG, Riaño-Pachón DM, Schrago CG, dos Santos RV, Mueller-Roeber B, Vincentz M (2008) The Role of bZIP Transcription Factors in Green Plant Evolution:

Adaptive Features Emerging from Four Founder Genes. PLoS One. doi: 10.1371/journal.pone.0002944

Czechowski T, Stitt M, Altmann T, Udvardi MK, Scheible W-R (2005) Genome-Wide Identification and Testing of Superior Reference Genes for Transcript Normalization in *Arabidopsis*. Plant Physiol **139**: 5–17

Damour G, Simonneau T, Cochard H, Urban L (2010) An overview of models of stomatal conductance at the leaf level. Plant, Cell Environ **33**: 1419–1438

Davies WJ, Zhang J (1991) Root Signals and the Regulation of Growth and Development of Plants in Drying Soil. Ann Rev Plant Physiol Plant Mol Biol **42**: 55–76

De Schepper V, De Swaef T, Bauweraerts I, Steppe K (2013) Phloem transport: a review of mechanisms and controls. J Exp Bot **64**: 4839–4850

Dekkers BJW, Schuurmans JAMJ, Smeekens SCM (2004) Glucose delays seed germination in *Arabidopsis thaliana*. Planta **218**: 579–588

Delport W, Poon AFY, Frost SDW, Kosakovsky Pond SL (2010) Datamonkey 2010: a suite of phylogenetic analysis tools for evolutionary biology. Bioinformatics **26**: 2455–2457

Denekamp M, Smeekens SC (2003) Integration of Wounding and Osmotic Stress Signals Determines the Expression of the AtMYB102 Transcription Factor Gene. Plant Physiol **132**: 1415–1423

Deng X, An B, Zhong H, Yang J, Kong W, Li Y (2019) A Novel Insight into Functional Divergence of the MST Gene Family in Rice Based on Comprehensive Expression Patterns. Genes (Basel). doi: 10.3390/genes10030239

Desrut A, Moumen B, Thibault F, Le Hir R, Coutos-Thévenot P, Vriet C (2020) Beneficial rhizobacteria *Pseudomonas simiae* WCS417 induce major transcriptional changes in plant sugar transport. J Exp Bot **71**: 7301–7315

D'Hont A, Denoeud F, Aury J-M, Baurens F-C, Carreel F, Garsmeur O, Noel B, Bocs S, Droc G, Rouard M, et al (2012) The banana (*Musa acuminata*) genome and the evolution of monocotyledonous plants. Nature **488**: 213–217

Doidy J, Vidal U, Lemoine R (2019) Sugar transporters in Fabaceae, featuring SUT MST and SWEET families of the model plant *Medicago truncatula* and the agricultural crop *Pisum sativum.* PLOS ONE **14**: e0223173

Durand M, Porcheron B, Hennion N, Maurousset L, Lemoine R, Pourtau N (2016) Water Deficit Enhances C Export to the Roots in *Arabidopsis thaliana* Plants with Contribution of Sucrose Transporters in Both Shoot and Roots. Plant Physiol **170**: 1460–1479

Edwards K, Johnstone C, Thompson C (1991) A simple and rapid method for the preparation of plant genomic DNA for PCR analysis. Nucleic Acids Res **19**: 1349–1349

Ehness R, Ecker M, Godt DE, Roitsch T (1997) Glucose and Stress Independently Regulate Source and Sink Metabolism and Defense Mechanisms via Signal Transduction Pathways Involving Protein Phosphorylation. Plant Cell **9**: 1825–1841

Elster J, Degma P, Kováčik Ľ, Valentová L, Šramková K, Batista Pereira A (2008) Freezing and desiccation injury resistance in the filamentous green alga *Klebsormidium* from the Antarctic, Arctic and Slovakia. Biologia **63**: 843–851

Endler A, Meyer S, Schelbert S, Schneider T, Weschke W, Peters SW, Keller F, Baginsky S, Martinoia E, Schmidt UG (2006) Identification of a Vacuolar Sucrose Transporter in Barley and *Arabidopsis* Mesophyll Cells by a Tonoplast Proteomic Approach. Plant Physiol **141**: 196–207

Endo A, Sawada Y, Takahashi H, Okamoto M, Ikegami K, Koiwai H, Seo M, Toyomasu T, Mitsuhashi W, Shinozaki K, et al (2008) Drought Induction of *Arabidopsis* 9-cis-Epoxycarotenoid Dioxygenase Occurs in Vascular Parenchyma Cells. Plant Physiol **147**: 1984–1993

Engel ML, Holmes-Davis R, McCormick S (2005) Green Sperm. Identification of Male Gamete Promoters in *Arabidopsis*. Plant Physiol **138**: 2124–2133

Eulgem T, Rushton PJ, Robatzek S, Somssich IE (2000) The WRKY superfamily of plant transcription factors. Trends Plant Science **5**: 199–206

Fang Y, Xiong L (2015) General mechanisms of drought response and their application in drought resistance improvement in plants. Cell Mol Life Sci **72**: 673–689

Farooq M, Wahid A, Kobayashi N, Fujita D, Basra SMA (2009) Plant drought stress: effects, mechanisms and management. Agron Sustain Dev **29**: 185–212

Feller A, Machemer K, Braun EL, Grotewold E (2011) Evolutionary and comparative analysis of MYB and bHLH plant transcription factors. Plant J**66**: 94–116

Finch- Savage WE, Leubner- Metzger G (2006) Seed dormancy and the control of germination. New Phytologist **171**: 501–523

Finkelstein R, Reeves W, Ariizumi T, Steber C (2008) Molecular Aspects of Seed Dormancy. Ann Rev Plant Biol **59**: 387–415

Finkelstein RR, Gampala SSL, Rock CD (2002) Abscisic Acid Signaling in Seeds and Seedlings. Plant Cell **14**: s15–s45

Finkelstein RR, Wang ML, Lynch TJ, Rao S, Goodman HM (1998) The *Arabidopsis* Abscisic Acid Response Locus ABI4 Encodes an APETALA2 Domain Protein. Plant Cell **10**: 1043–1054

Fleurat-Lessard P, Béré E, Lallemand M, Dédaldéchamp F, Roblin G (2016) Co-occurrence of tannin and tannin-less vacuoles in sensitive plants. Protoplasma **253**: 821–834

Flexas J, Bota J, Cifre J, Escalona J, Galmés J, Gulias J, Lefi E-K, Martínez-Cañellas S, Moreno M, Ribas-Carbo M, et al (2004) Understanding down-regulation of

photosynthesis under water stress: Future prospects and searching for physiological tools for irrigation management. Ann appl Biol **144**: 273–283

França M, AT P, Pimentel C, Rossiello R, Zuily-Fodil Y, Laffray D (2000) Differences in growth and water relations among *Phaseolus vulgaris* cultivars response to induced drought stress. Environ Exp Bot **43**: 227–237

Frommer WB, Sonnewald U (1995) Molecular analysis of carbon partitioning in solanaceous species. J Exp Bot **46**: 587–607

Fujita Y, Fujita M, Satoh R, Maruyama K, Parvez MM, Seki M, Hiratsu K, Ohme-Takagi M, Shinozaki K, Yamaguchi-Shinozaki K (2005) AREB1 Is a Transcription Activator of Novel ABRE-Dependent ABA Signaling That Enhances Drought Stress Tolerance in *Arabidopsis*. Plant Cell **17**: 3470–3488

Fujita Y, Fujita M, Shinozaki K, Yamaguchi-Shinozaki K (2011) ABA-mediated transcriptional regulation in response to osmotic stress in plants. J Plant Res **124**: 509–525

Gallegos JE, Rose AB (2019) An intron-derived motif strongly increases gene expression from transcribed sequences through a splicing independent mechanism in *Arabidopsis thaliana*. Sci Rep **9**: 13777

Galmés J, Ochogavía JM, Gago J, Roldán EJ, Cifre J, Conesa MÀ (2013) Leaf responses to drought stress in Mediterranean accessions of *Solanum lycopersicum*: anatomical adaptations in relation to gas exchange parameters. Plant, Cell Environ **36**: 920–935

Gattolin S, Sorieul M, Frigerio L (2010) Tonoplast intrinsic proteins and vacuolar identity. Biochem Soc Trans **38**: 769–773

Ghassemian M, Nambara E, Cutler S, Kawaide H, Kamiya Y, McCourt P (2000) Regulation of Abscisic Acid Signaling by the Ethylene Response Pathway in *Arabidopsis*. Plant Cell **12**: 1117–1126

Gibson SI, Laby RJ, Kim D (2001) The sugar-insensitive1 (sis1) Mutant of *Arabidopsis* Is Allelic to ctr1. Biochemical and Biophysical Research Communications **280**: 196–203

Godt DE, Riegel A, Roitsch T (1995) Regulation of Sucrose Synthase Expression in *Chenopodium rubrum*: Characterization of Sugar Induced Expression in Photoautotrophic Suspension Cultures and Sink Tissue Specific Expression in Plants. J Plant Physiol**146**: 231–238

Gómez-Porras JL, Riaño-Pachón D, Dreyer I, Mayer JE, Mueller-Roeber B (2007) Genome-wide analysis of ABA-responsive elements ABRE and CE3 reveals divergent patterns in *Arabidopsis* and rice. BMC Genomics **8**: 260

Gong X, Liu M, Zhang L, Ruan Y, Ding R, Ji Y, Zhang N, Zhang S, Farmer J, Wang C (2015) *Arabidopsis* AtSUC2 and AtSUC4, encoding sucrose transporters, are required for abiotic stress tolerance in an ABA-dependent pathway. Physiologia Plantarum **153**: 119–136

Gottwald JR, Krysan PJ, Young JC, Evert RF, Sussman MR (2000) Genetic evidence for the *in planta* role of phloem-specific plasma membrane sucrose transporters. PNAS **97**: 13979–13984

Guo W-J, Nagy R, Chen H-Y, Pfrunder S, Yu Y-C, Santelia D, Frommer WB, Martinoia E (2014) SWEET17, a Facilitative Transporter, Mediates Fructose Transport across the Tonoplast of Arabidopsis Roots and Leaves. Plant Physiol **164**: 777–789

Haake V, Cook D, Riechmann JL, Pineda O, Thomashow MF, Zhang JZ (2002) Transcription Factor CBF4 Is a Regulator of Drought Adaptation in Arabidopsis. Plant Physiol **130**: 639–648

Halford NG, Hey S, Jhurreea D, Laurie S, McKibbin RS, Paul M, Zhang Y (2003) Metabolic signalling and carbon partitioning: role of Snf1- related (SnRK1) protein kinase. J Exp Bot **54**: 467–475

Hanada K, Zou C, Lehti-Shiu MD, Shinozaki K, Shiu S-H (2008) Importance of Lineage-Specific Expansion of Plant Tandem Duplicates in the Adaptive Response to Environmental Stimuli. Plant Physiology **148**: 993–1003

Haouazine-Takvorian N, Tymowska-Lalanne Z, Takvorian A, Tregear J, Lejeune B, Lecharny A, Kreis M (1997) Characterization of two members of the *Arabidopsis thaliana* gene family, Atβfruct3 and Atβfruct4, coding for vacuolar invertases. Gene **197**: 239–251

Harb A, Krishnan A, Ambavaram MMR, Pereira A (2010) Molecular and Physiological Analysis of Drought Stress in *Arabidopsis* Reveals Early Responses Leading to Acclimation in Plant Growth. Plant Physiology **154**: 1254–1271

Hare PD, Cress WA (1997) Metabolic implications of stress-induced proline accumulation in plants. Plant Growth Regulation **21**: 79–102

Hare PD, Cress WA, Staden JV (1998) Dissecting the roles of osmolyte accumulation during stress. Plant, Cell & Environment **21**: 535–553

Hedges SB, Dudley J, Kumar S (2006) TimeTree: a public knowledge-base of divergence times among organisms. Bioinformatics **22**: 2971–2972

Hedrich R, Sauer N, Neuhaus HE (2015) Sugar transport across the plant vacuolar membrane: nature and regulation of carrier proteins. Current Opinion in Plant Biology **25**: 63–70

Hernandez-Garcia CM, Finer JJ (2014) Identification and validation of promoters and cis-acting regulatory elements. Plant Science **217–218**: 109–119

Higo K, Ugawa Y, Iwamoto M, Korenaga T (1999) Plant cis-acting regulatory DNA elements (PLACE) database: 1999. Nucleic Acids Res **27**: 297–300

Hori K, Maruyama F, Fujisawa T, Togashi T, Yamamoto N, Seo M, Sato S, Yamada T, Mori H, Tajima N, et al (2014) *Klebsormidium flaccidum* genome reveals primary factors for plant terrestrial adaptation. Nature Communications **5**: 3978

Hsiao TC (1973) Plant Responses to Water Stress. Annu Rev Plant Physiol **24**: 519–570

Hu B, Jin J, Guo A-Y, Zhang H, Luo J, Gao G (2015) GSDS 2.0: an upgraded gene feature visualization server. Bioinformatics **31**: 1296–1297

Hummel I, Pantin F, Sulpice R, Piques M, Rolland G, Dauzat M, Christophe A, Pervent M, Bouteillé M, Stitt M, et al (2010) *Arabidopsis* Plants Acclimate to Water Deficit at Low Cost through Changes of Carbon Usage: An Integrated Perspective Using Growth, Metabolite, Enzyme, and Gene Expression Analysis. Plant Physiology **154**: 357–372

Ikegami K, Okamoto M, Seo M, Koshiba T (2009) Activation of abscisic acid biosynthesis in the leaves of *Arabidopsis thaliana* in response to water deficit. J Plant Res **122**: 235–243

Ilyas M, Nisar M, Khan N, Hazrat A, Khan A, Hayat K, Fahad S, Khan A, Ullah A (2020) Drought Tolerance Strategies in Plants: A Mechanistic Approach. Journal of Plant Growth Regulation. doi: 10.1007/s00344-020-10174-5

Innan H, Kondrashov F (2010) The evolution of gene duplications: classifying and distinguishing between models. Nat Rev Genet **11**: 97–108

Jackson RB, Sperry JS, Dawson TE (2000) Root water uptake and transport: using physiological processes in global predictions. Trends in Plant Science **5**: 482–488

Jakoby M, Weisshaar B, Dröge-Laser W, Vicente-Carbajosa J, Tiedemann J, Kroj T, Parcy F (2002) bZIP transcription factors in *Arabidopsis*. Trends in Plant Science **7**: 106–111

Jang JC, León P, Zhou L, Sheen J (1997) Hexokinase as a sugar sensor in higher plants. Plant Cell **9**: 5–19

Jang JC, Sheen J (1994) Sugar sensing in higher plants. Plant Cell **6**: 1665–1679

Jefferson R, Goldsbrough A, Bevan M (1990) Transcriptional regulation of a patatin-1 gene in potato. Plant Mol Biol **14**: 995–1006

Jiao Y, Leebens-Mack J, Ayyampalayam S, Bowers JE, McKain MR, McNeal J, Rolf M, Ruzicka DR, Wafula E, Wickett NJ, et al (2012) A genome triplication associated with early diversification of the core eudicots. Genome Biology **13**: R3

Jiao Y, Wickett NJ, Ayyampalayam S, Chanderbali AS, Landherr L, Ralph PE, Tomsho LP, Hu Y, Liang H, Soltis PS, et al (2011) Ancestral polyploidy in seed plants and angiosperms. Nature **473**: 97–100

Johnson DA, Hill JP, Thomas MA (2006) The monosaccharide transporter gene family in land plants is ancient and shows differential subfamily expression and expansion across lineages. BMC Evolutionary Biology **6**: 64

Johnson DA, Thomas MA (2007) The Monosaccharide Transporter Gene Family in Arabidopsis and Rice: A History of Duplications, Adaptive Evolution, and Functional Divergence. Mol Biol Evol **24**: 2412–2423

Julius BT, Leach KA, Tran TM, Mertz RA, Braun DM (2017) Sugar Transporters in Plants: New Insights and Discoveries. Plant and Cell Physiology **58**: 1442–1460

Jung C, Seo JS, Han SW, Koo YJ, Kim CH, Song SI, Nahm BH, Choi YD, Cheong J-J (2008) Overexpression of AtMYB44 Enhances Stomatal Closure to Confer Abiotic Stress Tolerance in Transgenic *Arabidopsis*. Plant Physiology **146**: 623–635

Jung S (2004) Variation in antioxidant metabolism of young and mature leaves of *Arabidopsis thaliana* subjected to drought. Plant Science **166**: 459–466

Kagale S, Robinson SJ, Nixon J, Xiao R, Huebert T, Condie J, Kessler D, Clarke WE, Edger PP, Links MG, et al (2014) Polyploid Evolution of the Brassicaceae during the Cenozoic Era. Plant Cell **26**: 2777–2791

Kang J, Choi H, Im M, Kim SY (2002) *Arabidopsis* Basic Leucine Zipper Proteins That Mediate Stress-Responsive Abscisic Acid Signaling. Plant Cell **14**: 343–357

Karsten U, Holzinger A (2011) Light, Temperature, and Desiccation Effects on Photosynthetic Activity, and Drought-Induced Ultrastructural Changes in the Green Alga *Klebsormidium dissectum* (Streptophyta) from a High Alpine Soil Crust. Microbial ecology **63**: 51–63

Kay R, Chan A, Daly M, Mcpherson J (1987) Duplication of CaMV 35S Promoter Sequences Creates a Strong Enhancer for Plant Genes. Science **236**: 1299–1302

Khalil A a. M, Grace J (1993) Does Xylem Sap ABA Control the Stomatal Behaviour of Water-Stressed Sycamore (*Acer pseudoplatanus L.*) Seedlings? J Exp Bot **44**: 1127–1134

Kieber JJ, Rothenberg M, Roman G, Feldmann KA, Ecker JR (1993) CTR1, a negative regulator of the ethylene response pathway in *Arabidopsis*, encodes a member of the Raf family of protein kinases. Cell **72**: 427–441

Kim J-M, To TK, Ishida J, Morosawa T, Kawashima M, Matsui A, Toyoda T, Kimura H, Shinozaki K, Seki M (2008) Alterations of lysine modifications on the histone H3 N-tail under drought stress conditions in *Arabidopsis thaliana*. Plant Cell Physiol **49**: 1580–1588

Kim S, Kang J, Cho D-I, Park JH, Kim SY (2004) ABF2, an ABRE-binding bZIP factor, is an essential component of glucose signaling and its overexpression affects multiple stress tolerance. The Plant Journal **40**: 75–87

Kim S, Soltis PS, Wall K, Soltis DE (2006) Phylogeny and Domain Evolution in the APETALA2-like Gene Family. Molecular Biology and Evolution **23**: 107–120

Kim T-H, Böhmer M, Hu H, Nishimura N, Schroeder JI (2010) Guard Cell Signal Transduction Network: Advances in Understanding Abscisic Acid, CO2, and Ca2+ Signaling. Annu Rev Plant Biol **61**: 561–591

Kiyosue T, Abe H, Yamaguchi-Shinozaki K, Shinozaki K (1998) ERD6, a cDNA clone for an early dehydration-induced gene of *Arabidopsis*, encodes a putative sugar transporter. Biochimica et Biophysica Acta (BBA) - Biomembranes **1370**: 187–191

Kiyosue T, Yamaguchi-Shinozaki K, Shinozaki K (1994) Cloning of cDNAs for genes that are early-responsive to dehydration stress (ERDs) in *Arabidopsis thaliana* L.: identification of three ERDs as HSP cognate genes. Plant Mol Biol **25**: 791–798

Klemens PAW, Patzke K, Deitmer J, Spinner L, Hir RL, Bellini C, Bedu M, Chardon F, Krapp A, Neuhaus HE (2013) Overexpression of the Vacuolar Sugar Carrier AtSWEET16 Modifies Germination, Growth, and Stress Tolerance in *Arabidopsis*. Plant Physiology **163**: 1338–1352

Klemens PAW, Patzke K, Trentmann O, Poschet G, Büttner M, Schulz A, Marten I, Hedrich R, Neuhaus HE (2014) Overexpression of a proton-coupled vacuolar glucose exporter impairs freezing tolerance and seed germination. New Phytologist **202**: 188–197

Klepek Y-S, Geiger D, Stadler R, Klebl F, Landouar-Arsivaud L, Lemoine R, Hedrich R, Sauer N (2005) *Arabidopsis* Polyol Transporter 5, a New Member of the Monosaccharide Transporter-Like Superfamily, Mediates H^+-Symport of Numerous Substrates, Including myo-Inositol, Glycerol, and Ribose. Plant Cell **17**: 204–218

Klepek Y-S, Volke M, Konrad KR, Wippel K, Hoth S, Hedrich R, Sauer N (2010) Arabidopsis thaliana Polyol/Monosaccharides Transporters 1 and 2: fructose and xylitol/H+ symporters in pollen and young xylem cells. J Exp Bot **61**: 537–550

Koornneef M, Hanhart CJ, Hilhorst HWM, Karssen CM (1989) *In Vivo* Inhibition of Seed Development and Reserve Protein Accumulation in Recombinants of Abscisic Acid Biosynthesis and Responsiveness Mutants in *Arabidopsis thaliana*. Plant Physiol **90**: 463–469

Kosakovsky Pond SL, Frost SDW (2005) Not So Different After All: A Comparison of Methods for Detecting Amino Acid Sites Under Selection. Molecular Biology and Evolution **22**: 1208–1222

Kuhn C (1997) Macromolecular Trafficking Indicated by Localization and Turnover of Sucrose Transporters in Enucleate Sieve Elements. Science **275**: 1298–1300

Kühn C, Barker L, Bürkle L, Frommer W-B (1999) Update on sucrose transport in higher plants. Journal of Experimental Botany **50**: 935–953

Kühn C, Grof CP (2010) Sucrose transporters of higher plants. Current Opinion in Plant Biology **13**: 287–297

Kumar S, Stecher G, Suleski M, Hedges SB (2017) TimeTree: A Resource for Timelines, Timetrees, and Divergence Times. Molecular Biology and Evolution **34**: 1812–1819

Lalonde S, Frommer WB (2012) SUT Sucrose and MST Monosaccharide Transporter Inventory of the *Selaginella* Genome. Front Plant Sci. doi: 10.3389/fpls.2012.00024

Lalonde S, Tegeder M, Throne- Holst M, Frommer WB, Patrick JW (2003) Phloem loading and unloading of sugars and amino acids. Plant, Cell & Environment **26**: 37–56

Lalonde S, Wipf D, Frommer WB (2004) Transport mechanisms for organic forms of carbon and nitrogen between source and sink. Annu Rev Plant Biol **55**: 341–372

Lata C, Prasad M (2011) Role of DREBs in regulation of abiotic stress responses in plants. J Exp Bot **62**: 4731–4748

Law CJ, Maloney PC, Wang D-N (2008) Ins and Outs of Major Facilitator Superfamily Antiporters. Annu Rev Microbiol **62**: 289–305

Lawlor DW (2013) Genetic engineering to improve plant performance under drought: physiological evaluation of achievements, limitations, and possibilities. EXBOTJ **64**: 83–108

Lawlor DW, Cornic G (2002) Photosynthetic carbon assimilation and associated metabolism in relation to water deficits in higher plants. Plant, Cell & Environment **25**: 275–294

Laxa M (2016) Intron-Mediated Enhancement: A Tool for Heterologous Gene Expression in Plants? Frontiers in Plant Science. doi: 10.3389/fpls.2016.01977

Lecourieux F, Kappel C, Lecourieux D, Serrano A, Torres E, Arce-Johnson P, Delrot S (2014) An update on sugar transport and signalling in grapevine. J Exp Bot **65**: 821–832

Lee TI, Young RA (2000) Transcription of eukaryotic protein-coding genes. Annu Rev Genet **34**: 77–137

Leliaert F, Smith DR, Moreau H, Herron MD, Verbruggen H, Delwiche CF, Clerck OD (2012) Phylogeny and Molecular Evolution of the Green Algae. Critical Reviews in Plant Sciences **31**: 1–46

Lemoine R (2000) Sucrose transporters in plants: update on function and structure. Biochimica et Biophysica Acta (BBA) - Biomembranes **1465**: 246–262

Lemoine R, Camera SL, Atanassova R, Dédaldéchamp F, Allario T, Pourtau N, Bonnemain J-L, Laloi M, Coutos-Thévenot P, Maurousset L, et al (2013) Source-to-sink transport of sugar and regulation by environmental factors. Front Plant Sci. doi: 10.3389/fpls.2013.00272

León P, Sheen J (2003) Sugar and hormone connections. Trends Plant Sci **8**: 110–116

Lewis LA, McCourt RM (2004) Green algae and the origin of land plants. Am J Bot **91**: 1535–1556

Lin H, Zhu W, Silva JC, Gu X, Buell CR (2006) Intron gain and loss in segmentally duplicated genes in rice. Genome Biology **7**: R41

Lin P-C, Hwang S-G, Endo A, Okamoto M, Koshiba T, Cheng W-H (2007) Ectopic Expression of ABSCISIC ACID 2/GLUCOSE INSENSITIVE 1 in *Arabidopsis* Promotes Seed Dormancy and Stress Tolerance. Plant Physiol **143**: 745–758

Liu F, Andersen MN, Jacobsen SE, Jensen CR (2005) Stomatal control and water use efficiency of soybean (Glycine max L. Merr.) during progressive soil drying. Environmental and experimental botany

Liu Q, Kasuga M, Sakuma Y, Abe H, Miura S, Yamaguchi-Shinozaki K, Shinozaki K (1998) Two transcription factors, DREB1 and DREB2, with an EREBP/AP2 DNA binding domain separate two cellular signal transduction pathways in drought- and low-temperature-responsive gene expression, respectively, in *Arabidopsis*. Plant Cell **10**: 1391–1406

Liu S, Lv Z, Liu Y, Li L, Zhang L (2018) Network analysis of ABA-dependent and ABA-independent drought responsive genes in *Arabidopsis thaliana*. Genet Mol Biol **41**: 624–637

Liu T, Zhou T, Lian M, Liu T, Hou J, Ijaz R, Song B (2019) Genome-Wide Identification and Characterization of the AREB/ABF/ABI5 Subfamily Members from Solanum tuberosum. Int J Mol Sci. doi: 10.3390/ijms20020311

Loreti E, Alpi A, Perata P (2000) Glucose and Disaccharide-Sensing Mechanisms Modulate the Expression of α-amylase in Barley Embryos. Plant Physiol **123**: 939–948

Ludewig F, Flügge U-I (2013) Role of metabolite transporters in source-sink carbon allocation. Front Plant Sci. doi: 10.3389/fpls.2013.00231

Lysak MA, Koch MA, Pecinka A, Schubert I (2005) Chromosome triplication found across the tribe Brassiceae. Genome Res **15**: 516–525

Ma Y, Szostkiewicz I, Korte A, Moes D, Yang Y, Christmann A, Grill E (2009) Regulators of PP2C Phosphatase Activity Function as Abscisic Acid Sensors. **324**: 7

Magome H, Yamaguchi S, Hanada A, Kamiya Y, Oda K (2008) The DDF1 transcriptional activator upregulates expression of a gibberellin-deactivating gene, GA2ox7, under high-salinity stress in Arabidopsis. The Plant Journal **56**: 613–626

Mao G-L, Yan Y, Chen Y, Wang B-F, Xu F-F, Zhang Z-X, Lin F, Xu H-H (2017) Family of Ricinus communis Monosaccharide Transporters and RcSTP1 in Promoting the Uptake of a Glucose–Fipronil Conjugate. J Agric Food Chem **65**: 6169–6178

Marger MD, Saier MH (1993) A major superfamily of transmembrane facilitators that catalyse uniport, symport and antiport. Trends in Biochemical Sciences **18**: 13–20

Martin T, Hellmann H, Schmidt R, Willmitzer L, Frommer WB (1997) Identification of mutants in metabolically regulated gene expression. Plant J **11**: 53–62

Martinoia E, Massonneau A, Frangne N (2000) Transport Processes of Solutes across the Vacuolar Membrane of Higher Plants. Plant Cell Physiol **41**: 1175–1186

Martinoia E, Meyer S, De Angeli A, Nagy R (2012) Vacuolar Transporters in Their Physiological Context. Annual Review of Plant Biology **63**: 183–213

Maurel C, Verdoucq L, Luu D-T, Santoni V (2008) Plant Aquaporins: Membrane Channels with Multiple Integrated Functions. Annu Rev Plant Biol **59**: 595–624

Mewis I, Khan MAM, Glawischnig E, Schreiner M, Ulrichs C (2012) Water Stress and Aphid Feeding Differentially Influence Metabolite Composition in *Arabidopsis thaliana* (L.). PLOS ONE **7**: e48661

Meyer S, Lauterbach C, Niedermeier M, Barth I, Sjolund RD, Sauer N (2004) Wounding Enhances Expression of AtSUC3, a Sucrose Transporter from *Arabidopsis* Sieve Elements and Sink Tissues. Plant Physiology **134**: 684–693

Ming R, VanBuren R, Liu Y, Yang M, Han Y, Li L-T, Zhang Q, Kim M-J, Schatz MC, Campbell M, et al (2013) Genome of the long-living sacred lotus (*Nelumbo nucifera* Gaertn.). Genome Biol **14**: R41

Misra VA, Wafula EK, Wang Y, dePamphilis CW, Timko MP (2019) Genome-wide identification of MST, SUT and SWEET family sugar transporters in root parasitic angiosperms and analysis of their expression during host parasitism. BMC Plant Biology **19**: 196

Mizoi J, Shinozaki K, Yamaguchi-Shinozaki K (2012) AP2/ERF family transcription factors in plant abiotic stress responses. Biochimica et Biophysica Acta (BBA) - Gene Regulatory Mechanisms **1819**: 86–96

Moore B, Zhou L, Rolland F, Hall Q, Cheng W-H, Liu Y-X, Hwang I, Jones T, Sheen J (2003) Role of the *Arabidopsis* Glucose Sensor HXK1 in Nutrient, Light, and Hormonal Signaling. Science **300**: 332–336

Moore JP, Vicré-Gibouin M, Farrant JM, Driouich A (2008) Adaptations of higher plant cell walls to water loss: drought vs desiccation. Physiologia Plantarum **134**: 237–245

Morgan JM (1984) Osmoregulation and Water Stress in Higher Plants. Annual Review of Plant Physiology **35**: 299–319

Morison MO, Sheath RG (1985) Responses to desiccation stress by *Klebsormidium rivulare* (Ulotrichales, Chlorophyta) from a Rhode Island stream. Phycologia **24**: 129–145

Muller B, Pantin F, Génard M, Turc O, Freixes S, Piques M, Gibon Y (2011) Water deficits uncouple growth from photosynthesis, increase C content, and modify the relationships between C and growth in sink organs. J Exp Bot **62**: 1715–1729

Müller J, Aeschbacher RA, Wingler A, Boller T, Wiemken A (2001) Trehalose and Trehalase in Arabidopsis. Plant Physiol **125**: 1086–1093

Munns R (2002) Comparative physiology of salt and water stress. Plant, Cell & Environment **25**: 239–250

Myburg AA, Grattapaglia D, Tuskan GA, Hellsten U, Hayes RD, Grimwood J, Jenkins J, Lindquist E, Tice H, Bauer D, et al (2014) The genome of *Eucalyptus grandis*. Nature **510**: 356–362

Nagao M, Matsui K, Uemura M (2008) Klebsormidium flaccidum, a charophycean green alga, exhibits cold acclimation that is closely associated with compatible solute accumulation and ultrastructural changes. Plant, Cell & Environment **31**: 872–885

Nakano T, Suzuki K, Fujimura T, Shinshi H (2006) Genome-Wide Analysis of the ERF Gene Family in Arabidopsis and Rice. Plant Physiol **140**: 411–432

Narusaka Y, Nakashima K, Shinwari ZK, Sakuma Y, Furihata T, Abe H, Narusaka M, Shinozaki K, Yamaguchi-Shinozaki K (2003) Interaction between two cis-acting elements, ABRE and DRE, in ABA-dependent expression of Arabidopsis rd29A gene in response to dehydration and high-salinity stresses. Plant J **34**: 137–148

Neales TF, Masia A, Zhang J, Davies WJ (1989) The Effects of Partially Drying Part of the Root System of Helianthus annuus on the Abscisic Acid Content of the Roots, Xylem Sap and Leaves. J Exp Bot **40**: 1113–1120

Ng DW-K, Abeysinghe JK, Kamali M (2018) Regulating the Regulators: The Control of Transcription Factors in Plant Defense Signaling. Int J Mol Sci. doi: 10.3390/ijms19123737

Ni F-T, Chu L-Y, Shao H-B, Liu Z-H (2009) Gene Expression and Regulation of Higher Plants Under Soil Water Stress. Curr Genomics **10**: 269–280

Nishiyama T, Sakayama H, de Vries J, Buschmann H, Saint-Marcoux D, Ullrich KK, Haas FB, Vanderstraeten L, Becker D, Lang D, et al (2018) The Chara Genome: Secondary Complexity and Implications for Plant Terrestrialization. Cell **174**: 448-464.e24

Noiraud N, Maurousset L, Lemoine R (2001a) Transport of polyols in higher plants. Plant Physiology and Biochemistry **39**: 717–728

Noiraud N, Maurousset L, Lemoine R (2001b) Identification of a Mannitol Transporter, AgMaT1, in Celery Phloem. Plant Cell **13**: 695–706

Nonogaki H (2014) Seed dormancy and germination—emerging mechanisms and new hypotheses. Front Plant Sci. doi: 10.3389/fpls.2014.00233

Norholm MHH, Nour-Eldin HH, Brodersen P, Mundy J, Halkier BA (2006) Expression of the Arabidopsis high-affinity hexose transporter STP13 correlates with programmed cell death. FEBS Lett **580**: 2381–2387

Olsen AN, Ernst HA, Leggio LL, Skriver K (2005) NAC transcription factors: structurally distinct, functionally diverse. Trends in Plant Science **10**: 79–87

Ooka H, Satoh K, Doi K, Nagata T, Otomo Y, Murakami K, Matsubara K, Osato N, Kawai J, Carninci P, et al (2003) Comprehensive analysis of NAC family genes in Oryza sativa and Arabidopsis thaliana. DNA Res **10**: 239–247

Pao SS, Paulsen IT, Saier MH (1998) Major Facilitator Superfamily. Microbiol Mol Biol Rev **62**: 1–34

Park S-Y, Fung P, Nishimura N, Jensen DR, Fujii H, Zhao Y, Lumba S, Santiago J, Rodrigues A, Chow TF, et al (2009) Abscisic Acid Inhibits Type 2C Protein Phosphatases via the PYR/PYL Family of START Proteins. Science **324**: 1068–1071

Paterson AH, Bowers JE, Chapman BA (2004) Ancient polyploidization predating divergence of the cereals, and its consequences for comparative genomics. PNAS **101**: 9903–9908

Patrick JW (1997) PHLOEM UNLOADING: Sieve Element Unloading and Post-Sieve Element Transport. Annu Rev Plant Physiol Plant Mol Biol **48**: 191–222

Peng D, Gu X, Xue L-J, Leebens-Mack JH, Tsai C-J (2014) Bayesian phylogeny of sucrose transporters: ancient origins, differential expansion and convergent evolution in monocots and dicots. Front Plant Sci. doi: 10.3389/fpls.2014.00615

Polge C, Thomas M (2007) SNF1/AMPK/SnRK1 kinases, global regulators at the heart of energy control? Trends in Plant Science **12**: 20–28

Poschet G, Hannich B, Büttner M (2010) Identification and Characterization of AtSTP14, a Novel Galactose Transporter from Arabidopsis. Plant Cell Physiol **51**: 1571–1580

Poschet G, Hannich B, Raab S, Jungkunz I, Klemens PAW, Krueger S, Wic S, Neuhaus HE, Büttner M (2011) A Novel Arabidopsis Vacuolar Glucose Exporter Is Involved in Cellular Sugar Homeostasis and Affects the Composition of Seed Storage Compounds. Plant Physiology **157**: 1664–1676

Price J, Laxmi A, St. Martin SK, Jang J-C (2004) Global Transcription Profiling Reveals Multiple Sugar Signal Transduction Mechanisms in Arabidopsis. Plant Cell **16**: 2128–2150

Price J, Li T-C, Kang SG, Na JK, Jang J-C (2003) Mechanisms of Glucose Signaling during Germination of Arabidopsis. Plant Physiol **132**: 1424–1438

Prouse MB, Campbell MM (2012) The interaction between MYB proteins and their target DNA binding sites. Biochim Biophys Acta **1819**: 67–77

Quirino BF, Reiter W-D, Amasino RD (2001) One of two tandem Arabidopsis genes homologous to monosaccharide transporters is senescence-associated. Plant Mol Biol **46**: 447–457

Ramon M, Rolland F, Sheen J (2008) Sugar Sensing and Signaling. Arabidopsis Book. doi: 10.1199/tab.0117

Raza A, Razzaq A, Mehmood SS, Zou X, Zhang X, Lv Y, Xu J (2019) Impact of Climate Change on Crops Adaptation and Strategies to Tackle Its Outcome: A Review. Plants (Basel). doi: 10.3390/plants8020034

Reddy VS, Shlykov MA, Castillo R, Sun EI, Saier MH (2012) The Major Facilitator Superfamily (MFS) Revisited. FEBS J **279**: 2022–2035

Reinders A, Panshyshyn JA, Ward JM (2005) Analysis of transport activity of Arabidopsis sugar alcohol permease homolog AtPLT5. J Biol Chem **280**: 1594–1602

Reinders A, Sivitz AB, Ward JM (2012) Evolution of plant sucrose uptake transporters. Front Plant Sci **3**: 22

Remy E, Cabrito TR, Batista RA, Hussein MAM, Teixeira MC, Athanasiadis A, Sá-Correia I, Duque P (2014) Intron Retention in the 5′UTR of the Novel ZIF2 Transporter Enhances Translation to Promote Zinc Tolerance in Arabidopsis. PLOS Genetics **10**: e1004375

Ren X, Chen Z, Liu Y, Zhang H, Zhang M, Liu Q, Hong X, Zhu J-K, Gong Z (2010) ABO3, a WRKY transcription factor, mediates plant responses to abscisic acid and drought tolerance in Arabidopsis. Plant J **63**: 417–429

Rennie EA, Turgeon R (2009) A comprehensive picture of phloem loading strategies. PNAS **106**: 14162–14167

Reuscher S, Akiyama M, Yasuda T, Makino H, Aoki K, Shibata D, Shiratake K (2014) The Sugar Transporter Inventory Of Tomato: Genome-Wide Identification And Expression Analysis. Plant & cell physiology. doi: 10.1093/pcp/pcu052

Rhodes D, Nadolska-Orczyk A (2001) Plant Stress Physiology. doi: 10.1038/npg.els.0001297

Riesmeier JW, Willmitzer L, Frommer WB (1992) Isolation and characterization of a sucrose carrier cDNA from spinach by functional expression in yeast. The EMBO Journal **11**: 4705–4713

Riethoven J-JM (2010) Regulatory regions in DNA: promoters, enhancers, silencers, and insulators. Methods Mol Biol **674**: 33–42

Roitsch T, Bittner M, Godt DE (1995) Induction of Apoplastic Invertase of Chenopodium rubrum by D-Glucose and a Glucose Analog and Tissue-Specific Expression Suggest a Role in Sink-Source Regulation. Plant Physiology **108**: 285–294

Rolland F, Baena-Gonzalez E, Sheen J (2006) Sugar sensing and signaling in plants: conserved and novel mechanisms. Annu Rev Plant Biol **57**: 675–709

Rolland F, Moore B, Sheen J (2002) Sugar Sensing and Signaling in Plants. Plant Cell **14**: s185–s205

Rook F, Bevan MW (2003) Genetic approaches to understanding sugar- response pathways. J Exp Bot **54**: 495–501

Rook F, Gerrits N, Kortstee A, Kampen MV, Borrias M, Weisbeek P, Smeekens S (1998) Sucrose-specific signalling represses translation of the Arabidopsis ATB2 bZIP transcription factor gene. The Plant Journal **15**: 253–263

Rosa NM la, Lin C-W, Kang YJ, Dhondt S, Gonzalez N, Inzé D, Falter- Braun P (2019) Drought resistance is mediated by divergent strategies in closely related Brassicaceae. New Phytologist **223**: 783–797

Rottmann T, Klebl F, Schneider S, Kischka D, Rüscher D, Sauer N, Stadler R (2018a) Sugar Transporter STP7 Specificity for l-Arabinose and d-Xylose Contrasts with the Typical Hexose Transporters STP8 and STP12. Plant Physiol **176**: 2330–2350

Rottmann T, Zierer W, Subert C, Sauer N, Stadler R (2016) STP10 encodes a high-affinity monosaccharide transporter and is induced under low-glucose conditions in pollen tubes of Arabidopsis. J Exp Bot **67**: 2387–2399

Rottmann TM, Fritz C, Lauter A, Schneider S, Fischer C, Danzberger N, Dietrich P, Sauer N, Stadler R (2018b) Protoplast-Esculin Assay as a New Method to Assay

Plant Sucrose Transporters: Characterization of AtSUC6 and AtSUC7 Sucrose Uptake Activity in Arabidopsis Col-0 Ecotype. Front Plant Sci **9**: 430

Rouhi V, Samson R, Lemeur R, Damme PV (2007) Photosynthetic gas exchange characteristics in three different almond species during drought stress and subsequent recovery. Environmental and Experimental Botany **59**: 117–129

Roy SW, Gilbert W (2005) Rates of intron loss and gain: Implications for early eukaryotic evolution. PNAS **102**: 5773–5778

Roycewicz P, Malamy JE (2012) Dissecting the effects of nitrate, sucrose and osmotic potential on Arabidopsis root and shoot system growth in laboratory assays. Philos Trans R Soc Lond B Biol Sci **367**: 1489–1500

Roychoudhury A, Paul S, Basu S (2013) Cross-talk between abscisic acid-dependent and abscisic acid-independent pathways during abiotic stress. Plant Cell Rep **32**: 985–1006

Ruan Y-L, Patrick JW (1995) The cellular pathway of postphloem sugar transport in developing tomato fruit. Planta **196**: 434–444

Rushton PJ, Somssich IE, Ringler P, Shen QJ (2010) WRKY transcription factors. Trends Plant Sci **15**: 247–258

Sakuma Y, Maruyama K, Osakabe Y, Qin F, Seki M, Shinozaki K, Yamaguchi-Shinozaki K (2006) Functional Analysis of an *Arabidopsis* Transcription Factor, DREB2A, Involved in Drought-Responsive Gene Expression. Plant Cell **18**: 1292–1309

dos Santos Gouvêa PR, Marenco RA (2018) Is a reduction in stomatal conductance the main strategy of Garcinia brasiliensis (Clusiaceae) to deal with water stress? Theor Exp Plant Physiol **30**: 321–333

Sato S, Nakamura Y, Kaneko T, Asamizu E, Kato T, Nakao M, Sasamoto S, Watanabe A, Ono A, Kawashima K, et al (2008) Genome structure of the legume, Lotus japonicus. DNA Res **15**: 227–239

Sauer N (2007) Molecular physiology of higher plant sucrose transporters. FEBS Letters **581**: 2309–2317

Sauer N, Friedländer K, Gräml-Wicke U (1990) Primary structure, genomic organization and heterologous expression of a glucose transporter from Arabidopsis thaliana. EMBO J **9**: 3045–3050

Sauer N, Ludwig A, Knoblauch A, Rothe P, Gahrtz M, Klebl F (2004) AtSUC8 and AtSUC9 encode functional sucrose transporters, but the closely related AtSUC6 and AtSUC7 genes encode aberrant proteins in different Arabidopsis ecotypes. The Plant Journal **40**: 120–130

Sauer N, Tanner W (1989) The hexose carrier from Chlorella. cDNA cloning of a eucaryotic H+-cotransporter. FEBS Lett **259**: 43–46

Scharwies JD, Dinneny JR (2019) Water transport, perception, and response in plants. J Plant Res **132**: 311–324

Schneider S, Beyhl D, Hedrich R, Sauer N (2008) Functional and Physiological Characterization of Arabidopsis INOSITOL TRANSPORTER1, a Novel Tonoplast-Localized Transporter for myo-Inositol. The Plant Cell **20**: 1073–1087

Schneider S, Hulpke S, Schulz A, Yaron I, Höll J, Imlau A, Schmitt B, Batz S, Wolf S, Hedrich R, et al (2012) Vacuoles release sucrose via tonoplast-localised SUC4-type transporters. Plant Biol (Stuttg) **14**: 325–336

Schneider S, Schneidereit A, Konrad KR, Hajirezaei M-R, Gramann M, Hedrich R, Sauer N (2006) Arabidopsis INOSITOL TRANSPORTER4 Mediates High-Affinity H+ Symport of Myoinositol across the Plasma Membrane. Plant Physiology **141**: 565–577

Schneider S, Schneidereit A, Udvardi P, Hammes U, Gramann M, Dietrich P, Sauer N (2007) Arabidopsis INOSITOL TRANSPORTER2 Mediates H+ Symport of Different Inositol Epimers and Derivatives across the Plasma Membrane. Plant Physiology **145**: 1395–1407

Schulz A, Beyhl D, Marten I, Wormit A, Neuhaus E, Poschet G, Büttner M, Schneider S, Sauer N, Hedrich R (2011) Proton-driven sucrose symport and antiport are provided by the vacuolar transporters SUC4 and TMT1/2. Plant J **68**: 129–136

Scott P (2000) Resurrection Plants and the Secrets of Eternal Leaf. Annals of Botany **85**: 159–166

Seki M, Narusaka M, Ishida J, Nanjo T, Fujita M, Oono Y, Kamiya A, Nakajima M, Enju A, Sakurai T, et al (2002) Monitoring the expression profiles of 7000 Arabidopsis genes under drought, cold and high-salinity stresses using a full-length cDNA microarray. Plant J **31**: 279–292

Seki M, Umezawa T, Urano K, Shinozaki K (2007) Regulatory metabolic networks in drought stress responses. Curr Opin Plant Biol **10**: 296–302

Shao H, Wang H, Tang X (2015) NAC transcription factors in plant multiple abiotic stress responses: progress and prospects. Front Plant Sci. doi: 10.3389/fpls.2015.00902

Sharp RE, Poroyko V, Hejlek LG, Spollen WG, Springer GK, Bohnert HJ, Nguyen HT (2004) Root growth maintenance during water deficits: physiology to functional genomics. J Exp Bot **55**: 2343–2351

Sherson SM, Hemmann G, Wallace G, Forbes S, Germain V, Stadler R, Bechtold N, Sauer N, Smith SM (2000) Monosaccharide/proton symporter AtSTP1 plays a major role in uptake and response of Arabidopsis seeds and seedlings to sugars. Plant J **24**: 849–857

Shinozaki K, Yamaguchi-Shinozaki K (2000) Molecular responses to dehydration and low temperature: differences and cross-talk between two stress signaling pathways. Current Opinion in Plant Biology **3**: 217–223

Shinozaki K, Yamaguchi-Shinozaki K (2007) Gene networks involved in drought stress response and tolerance. J Exp Bot **58**: 221–227

Shinozaki K, Yamaguchi-Shinozaki K, Seki M (2003) Regulatory network of gene expression in the drought and cold stress responses. Curr Opin Plant Biol **6**: 410–417

Shu K, Liu X, Xie Q, He Z (2016) Two Faces of One Seed: Hormonal Regulation of Dormancy and Germination. Molecular Plant **9**: 34–45

Simonneau T, Lebon E, Coupel-Ledru A, Marguerit E, Rossdeutsch L, Ollat N (2017) Adapting plant material to face water stress in vineyards: which physiological targets for an optimal control of plant water status? OENO One **51**: 167–179

Sirichandra C, Wasilewska A, Vlad F, Valon C, Leung J (2009) The guard cell as a single-cell model towards understanding drought tolerance and abscisic acid action. J Exp Bot **60**: 1439–1463

Sivitz AB, Reinders A, Johnson ME, Krentz AD, Grof CPL, Perroux JM, Ward JM (2007) Arabidopsis Sucrose Transporter AtSUC9. High-Affinity Transport Activity, Intragenic Control of Expression, and Early Flowering Mutant Phenotype. Plant Physiology **143**: 188–198

Sivitz AB, Reinders A, Ward JM (2008) Arabidopsis Sucrose Transporter AtSUC1 Is Important for Pollen Germination and Sucrose-Induced Anthocyanin Accumulation. Plant Physiology **147**: 92–100

Skirycz A, Vandenbroucke K, Clauw P, Maleux K, De Meyer B, Dhondt S, Pucci A, Gonzalez N, Hoeberichts F, Tognetti VB, et al (2011) Survival and growth of Arabidopsis plants given limited water are not equal. Nat Biotechnol **29**: 212–214

Slawinski L (2017) La famille de transporteurs de monosaccharides ERD6-like (Early Response to Dehydration six-like): émergence, évolution chez les plantes terrestres et réponses au déficit hydrique dans les feuilles d'Arabidopsis thaliana. Thèse. Université de Poitiers.

Slewinski TL (2011) Diverse functional roles of monosaccharide transporters and their homologs in vascular plants: a physiological perspective. Mol Plant **4**: 641–662

Smeekens S (2000) Sugar-Induced Signal Transduction in Plants. Annual Review of Plant Physiology and Plant Molecular Biology **51**: 49–81

Somerville C, Briscoe J (2001) Genetic Engineering and Water. Science **292**: 2217–2217

Souer E, van Houwelingen A, Kloos D, Mol J, Koes R (1996) The no apical meristem gene of Petunia is required for pattern formation in embryos and flowers and is expressed at meristem and primordia boundaries. Cell **85**: 159–170

Sperdouli I, Moustakas M (2012) Interaction of proline, sugars, and anthocyanins during photosynthetic acclimation of Arabidopsis thaliana to drought stress. Journal of Plant Physiology **169**: 577–585

Stadler R, Büttner M, Ache P, Hedrich R, Ivashikina N, Melzer M, Shearson SM, Smith SM, Sauer N (2003) Diurnal and Light-Regulated Expression of AtSTP1 in Guard Cells of Arabidopsis. Plant Physiology **133**: 528–537

Stadler R, Sauer N (1996) The *Arabidopsis thaliana AtSUC2* Gene is Specifically Expressed in Companion Cells. Botanica Acta **109**: 299–306

Stadler R, Truernit E, Gahrtz M, Sauer N (1999) The AtSUC1 sucrose carrier may represent the osmotic driving force for anther dehiscence and pollen tube growth in Arabidopsis. The Plant Journal **19**: 269–278

Stadler R, Wolf K, Hilgarth C, Tanner W, Sauer N (1995) Subcellular localization of the inducible Chlorella HUP1 monosaccharide-H+ symporter and cloning of a Co-induced galactose-H+ symporter. Plant Physiol **107**: 33–41

Sun C, Palmqvist S, Olsson H, Borén M, Ahlandsberg S, Jansson C (2003) A Novel WRKY Transcription Factor, SUSIBA2, Participates in Sugar Signaling in Barley by Binding to the Sugar-Responsive Elements of the iso1 Promoter. Plant Cell **15**: 2076–2092

Taiz L, Zeiger E (1998) Plant physiology 2nd Edition, Sinauer.

Taiz L, Zeiger E, Møller IM, Murphy A (2014) Plant Physiology and Development 6th Edition, Sinauer.

Taji T, Ohsumi C, Iuchi S, Seki M, Kasuga M, Kobayashi M, Yamaguchi- Shinozaki K, Shinozaki K (2002) Important roles of drought- and cold-inducible genes for galactinol synthase in stress tolerance in Arabidopsis thaliana. The Plant Journal **29**: 417–426

Tamura K, Stecher G, Peterson D, Filipski A, Kumar S (2013) MEGA6: Molecular Evolutionary Genetics Analysis version 6.0. Mol Biol Evol **30**: 2725–2729

Tang H, Bowers JE, Wang X, Paterson AH (2010) Angiosperm genome comparisons reveal early polyploidy in the monocot lineage. PNAS **107**: 472–477

Tardieu F (2013) Plant response to environmental conditions: assessing potential production, water demand, and negative effects of water deficit. Front Physiol. doi: 10.3389/fphys.2013.00017

Tardieu F, Granier C, Muller B (1999) Modelling leaf expansion in a fluctuating environment: are changes in specific leaf area a consequence of changes in expansion rate? New Phytologist **143**: 33–43

Tardieu F, Granier C, Muller B (2011) Water deficit and growth. Co-ordinating processes without an orchestrator? Current Opinion in Plant Biology **14**: 283–289

Timme RE, Bachvaroff TR, Delwiche CF (2012) Broad Phylogenomic Sampling and the Sister Lineage of Land Plants. PLOS ONE **7**: e29696

Tora L, Timmers HThM (2010) The TATA box regulates TATA-binding protein (TBP) dynamics in vivo. Trends in Biochemical Sciences **35**: 309–314

Tran L-SP, Nakashima K, Sakuma Y, Osakabe Y, Qin F, Simpson SD, Maruyama K, Fujita Y, Shinozaki K, Yamaguchi- Shinozaki K (2007) Co-expression of the stress-inducible zinc finger homeodomain ZFHD1 and NAC transcription factors enhances expression of the ERD1 gene in Arabidopsis. The Plant Journal **49**: 46–63

Tran L-SP, Nakashima K, Sakuma Y, Simpson SD, Fujita Y, Maruyama K, Fujita M, Seki M, Shinozaki K, Yamaguchi-Shinozaki K (2004) Isolation and Functional Analysis of Arabidopsis Stress-Inducible NAC Transcription Factors That Bind to a Drought-Responsive *cis* -Element in the *early responsive to dehydration stress 1* Promoter. Plant Cell **16**: 2481–2498

Truernit E (2001) Plant physiology: The importance of sucrose transporters. Current Biology **11**: R169–R171

Truernit E, Sauer N (1995) The promoter of the Arabidopsis thaliana SUC2 sucrose-H+ symporter gene directs expression of ?-glucuronidase to the phloem: Evidence for phloem loading and unloading by SUC2. Planta. doi: 10.1007/BF00203657

Truernit E, Schmid J, Epple P, Illig J, Sauer N (1996) The sink-specific and stress-regulated Arabidopsis STP4 gene: enhanced expression of a gene encoding a monosaccharide transporter by wounding, elicitors, and pathogen challenge. Plant Cell **8**: 2169–2182

Turgeon R (1989) The Sink-Source Transition in Leaves. Annual Review of Plant Physiology and Plant Molecular Biology **40**: 119–138

Turner NC (2018) Turgor maintenance by osmotic adjustment: 40 years of progress. J Exp Bot **69**: 3223–3233

Tuskan GA, Difazio S, Jansson S, Bohlmann J, Grigoriev I, Hellsten U, Putnam N, Ralph S, Rombauts S, Salamov A, et al (2006) The genome of black cottonwood, Populus trichocarpa (Torr. & Gray). Science **313**: 1596–1604

Uno Y, Furihata T, Abe H, Yoshida R, Shinozaki K, Yamaguchi-Shinozaki K (2000) Arabidopsis basic leucine zipper transcription factors involved in an abscisic acid-dependent signal transduction pathway under drought and high-salinity conditions. Proc Natl Acad Sci USA **97**: 11632–11637

Varshney RK, Song C, Saxena RK, Azam S, Yu S, Sharpe AG, Cannon S, Baek J, Rosen BD, Tar'an B, et al (2013) Draft genome sequence of chickpea (Cicer arietinum) provides a resource for trait improvement. Nat Biotechnol **31**: 240–246

Velasco R, Zharkikh A, Affourtit J, Dhingra A, Cestaro A, Kalyanaraman A, Fontana P, Bhatnagar SK, Troggio M, Pruss D, et al (2010) The genome of the domesticated apple (Malus × domestica Borkh.). Nature Genetics **42**: 833–839

Venter M, Botha F (2010) Synthetic Promoter Engineering. Plant Developmental Biology. pp 393–414

Verslues PE, Agarwal M, Katiyar- Agarwal S, Zhu J, Zhu J-K (2006) Methods and concepts in quantifying resistance to drought, salt and freezing, abiotic stresses that affect plant water status. The Plant Journal **45**: 523–539

Wang HX, Weerasinghe RR, Perdue TD, Cakmakci NG, Taylor JP, Marzluff WF, Jones AM (2006) A Golgi-localized Hexose Transporter Is Involved in Heterotrimeric G Protein-mediated Early Development in Arabidopsis. Mol Biol Cell **17**: 4257–4269

Wang Y, Wang X, Paterson AH (2012) Genome and gene duplications and gene expression divergence: a view from plants: Gene duplication and expression divergence. Annals of the New York Academy of Sciences **1256**: 1–14

Watanabe S, Kojima K, Ide Y, Sasaki S (2000) Effects of saline and osmotic stress on proline and sugar accumulation in Populus euphratica in vitro. Plant Cell, Tissue and Organ Culture **63**: 199

Weber H, Borisjuk L, Heim U, Sauer N, Wobus U (1997) A role for sugar transporters during seed development: molecular characterization of a hexose and a sucrose carrier in fava bean seeds. Plant Cell **9**: 895–908

Wei X, Liu F, Chen C, Ma F, Li M (2014) The Malus domestica sugar transporter gene family: identifications based on genome and expression profiling related to the accumulation of fruit sugars. Front Plant Sci. doi: 10.3389/fpls.2014.00569

Weise A, Lalonde S, Kühn C, Frommer WB, Ward JM (2008) Introns control expression of sucrose transporter LeSUT1 in trichomes, companion cells and in guard cells. Plant Mol Biol **68**: 251–262

Weitbrecht K, Müller K, Leubner-Metzger G (2011) First off the mark: early seed germination. Journal of Experimental Botany **62**: 3289–3309

Wieczorke R, Krampe S, Weierstall T, Freidel K, Hollenberg CP, Boles E (1999) Concurrent knock-out of at least 20 transporter genes is required to block uptake of hexoses in Saccharomyces cerevisiae. FEBS Letters **464**: 123–128

Wilkinson S (1999) PH as a stress signal. Plant Growth Regulation **29**: 87–99

Wilkinson S, Davies WJ (2002) ABA-based chemical signalling: the co-ordination of responses to stress in plants. Plant, Cell & Environment **25**: 195–210

Williams LE, Lemoine R, Sauer N (2000) Sugar transporters in higher plants – a diversity of roles and complex regulation. Trends in Plant Science **5**: 283–290

Wingenter K, Schulz A, Wormit A, Wic S, Trentmann O, Hoermiller II, Heyer AG, Marten I, Hedrich R, Neuhaus HE (2010) Increased Activity of the Vacuolar

Monosaccharide Transporter TMT1 Alters Cellular Sugar Partitioning, Sugar Signaling, and Seed Yield in Arabidopsis. Plant Physiol **154**: 665–677

Wingler A, Fritzius T, Wiemken A, Boller T, Aeschbacher RA (2000) Trehalose Induces the ADP-Glucose Pyrophosphorylase Gene,ApL3, and Starch Synthesis in Arabidopsis. Plant Physiology **124**: 105–114

Wipf D, Pfister C, Mounier A, Leborgne-Castel N, Frommer WB, Courty P-E (2021) Identification of Putative Interactors of Arabidopsis Sugar Transporters. Trends in Plant Science **26**: 13–22

Wormit A, Trentmann O, Feifer I, Lohr C, Tjaden J, Meyer S, Schmidt U, Martinoia E, Neuhaus HE (2006) Molecular Identification and Physiological Characterization of a Novel Monosaccharide Transporter from Arabidopsis Involved in Vacuolar Sugar Transport. The Plant Cell **18**: 3476–3490

Xiao W, Sheen J, Jang J-C (2000) The role of hexokinase in plant sugar signal transduction and growth and development. Plant Mol Biol **44**: 451–461

Xiong L, Wang R-G, Mao G, Koczan JM (2006) Identification of Drought Tolerance Determinants by Genetic Analysis of Root Response to Drought Stress and Abscisic Acid. Plant Physiol **142**: 1065–1074

Xiong L, Zhu J-K (2002) Molecular and genetic aspects of plant responses to osmotic stress. Plant Cell Environ **25**: 131–139

Yamada K, Osakabe Y, Mizoi J, Nakashima K, Fujita Y, Shinozaki K, Yamaguchi-Shinozaki K (2010) Functional Analysis of an Arabidopsis thaliana Abiotic Stress-inducible Facilitated Diffusion Transporter for Monosaccharides. J Biol Chem **285**: 1138–1146

Yamaguchi-Shinozaki K, Shinozaki K (2005) Organization of cis-acting regulatory elements in osmotic- and cold-stress-responsive promoters. Trends in Plant Science **10**: 88–94

Yamaguchi-Shinozaki K, Shinozaki K (2006) Transcriptional regulatory networks in cellular responses and tolerance to dehydration and cold stresses. Annu Rev Plant Biol **57**: 781–803

Yamauchi Y, Ogawa M, Kuwahara A, Hanada A, Kamiya Y, Yamaguchi S (2004) Activation of Gibberellin Biosynthesis and Response Pathways by Low Temperature during Imbibition of Arabidopsis thaliana Seeds. Plant Cell **16**: 367–378

Yan N (2013) Structural advances for the major facilitator superfamily (MFS) transporters. Trends in Biochemical Sciences **38**: 151–159

Yanagisawa S, Yoo S-D, Sheen J (2003) Differential regulation of EIN3 stability by glucose and ethylene signalling in plants. Nature **425**: 521–525

Yoshida T, Fujita Y, Maruyama K, Mogami J, Todaka D, Shinozaki K, Yamaguchi-Shinozaki K (2015) Four Arabidopsis AREB/ABF transcription factors function

predominantly in gene expression downstream of SnRK2 kinases in abscisic acid signalling in response to osmotic stress. Plant Cell Environ **38**: 35–49

Yoshida T, Fujita Y, Sayama H, Kidokoro S, Maruyama K, Mizoi J, Shinozaki K, Yamaguchi- Shinozaki K (2010) AREB1, AREB2, and ABF3 are master transcription factors that cooperatively regulate ABRE-dependent ABA signaling involved in drought stress tolerance and require ABA for full activation. The Plant Journal **61**: 672–685

Yoshida T, Mogami J, Yamaguchi-Shinozaki K (2014) ABA-dependent and ABA-independent signaling in response to osmotic stress in plants. Current Opinion in Plant Biology **21**: 133–139

Zhang C, Turgeon R (2018) Mechanisms of phloem loading. Current Opinion in Plant Biology **43**: 71–75

Zhang L, Zhang C, Yang B, Xiao Z, Ma J, Liu J, Jian H, Qu C, Lu K, Li J (2020) Genome-Wide Identification and Expression Profiling of Monosaccharide Transporter Genes Associated with High Harvest Index Values in Rapeseed (*Brassica napus* L.). Genes (Basel). doi: 10.3390/genes11060653

Zhang W, Ruan J, Ho T -h. D, You Y, Yu T, Quatrano RS (2005) Cis-regulatory element based targeted gene finding: genome-wide identification of abscisic acid- and abiotic stress-responsive genes in Arabidopsis thaliana. Bioinformatics **21**: 3074–3081

Zhang Y, Liu Z, Khan AA, Lin Q, Han Y, Mu P, Liu Y, Zhang H, Li L, Meng X, et al (2016) Expression partitioning of homeologs and tandem duplications contribute to salt tolerance in wheat (*Triticum aestivum* L.). Sci Rep **6**: 21476

Zhao L, Wang P, Yan S, Gao F, Li H, Hou H, Zhang Q, Tan J, Li L (2014) Promoter-associated histone acetylation is involved in the osmotic stress-induced transcriptional regulation of the maize ZmDREB2A gene. Physiologia Plantarum **151**: 459–467

Zhao W, Liu L, Shen Q, Yang J, Han X, Tian F, Wu J (2020) Effects of Water Stress on Photosynthesis, Yield, and Water Use Efficiency in Winter Wheat. Water **12**: 2127

Zhou A, Ma H, Feng S, Gong S, Wang J (2018) DsSWEET17, a Tonoplast-Localized Sugar Transporter from Dianthus spiculifolius, Affects Sugar Metabolism and Confers Multiple Stress Tolerance in Arabidopsis. IJMS **19**: 1564

Zhou L, Jang J, Jones TL, Sheen J (1998) Glucose and ethylene signal transduction crosstalk revealed by an Arabidopsis glucose-insensitive mutant. Proc Natl Acad Sci U S A **95**: 10294–10299

Zhu L, Li B, Wu L, Li H, Wang Z, Wei X, Ma B, Zhang Y, Ma F, Ruan Y-L, et al (2021) MdERDL6-mediated glucose efflux to the cytosol promotes sugar accumulation in the vacuole through up-regulating TSTs in apple and tomato. Proc Natl Acad Sci USA **118**: e2022788118

Živanović B, Milić Komić S, Tosti T, Vidović M, Prokić L, Veljović Jovanović S (2020) Leaf Soluble Sugars and Free Amino Acids as Important Components of Abscisic Acid—Mediated Drought Response in Tomato. Plants **9**: 1147

Zou C, Sun K, Mackaluso JD, Seddon AE, Jin R, Thomashow MF, Shiu S-H (2011) Cis-regulatory code of stress-responsive transcription in *Arabidopsis thaliana*. Proceedings of the National Academy of Sciences **108**: 14992–14997

ANNEXES

Annex I

Composition of minimal Murashige and Skoog (MS) medium used *in vitro* culture

Composition	Concentration
KNO_3	5 mM
KH_2PO_4	2.5 mM
$MgSO_4$	2 mM
$Ca(NO_3)_2$	2 mM
Fe. EDTA	50 µM
H_3BO_3	70 µM
$MnCl_2$	14 µM
$CuSO_4$	0.5 µM
$ZnSO_4$	1 µM
$NaMoO_4$	0.2 µM
NaCl	0.01µM
$CoCl_2$	0.1 µM

Annex II : Bacterial culture media

Luria-Bertrani (LB) medium

LB	Composition (g/liter)
Tryptone	10.0 g
Yeast extract	5.00 g
NaCl	5.00 g
Agar type E	15.00 g
Water to	1.0 l

pH of the LB medium adjusted to 7 with KOH, prior to autoclave sterilization for 20 min at 120°C.

Yeast extract beef (YEB) medium

YEB	Composition (g/liter)
Beef extract	5.00 g
Yeast extract	1.00 g
Bactopeptone	5.00 g
Sucrose	5.00 g
Agar type E	15.0 g
Water to	1.0 l

pH of the YEB medium adjusted to 7.2 with NaOH. Following autoclave sterilization for 20 min at 120°C, and prior to use, one liter of medium is supplemented with 2 ml of 1 M $MgSO_4$ to a final concentration of 5 mM.

Annex III: Yeast culture medium

Yeast peptone maltose (YPM) medium

YPM	Composition (g/liter)
Yeast extract	10 g
Peptone	10 g
Maltose	20 g
Agar type E	15 g
Water to	1.0 l

Yeast nitrogen base (YNB) medium

YNB	Composition (g/liter)
DIFCO Yeast nitrogen base without amino acids	5.00 g
Ammonium sulfate	5.00 g
Agar type E	15.0 g
Water to	1.0 l

YNB medium autoclaved at 110°C for 20 min and cooled before supplementation with filtered-sterilized stock solutions of L-tryptophane, L-histidine and L-leucine (all amino acids at final concentration of 20 mg/l), and maltose, fructose, glucose, galactose, or mannose (all sugars at final concentration of 2% (w/v)). Medium not supplemented with uracil.

Annex IV: Media used for agroinfiltration of *N. benthamiana* leaves

Induction medium

Compounds	Composition (g or ml per liter)
K_2HPO_4	10.5 g
KH_2PO_4	4.50 g
$(NH_4)_2SO_4$	1.00 g
Sodium citrate	0.50 g
Glucose	1.00 g
Fructose	1.00 g
Glycerol	4.00 ml
$MgSO_4$	0.12 g
MES	1.96 g
Water to	1.0 l

pH of the induction medium adjusted with KOH to 5.6 before autoclave sterilization for 20 min at 120℃

Infiltration medium

Compounds	Composition (g/liter)
10 mM $MgSO_4.7\ H_2O$	2.46 g
10 mM MES	1.95 g
Water to	1.0 l

pH of the infiltration medium adjusted with KOH to 5.6 before autoclave sterilization for 20 min at 120℃

Annex V: Primers

Table 1. Primers used in qPCR for gene expression analysis

Gene	accession	Primer name	Sequence 5'-3'
ESL3.07	At1g08920	qESL3.7-F	TCGGTCTCATTCCATGTGCG
		qESL3.7-R	TGCATCATCTCCGCGAAGAC
ESL1.02	At1g75220	qESL1.2-F	GTGGAGGAACTTTCACTCTGTA
		qESL1.2-R	GTTCTTCAAGAGTTTTGCCTT
ESL3.05	At1g08890	qESL3.5-F	TGGAGTGCTTTCGGAACATATT
		qESL3.5-R	GAGTAAAGAATCAACTTTGGAT
ESL3.03	At4g04760	qESL3.3-F	CAGAGATTTATCCAGTAGATGT
		qESL3.3-R	TGGCTATGAACACAAATCCAA
PP2a	At1g13320	qPP2a-F	
		qPP2a-R	

Table 2. Primers used for genotyping

Gene	Accession	Salk	Primer name	Sequence 5'-3'
ESL3.07	At1g08920	SALK_025646	25646 LP	AGAACCAAAACGACATCAACG
			25646 RP	TCCCCATTTTCCCTATACACC
ESL1.02	At1g75220	SALK_106049	106049 LP	GCAACAAATCCAAGATTCGAC
			106049 RP	TATCCCCAAGTTTTGTTTCC
ESL3.05	At1g08890	SALK_047351	47351 LP	TGCTCTTGCAACAATTTTGTG
			47351 RP	TTTACCGAAAGCACTCCATTG
ESL3.03	At4g04760	SALK_132009	132009 LP	TTTACCGAAAGCACTCCATTG
			132009 RP	ATTGATCCCATACCAGAACC
			LBb1.3	ATTTTGCCGATTTCGGAAC

Table 3. Primers used in Gateway cloning for *AtESL* amplification for yeast expression and subcellular localization experiments

Name	Sequences (5'-3')
ESL1.02-F GW	CACCATGAGTTTCAGGGATGATAA
ESL1.02-R GW	TCATCTGAACAAGGATTGAAGTTC
ESL3.07-F GW	CACCATGACGATGTCGGAGA
ESL3.07-R GW	TCATTGTAGAAAATCTGTAAGAGAAGC
ESL3.05-F GW	CACCATGGAATCTGGAAGTATGAA
ESL3.05-R GW	TTATGAAAGTTGGCCTAGTGATTG
ESL3.03-F GW	CACCATGGCAGAAGAAGGTTTA
ESL3.03-R GW	TTAGAAAATTGTAGAATCTTGAGGAGG
ESL3.07-GFP-R GW	TTGTAGAAAATCTGTAAGAGAAGCTTG
ESL3.05-GFP-R	TGAAAGTTGGCCTAGTGATTGTTG
M13-F (-20)	GTAAAACGACGGCCAG
T7	TAATACGACTCACTATAGGG
PMA-F GW	CTCTCTTTTATACACACATTC
ADH close R GW	CGTAATACGACTCACTATAGG
p35S F	CTATCCTTCGCAAGACCCTTCCTC
t35S R	CATGAGCGAAACCCTATAAGAACC

Table 4. Primers used in restriction cloning for *AtESL* amplification for yeast experiments

Name	Sequences (5'-3')
ESL3.05-XhoI-F	GAG**CTCGAG**ATGGAATCTGGAAGTATGAA
ESL3.05-BamHI-R	AGA***GGATCC***TTATGAAAGTTGGCCTA
ESL3.03-XhoI-F	GAG**CTCGAG**ATGGCAGAAGAAGGTTTAT
ESL3.03- BamHI -R	***GGATCC***TTAGAAAATTGTAGAATCTTGAGGAGG
SP6	TATTTAGGTGACACTATAG
T7	TAATACGACTCACTATAGGG

Underlined sequence in bold (**CTCGAG**) - restriction site for XhoI.
Sequence in italics and bold (***GGATCC***) - restriction site for BamHI in the primers pairs.

Functional diversity of AtESL sugar transporters in the development and the response of *Arabidopsis thaliana* to abiotic constraints

Water deficit is among the most important abiotic factors, which severely affects plant growth, development, and crop yield. In *Arabidopsis thaliana*, the monosaccharide transporters ESL (Early response to dehydration Six-Like) represent one of the largest sugar transporter subfamilies, but until now their biological functions remain not elucidated. Our phylogenetic analysis revealed the emergence of the *ESL* gene family in Streptophyta, while their diversification and distribution in three groups (ESL1, ESL2, and ESL3) are closely related to the evolution of land plants. In the aim to unravel the functional diversity of AtESLs in plant development and stress responses, phenotyping of wild-genotype Col0 and *esl* mutant plants was performed at morphological, physiological, biochemical, and molecular levels, under conditions of watering and water deprivation. The expression profiling of *ESL* genes revealed up-regulation of four genes and down-regulation of eight genes in response to water deficit. In order to decipher the roles of ESL transporters, four T-DNA insertional mutants corresponding to each of the four drought-responsive genes were identified. Given the lack of specific phenotypes for single mutants, we created through their genetic crossing in different combinations three double and two triple *esl* mutants. Using seed germination assays for *esl* single, double, and triple mutants we provided evidence for their differential germination sensitivity/resistance to ABA, glucose, salinity and cold treatments. To gain further insight into the sugar transport activity of AtESL3.05 and AtESL3.03, heterologous expression in *S. cerevisiae*, as well as sugar transport assays on plant isolated vacuoles were developed. Eventually, through using protein fusion constructs with two different fluorescent markers, and their transient expression in protoplasts isolated from agro-infiltrated tobacco leaves, we demonstrated that AtESL3.05 is localized on the tonoplast.

Key words: *Arabidopsis thaliana*, abiotic stresses, ESL/ERD6, germination, monosaccharides, subcellular localization, sugar transport, vacuole

Diversité fonctionnelle des transporteurs de sucres AtESL dans le développement et la réponse d'*Arabidopsis thaliana* aux contraintes abiotiques

Le déficit hydrique est l'un des facteurs abiotiques les plus importants, qui affecte gravement la croissance et le développement des plantes, ainsi que le rendement des cultures. Chez *Arabidopsis thaliana*, les transporteurs de monosaccharides ESL (Early response to dehydration Six-Like) forment l'une des plus grandes sous-familles de transporteurs de sucre, cependant leurs fonctions biologiques ne sont pas encore élucidées. Notre analyse phylogénétique a révélé l'émergence de cette famille de gènes chez les Streptophytes, leur répartition en trois principaux groupes (ESL1, ESL2 et ESL3), ainsi que leur diversification qui est étroitement liée à l'évolution des plantes terrestres. Dans le but d'élucider la diversité fonctionnelle des AtESL dans le développement des plantes et leurs réponses aux stress abiotiques, le phénotypage de plantes sauvages Col-0 et mutantes *esl* a été effectué aux niveaux morphologique, physiologique, biochimique et moléculaire, dans des conditions d'arrosage et de carence en eau. Le profil d'expression des gènes *ESL,* en réponse au déficit en eau, a révélé l'induction de quatre d'entre eux et la répression de huit autres gènes. Afin de comprendre les rôles des transporteurs ESL induits par la carence en eau, quatre simples mutants d'insertion T-DNA ont été identifiés et caractérisés. L'absence de phénotypes marquants pour ces simples mutants nous a conduit à créer par croisements génétiques dans différentes combinaisons trois doubles et deux triples mutants *esl*. Grace à des tests de germination de graines des simples, doubles et triples mutants *esl*, nous avons fourni des preuves de leur sensibilité/résistance différentielle à la germination à l'ABA, au glucose, à la salinité et au froid. Pour mieux comprendre l'activité de transport de sucres de AtESL30.5 et de AtESL3.03, nous avons réalisé une expression hétérologue dans *S. cerevisiae*, ainsi que des essais de transport de sucres sur des vacuoles isolées de la plante. Finalement, en utilisant des constructions de fusion de protéines avec deux marqueurs fluorescents différents exprimées de façon transitoire dans des protoplastes isolés de feuilles de tabac agro-infiltrées, nous avons démontré que AtESL3.05 est localisé au niveau du tonoplaste.

Mots clés : *Arabidopsis thaliana*, stress abiotique, ESL/ERD6, germination, monosaccharides, localisation subcellulaire, transport du sucre, vacuole